WA School of Mines: Minerals, Energy and Chemical Engineering

Relative Permeability Modification in Gas Wells with Excessive Water Production- An Experimental Investigation

Faaiz Al-Shajalee
0000-0002-0590-7694

This thesis is presented for the Degree of
Doctor of Philosophy
of
Curtin University

December 2021

Declaration

To the best of my knowledge and belief, this thesis contains no material previously published by any other person except where due acknowledgment has been made.

This thesis contains no material which has been accepted for the award of any other degree or diploma in any university.

Faaiz Hadi Rasheed Al-Shajalee

Signature:

Date: 10 / 09 /2022

Copyright

I warrant that I have obtained, where necessary, permission from the copyright owners to use any of my own published work (e.g. journal articles) in which the copyright is held by another party (e.g. publisher, co-author).

Faaiz Hadi Rasheed Al-Shajalee

Signature:

Date: 10 / 09 /2022

To my beloved family

Abstract

Excessive water production is becoming common in many gas reservoirs. Polymers have been used as relative permeability modifiers (RPM) to selectively reduce water production with minimum effect on the hydrocarbon phase. The effect of initial rock permeability (low, moderate, and high), fluid flow (water and gas) rate, RPM strength and brine salinity on the outcome of an RPM treatment for a gas/water system were experimentally examined.

As a key study, the effect of high rock permeability range (low, moderate, high) on polymer performance were first investigated. The results obtained in this work are insightful in pointing out that the initial rock permeability can be used as an important screening parameter in planning an RPM treatment for gas producing wells. Using a non-crossed-linked polymer (cationic polyacrylamide, CPAM), in low permeability rocks, the treatment resulted in greater reduction in gas relative permeability than that of water. In a moderate permeability case, the treatment was found to reduce water relative permeability significantly but improve gas relative permeability. In high permeability rocks, the treatment may have no significant effect on either of water or gas relative permeabilities. The relative pore size alteration (wall-steric effect) due to the RPM treatment impacts on how water-gas may redistribute and RPM performance.

On the basis of the above results, the polymer treatment caused gas plugging due to the relative pore size reduction is the highest in the lowest rock permeability. To expand the use of polymer in low permeability rocks, core-flooding results show that lowering salinity decreases the water relative permeability but with marginal effect on the gas relative permeability through decreasing the effective polymer layer thickness at pore surfaces. Moreover, the adsorption of the CPAM onto the negatively charged sandstone rock, together with lowering brine salinity, increases hydrophobicity of the rock and in turn reduced water layer thickness. Thus, the results suggest that rock-polymer-brine interactions at pore surfaces govern the performance of CPAM in low permeability sandstone rocks.

In the next step, to further improve the RPM performance in moderate permeability rock the cross-linked anionic polyacrylamide gel was investigated. In general, utilizing crossed-linked polymer resulted in greater and more stable RPM efficiency than using polymer alone. However, unexpectedly, as gas flow rate increased the gel shows shear thickening behavior due to the gas dissolved in and expanded the gel layer. Furthermore, stronger gels increased water retention inside the porous media, yet decreased the lubrication effect of the gel.

Finally, as another important factor, the CPAM concentration effect was also investigated as how it may modify the performance of RPM in moderate permeability rocks. The results show that a uniform trend of ever decreasing or increasing Frr_w versus the concentration of non-cross-linked polymer and rock permeability may not be expected. This would be dictated by the competing and opposite effects of pore radius (which increases with increase in permeability) and adsorbed polymer layer (which increases with increase in polymer concentration).With regard to the gas phase, the results reveal an increasing Frr_g with an increase in both rock permeability and polymer concentration. This is due to the fact that the adsorbed polymer layer may impact on the gas flow in different ways compared with the water flow.

Furthermore, the results show that the RPM performance is significantly fluid flow rate dependent. Therefore flow rate should be considered during RPM design. The results show that, as the water flow rate increased, Frr_w decreased due to decreasing gas saturation (Sgr) and RPM shear thinning behavior. As gas flow rate increased, in low permeability the RPM show shear thinning behavior due to interstitial fluid velocity is higher that may compress the polymer layer. On the other hand, in moderate and high permeability the performance of RPMs reduces (i.e. Frr_g increased with increasing the gas flow rate) due to decreasing water saturation (decreasing RPM lubrication effect) and RPM shear thickening behavior (due to increasing RPM rigidity, expanding RPM and/or changing gas flow regime). Moreover, at low gas flow rates, RPM performance is mainly controlled by the lubrication effect whereas at higher gas flow rates, RPM rigidity is the dominant factor.

Acknowledgements

I would like to thank my family, who continue to provide their support. To my supervisors (Prof. Ali Saeedi, Prof. Moses O. Tadé, and Dr. Colin wood) who provided me with the support, material, structure, and scope to complete this project.

The Iraqi Ministry of Higher Education and Scientific Research is thanked for providing financial support during my study. I also owe a debt to the Department of Petroleum Engineering at Curtin University for providing lab equipment and facilities.

Finally, I wish to thank all the respected academics whose works have been cited throughout this dissertation. None of this would have been possible without prior study and documentation.

List of publications included as part of the thesis:

1. AL-SHAJALEE, F., ARIF, M., MYERS, M., TADÉ, M. O., WOOD, C. & SAEEDI, A. 2021. Rock/Fluid/Polymer Interaction Mechanisms: Implications for Water Shut-off Treatment. Energy & Fuels, 35, 12809-12827.
2. AL-SHAJALEE, F., WOOD, C., XIE, Q. & SAEEDI, A. 2019. Effective Mechanisms to Relate Initial Rock Permeability to Outcome of Relative Permeability Modification. Energies, 12, 4688.
3. AL-SHAJALEE, F., ARIF, M., SARI, A., WOOD, C., AL-BAYATI, D., XIE, Q. & SAEEDI, A. 2020. Low-Salinity-Assisted Cationic Polyacrylamide Water Shutoff in Low-Permeability Sandstone Gas Reservoirs. Energy & Fuels, 34, 5524-5536.
4. AL-SHAJALEE, F., ARIF, M., MACHALE, J., VERRALL, M., ALMOBARAK, M., IGLAUER, S. & WOOD, C. 2020a. A Multiscale Investigation of Cross-Linked Polymer Gel Injection in Sandstone Gas Reservoirs: Implications for Water Shutoff Treatment. Energy & Fuels, 34, 14046-14057.
5. AL-SHAJALEE, F., SAEEDI, A. & WOOD, C. 2019a. A New Dimensionless Approach to Assess Relative Permeability Modifiers. Energy & Fuels, 33, 3448-3455.

Permissions have been obtained from the journal publishers to use the above papers in support of this thesis. The permissions can be found in Appendix B.

List of publications not included in the thesis:

1. ALSHAJALEE, F., SEYYEDI, M., VERRALL, M., WOOD, C. & SAEEDI, A. Role of Prolonged Successive Fluid Flow on the Performance of Relative Permeability Modifiers in Gas Reservoirs. 82nd EAGE Annual Conference & Exhibition, 2020. European Association of Geoscientists & Engineers, 1-5.
2. AL-SHAJALEE, F., SEYYEDI, M., VERRALL, M., ARIF, M., AL-YASERI, A. Z., TADÉ, M. O., WOOD, C., IGLAUER, S. & SAEEDI, A. Impact of prolonged

water-gas flow on the performance of polyacrylamide. Journal of Applied Polymer Science, n/a, 52037.

Table of Contents

List of Figures

List of Tables

Abbreviations/Symbols/Nomenclature

γ	Shear rate (s^{-1})
k	Absolute permeability (μm^2).
r^-	Dimensionless effective pore radius (fraction)
r_{eff}	The effective porous radius (μm)
A	Core cross-sectional surface area (m^2)
e	Average hydrodynamic polymer layer thickness (μm)
F_{rr}	Residual resistance factor
K	Absolute permeability (μm^2).
k_{rg1}	The end-point relative permeability of gas before the treatment
k_{rg1}	The end-point relative permeability of gas before the treatment
k_{rg2}	The end-point relative permeability of gas after the treatment
k_{rw1}	The end-point relative permeability of water before the treatment
k_{rw2}	The end-point relative permeability of water after the treatment
L	Core length (m)
M	Molar mass ($kg.mol^{-1}$)

P =	Pressure (Pa)
P_c	Capillary pressure
Q	Inlet flow rate ($m^3.sec^{-1)}$
Q	Flow rate ($m^3.sec^{-1)}$
r	Average pore radius (μm)
R	Perfect gas constant ($J.mol^{-1}.K^{-1}$)
Rei	Reynold's number
S_{gr}	Residual gas saturations
S_{wirr}	Irreducible water saturation
T =	Temperature (K)
w,g	water , gas
X	Forchheimer variable (Eq. 6)
Y	Forchheimer variable (Eq. 7)
β	Inertial resistance coefficient (m^{-1})
μ	Dynamic viscosity (Pa.s).
ρ	Fluid density ($kg.m^{-3}$)

σ	Interfacial tension, mN/m.
σ	Interfacial tension
Vsi	Interstitial velocity, (cm/sec)
θ	Contact angle, 0-180.
φ	Porosity.

Chapter 1: Introduction

1.1 Significance and motivation

Natural gas as a geo-energy resource presents an important viable supply for the rest of the 21st century, beacuase has a far less global carbon footprint, compared to the other fossile fuels; oil and coal (Chen et al., 2019a, Ahmed and Rezaei-Gomari, 2019, Chen et al., 2019b). However, with many hydrocarbon fields nearing their maturity, excessive water production from production wells has become a major challenge. It has been reported that in the U.S., the daily volumetric water/oil ratio is 9/1, approximately (Kalfayan and Dawson, 2004). It was reported that 24.4 billion barrels of water were produced in the USA during 2017 (Seright and Brattekas, 2021). Although globally the water/oil ratio is about 3/1, it still translates to around 250 million barrels of produced water on a daily basis worldwide (Rae & di Lullo, 2002)(Hajilary and Shahmohammadi, 2018, Hajilary et al., 2015b, Di Lullo et al., 2002, Joseph and Ajienka, 2010).

In the first instance, excessive water production means a considerable decrease in well productivity in terms of the hydrocarbon yield (Hajilary et al., 2015b, El-Karsani et al., 2014, Hajilary and Shahmohammadi, 2018). Substantial increase in the operating costs is also among the problems associated with water production (Seright and Brattekas, 2021, Al-Hulail et al., 2017, Hajilary and Shahmohammadi, 2018). Such costs relate to the lifting of water from the formation to surface, corrosion of tubulars and surface equipment, water separation and transportation, effluent disposal and handling, sand production and the required environmental protection measures (Seright and Brattekas, 2021, El-Karsani et al., 2014, Hajilary and Shahmohammadi, 2018). It has been reported that the cost of the water handling may reach up to $4 per every barrel of the water produced costing the oil and gas industry around $440B per year (Kalfayan and Dawson, 2004, Al-shajalee et al., 2019b). It is worth noting that these costs are associated with only treating the water and do not cover effects such as corrosion, loss of hydrocarbon production, etc.(Al-shajalee et al., 2019b).

Therefore, water production can greatly affect the economic feasibility of hydrocarbon wells and, even result in their abandonment (Anokwuru, 2015, Liao, 2014, Al-Hulail et al., 2017, Karimi et al., 2014b, Hajilary et al., 2015b).

The above challenges provide the motivation for this thesis and hence its significance for industrial applications in the area. Consequently, the main contributions of the thesis are as listed below:

a) Add to the limited existing data and knowledge around the application of RPMs for the gas/water system in sandstone media. Thus, improve our understanding to the RPM mechanisms.
b) Show the importnance of rock permability on planning an RPM treatment for gas producing wells.
c) Demonstrate how the relative pore size alteration due to the RPM treatment significantly impacts the RPM performance.
d) Demonstrate how rock-polymer-water intractons could significantly affect the RPM performance.
e) Demonstrate the performance of both polymer and gel treatment in sandstone-gas-water system.
f) Demonstrate how fluid flow-rate/type significantly affects RPM performance. Therefore, they should be considered during RPM design.
g) Demonstrate how the RPM lubrication effect has a great role on RPM performance.

1.2 Water control systems

In order to improve the well productivities and extend the economic life of many reservoirs, there is a pressing need to cut back on the undesirable water production. Numerous endeavours have already been made to limit water production leading to the development of a range of water control techniques. Such techniques may fall into the three categories of mechanical, chemical and biological (Xindi and Baojun, 2017, Karimi et al., 2014b, Hajilary and Shahmohammadi, 2018). Mechanical techniques, for example, may include re-

completing the well, horizontal or deviated drilling, applying wellhead isolation devise or using a central pipe in the stream of water production while the chemical techniques may involve polymer/gel treatments or squeeze cementing a water producing zone (Xindi and Baojun, 2017, Joseph and Ajienka, 2010, Hajilary and Shahmohammadi, 2018, Yi et al., 2017, Kalfayan and Dawson, 2004). High operational and maintenance costs associated with the mechanical techniques and the complex nature of the biological methods have led the researchers and field operators to pay an ever increasing attention to the more economical and operationally viable chemical techniques (Xindi and Baojun, 2017, Hajilary and Shahmohammadi, 2018, Hajilary et al., 2015b, Amir et al., 2019). These techniques often involve the application of a polymer/gel as a water shut-off or relative permeability modification (RPM) agent to control and diminish the high water-to-hydrocarbon ratio (Al-Shajalee et al., 2020d, Al-Shajalee et al., 2020a, Song et al., 2015, Yadav et al., 2020, Heidari et al., 2019, El-hoshoudy et al., 2019, Liang et al., 2018, Al-Hulail et al., 2017, Askarinezhad et al., 2016, Karimi et al., 2014b, Xindi and Baojun, 2017)

1.3 Relative permeability modifiers (RPM)

The relative permeability modifiers (RPM), which are sometimes also referred to as the disproportionate permeability reducers (DPR) or selective plugging systems, have been applied effectively in the oil and gas wells to restrain undesirable water production. Polyacrylamide (PAM) and hydrolyzed polyacrylamide (HPAM) are the most common chemical systems utilised as RPM agents (Song et al., 2015, Yi et al., 2017, Liang et al., 2017, Liang et al., 2018, Hajilary et al., 2015b, El-Karsani et al., 2014, Karimi et al., 2014b). Suitable polymers can lower the wetting phase relative permeability more than that for the non-wetting phase (oil/gas) (Al-shajalee et al., 2019b, Al-Shajalee et al., 2020d). The viability of PAM as an RPM agent has been exhibited through laboratory and field scale results (Zaltoun et al., 1991, Dovan and Hutchins, 1994, Lockhart and Burrafato, 2000, Park et al., 2015, Song et al., 2015, Liang et al., 2017, Liang et al., 2018, Al-Shajalee et al., 2019a, Al-Shajalee et al., 2020a, Heidari et al., 2019). As elaborated by some researchers, the most important advantages of PAM are the low cost, minor operational risks and low

environmental effects (Amir et al., 2019, Song et al., 2015, Yi et al., 2017, Liang et al., 2017, Liang et al., 2018, Hajilary et al., 2015b).

1.4 Gaps in knowledge

To date, a number of experimental investigations and field trials have been carried out to understand the behavior of RPMs with regards to the oil/water system (Yadav et al., 2020, Moghadasi et al., 2019, Heidari et al., 2019, El-hoshoudy et al., 2019, Salehi et al., 2019, Liang et al., 2017, Liang et al., 2018, Hajilary and Shahmohammadi, 2018, Dai et al., 2017a, Askarinezhad and Hatzignatiou, 2017, Norouzi et al., 2017, Li et al., 2017, Al-Hulail et al., 2017, Askarinezhad et al., 2016, Bhatnagar and Eoff, 2016, Aghabozorgi and Rostami, 2016, Song et al., 2018b, Park et al., 2015, Dang et al., 2014, Mishra et al., 2014). However, there is limited data regarding the gas/water systems (Song et al., 2015, Liu, 2015, Hajilary et al., 2015b, Al-shajalee et al., 2019b, Al-Shajalee et al., 2019a, Al-Shajalee et al., 2020d, Al-Shajalee et al., 2020a, Sharifpour et al., 2016), even though the effect of water production on productivity of gas wells is extreme and introduction of water could render a gas well inoperable in a short space of time (Al-shajalee et al., 2019b, Chen et al., 2019b, Elmkies et al., 2002, Tielong et al., 1996). This is becuase the effect of water phase on the mobility of the gas phase is much more pronounced compared to the liquid oil phase. In addition, water shuttoff in gas wells is not practiced commonly due to the risk of face plugging with high molecular weight polymer solutions (Pusch et al., 1995, Dovan and Hutchins, 1994, Al-shajalee et al., 2019b, Al-Shajalee et al., 2020d). Thus, there is a need for studies concentrating on gas reservoirs.

Furthermore, it has also been reported that the efficiency of a polymer/gel as an RPM agent may vary with the flow rate of produced water, oil (Mishra et al., 2014, Al-Sharji et al., 2001b, Al-Sharji et al., 1999a) and gas (Song et al., 2015). In general, the performance of an RPM agent declines as the fluid flow rate rises, posing a risk of overestimating its water-cut reduction potential. Therefore, fluid flow rate needs to be considered as a critical design criterion in an RPM treatment (Stavland, 2010, Al-Shajalee et al., 2020a). This is particularly

important for gas producing wells as high gas flow rate is expected in the wellbore vicinity (Elmkies et al., 2002). Morover, many DPR mechanisms have been proposed in literature for water shutoff treatment using RPM. However, there is still a lack of detailed understanding about some mechanisms and how these mechanisms may work together or against each other.

1.5 Study objectives

The primary objective of this work is to investigate the efficiency of the RPM treatment to favorably modify the relative permeability of water and gas phases towards reducing water production in gas wells. The study has examined the feasibility of the RPM application for gas/water fluid system using sandstone rocks with a wide range of permeability values (low, moderate and high). In addition, the research has used a wide range of fluid flow rates expected to occur during the production from gas wells. This investigation has also investigated the effect of a number of factors relating to the polymers used for RPM treatment. Finding the optimum polymer characteristics would result in the maximum reduction of water permeability with minimum effect on gas permeability for every permeability range tested. In general, this research has attempted to increase the industry's confidence in the application of the RPM as an effective water control technique.

In summary, to achieve the above overall research goals, the following specific objectives have been be pursued:

1. To investigate the effect of cationic Polyacrylamide (CPAM) treatment on sandstone samples with a wide range of permeabilities (low, moderate, and high).
2. To evaluate the effect of brine salinity-CPAM treatment on sandstone samples with low permeabilities range.
3. To study the effect of crossed-linked-anomic PAM treatment on sandstone samples with a moderate permeabilities range.
4. To determine the effect of CPAM-concertation during treatment of sandstone samples with a moderate permeabilities range.

5. To evaluate the effect of flow rate (gas and water) on the results of all the above investigations
6. To use the interpretations done around the experimental results obtained in this study to improve the current fundamental understanding of the DPR mechanisms associated with RPM treatment for a water/gas system.
7. To provide a comprehensive review of the mechanisms behind the RPMs particularly about the effect of initial rock permeability on the RPM performance.

1.6 Organization of thesis

Besides the current introductory chapter (Chapter 1), this thesis includes six more chapters, Figure 1-1.

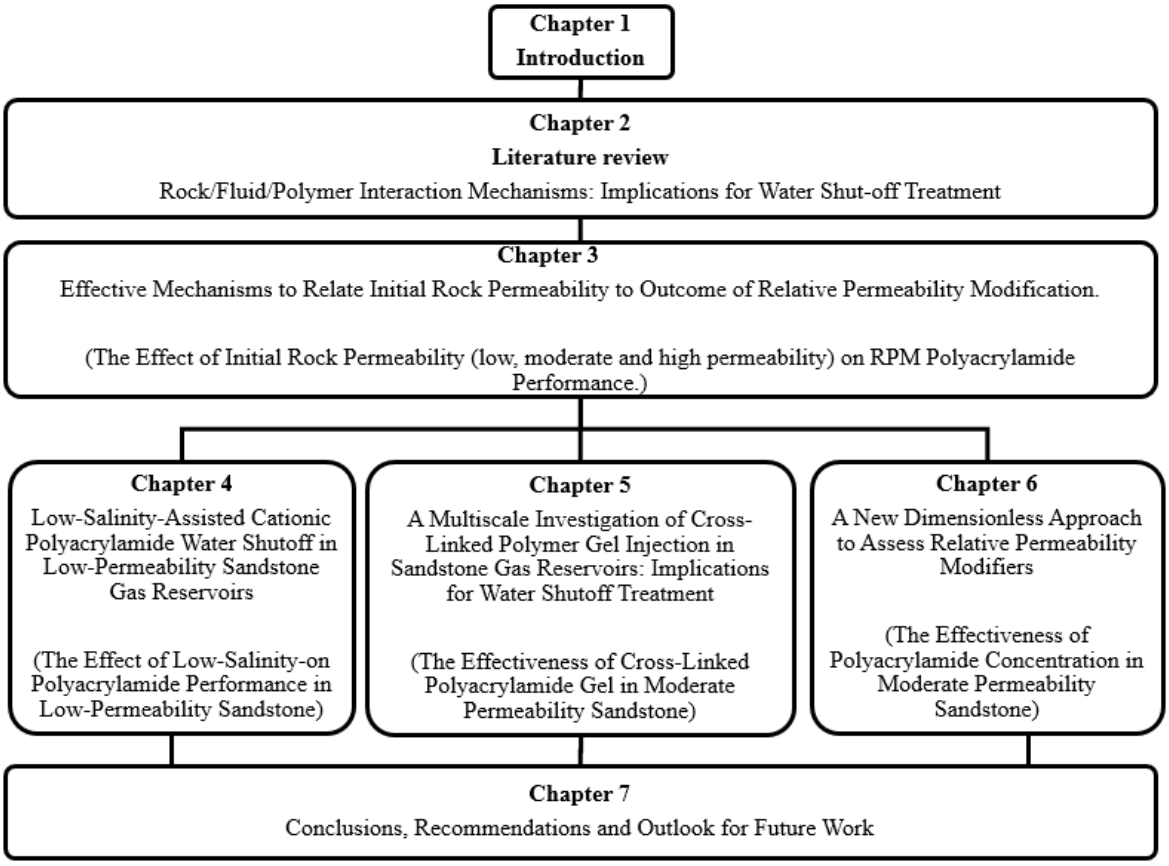

Figure 1-1: Thesis flow chart

Chapter 2 (Literature Review: Rock/Fluid/Polymer Interaction Mechanisms: Implications for Water Shut-off Treatment) provides a critical parametric evaluation of the factors

affecting the performance of polymer-based RPM solutions. This review covers systematic tools and approaches that explain the relationship among two dominant factors: the adsorption process and the mechanisms (or combination of mechanisms) responsible for selective permeability reduction.

Chapter 3 (Effective Mechanisms to Relate Initial Rock Permeability to Outcome of Relative Permeability Modification), presents the experimental results where the effect of initial rock permeability on the outcome of a cationic Polyacrylamide (CPAM) treatment for a gas/water system is examined. This investigation uses a number of sandstone rocks with different permeabilities (low, moderate and high). Using the data generated, the underlying mechanisms behind the DPR effect of the RPM agent are discussed. Moreover, the experimental work covered in this chapter also examine the feasibility of the CPAM application under a wide range of fluid (water and gas) flow rates.

Chapter 4 (Low-Salinity-Assisted Cationic Polyacrylamide Water Shutoff in Low-Permeability Sandstone Gas Reservoirs), presents the experimental results relating to the relative permeabilities to water and gas before and after CPAM treatment as a function of brine salinity in low permeability rock. The chapter reports on the outcome of core flooding experiments conducted to study the impacts of brine concentration on possible variations to the water and gas relative permeabilities due to cationic polyacrylamide treatment (CPAM) on three low permeability sandstones. The core flooding experiments were complemented by Zeta potential measurements and contact angle evaluation.

Chapter 5 (A Multiscale Investigation of Cross-Linked Polymer Gel Injection in Sandstone Gas Reservoirs: Implications for Water Shutoff Treatment), presents the results of the experimental investigation performed into the impact of cross-linked polyacrylamide (Poly (acrylamide-co-acrylic acid) partial sodium salt) gel as an RPM for a moderate permeability sandstone/gas/water system and provides insights into the detailed in-situ gel behaviour inside the porous medium as a function of gas/water flow rate. First, this chapter investigates the rheological behaviour of P(AAM-co-AA)Na -chromium gels for a broad range of shear

rates, chromium concentrations and temperatures. Then, core- and pore-scale flow experiments would be used to determine the gel performance in terms of reducing water production. To interpret the core flooding results and to visualize the flow behavior of the gel and how it may influence gas flow at the pore-scale, a set of systematic visualization experiments were conducted on a transparent 2D-micromodel using borosilicate glass and a capillary tube. This chapter therefore adds to the current understanding of the gel/water/gas interactions in porous media, and aids in the reduction of excess water production.

Chapter 6 (A New dimensionless Approach to Assess Relative Permeability Modifiers), presents the outcomes of the research conducted to evaluate the effect of CPAM and its concentration on water and gas permeability reductions in a number of sandstone rock samples with moderate permeability. In this chapter the competing and opposite effects of rock permeability and polymer concentration on water and gas permeability reductions during the experimental evaluation of CPAM treatment are evaluated. The results are interpreted and discussed initially using a common technique where Frr is used as a critical parameter in evaluating the effectives of such a treatment. Subsequently, a new dimensionless parameter referred to as the dimensionless effective pore radius (r_{eff}^{-}) is developed and used to interpret the same data. Finally, the Forchheimer equation is used to analyse the possible flow regimes that may be encountered during gas injection as the injection flow rate varies.

Finally, in Chapter 7 (Conclusions, Recommendations and Outlook for Future Work), includes a condensed summary of the research findings together with a number of recommendations for possible future investigations.

It is worth noting that chapters 2 to 6 have been each published as a peer-reviewed journal publication whose details are provided below:

Chapter 2

AL-SHAJALEE, F., ARIF, M., MYERS, M., TADÉ, M. O., WOOD, C. & SAEEDI, A. 2021. Rock/Fluid/Polymer Interaction Mechanisms: Implications for Water Shut-off Treatment. Energy & Fuels, 35, 12809-12827.

Chapter 3

AL-SHAJALEE, F., WOOD, C., XIE, Q. & SAEEDI, A. 2019. Effective Mechanisms to Relate Initial Rock Permeability to Outcome of Relative Permeability Modification. Energies, 12, 4688.

Chapter 4

AL-SHAJALEE, F., ARIF, M., SARI, A., WOOD, C., AL-BAYATI, D., XIE, Q. & SAEEDI, A. 2020b. Low-Salinity-Assisted Cationic Polyacrylamide Water Shutoff in Low-Permeability Sandstone Gas Reservoirs. Energy & Fuels, 34, 5524-5536.

Chapter 5

AL-SHAJALEE, F., ARIF, M., MACHALE, J., VERRALL, M., ALMOBARAK, M., IGLAUER, S. & WOOD, C. 2020a. A Multiscale Investigation of Cross-Linked Polymer Gel Injection in Sandstone Gas Reservoirs: Implications for Water Shutoff Treatment. Energy & Fuels, 34, 14046-14057.

Chapter 6

AL-SHAJALEE, F., SAEEDI, A. & WOOD, C. 2019a. A New Dimensionless Approach to Assess Relative Permeability Modifiers. Energy & Fuels, 33, 3448-3455.

Chapter 2: Rock/Fluid/Polymer Interaction Mechanisms: Implications for Water Shut-off Treatment: Literature review

2.1 Introduction

Excessive water production is a major challenge in the oil and gas industry as water production can subsequently cause a significant reduction in hydrocarbon productivity(Hajilary and Shahmohammadi, 2018, Chen et al., 2019b, Yi et al., 2017, Karimi et al., 2014b) and increase the operational costs related to surface water treatment and handling(Kalfayan and Dawson, 2004, Pusch et al., 1995, Evans, 2001, Inikori, 2002, Mohanty, 2003, Karimi et al., 2014a, Hajilary et al., 2015a, Hajilary and Shahmohammadi, 2018, Yi et al., 2017, Karimi et al., 2014b). Three different types of methods (i.e. chemical, mechanical and biological) can be applied to regulate or decrease water production (Karimi et al., 2014b, Hajilary and Shahmohammadi, 2018, Yi et al., 2017, Xindi and Baojun, 2017, Zaltoun et al., 1991). This review will focus on chemical treatments which have been extensively utilized to reduce water production. One class of chemical materials that have received widespread attention(Song et al., 2015, Qi et al., 2013, Qin et al., 2021, Qin et al., 2020), due to their potential performance, low costs, and ease of implementation(Amir et al., 2019, Karimi et al., 2014b), are relative permeability modifiers (RPM) that can selectively reduce the permeability to water while ideally having minimal effect on oil/gas permeability.

The ability of polymers to induce a reduction in relative permeability of water (and thus assist towards improving the hydrocarbon flow) in porous media was documented as early as 1964. The main objective was to improve the water flooding performance by using hydrolyzed polyacrylamide to lower water-oil mobility ratio and to achieve better sweep efficiency and efficient displacement in the swept zone (i.e. from injection well to production well(s), EOR)(Sandiford, 1964). Furthermore, Sandiford (1964) realized a significant decline in the relative permeability to water after polymer flooding. Subsequently, in 1971, Jennings et al., (1971) introduced the term “residual resistance factor” to indicate water mobility reduction ratio due to polymer flooding (Jennings et al., 1971). However, to the better of our research,

White and co-authors were the first one to introduce the use of polymers as RPM agents for water shut-off treatment in 1973 (White et al., 1973).

Several mechanisms are reported in the literature to explain the behaviour of relative permeability modifiers (RPM) which exhibit disproportionate permeability reduction. However, as there are many RPM approaches or technologies, there is no single mechanism that can be claimed to explain their behaviour. Furthermore, in many instances, the mechanism is either intensely debated or it may be the case that multiple mechanisms eventuate simultaneously or to varying extents depending on the conditions. There are scores of publications which investigate, discuss or propose different mechanisms to explain disproportionate permeability reduction (DPR) behaviour for an RPM implementation. These mechanisms include: RPM adsorption onto the rock surface, fluid segregation pathways, steric effect, lubrication effect, wettability effect, and swelling/shrinking(Al-shajalee et al., 2019b, Al-Shajalee et al., 2020c, Scott et al., 2020, Browne et al., 2020, Imqam, 2015, Mishra et al., 2014, Liang et al., 2018, Liang et al., 2017)**.**

The current review provides a critical parametric evaluation of the factors affecting the performance of polymer-based RPM solutions. To this end, this review provides flow charts that explain the relationship among two dominant factors: the adsorption process and the mechanisms (or combination of mechanisms) responsible for selective permeability reduction (SPR).

2.2 Polymer adsorption

The adsorption of polymers in porous media is considered necessary for DPR as it immobilizes the polymer within the rock matrix thus allowing subsequent DPR mechanisms to manifest.(Al-Shajalee et al., 2019a, Vasquez and Eoff, 2013a, Qi et al., 2013, Chiappa et al., 1997, Elmkies et al., 2002, Ranjbar and Schaffie, 2000, Dovan and Hutchins, 1994, Pusch et al., 1995, Tielong et al., 1996, Zaitoun and Pichery, 2001, Grattoni et al., 2004) Furthermore, it is well-established that the fluid (water and oil/gas)-rock interactions

(attraction/repulsion) govern rock wettability(Awolayo et al., 2019), and this, controls fluid distributions, capillary pressure, relative permeabilities, fluid transportation, and oil/gas recovery(Arjomand et al., 2020, Sidiq, 2007, Katika et al., 2016, Al-Muthana et al., 2012). Consequently, the adsorption of polymer in porous media is also a strong function of rock wettability. More specifically, during injection, a DPR fluid that wets the porous medium will be *segregated* mainly in the preferred pathways for wetting fluid(Stavland and Nilsson, 2001), thus promoting its adsorption onto the rock surface. Subsequently, the wetting phase relative permeability will be more affected by the RPM treatment. Overall, this mechanism is generally referred to in the literature as *fluid segregation pathways* (see Figure 2-1)(Liang et al., 2018, Liang et al., 2017, Liang and Seright, 1997, Liang et al., 1995), and the *initial fluid segregation pathways* (i.e. oil/gas and water) may segregate differently following polymer adsorption.

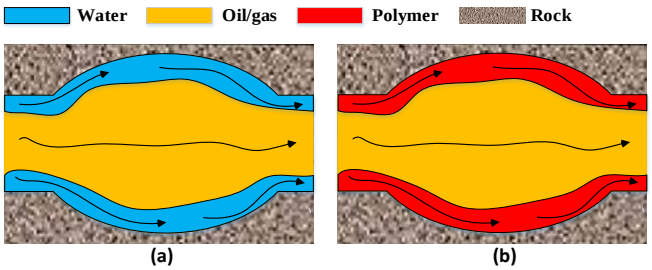

Figure 2-1: Initial fluid segregation during polymer placement. (a) In water-wet pores, water flows close to the pore wall while oil/gas flows in the center of the pore channel. (b) Water-based RPM flow in the same path water flows.

Polymers (as RPMs) should be nominated based on their ability to show strong attractive interactions with the rock surface to maximize adsorption, stability and irreversibility. Rock-polymer interactions are: 1) van Der Waals interactions (dispersion), which are usually attractive and are governed by polymer structure/molecular weight, and 2) electrostatic interactions (which can be attractive or repulsive) exist at the interfaces of rock/brine and brine/polymer (Hamouna et al., 2021, Kawelah et al., 2020, Shi et al., 2020, Shoaib et al., 2020, Broseta and Medjahed, 1995). The total interaction, i.e. the sum of van der Waals and

electrostatic interactions (DLVO), is defined by the prevailing physicochemical conditions (Canseco et al., 2009). In general, electrostatic interactions has a vital role in the adsorption process, because they can be either attractive or repulsive forces (Sidiq, 2007). Both interactions (i.e. van Der Waals and electrostatic interactions) also govern the interactions between polymer monomers (or in general fluid-fluid) i.e. they govern the solvent quality and whether the polymer chain swells or shrinks (Schmidt et al., 2019, Kawelah et al., 2020, Hamouna et al., 2021, Broseta and Medjahed, 1995). Solvent quality is also a function to brine ionic charge and strength (Bera et al., 2013, Kawelah et al., 2020, Sun et al., 2021, Omari et al., 2006). A low electrolyte (or brine) concentration enhances the repulsive charges between the charges monomers and therefore anionic polymer swells and also reduces the anionic polymer/positively charged rock adsorption (Shi et al., 2020). On the other hand, if the electrolyte concentration increases (i.e. solvent quality is poorer), anionic polymers shrink/contract and increase the polymer-rock adsorption (Shi et al., 2020) .

Furthermore, during polymer placement in porous medium, several chemical/physical factors will affect the electrostatic interactions process between the absorbed polymer and rock surface (Figure 2-2). These factors are responsible for controlling the polymer adsorption and the polymer efficiency after the placement in porous media.

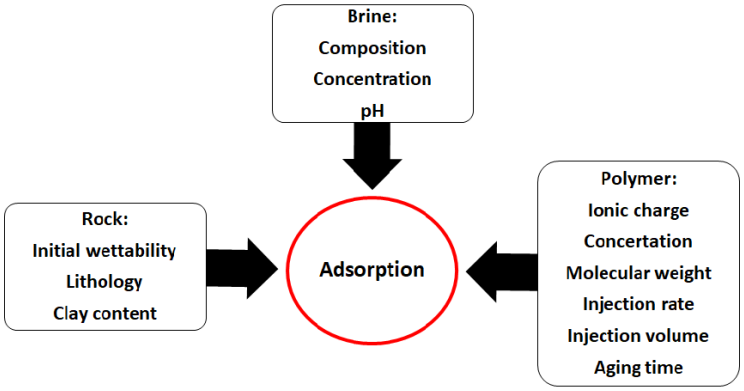

Figure 2-2: Flow chart of the factors affecting RPM adsorption

The injection of polymers into subsurface reservoirs for enhanced oil/gas recovery (EOR) has attracted substantial interest in the petroleum industry. Polymers increase the viscosity of the injected water and thereby control fluid mobility and enhance the displacement and the volumetric sweep efficiency. However, significant polymer adsorption on the rock surface can reduce the efficiency of the polymer flooding due to reducing polymer viscosity because of polymer loss, limiting the propagation through the reservoir and consequently the hydrocarbon relative permeability may reduce (Kawelah et al., 2020, Shi et al., 2020, Tamsilian et al., 2020, Al-Hashmi and Luckham, 2010, Dang et al., 2014, Satken et al., 2021). On the contrary, in water shutoff or relative permeability modification (RPM) applications, the purpose is to have enough adsorption. Therefore, these two oil/gas field applications (i.e., the EOR and water shut-off) require different adsorption characteristics. If the rock carries negative charges, non-adsorbing polymers (i.e. nonionic and anionic polyacrylamides) are frequently used for EOR (Kawelah et al., 2020), while strongly adsorbing polymers (i.e. cationic polyacrylamide) are used for water shut-off applications (Al-shajalee et al., 2019b). One more difference between EOR and RPM application that the EOR is applied in a reservoir scale where injector(s) and producer(s) wells are required, whereas RPM is applied at well scale where and the RPM agent is injected in the vicinity of the wellbore of one producer well, see *Figure 2-3*.

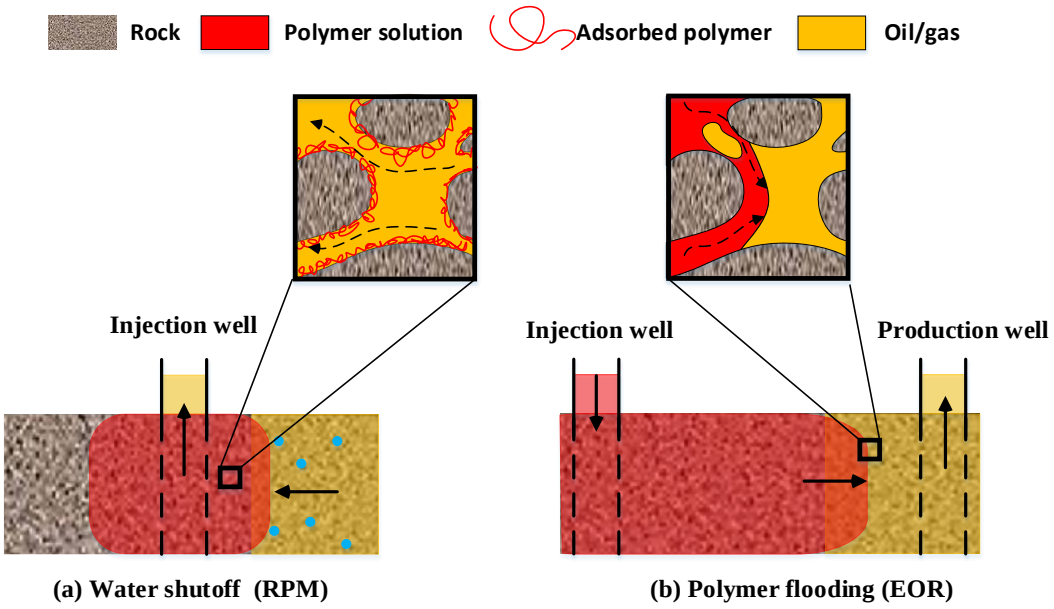

Figure 2-3: A comparison between (a) RPM and (b) EOR

Therefore, to keep up with the context of interest (i.e. RPM implication), most of the results presented here are from water-shutoff/RPM publications. However, a considerable body of literature has been devoted to polymer applications for EOR. Thus, where possible, the implications of polymers for EOR have been used here to supplement the interpretation for RPM applications.

2.2.1 Rock-polymer interactions

For most polymers used as relative permeability modifiers, the polymer is immobilized on the rock surface in an adsorption process dominated by rock/brine/polymer interactions. This in turn depends on the polymer ionic charge and rock surface charge(Chiappa et al., 1997, Burrafato et al., 1999, Lockhart and Burrafato, 2000, Chiappa et al., 1998, Qi et al., 2013, Zaltoun et al., 1991, Al-Hajri et al., 2018, Chiappa et al., 1999, Aghabozorgi and Rostami, 2016, Ahsani et al., 2020, Vasquez and Eoff, 2013b, Al-Hulail et al., 2017, Al-Hashmi et al., 2013, Stavland and Nilsson, 2001, Al-Shajalee et al., 2020c).

To examine this aspect, Al-Hashmi et al., (2013) performed colloidal force measurements and concluded that the instantaneous adsorption of polymer cationic groups onto the negatively charged rock surface is due to polymer-rock attraction(Al-Hashmi et al., 2013).

Polymers can be divided into two categories based on their affinity for sorption onto sandstone rocks: high affinity (generally cationic and some non-ionic) and low-affinity polymers (generally anionic and some non-ionic) (Burrafato et al., 1999). These observations are consistent with(Chiappa et al., 1997, Chiappa et al., 1999, Qi et al., 2013, Al-Hashmi et al., 2013). This is confirmed by Chiappa et al., (1997) who used cationic, non-ionic, and anionic polyacrylamide derivatives on a Clashach sandstone core (which is composed mainly of quartz and silicates with less than 2% clays) in a 2% KCl brine. They showed equilibrium adsorption masses of 1.85, 0.9 and ≈ 0 mg/g for cationic, non-ionic and anionic polymers, respectively. This behaviour is attributed to the strong attraction between the cationic polymer and the negatively charged sandstone rock. To investigate the effect of calcite on polymer adsorption, Chiappa et al., (1997) used sand packs containing reservoir sands (consisting mainly of silicates and alumina-silicate with approximately 20 % calcite) and observed adsorption masses for cationic, non-ionic, and anionic polymers were 2.8, 1.6, and < 0.2 mg/g, respectively. Interestingly, despite the presence of positively charged calcites (20%) in their sand pack sample at pH < 10, anionic polymers still demonstrated negligible adsorption. Apparently, the high pH value shifted the calcite charge towards a negative value or at least to a less positive value. Similarly Qi et al. (2013) showed that the approximate adsorption of cationic and anionic polymer on quartz sands were 1.1 and 0.3mg/g, respectively, while the adsorption of cationic polymer on reservoir sands was 0.5 mg/g. The adsorption of cationic polymers onto quartz sands (which are water-wet and negatively charged) is significantly greater than that onto reservoir sands (which are oil-wet sands and mainly positively charged). Again, unexpectedly the adsorption of cationic polymers onto oil-wet sands is also greater than the adsorption of anionic polymer on water-wet sands(Qi et al., 2013). Qi et al. (2013) explained that even though the reservoir sands is oil-wet as a whole, there are still water-wet regions on the sand surface and cationic polymer can adsorb on these water-wet regions. It has also been shown that clay content can impact the adsorption process, especially for cationic polymers because of the negative charge and high specific

surface area of clays(Sidiq, 2007, Tekin et al., 2010, Chiappa et al., 1999, Tekin et al., 2005, Grattoni et al., 2004, Ferreira and Moreno, 2019).

In summary, these results confirm the importance of wettability and associated electrostatic attraction on polymer adsorption (polymer affinity). RPMs should be nominated based on their ability to exhibit strong attraction with the rock surface to maximize the adsorption and polymer layer stability. However, polymer-rock attraction is arguably not the only factor that controls the adsorption process, there are indeed other influencing factors too. These factors, especially brine-polymer interaction, will be discussed in the next sections.

2.2.2 Polymer-brine interactions

The success of a polymer treatment often also depends on reservoir brine composition(Pusch et al., 1995, Ranjbar et al., 1995, Zaitoun and Pichery, 2001, Nieves et al., 2002, Sydansk, 1993, Karimi et al., 2014b, Qi et al., 2013, Zaltoun et al., 1991, Mishra et al., 2014, Al-Hashmi and Luckham, 2010, Kalfayan and Dawson, 2004, Al-Shajalee et al., 2020c). Brine composition (in particular, ionic charge and ionic strength) can affect the polymer-rock interaction and the associated adsorbed polymer thickness(Chiappa et al., 1999, Sidiq, 2007, Park et al., 2015, Dang et al., 2014, Ali and Mahmud, 2015, Al-Shajalee et al., 2020c, Tekin et al., 2010, Mishra et al., 2014).

Chiappa et al. (1999) showed that increasing the concentration of K^+ (i.e. 0 to 13% of KCl) or Ca^{2+} (i.e. 0 to 8 wt.% $CaCl_2$) slightly decreases the adsorption of cationic polymer onto the otherwise negatively charged pure quartzite. Moreover, Tekin et al. (2010) showed that the adsorption of cationic polyacrylamide onto negatively charged expanded perlite (EP) significantly decreases with increasing Na^+ concentration (i.e. increasing NaCl). This trend has been attributed to positively charged ions inducing electrostatic screening between the rock surface and the polymer molecules(Tekin et al., 2010, Chiappa et al., 1999). Based on core flooding, contact angle, and zeta potential measurements, Al-Shajalee et al. (2020) found that increasing K^+ with a cationic polymer solution causes the zeta potential of the rock-polymer system to decrease (i.e. more negative or less positive) leading to a reduction in

electrostatic attraction. However, if the zeta potential of the polymer-brine-polymer becomes negative, the repulsion between positively charged polymer-polymer molecules increases eventually leading to an increased polymer layer thickness; this mechanism has also been confirmed elsewhere(Grattoni et al., 2004, Al-Hashmi and Luckham, 2010, Tekin et al., 2010, Dang et al., 2014).

In summary, increasing salt cation concentration in a cationic polymer solution can bring about two effects: (1) a decrease in the electrostatic attraction between negatively charged rocks and positively charged polymers and, (2) an increase in the polymer layer thickness (swells) due to increasing the repulsion force between the positively charged polymer-polymer molecules. However, in other instances, different results were observed. For example, Tekin et al., (2005) showed that the adsorption of cationic polymer onto a negatively charged kaolinite (a clay mineral, $Al_2Si_2O_4$) increases with increasing NaCl concentration(Tekin et al., 2005).

In contrast, the cations in brine tend to improve polymer adsorption in situations where polymer and solid surfaces are like-charged i.e. when electrostatic interactions do not govern the adsorption process (Chiappa et al., 1999, Mishra et al., 2014, Deng et al., 2006, Vermöhlen et al., 2000, Bragança et al., 2007, Ait-Akbour et al., 2015, Dos Santos et al., 2016, Wang et al., 2010, Shoaib et al., 2020). For example, increasing the concentration of Ca^{2+} (from 0 to 8 wt.%) causes a significant increase in adsorption for anionic polymers onto the negatively charged quartz surface(Chiappa et al., 1999). Similarly, Mishra et al. (2014) show that the adsorption of anionic polymer onto negatively charged sand particles (silica-dominant) increases with increasing NaCl concentration (1- 4 wt%) due to increasing the monovalent cation (Na^+)(Mishra et al., 2014). It has been explained that the presence of brine cationic ions in anionic polymer solution generally increases the polymer adsorption on negatively charged rocks. This is a result of two opposing effects: a)cationic ions reduce the electrostatic repulsion between the negatively charged polymer and rock, and b) cationic ions help reduce intermolecular repulsion between the molecules in the anionic polymer solution.

Consequently, the hydrodynamic radius of the polymer molecule also reduces (i.e. shrinks or compresses) (Mishra et al., 2014, Zaltoun et al., 1991, Ferreira and Moreno, 2019). This observation was also referred to as the electrical double layer compression triggered by high cationic concentration of salt, which leads to improved polymer adsorption and inhibit electrostatic repulsion among the polymer monomers (Sun et al., 2021). This hypothesis was confirmed via zeta potential measurements which displayed a less negative surface charge on the solid particles in high cationic brines compared to that of low concentration (Sun et al., 2021).

In summary, according to the literature, increasing salt concentration (specifically, Na^+ or Ca^{2+}) in anionic polymer solutions increases the electrostatic attraction between negatively charged rock surfaces and polymer. However, contradictory behaviour is also reported. For example,(Chiappa et al., 1999) showed that the adsorption of anionic polymer onto quartz surfaces was marginally affected by increasing the concentration of monovalent cation (K^+) (0-13 wt% KCl brine). This suggests that not only the brine ionic charge plays a role in rock-polymer attraction but also other factors such as brine composition may have their effect.

It was presumed that anionic polymers bound more strongly to anionic surfaces in solutions having divalent cations (Mg^{2+} and Ca^{2+}) than those solutions having monovalent cations (Na^+ and K^+)(Deng et al., 2006, Sun et al., 2021, Bragança et al., 2007). It has been observed that divalent cation bridging, depending on the charge density, plays a vital role in physicochemical interactions between two negatively charged species (fluid-fluid and rock-fluid) (Jha et al., 2019a, Jha et al., 2019b, Kobayashi et al., 2017, Griffin et al., 2016). In other words, divalent cations serve as bridges between the negatively charged polymers and the particle surfaces, destroying the electrostatic repulsion between them, in addition to reducing the electrostatic repulsion between the polymer molecules via coordination process (Chiappa et al., 1999, Ait-Akbour et al., 2015, Deng et al., 2006, Sun et al., 2021) , see Figure 2-4. However, an opposite result was also reported in the literature, where anionic polymers/anionic surface adsorption is higher in presence of Na^+ than in Mg^{2+}/Ca^{2+}(Ait-

Akbour et al., 2015). In addition, using the neutron reflection method, Allen et al. (2017) demonstrated that the monovalent cations, depending on their charge density and hydration energy, can also serve as a bridge between the negatively charged substrate and negatively charged fluid (Allen et al., 2017, Salis et al., 2010). However, the hydration effect and the bridging efficiency of monovalent cations are not fully understood and still need more investigation.

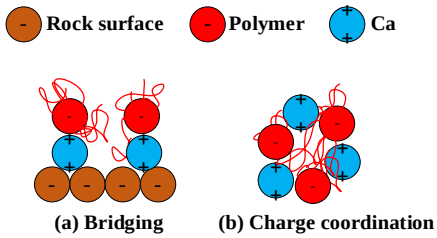

Figure 2-4: Presence of the divalent positive cation (Ca^{2+}) in brine enhances the adsorption of negatively charged polymer molecules on the negatively charged quartzite due to (a) Bridging mechanisms: Ca^{2+} link polymer – and quartzite – or (b) Charge coordination mechanism: Ca^{2+} reduces the electrostatic repulsion between the negatively charged polymer molecules

Moreover, several other aspects related to brine salinity that contribute to a better understanding of RPM implications for EOR are also investigated. For instance, it has been reported that if brine salinity is reduced below a critical, double layer expansion (DLE) causes clay particles to detach which consequently promotes fines migration (Jha et al., 2020, Morrow and Buckley, 2011, Jackson et al., 2016, Lever and Dawe, 1984, Tang and Morrow, 1999) (Pingo-Almada et al., 2013). However, relating fines migration to the low salinity effect is also controversial (Nasralla and Nasr-El-Din, 2014a, Alagic and Skauge, 2010, Alotaibi et al., 2010, Cissokho et al., 2010, Lager et al., 2008a, Lager et al., 2008b, Pingo-Almada et al., 2013). Nevertheless, the literature suggests that fines migration could be effectively suppressed using nanoparticles (Jha et al., 2020). On the contrary, very high salinity may even shift the zeta potential of sandstone surface from negative to a constant lower value or even positive value due to the thickness of the electrical double layer reaching the sub-atomic range (or counter-ion size) as a result of diffuse layer collapsing (Jaafar et

al., 2009, Yang et al., 2004). However, further increase in brine concentration cannot further reduce the double layer thickness because of the finite size of the ions (Jackson et al., 2016). Predicting the critical salinity values (that promote low salinity effect, fines migration, and constant zeta potential) for a given chemical-oil/gas-brine-rock system is thus an area of active research (Jackson et al., 2016, Alotaibi et al., 2010, Cissokho et al., 2010, Nasralla and Nasr-El-Din, 2014a, RezaeiDoust et al., 2010, Skrettingland et al., 2011, Pingo-Almada et al., 2013). Importantly, selecting polymers with the suitable ionic charge for a reservoir candidate with certain brine salinity can play a critical role in the adsorption process. Furthermore, the brine salinity can also induce significant changes in the thickness of the adsorbed polymer. However, as the second mechanism can affect the DPR outcomes after polymer adsorption, this mechanism will be discussed with more detail on the swelling/shrinkage mechanism due to the brine salinity effect. Nevertheless, more studies are needed to further understand these mechanisms for different candidate wells (i.e. rock type and brine composition, and ionic charge).

2.2.3 The effect of pH

Solution pH can significantly affect polymer adsorption(Tekin et al., 2005, Tekin et al., 2010, Mishra et al., 2014, Dang et al., 2014). The isoelectric point (IEP) is the pH at which a molecule/ surface carries no net electrical charge. Thus, a surface below IEP will have positive charges and above IEP will have negative charges (Kamal et al., 2015, Jaafar et al., 2014, Ferreira and Moreno, 2019). For sandstones, the IEP is around 2.4 while it is around 9.5 for carbonates (Ferreira and Moreno, 2019, Jaafar et al., 2014, Qi et al., 2013, Mishra et al., 2014, Bera et al., 2013, Yefei and Kai, 2006), see Figure 2-5.

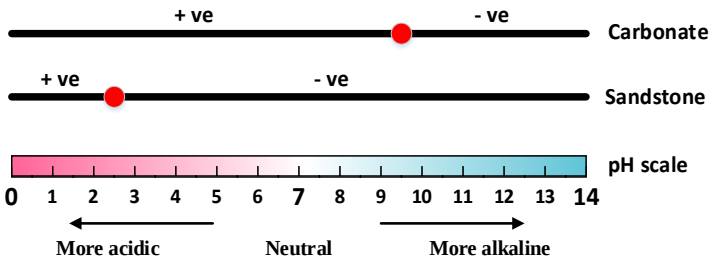

Figure 2-5: pH natural scale with isoelectric points for Sandstone and Carbonate rocks

Tekin et al., (2010) reported that the adsorption of cationic polyacrylamide onto negatively charged expanded perlite (EP) increased with increasing pH. This is consistent with decreasing measured zeta potential measurements (toward more negative) for both treated and non-treated EP with increasing pH value from 2 to 10. The non-treated EP particles demonstrated negative electrophoretic mobility values at all ranges of pH values, while EP-polymer had zero charge at pH value around 8.7(Tekin et al., 2010), implying pH-dependent polymer behaviour. Similar results were attained for negatively charged kaolinite particles with cationic polyacrylamide(Tekin et al., 2005). On the other hand, Mishra et al., (2014) show that the adsorption of anionic partially hydrolysed polyacrylamide on negatively charged sand increases with decreasing pH. This is because the sand surface is more positive when the pH of the aqueous solution is lowered (from 9 to 3) leading to a decrease in the electrostatic repulsion between sand surface and the polymer (Mishra et al., 2014). However, at high pH, the adsorption is lower due to the repulsion force between the anionic polymers with the negatively charged carboxylic acid group and the negatively charged sand surface. Similar results were reported elsewhere (Dang et al., 2014). In addition to the dependency of rock surface charges on pH, Dang et al., (2014) also explained that increasing the pH value results in increasing the molecular sizes of anionic polymers, which eventually leads to a decrease in adsorption (Dang et al., 2014), and vice versa if pH is decreased.

Moreover, Chiappa et al. (1999) reported adsorption of anionic and cationic polymers onto: a) negatively charged quartz surfaces at low pH (pH >2), and b) sand particles having significant amount of positively charged calcite (20%) at high pH (pH < 9.5). In both cases,

the adsorption of cationic polymer was higher than anionic polymer, probably due to the presence of high amount of positively charged particles in both cases. However, even though the second sample (i.e., the sample with pH < 9.5) had a significant amount of positively charged calcite, the anionic polymer adsorption on the second sample was almost negligible (0.2 mg/m^2) compared to that on the first sample (6.5 mg/m^2). This is consistent with our earlier explanation (refer to section 2.2.1) that the high pH value may shift the positive calcite charge towards a negative value or at least to a less positive value (Chiappa et al., 1999).

To summarise, sandstone rocks exhibit high adsorption efficiency at high pH for cationic polymers, whereas the opposite trend was found for anionic polymer. In other words, depending on the acid-base characteristics of the polymer, adsorption onto rock surfaces can be improved by adjusting the solution pH. The pH value in aqueous solution can affect rock surface charges and how the polymer/rock electrostatic interactions (attraction/repulsion) play a significant role in the adsorption process.

2.2.4 The effect of polymer concentrations

Generally, the current literature widely agrees that increasing the concentration of injected polymer leads to increased adsorption and this is fairly common with other sorption processes(Chiappa et al., 1999, Chiappa et al., 1997, Grattoni et al., 2001d, Mennella et al., 1998, Ogunberu and Asghari, 2004a, Mishra et al., 2014, Zheng et al., 1998, Qi et al., 2013, Al-Shajalee et al., 2019a, Sidiq, 2007, Tekin et al., 2005, Park et al., 2015). Similarly, with increasing polymer concentration, the layer thickness increases on the internal pore walls of a porous medium and may eventually severely impact the permeability to flowing fluids. Mishra et al. (2014) explained that increasing polymer concentration can lead to an increase in the interaction between the polymer molecules which may cause further adsorption(Mishra et al., 2014, Tekin et al., 2005). Moreover, Tekin et al., (2005) experimentally measured the relationship between adsorption amount of a positively charged polymer onto a negatively charged kaolinite surface and zeta potential values; higher sorption or increasing polymer

concentration led to the zeta potential becoming larger (i.e. a shift from negative values to positive values and then to larger positive values)(Tekin et al., 2005).

2.2.5 The effect of polymer molecular weight

Generally, polymer adsorption increases with polymer molecular weight (Mw) and this is consistent with thermodynamic principles showing that larger molecules will have a stronger interaction (whether attractive or repulsive) with a surface(Chiappa et al., 1997, Chiappa et al., 1998, Chiappa et al., 1999, Lockhart and Burrafato, 2000, Nieves et al., 2002, Li et al., 2017, Grattoni et al., 2004). For RPM applications, it is suggested that lower molecular weight polymers are utilized to zminimize the injectivity or plugging issues(Lockhart and Burrafato, 2000). Furthermore, using polyacrylamide polymers with molecular weight ranging from 15 to 20 milion g/moland and prepared in the same brine, the cationic polymer demonstrated a thickness in the range tens nanometers while an anionic polymer gave a thickness of hundreds nanometers, i.e. 3-4 times greater than the cationic polymer (Grattoni et al., 2004).. One explanation for this difference is that the cationic polymer is more tightly bound to the surface due to stronger electrostatic interaction.

2.2.6 The effect polymer aging time (static adsorption)

After RPM injection into a porous media, the RPM can be left statically for a certain time (or an aging period) to ensure equilibrium (i.e. plateau) adsorption onto the pore surface (or until there is no further sorption)(Chiappa et al., 1997, Chiappa et al., 1999, Mishra et al., 2014, Tekin et al., 2010, Tekin et al., 2005, Li et al., 2017). Table 2-1 includes a summary of the studies which reported different plateau times. Moreover, Mishra et al. (2014) explain that as aging time increases, the adsorption sites on the sand surface decrease due to saturation. Therefore, when all the sites are covered with polymer, no further adsorption takes place(Mishra et al., 2014). Furthermore, during the static adsorption process, some polymer molecules possibly will be unlocked owing to the fragile associations with solid surface and/or the adsorbed polymers(Li et al., 2017).

Table 2-1: Studies on equilibrium aging time

Reference	Plateau time, hrs	Polymer type	Rock / solid type
(Li et al., 2017)	20	KYPAM polymer (acrylamide-based copolymer)	sand
(Mishra et al., 2014)	7	partially hydrolyzed polyacrylamide (PHPAM)	sand
(Tekin et al., 2010)	13	cationic polyacrylamide	expanded perlite (EP)
(Chiappa et al., 1997)	18	cationic, non-ionic and anionic polyacrylamide	sand
(Chiappa et al., 1999)	18-24	cationic and anionic polyacrylamide	quartzite and reservoir sand

2.2.7 The effect of polymer injection volume (dynamic adsorption)

The literature data differentiates between static adsorption (i.e. static aging of rock with polymer) and dynamic adsorption (i.e. polymer injection). *Table 2-2* presents a summary of studies that investigated the effect of polymer injection volume on dynamic adsorption behaviour. In a micro-capillary model, with a cationic polyacrylamide, dynamic adsorption was approximately 15 times greater than that achieved with static adsorption(Al-Hashmi et al., 2013). Li et al., (2017) showed that with polymer injection, the differential pressure increases due to polymer adsorption until it stabilized when adsorption saturation is achieved(Li et al., 2017, El-hoshoudy et al., 2019, Mishra et al., 2014, Cozic et al., 2009, Denys et al., 2001).

Al-Sharji et al. (2001 a) and Grattoni et al. (2004) propose that the layer formation during dynamic polymer adsorption begins with a dense layer on the surface followed by a dilute layer further from the surface (see Figure 2-6)(Grattoni et al., 2004, Ranjbar et al., 1995, Cohen and Christ, 1986, Al-Sharji et al., 2001a, Al-Hashmi et al., 2013, Vasquez and Eoff, 2013b). Initially, a polymer layer of few hundred nanometers in thickness forms where some of its loops-tails are closed to the rock surface and sticking out into the solution. In the second step, polymer-polymer entanglement of the loops-tails from the fresh flowing polymer onto the adsorbed polymer. It is called the dilute layer(Grattoni et al., 2004, Al-Sharji et al., 2001a). Furthermore, Ranjbar et al., (1991) and Cohen and Christ, (1986) claim that multi-layer entanglement increases as more fresh polymer solution flows through the porous media(Ranjbar et al., 1991, Cohen and Christ, 1986).

Table 2-2: Studies on the effect of polymer injection volume on dynamic adsorption at a constant flow rate. As polymer injection volume increases pressure drop increases (at constant injection rate) or injection flow rate decreases (at constant pressure).

Reference	PV injected or injection time (min)	Pressure drop (kPa), flow rate (cm^3/s) or mobility reduction Rm
(Li et al., 2017)	0.1-2 (critical) -3 PV	190-750 (critical) -750 kPa
(Mishra et al., 2014)	0.1-0.6 (critical) -1 PV	0.25-0.2(critical) -0.2 cm^3/s
(Al-Sharji et al., 2001a)	0.0-160 (critical) -275 min	4.1-9.7 (critical) -9.7 kPa
(Denys et al., 2001)	0.0-3.5(critical) -20 PV	1-3.2(critical) -3.5 Rm

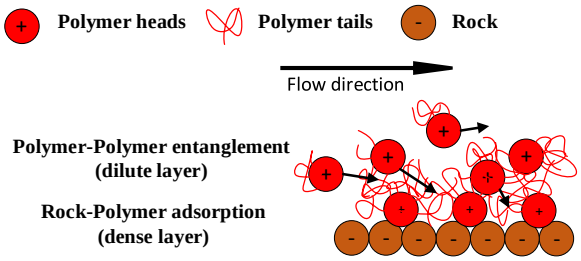

Figure 2-6: polymer PV dependent adsorption

2.2.8 The effect of polymer injection rate (dynamic adsorption)

As the RPM injection rate increases, the adsorption amount and the adsorption hydrodynamic thickness gradually increase, consequently causing more permeability reduction(Bhatnagar and Eoff, 2016, Qi et al., 2013, Al-Sharji et al., 2001a). It has been reported that extensional flows can stretch and orientate the chains/macromolecule of flexible polymers (such as polyacrylamide and poly(ethylene oxide)). This is also called shear-induced elongation (Hoagland and Prud'homme, 1989, Babcock et al., 2003, Browne et al., 2020, Moan and Omari, 1992, Skauge et al., 2018, Denys et al., 2001, Gao et al., 2021). Polymer molecules can be imagined as entangled coils. Above a critical shear rate, flexible polymers can experience a coil-stretch transition or elongation (Schroeder et al., 2003, Chauveteau and Moan, 1981, Chauveteau et al., 1984, Moan and Omari, 1992, Skauge et al., 2018, Schmidt et al., 2019, Denys et al., 2001, Le Maout et al., 2021, Sun et al., 2021, Al Hashmi et al., 2013, Al-Hashmi et al., 2014, Georgelos and Torkelson, 1988, Al-Shakry et al., 2018). As polymer chains elongate, they can irreversibly and strongly adsorb onto pore walls due to higher contact area (*Figure 2-7*a and b) and can bridge pore throats depending on macromolecule stretching to pore throat size ratio (*Figure 2-7*c). This eventually can have significant consequences for pore-scale and macroscopic transport (Browne et al., 2020, De Gennes, 1976, Rubinstein and Colby, 2003, Denys et al., 2001). The formed adsorbed polymer layers can restrict pore size and create additional mobility-reduction/flow-resistance (Browne et al., 2020).

Elongation ability depends on many factors such as polymer molecular structure/type, solvent (brine) salinity, and flowing flow rate (Browne et al., 2020, Moan and Omari, 1992, Sugar et al., 2020). Decreasing solvent quality with increasing salinity (in HPAM, for example) generally reduces coil gyration and hydrodynamic radius due to compressing the electrical double layer on molecular chains and reducing electrostatic repulsion (as discussed in section 2.2.2). Therefore higher flow rates are necessary to such uncoil polymers thus making the apparent coil-stretch transition or elongation/thickening begin at higher flow rates (Skauge et al., 2018, Briscoe et al., 1999, Dupuis et al., 1994, Ait-Kadi et al., 1987, Maia et al., 2005, Maia et al., 2011). Moreover, the polymer bridging/plugging effect increases not only with increasing flow rate but also with decreasing polymer concentration as coil stretching becomes more difficult under overlapping conditions (i.e. high concentration) and decreasing pore size. The bridging effect resulting from polymer elongation also increases due to the presence of residual oil saturation that reduces the pore cross-section (in front of water-wet pore throats due to capillary forces) and increases shear rate(Denys et al., 2001, Moan and Omari, 1992).

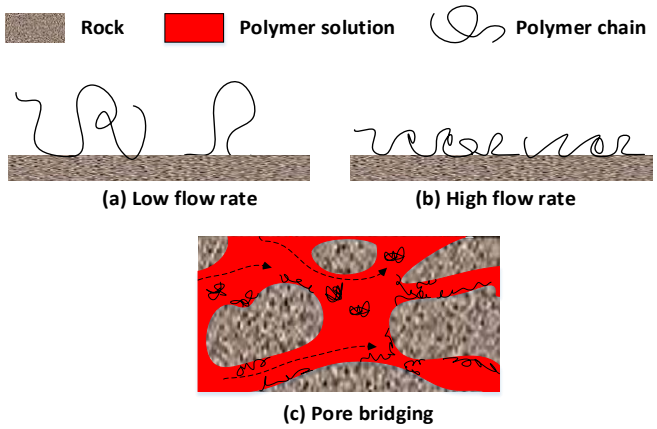

Figure 2-7: Schematic diagram of flexible polymer adsorption in pore media; (a) under low rate injection, (b) under high rate injection, and (c) polymer bridging.

Moreover, Park et al., (2015) report that there is a critical polymer injection rate below which the adsorbed layer thickness is independent of the injection rate, above which the adsorbed layer thickness gradually increases(Park et al., 2015, Chauveteau et al., 2002, Ogunberu and

Asghari, 2005). Ogunberu and Asghari, (2005) showed that at polymer injection rate lower than a critical injection shear rate (300 s^{-1}), only static adsorption existed, while at higher injection rates the adsorbed polymer layer improved due to flow-induced adsorption. It was pointed out that at high injection rates (i.e. high hydrodynamic force), additional macromolecules penetrate inside the static adsorption layer by overcoming the osmotic force barrier), similar to Figure 2-6. As a result, the density of adsorbed macromolecules increases. Moreover, it is expected that hydrodynamic force is highest at the entrance of pore throats, where polymer adsorption has a strong effect on permeability reduction(Ogunberu and Asghari, 2005). Nevertheless, it seems that there is a higher critical injection rate after which the adsorption become almost stable(Qi et al., 2013).

Table 2-3 shows literature data on the effect of polymer flow/shear rate on polymer adsorption. This table shows polymer adsorption as a function of flow/shear rate, in different forms which are: increasing adsorption layer thickens (e), adsorption concentration or more obviously and traditionally by flow resistance (RF)/mobility reduction (Rm). Mobility reduction(Mishra et al., 2014) and polymer layer thickens(Al-shajalee et al., 2019b, Al-Shajalee et al., 2020b) are a function of pressure drop:

$$R_m = \frac{\lambda_w}{\lambda_p} \qquad (1)$$

where λ_w is the mobility of water and $\lambda_p$is the mobility of polymer solution. The mobility is calculated using Darcy's equation ($\lambda = qL/A\emptyset\Delta p$).

$$e = r\left(1 - \frac{1}{F_{rrw}^{0.25}}\right) \qquad (2)$$

Where r is the average pore radius and F_{rrw} is the residual resistance factor:

$$F_{rrw} = \frac{\lambda_{w\,before}}{\lambda_{w\,after}} \qquad (3)$$

Where $\lambda_{w\,before}$ is the mobility of water before polymer treatment and $\lambda_{w\,after}$ is the mobility of water after polymer treatment.

Table 2-3: Schematic illustration of static adsorption and flow-induced adsorption.

Reference	Flow rate (cm^3/min or Pv/min) or shear rate (s^{-1})	Adsorption layer thickness (μm), adsorption concentration ($mg.cm^{-2}$) or mobility reduction (R_m)
(Chauveteau et al., 2002)	18-60 (critical) -290 s^{-1}	0.6-0.8-1.8 μm
(Ogunberu and Asghari, 2005)	65-300 (critical) -3000 s^{-1}	0.12-4-4.3 μm
(Qi et al., 2013)	0.25-2 (critical) -4 cm^3/min	0.54-2.12-2.18 μm
(Al-Sharji et al., 2001a)	0.01, 0.02 and 0.04 cm^3/min	3, 3.6 and 4 R_m
(Bhatnagar and Eoff, 2016)	7 and 35 milli Pv/min	2 and 4 $mg.cm^{-2}$
(Denys et al., 2001)	59, 119 and 178 s^{-1}	5, 18 and 75 R_m

2.2.9 The effect of temperature

Previous studies are in general agreement that reservoir temperature affects RPM performance such that the temperature tends to increase polymer adsorption followed by a flattening with further temperature rise(Ranjbar and Schaffie, 2000, Ranjbar et al., 1996, Tekin et al., 2010, Tekin et al., 2005, Zaitoun and Pichery, 2001, Pusch et al., 1995, Karimi et al., 2014b, Nieves et al., 2002, Qi et al., 2013, Kalfayan and Dawson, 2004). However, it has been argued that most RPMs work well at low-temperature conditions and tend to depict poor thermal stability at high-temperature conditions. Thus finding suitable polymers, especially in gel form, that are thermally stable for application in high-temperature wells is currently an area of investigation(Zhu et al., 2017, El-Karsani et al., 2014).

2.3 Post-adsorption mechanisms

Different physical mechanisms have been suggested in the literature to explain the origin of DPR behaviour: wall effects (i.e. steric, lubrication, wettability, and swelling/shrinking) and

fluid segregation. Although, there is evidence that all of these mechanisms occur; however, a comprehensive understanding of how these mechanisms affect each other (either cooperatively or against each other) is still a matter of active research.

2.3.1 Fluid Segregated pathways

Studies on multiphase flow in porous media generally agree that preferred pathways for wetting and non-wetting fluids are dominated by pore wettability, pore size, and capillary entrance pressure(Nilsson et al., 1998, Stavland and Nilsson, 2001, Ali and Barrufet, 2001, Grattoni et al., 2001d, Zaitoun and Kohler, 1988, Al-Muthana et al., 2012, Katika et al., 2016, Ladutko et al., 2012, Jaripatke et al., 2009). In addition, Anderson (1986) proposed that the wetting fluid preferentially fills the smallest pores and is in contact with the rock surface; while the non-wetting fluid typically inhabits the centres of the larger pores and extends continuously from pore to pore(Anderson, 1986) (see Figure 2-8a). Furthermore, due to capillary effects, the non-wetting phase needs to exceed a threshold pressure (or entrance pressure) to flow through the pores filled with the wetting phase. If the entrance pressure is not surpassed, the non-wetting phase will not flow through the pores(Stavland and Nilsson, 2001) with smaller pores generally having a larger capillary effect(Ali and Barrufet, 2001, Al-Shajalee et al., 2020c, Al-shajalee et al., 2019b).

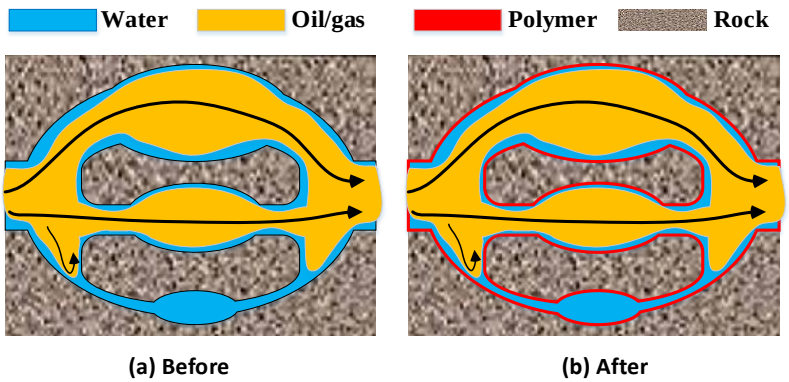

Figure 2-8: Fluid Segregated pathways of wetting (water), non-wetting (oil/gas) and water-based DPR fluids in water-wet pore network.

Therefore, fluid segregation has been identified as a crucial mechanism to achieve DPR with water and oil/gas flowing in separate pathways of a porous media or defined parts of a pore and water-based DPR fluid only affects the water network(White et al., 1973, Liang et al., 1995, Thompson and Fogler, 1997, Nilsson et al., 1998, Al-shajalee et al., 2019b, Al-Shajalee et al., 2020c, Stavland and Nilsson, 2001, Imqam et al., 2014, Jaripatke et al., 2009, Ladutko et al., 2012, You et al., 2013, Dovan and Hutchins, 1994, Liang et al., 1992, Liang and Seright, 1997, Seright, 1995, Zaitoun et al., 1998, Li et al., 2014, Sidiq, 2007, Zhao et al., 2014, Scott et al., 2020, Song et al., 2015). For example, if the injected RPM agent is hydrophilic (i.e. a water-based DPR agent), it flows preferentially in the water-wet paths avoiding non-wetting paths. Therefore, a water-based DPR fluid settles onto a water-wet surface through electrostatic interactions and this is referred to as a 'segregation mechanism'. However, as fluids may segregate differently after RPM sorption, the mechanism should be referred to as "initial fluid segregation" as the wettability characteristics evolve. Nevertheless, as the water (i.e. wetting fluid) flows close to the water-wet pore surface and oil/gas (i.e. non-wetting fluid) flows preferentially through the center of these pores, which is free of polymer, the water permeability is selectively reduced with minimal effects on the non-wetting fluid flow (see Figure 2-8b)(Stavland and Nilsson, 2001, Jaripatke et al., 2009, Ladutko et al., 2012, You et al., 2013, Sidiq, 2007, Scott et al., 2020). Similarly, these roles would reverse if the pore surface was oil/gas wet(Stavland and Nilsson, 2001, Scott et al., 2020). Elsewhere in the literature, this mechanism is referred to as segregated pathways(Stavland and Nilsson, 2001, Al Ali, 2012, Scott et al., 2020, Jaripatke et al., 2009, Ladutko et al., 2012, You et al., 2013, Zhao et al., 2014, Liang et al., 2018, Liang et al., 2017, Liang et al., 1995), fluid partitioning (Zaitoun et al., 1998, Sidiq, 2007) and fluid distribution (Al-Sharji et al., 2001a, Al-Sharji et al., 2001b, Al-Shajalee et al., 2020c, Al-shajalee et al., 2019b, Grattoni et al., 2001d, Zaitoun and Kohler, 1988, Mennella et al., 1998). For consistency, the term 'fluid segregated pathways' is used in this review.

2.3.1.1 Pore size effects (on fluid redistribution)

The literature indicates that during multiphase flow in porous rocks, the relative permeabilities are controlled by the fluid distribution (or fluid segregation) depending on pores sizes of a rock(Grattoni et al., 2001d, Zaitoun and Kohler, 1988, Jaripatke et al., 2009, Ladutko et al., 2012, Al-Shajalee et al., 2020c, Al-shajalee et al., 2019b). In the water-wet system, after a polymer treatment the induced changes in the pores sizes and the subsequent redistribution of the wetting and non-wetting fluids are claimed to control DPR(Grattoni et al., 2001d, Al-Shajalee et al., 2020c, Al-shajalee et al., 2019b), see Figure 2-9. To elaborate further, the very small pores that were before occupied with water (Figure 2-9a) will possibly be plugged by immovable RPM and water (Figure 2-9b). The moderate pores, that were formerly filled by wetting phase (water) and non-wetting phase (oil/gas) concurrently (Figure 2-9a), after polymer adsorption, have a smaller size and accordingly greater capillary pressure and consequently, become occupied only by water (Figure 2-9b). The largest pores, though, possibly will remain comparatively large to be occupied by both wetting fluid (water) and non-wetting fluid (oil/gas) concurrently (Figure 2-9b)(Al-Shajalee et al., 2020c, Al-shajalee et al., 2019b, Grattoni et al., 2001d).

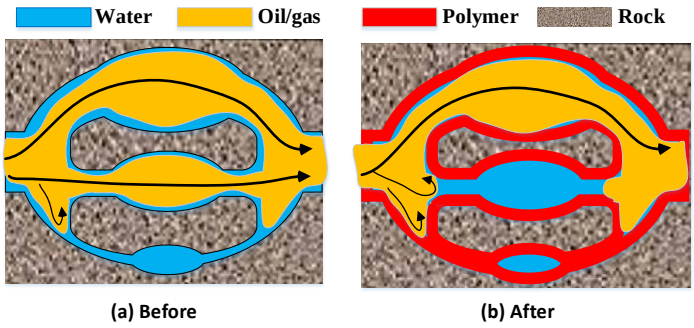

Figure 2-9: Pore size changing before and after treatment and its eventual effects on wetting and non-wetting fluids redistribution.

Another important condition to guarantee successful treatment is that the non-wetting fluid path remains continued after the treatment, else the treatment will cause permeability reduction for both wetting and non-wetting fluids(Stavland and Nilsson, 2001, Al-Shajalee

et al., 2020c, Al-shajalee et al., 2019b). This happens when polymers induce relatively high polymer thickness onto the pore surface, therefore, oil/gas needs to exceed higher entrance pressure to flow through the same pore filled with the wetting phase and an extra layer of the adsorbed polymer, which further reduces the pore size(Ali and Barrufet, 2001, Al-Shajalee et al., 2020c, Al-shajalee et al., 2019b, Grattoni et al., 2001d, Zaitoun and Kohler, 1988). This highlights the role of rock permeability on the RPM's performance(Al-shajalee et al., 2019b). Moreover, this effect also likely happens when placing a strong gel in a porous media at residual oil/gas (non-wetting fluid) saturation. Therefore, the remaining oil/gas will be discontinuous or immobile and the only way to flow is to break the gel and open a permanent channel through the gel and/or shrinking the gel by hydrodynamic force(Stavland and Nilsson, 2001, Al-Shajalee et al., 2020c).

2.3.1.2 Non-water-wet pores

The non-water-wet pores i.e. oil/gas-wet pores influence the fluid distribution and in turn, impact the RPM performance**.** The symmetric state (i.e. Figure 2-8) would follow in gas/oil-wet media, with water taking the place of gas/oil(Zaitoun et al., 1998, Stavland and Nilsson, 2001, Al Ali, 2012, Scott et al., 2020, Song et al., 2015). However, if the water-based RPM is used, the RPM will not adsorb on the oil/gas-wet pore surface and will not flow through the small pores. As elaborated earlier that this will not be applicable because the preferred "initial" fluid segregation is not achieved, yet the RPM may retain in large pores where non-wetting (water) and wetting (gas/oil) fluids can flow. Therefore, the DPR effect is not observed and the permeability reduction for both water and oil/gas will be minor(Stavland and Nilsson, 2001, Al Ali, 2012). If non-water-based DPR (i.e. oil/gas-based DPR) is used, the DPR will replace the oil/gas film and adsorb on the oil/gas-wet pore surface. Thus, the oil/gas permeability reduction will more likely be more than water, because the adsorbed layer will restrict the wetting fluid (oil/gas)(Stavland and Nilsson, 2001, Al Ali, 2012, Scott et al., 2020, Grattoni et al., 2002, Song et al., 2015). Unless the RPM is also capable of

altering the wettability from oil/gas-wet to water-wet state, thus wetting and non-wetting fluid will preferably be distributed ("final segregation") and eventually the DPR will be achieved(Al-Sharji et al., 2001a, Stavland and Nilsson, 2001, Al Ali, 2012), see Figure 2-10. Similarly, Vasquez and Eoff, (2013b) state that the wettability alteration stage for oil-wet media to water-wet should be done first so that the RPM agents can effectively adsorb onto the rock surface(Vasquez and Eoff, 2013b). As we mentioned earlier after treatment fluids may segregate differently due to pore size and/or wettability alteration. Therefore, for recognition purposes, the segregation mechanism after RPM settlement should be called "final fluid segregation".

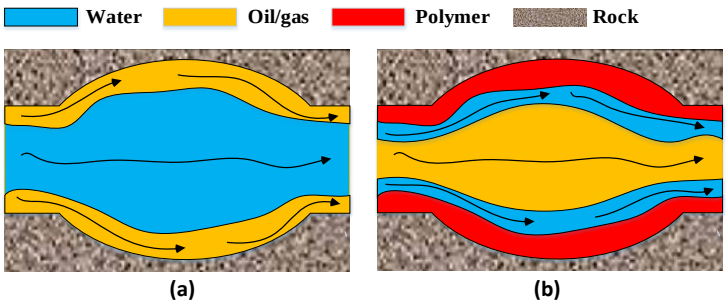

Figure 2-10: Fluid segregation during; (a) oil/gas-wet before polymer adsorption, and (b) after polymer adsorption and wettability alteration from oil/gas-wet to water-wet.

Moreover, the literature data, though limited, reported some oil-soluble RPM agents. The tetra-methyl-ortho-silicate (TMOS) is an oil-soluble or oil-based gelant that was first introduced by Thompson and Fogler (Thompson and Fogler, 1997). TMOS can be injected into the wellbore dissolved in oil to follow the oil pathways, yet only reacts with the water (mass transfer, hydrolyzing then condensation) to produce a rigid silicate gel. Therefore it effectively restricts/blocks the water pathways with less effect on oil pathways (segregation mechanism) that results in a greater reduction in water relative permeability (Grattoni et al., 2002, Karmakar et al., 2018, Karmakar et al., 2002).

In case of polymer interactions with an oil-wet rock, better theoretical approaches (e.g. theories related to disjoining press such as DLVO, double layer expansion, surface complexation and induced polarity) are required for wettability alteration and polymer

adsorption studies (Jha et al., 2019a, Takeya et al., 2020, Bordeaux-Rego et al., 2021, Hassan et al., 2020, Jha et al., 2020, Jha et al., 2021, Lopez et al., 2021, Arif et al., 2021).

2.3.1.3 Fluid segregation in gel

Polymer gels consist of polymer, cross-liker and solvent (often water, in case of water-based gel) (Karimi et al., 2016, Amir et al., 2019, Yi et al., 2017, Zhu et al., 2017). Gels are divided into two groups (organic or inorganic) depending on the cross-linker type, which is organic (such as polyethyleneimine, aldehydes and formaldehyde) and inorganic (which are usually a trivalent/tetravalent cation such as Al^{+3}, Cr^{+3}, Zr^{+3}) (Amir et al., 2019, Karimi et al., 2014b, Yi et al., 2017, Zhu et al., 2017). Cross-linker chemically helps to connect two polymer molecules, where this process depends on the concentration of each component, temperature, and time. Additives help to control gel strength, gelation time, and thermos-stability. Therefore, they are normally used in high-permeability and fractured reservoirs for EOR and RPM applications (Karimi et al., 2014b, Yi et al., 2017, Sidiq, 2007, Jinxiang et al., 2013, Yadav et al., 2020, Liang et al., 2017, Liang et al., 2018, Zaltoun et al., 1991, Grattoni et al., 2004, Hajilary et al., 2015b).

Therefore, the segregation mechanisms presented earlier, the literature proposed that oil/gas and water segregate through gels by a somewhat different mechanism to that in the presence of non-gel polymer(Liang et al., 2018, Liang et al., 2017, Willhite et al., 2000, Nguyen et al., 2006, Seright et al., 2004, Seright et al., 2006, Al-Shajalee et al., 2020c). Literature advocated that post gel placement, oil fingers through the gel by rupturing the gel, Figure 2-11a. Yet, the rupture can also be created by water if the gel placement is directly followed by water injection. Nevertheless, water flows mainly in the channels created and also causes water-based gel to swell due to rehydration, Figure 2-11b. This in turn reduces the size of the created channel and forces the water (i.e. solvent) to flow (i.e. diffuse) through the gel itself, Figure 2-11c. Thus, the permeability of water gets reduced as the water's pathways get partially closed due to a) the swelled gel due to rehydration by water and/or (b) the presence of the

trapped residual oil/gas saturation as water and oil/gas flow through the same channels. Notably, however gel shrinkage during oil flow can be beneficial to increase oil continuity that eventually leads to the DPR(Willhite et al., 2000, Stavland and Nilsson, 2001, Seright et al., 2004, Seright et al., 2006, Dawe and Zhang, 1994, Al-Shajalee et al., 2020b). More details about swelling/shrinkage will be presented in a separate section.

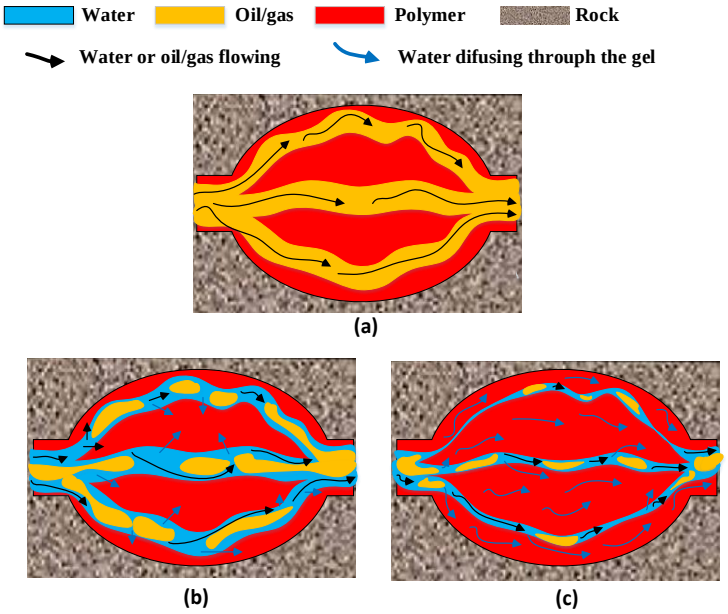

Figure 2-11: oil and water flowing through gel-treated porous media. a) Oil flowing through gel-treated porous media, b) subsequent water flowing through gel-treated porous media, in presence of residual oil saturation, c) continues water flowing through gel-treated porous media, in presence of residual oil saturation after gel rehydration and swelling.

Thus, in summary, the fluid segregation mechanism is applicable before the treatment as a primary condition to achieve RPM adsorption (or placement) and after the treatment where the RPM treatment is expected to preferably modify fluid segregation to achieve DPR. Therefore, it is better to differentiate between the initial and final fluid segregation. Moreover, having the segregation mechanism been supported as the main mechanism to achieve the DPR, it is still not the single explanation for the DPR.

2.3.2 Wall Effects

Wall effects have been recognized as an important post-treatment factor. Generally, it is agreed that wall effects appear due to the presence of the layer of the adsorbed polymer on the pore walls(Zaitoun et al., 1998, Elmkies et al., 2002, Rellegadla et al., 2017, Scott et al., 2020, Norouzi et al., 2017, Al-Shajalee et al., 2020c, Al-Shajalee et al., 2019a, Al-shajalee et al., 2019b, Browne et al., 2020, Al Ali, 2012, Lewis, 2014, Song et al., 2015, Sidiq, 2007, Bhatnagar and Eoff, 2016). The wall effect of RPMs can cause a noticeable reduction to water relative permeability but the minimum effect on oil/gas relative permeability due to the physical or chemical properties of the adsorbed layer(Lewis, 2014). It is claimed that the wall effect is expected to induce one or a combination of sub-effects that altogether determine the outcome of RPM treatment, and these include:

2.3.2.1 Steric effect

The steric effect is defined as a physical pore size restriction/reduction that can be caused by the firm and impenetrable layer of the adsorbed polymer on the pore walls(Zaitoun et al., 1998, Lewis, 2014, Scott et al., 2020, Browne et al., 2020, Sidiq, 2007, Al-Shajalee et al., 2020c, Al-Shajalee et al., 2019a, Al-shajalee et al., 2019b, Hirasaki and Pope, 1974, Tielong et al., 1996, Li et al., 2014). Therefore, in water-wet rocks as the water flow close to the pore walls the RPM layer restricts the flow of water fluid. In contrast, as non-wetting fluid (i.e. oil/gas) tend to flow through the center of the pore channels, which is free of polymer, the non-wetting fluid is insignificantly affected(Zaltoun et al., 1991, Tielong et al., 1996, Stavland and Nilsson, 2001, Scott et al., 2020, Al Ali, 2012, Lewis, 2014, Sidiq, 2007, Song et al., 2015).

As the polymer layer thickness increases, water permeability decreases(Sidiq, 2007). However, it is also reported that RPM's can remarkably reduce both wetting and non-wetting fluid(Al-Shajalee et al., 2020c, Al-shajalee et al., 2019b, Nieves et al., 2002). Therefore, it has been claimed that the efficiency of an RPM to restrict the water flow with less effect on oil/gas flow (i.e. DPR) is directly related to the ratio of polymer layer thickness over the pore

radius (i.e e/r) rather than to only polymer layer thickness (e)(Zaltoun et al., 1991, Al-Sharji et al., 2001a, Grattoni et al., 2004, Al-Shajalee et al., 2020c, Al-shajalee et al., 2019b, Browne et al., 2020). This implies that both initial pore sizes or initial rock permeability and the layer thickness of the adsorbed polymer play an important role in determining the success/efficiency of an RPM treatment(Kalfayan and Dawson, 2004, Al-shajalee et al., 2019b, Mennella et al., 1998, Qi et al., 2013, Elmkies et al., 2002, Zaitoun and Pichery, 2001, Burrafato et al., 1999, Jinxiang et al., 2013, Al-Shajalee et al., 2020c, Al-Shajalee et al., 2019a). Beside polymer adsorption there are other restrictions also that can cause the steric effect:

2.3.2.1.1 Water saturation

It has been stated that after polymer treatment the water retention (i.e. water saturation) increases(Scott et al., 2020) and subsequently this can also cause more pore size restriction to flowing oil/gas fluid(Stavland and Nilsson, 2001). It is worth mentioning that water saturation increment has been attributed to three factors; 1) the hydration property of the polymer molecules, 2) rock surface alteration to more water-wet, and 3) the capillary trapping phenomena(Zaitoun et al., 1998, Tielong et al., 1996, Elmkies et al., 2002, Scott et al., 2020). The latter one is due to the steric effect of the adsorbed polymer where the small pores become even smaller and only accessible to wetting fluid due to capillary effect, which is inversely proportionate to the pore size(Ali and Barrufet, 2001, Grattoni et al., 2004, Al-Shajalee et al., 2020c, Al-shajalee et al., 2019b). This implies that increasing the capillary pressure can render the non-wetting fluid inaccessible into small pores (Ali and Barrufet, 2001). In other words, increasing water saturation automatically induces a reduction in non-wetting fluid relative permeability(Chiappa et al., 1997, Zaitoun and Pichery, 2001). Therefore, the reduction in the non-wetting fluid permeability cannot be attributed only due to the polymer layer, but also to the increase in water saturation or water layer thickness(Chiappa et al., 1997, Al-Shajalee et al., 2020c), see Figure 2-12.

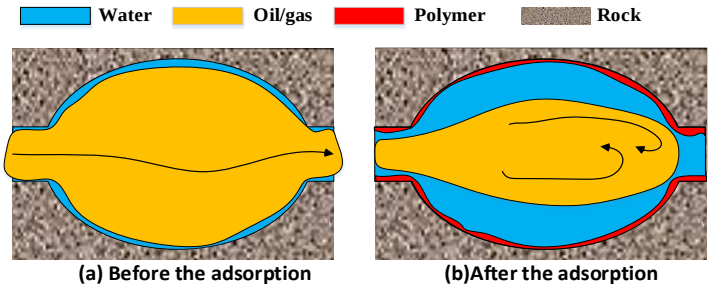

Figure 2-12: The effect of increasing water saturation on non-wetting fluid accessibility.

2.3.2.1.2 S_{or}/S_{gr} residual saturation

It has been stated that the trapping of residual saturation of non-wetting fluid (i.e. oil/gas) can also assist towards more DPR(Seright et al., 2006, Seright et al., 2004, Al Ali, 2012, Al-Shajalee et al., 2020b, Song et al., 2015). Investigations(Yadav et al., 2020, Liang et al., 2017, Liang et al., 2018, Prado Paez et al., 2009, Al-Shajalee et al., 2020b) suggest that the significant trapping of residual non-wetting saturation (S_{gr}/S_{or}) due to RPM treatment can cause greater restriction to wetting fluid flow (water) and eventually significantly increase the water permeability reduction, see Figure 2-13.

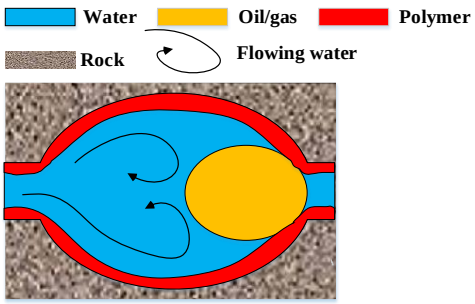

Figure 2-13: Decreasing water permeability due to the trapped residual saturation of non-wetting fluid (i.e. oil/gas).

2.3.2.2 Lubrication Effects

Polymer adsorption on the pore wall can induce a major lubrication effect that favours the flow of non-wetting fluids (i.e. oil/gas), and ultimately leads to DPR(Scott et al., 2020, Rellegadla et al., 2017, Lewis, 2014, Al-Shajalee et al., 2020b, Al-Shajalee et al., 2019a, Al-shajalee et al., 2019b, Al-Sharji et al., 2001a, Zaitoun and Kohler, 1988, Zaitoun et al., 1990,

Dovan and Hutchins, 1994, Norouzi et al., 2017). To elucidate, the lubrication effect can facilitate the flow of the non-wetting phase (i.e. oil/gas) and facilitate its displacement by; 1) making it slip through the centre of pore channels, and 2) reducing the roughness of the pore surface(Zaitoun and Kohler, 1988, Tielong et al., 1996, Zaitoun et al., 1998, Elmkies et al., 2002, Nieves et al., 2002, Scott et al., 2020, Rellegadla et al., 2017). Further, the formed water film on the RPM-covered pore surface can increase the lubrication effect(Zaitoun et al., 1998, Zaitoun and Kohler, 1988, Al-Shajalee et al., 2020b, Al-Shajalee et al., 2019a, Al-shajalee et al., 2019b). Studies also show that the adsorbed RPM layer on the pore wall can improve the flow of non-wetting fluids via extending the laminar flow region, avoiding the turbulent flow regime, or decreasing inertial effects(Zaitoun et al., 1990, Al-Shajalee et al., 2019a, Song et al., 2015, Elmkies et al., 2002).

2.3.2.3 Wettability alteration due to treatment (final wettability)

Literature reported that the DPR outcome of RPM treatment is attributed to the rock surface wettability alteration from oil-wet to water-wet. This is because the RPM agents (e.g. polymers) adsorb onto the rock surfaces and thus renders it more water-wet. Consequently, the water phase flows close (or closer) to the pore surfaces that subsequently helps the non-wetting fluid unrestrictedly flow through the centre of the pore channels whereas the relative permeability of the water may be reduced as water flows in contact with the adsorbed polymer layer(Zaitoun et al., 1998, Zaitoun and Kohler, 1988, Zaltoun et al., 1991, Tielong et al., 1996, Al-Sharji et al., 2001a, Karimi et al., 2014b, Ahmed et al., 2020, Al Ali, 2012, Song et al., 2015, Rellegadla et al., 2017, Lewis, 2014, Qi et al., 2013). It is worth noting that both effect (i.e. wettability alteration and/or lubrication effect) eventually helps the non-wetting fluid flowing through the centre of the pores with less restriction(Zaitoun et al., 1998). In other words, lubrication effect and/or wettability alteration towards water wet counterbalance or compete steric effect toward less effect on non-wetting phase which eventually aid in DPR.

Qi et al. (2013) experimental results indicate that, for example, a cationic polyacrylamide treatment declines the contact angle of a glass surface from 105º to 75º. Similar observations have been reported by(Chiappa et al., 1999).e.g. a cationic polyacrylamide treatment declines the contact angle of a glass surface from 120º to 75º. However, both studies show that treating the same surface (oil-wet) with anionic/weakly-anionic polymer could barely change the contact angle. In addition, previous studies used water-wet core samples and the wettability alteration was interpreted via a change in k_{rw}/k_{rg} - S_w curves after the RPM treatment (Karimi et al., 2014b, Tielong et al., 1996, Schneider and Owens, 1982, Zaitoun and Kohler, 1988, Zaitoun et al., 1998). Before the treatment, the k_{rw} branch (of the relative permeability curve) was much lower than the k_{rg} branch and the water saturation at the intersecting point of k_{rw} and k_{rg} branches is greater than 50% (i.e. water-wet). After polymer treatment, the k_{rw} branch becomes much lower than that before the treatment and the water saturation at the intersecting point also becomes higher (Karimi et al., 2014b, Tielong et al., 1996). Similar observations have been reported by other studies (Schneider and Owens, 1982, Zaitoun and Kohler, 1988, Zaitoun et al., 1998). Karimi et al., (2014b) attribute the k_{rw}/k_{rg} - S_w curves modification to a combination of wettability alteration and steric effects of an RPM treatment.

However, Al-Shajalee et al., (2020b) showed that positively charged poly (acrylamide-co-diallyldimethylammonium chloride) on a negatively charged glass surface can change the water contact angle from 16º to 32 º (with 0.2 wt.% KCl). Nevertheless, the treatment resulted in significant water permeability reduction for low permeability rocks (Socito, ~3 mD, Gray Bandera, ~23 mD, and San Saba, ~70 mD)(Al-Shajalee et al., 2020d). Moreover, zeta potential measurements showed that treating negatively charged surfaces with positively charged polymers alters the surfaces from negative to less negative or to positive charge (Tekin et al., 2005, Tekin et al., 2010, Al-Shajalee et al., 2020d).

2.3.2.4 Swelling / shrinking effect

From wall effect considerations, the firm adsorbed polymer layer onto the pore surface reduces the pore cross-sectional area. This in turn can lead to reducing the relative permeability of both wetting and non-wetting fluids(Zaitoun and Kohler, 1988, Kalfayan and Dawson, 2004, Mishra et al., 2014, Al-Shajalee et al., 2020c, Al-Shajalee et al., 2019a, Al-shajalee et al., 2019b). However, for plausible interpretation to DPR observations, it has been reported that water-base RPMs swell (hydrates) in presence of water, therefore, resist water flow while they shrink (dehydrates) in presence of oil/gas fluid so oil/gas flow easily. In other words, RPM's swelling/shrinking characteristic depends on the flowing fluid phase that ultimately leads to DPR phenomena and aids in selective permeability reduction (SPR)(Imqam, 2015, Lewis, 2014, Seright et al., 2006, Sidiq, 2007, Askarinezhad et al., 2016, Li et al., 2014, Mennella et al., 1998, Mishra et al., 2014, Liang et al., 2018, Liang et al., 2017, Willhite et al., 2000, Nguyen et al., 2006, Al-Sharji et al., 1999b). The factors that influence the RPM's swelling/shrinking phenomenon are:

2.3.2.4.1 The type of flowing fluid (water, oil or gas)

It has been reported that as water can defuse through polymer/gel layer, the water induces charge repulsion between the hydrolyzed groups in polymer/gel which in turn the polymer/gel swells and subsequently resists the flow of water(Zaitoun and Pichery, 2001, Mishra et al., 2014, Lewis, 2014, Seright et al., 2006, Sidiq, 2007, Askarinezhad et al., 2016, Mennella et al., 1998), see Figure 2-14a. Furthermore, it has been stated that the mechanical force exerted by flowing oil/gas fluid on polymer/gel causes water expulsion from the polymer/gel which eventually causes gel shrinkage(Zaitoun et al., 1998, Al-Shajalee et al., 2020c, Al-Shajalee et al., 2019a, Al-shajalee et al., 2019b, Lewis, 2014, Seright et al., 2006, Mennella et al., 2001, Liang et al., 1995, Liang and Seright, 1997, Dawe and Zhang, 1994, Elmkies et al., 2002, Sidiq, 2007, Mennella et al., 1998) , see Figure 2-14b.

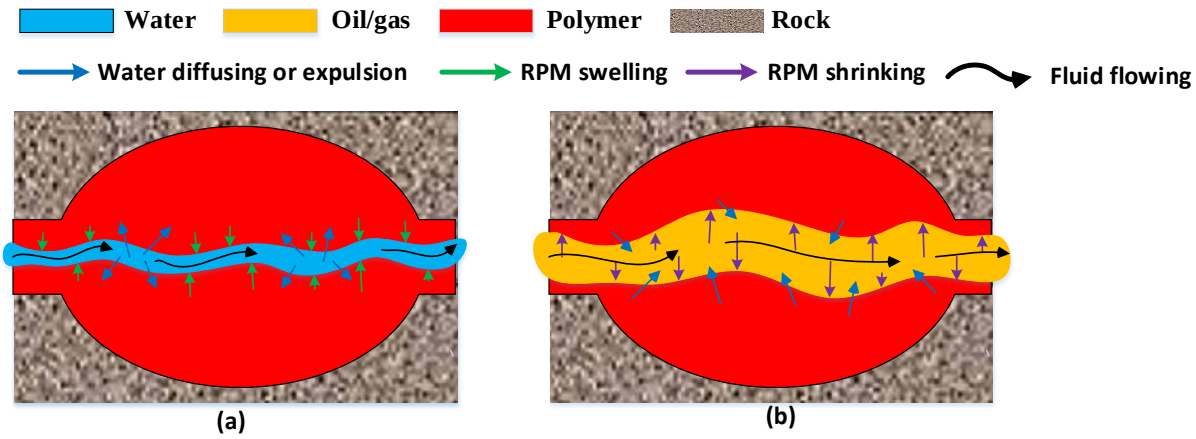

Figure 2-14: (a) water-based DPR swells (hydrates) during water flowing (b) water-based DPR shrikes (dehydrates) during oil flowing.

2.3.2.4.2 Brine and oil/gas injected PV

Studies emphasized the importance of brine injection volume on the swelling/shrinkage effect of placed RPM in porous media. It has been reported that as water fluid flows over the adsorbed polymer layer, the layer gradually swells and subsequently causes a reduction in water effective permeability(Barrufet and Ali, 1994, Mishra et al., 2014, Imqam, 2015, Wu et al., 2020). Likewise, field treatments also reported a similar trend as fluid production time passes(Ranjbar and Schaffie, 2000, Dovan and Hutchins, 1994, Kalfayan and Dawson, 2004). Moreover, polymer/gel swelling is also reported as a function of the time when polymer/gel is in contact with static brine. The literature shows that as time moves on the swelling ratio will gradually increase until it reaches a plateau and no further swelling occurs(Abdulfarraj and Imqam, 2019, Kalgaonkar et al., 2013, Sydansk, 1988, Song et al., 2018a, Chen et al., 2020a, Imqam, 2015, Chen et al., 2020b). The effect of oil injection volume on oil permeability reduction in cross-linked polymer treated permeable medium was also studied. The results showed that as oil-injected PV increases (up to 110PV), oil permeability reduction was gradually decreasing (i.e. oil permeability gradually recovering). This phenomenon is attributed to gel dehydration and that with greater oil PV flowing, more dehydration occurred(Liang et al., 2018, Liang et al., 2017). A similar observation was reported by(Dawe

and Zhang, 1994, Willhite et al., 2000, Nguyen et al., 2006). Literature also reported that RPM displacement may occur because of oil flow(Willhite et al., 2000, Liang et al., 2017).

2.3.2.4.3 Brine & oil/gas flow rate

The performance of placed RPMs is dependent on fluid flow rate. The permeabilities of water and oil/gas were found to vary with flow rate (more precisely shear rate) due to increasing the hydrodynamic forces exerted on the placed RPMs(Song et al., 2015, Al-Shajalee et al., 2020c, Al-Shajalee et al., 2019a, Al-shajalee et al., 2019b, Qi et al., 2013, Mishra et al., 2014, Al-Sharji et al., 2001b, Al-Sharji et al., 1999b, Zaitoun and Kohler, 1988). The flow rate dependency was attributed to the deformable fluids (i.e. flexible polymer/gel) due to their elastic properties(Cohen and Christ, 1986, Saphiannikova et al., 1998, Al-Sharji et al., 1999b, Al-Sharji et al., 2001b). Flexible polymer deformability (i.e. shear-thinning/thickening behaviour) is attributed to stretching properties of the adsorbed flexible polymers/gels, see section 2.8.

Brine: it has been reported that as water flow rate increases, RPM performance or water residual resistance factor (F_{rrw}, Equation 3) decreases. This trend has been attributed by numerous researchers to the shear-thinning behaviour of the placed-RPMs(Barrufet and Ali, 1994, Liang and Seright, 1997, Zaitoun and Kohler, 1988, Hajilary and Shahmohammadi, 2018, Nguyen et al., 2006, Song et al., 2015, Yadav et al., 2020, Stavland et al., 2011, Al-shajalee et al., 2019b, Al-Shajalee et al., 2020c). However, other trends, i.e. shear-thickening and shear-independency, which mainly depend on the flexibility property of polymers and the applied shear rate, were also reported(Al-Sharji et al., 2001a, Al-Shajalee et al., 2019a, LIU et al., 2009). For example, LIU et al. (2009) interpreted that as fluid injection rate increases, fluid has larger force to diffuse through the adsorption layer and subsequently the polymer layer swells further which eventually induces greater influence on the fluid permeability(LIU et al., 2009). Nevertheless, the maximum limit of polymer layer swelling/stretching is controlled by polymer chain length, therefore when the injection rate reaches a critical value, the swelling/stretching of the polymer layer reaches a maximum

too(Qi et al., 2013). Table 2-4 shows literature data regards the effect of brine flow rate on RPM behavior.

Table 2-4: Studies on the effect of brine flow rate on RPM performance.

	Used RPM	Porous media	Permeability, mD	Flow rate range, cm^3/min	F_{rrw} or PR%	RPM behaviour
(Al-Shajalee et al., 2020b)	P(AAM-co-AA)Na cross-linked with Cr^{3+}	Berea sandston	140	Q_w= 0.1 - 160	F_{rrw}= 3.8 - 1.7	shear-thinning
(Qi et al., 2013)	Cationic polyacrylamide	Sandpack	-	Q_w= 0.1 - 2 (criticle) - 4	F_{rrw}= 4.3 – 7 6.5	shear-thickening
(Al-Sharji et al., 2001a)	cationic polyacrylamide	Micromodel	-	Q_w= 0.01, 0.02, 0.04	PR_w = 60, 60, 60 %	shear-independency

Oil/gas: Reports show that with increasing oil shear rate, RPMs behaved as shear-independent(Nguyen et al., 2006, Hajilary and Shahmohammadi, 2018, Liang et al., 1995, Liang and Seright, 1997, Barrufet and Ali, 1994, Zaitoun and Kohler, 1988), shear-thinning(Song et al., 2018b), or shear-thickening agents(Qi et al., 2013). On the other hand, even though fewer works studied the gas effect, shear-thinning (Song et al., 2015) and shear-thickening behaviours(Al-Shajalee et al., 2020b, Al-Shajalee et al., 2019a, Al-shajalee et al., 2019b, Song et al., 2015) were also reported due to increasing gas shear rate. The above studies attribute the shear-independency to the immiscibility of oil with water-based RPMs while shear-thinning is attributed to RPM dehydration. However, shear-thickening behaviour is still more challenging. Micromodel results presented by (Al-Shajalee et al., 2020b) show that increasing gas flow rate causes trapping and dissolving of gas bubbles in the gel which causes gel expansion(Al-Shajalee et al., 2020b). Results also show shear thickening

behaviour for the used RPM with increasing oil flow rate(Qi et al., 2013). However, since the oil needs a bigger force to penetrate the adsorbed polymer layer, the polymer layer swells less in comparison to polymer swelling during water injection(Qi et al., 2013) and gas injection(Al-Shajalee et al., 2020b). Table 2-5 shows literature data regards the effect of gas flow rate on RPM behaviour.

Table 2-5: Studies on the effect of oil/gas flow rate on RPM performance.

	Used RPM	Porous media	Permeability, mD	Flow rate range, cm^3/min	Frr_g or Frr_o
(Al-Shajalee et al., 2020b)	P(AAM-co-AA)Na cross-linked with Cr^{3+}	Berea sandston	140	Q_g= 0.1 - 160	Frr_g= 0.1 -2
(Qi et al., 2013)	Cationic polyacrylamide	Sandpack	-	Q_o= 0.1 - 2 (criticle) - 4	Frr_o=1.8-2-2

2.3.2.4.4 Effect of brine salinity

Literature reports that polymers/gel layer either swells or shrinks when they are formed with or come in contact with brine(Al-Shajalee et al., 2020c, Zaltoun et al., 1991, Han et al., 2014, Farasat et al., 2017, Khamees and Flori, 2018, Heidari et al., 2019, Cozic et al., 2008, Imqam, 2015). It has been stated that the electrostatic interactions between the molecules of polymer and brine affect not only polymer adsorption on a surface (see section 2.2.2) but also the polymer layer thickness(Chiappa et al., 1999, Pusch et al., 1995, Ranjbar and Schaffie, 2000, Zaitoun and Pichery, 2001, Nieves et al., 2002, Sydansk, 1993, Karimi et al., 2014b, Qi et al., 2013, Zaltoun et al., 1991, Kalfayan and Dawson, 2004, Mishra et al., 2014, Al-Hashmi and Luckham, 2010, Tekin et al., 2005, Tekin et al., 2010, Al-Shajalee et al., 2020c).

It has been shown that increasing the positively charged ionic strength of brine in an anionic polymer causes reducing the hydrodynamic radius of polymer molecules due to decreasing

the electrostatic repulsion between the polymer-polymer molecules(Mishra et al., 2014, Zaltoun et al., 1991). However, the opposite will happen in the case of cationic polymer(Al-Shajalee et al., 2020c, Mishra et al., 2014, Zaltoun et al., 1991, Tekin et al., 2005, Tekin et al., 2010, Chiappa et al., 1999, Grattoni et al., 2004, Al-Hashmi and Luckham, 2010). Al-Shajalee et al., 2020b show that as the cations K^+ increases in the positively charged polymer, the zeta potential of polymer-brine-polymer shifted from positive to negative values. They interpreted that this is due to the polymer cation-cation electrostatic repellence increases or the attraction reduced(Al-Shajalee et al., 2020c), see Figure 2-15. Similar observations have also been reported in literature(Grattoni et al., 2004, Al-Hashmi and Luckham, 2010, Tekin et al., 2010, Dang et al., 2014). This phenomenon was interpreted that as the negatively charged surface being screened and henceforth more extended loops and tails of the adsorbed polymer molecules (Al-Hashmi and Luckham, 2010). In addition, Tekin et al., (2010) explained that increasing the salinity can increase the degree of dissociation of polymer molecules by facilitating the protonation(Tekin et al., 2010).

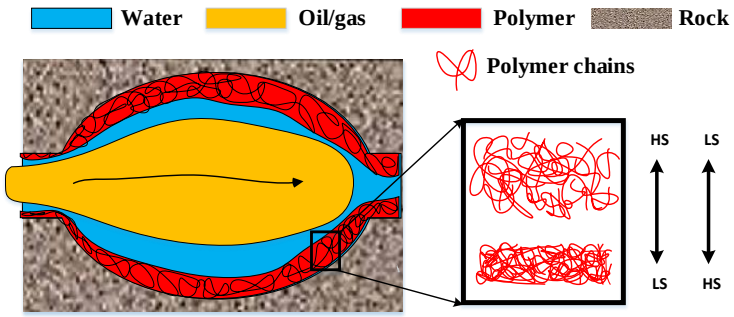

Figure 2-15: polymer layer thickness adjustment as a function to brine salinity.

To elaborate this further, Imqam, (2015) used particle gel (created with a super absorbent polymer (SAP)) to tackle water channeling in high-permeability streaks and fractures. These particles have a swelling ratio of 30-200 times the original volume. It was claimed that adjusting brine salinity can control the particle size. Further, the swelling pressure of such particles was regarded as a combination of osmotic pressure and elastic pressure. The osmotic pressure helps to swell the gel, whereas the elastic pressure constrains the swelling. The osmotic pressure in turn comprises two contributions, polymer-solvent mixing, and the

mobile ion concentration(Imqam, 2015). Moreover, regardless of reservoir brine salinity, brine-insensitive polymer (i.e. non-ionic polymers) with a swelling agent can also be used.(Zaltoun et al., 1991, Xindi and Baojun, 2017)

In summary, the brine salinity of a candidate reservoir plays a significant role to adjust RPM hydrodynamic thickness. This eventually can serve to achieve an optimum DPR and make the polymer suitable for broad implications. Therefore, the attention was to achieve; a) low polymer hydrodynamic thickness when treating low permeable rocks to avoid non-wetting fluid plugging (Al-Shajalee et al., 2020c, Moghadasi et al., 2019) and, b) high polymer hydrodynamic thickness to induce higher water permeability reduction in high permeable rocks(Zaltoun et al., 1991, Kohler et al., 1993, Xindi and Baojun, 2017, Imqam, 2015). Nevertheless, more studies are needed to serve certain implications for different well candidates (i.e. rock type and brine composition, and ionic charge).

2.3.2.4.5 The effect of pH

It is reported that the swelling ratio of pH-sensitive polymers can be controlled by adjusting the solution pH value(Al-Anazi and Sharma, 2002, Imqam, 2015). The results showed that the used polymers began to adsorb water then swell as the pH increased. Al-Anazi and Sharma, (2002) elucidate that as pH increases the electrostatic repulsion force and the polymer chain increase. This in turn causes the polymer to uncoil and stretch(Al-Anazi and Sharma, 2002).

2.3.2.4.6 The elasticity of polymer/gel

When water flows through water-affinity gels, the gels swell due to rehydration while gels shrink due to dehydration during oil flow(Liang et al., 2018, Liang et al., 2017, Willhite et al., 2000, Seright et al., 2006, Nguyen et al., 2006, Mishra et al., 2014, Al-Sharji et al., 1999b, Imqam, 2015, Lewis, 2014, Sidiq, 2007, Askarinezhad et al., 2016, Li et al., 2014, Mennella et al., 1998). However, the swelling/shrinkage process for RPMs depends not only on osmotic force (which causes swelling) but also on the elasticity (which restrains the swelling)(Imqam, 2015). It is also argued that when oil/gas droplets are forced to flow through gels, the droplets

compress the gel and create a path through the center of the channel. When the droplets move forward, the gel regains its original position. These movements, i.e. the opening and closing actions of the gel, are temporary and reproducible due to gel elasticity(Al-Sharji et al., 2001b, Al-Shajalee et al., 2020b, Dawe and Zhang, 1994), see Figure 2-16.

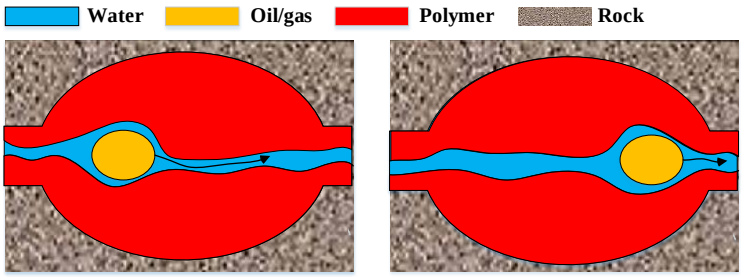

Figure 2-16: the opening and closing actions of the gel during oil/gas flowing due to gel elasticity

Furthermore, the literature explains that oil droplets can flow through the gel if capillary forces overcome the gel elastic force(Liang and Seright, 1997, Liang et al., 1995). In short, the capillary forces tend to keep or minimize the oil droplet radius thus keeping a path open through the gel layer, whereas the elastic forces of the gel layer tend to close this path(Liang and Seright, 1997, Liang et al., 1995, Kalfayan and Dawson, 2004, Nguyen et al., 2006, Hajilary et al., 2015a). Therefore efficient gel should be highly water-soluble and soft enough, thus the gel layer is easily compressed by capillary pressure so oil relative permeability is less affected(Omari et al., 2006). In other words, rheological behavior for shutoff gels should be well understood and monitored(Omari et al., 2006).

2.4 Conclusion

Excessive water production from oil and gas wells remains a key challenge for the oil and gas industry. To control this undesired water production, polymer treatments are often used. However, the success of polymer RPM treatment depends on a proper understanding of the factors influencing the polymer/rock/fluid interactions. This review, therefore, provides a comprehensive evaluation of all the possible mechanisms that are related to polymer/rock/fluid interactions in porous media. A better understanding of these mechanisms

is crucial for successful RPM treatment and thus a considerable control on water production. Moreover, the mechanisms pertinent to RPM were often reported either separately or as a combination of two or more mechanisms, however, their sequential order was not clear or was least emphasized. Thus, this review also provides a sequential order of RPM mechanisms.

The following conclusions can be drawn from this review:

1) The adsorption of polymers in porous media is a primary mechanism for the DPR.
2) Rock initial wettability and the associated fluid/polymer-rock interactions are significantly related to polymer adsorption. Polymers should be nominated based on their ability to exhibit strong attraction with the rock surface to maximize the adsorption and polymer layer stability. Polymer/rock interactions depend not only on the ionic charge of polymers but also on the brine composition, ionic charge, and ionic strength. Variable brine ionic strength may unfold two consequences: 1) increase/decrease adsorption, and 2) swell/shrink the adsorbed polymer layer.
3) The factors such as polymer concentration, polymer molecular weight, aging time, polymer injection volume, polymer injection rate, and reservoir temperature play a significant role in polymer adsorption.
    a) Increasing the concentration of the injected polymer enhances polymer adsorption.
    b) While increasing polymer molecular weight increases its adsorption, lower molecular weight polymers may still be preferred to avoid injectivity and fluid plugging problems.
    c) As polymer aging time increases, the static adsorption of a polymer increases until it reaches a maximum value (plateau, equilibrium, or saturation).
    d) With the increase in the pore volume of the injected polymer, the dynamic polymer adsorption increases due to polymer-polymer entanglement until it levels off due to adsorption saturation.

e) As the polymer injection rate increases, the adsorption amount and the hydrodynamic thickness of the adsorption layer also gradually increases. There is a critical polymer injection rate below which the adsorbed layer thickness is independent of the injection rate. At high hydrodynamic forces, flexible polymers can experience a coil-stretch transition which can lead to irreversible polymer adsorption onto pore walls Nevertheless, there is another critical injection rate after which the adsorption becomes almost stable.

f) Temperature tends to increase polymer adsorption followed by a flattening with further temperature rise. However, high temperatures (for example > 120 °C) compromise RPM's stability.

4) Fluid segregation has been identified as a crucial mechanism for DPR. The key trend is that water and oil/gas flow in separate pathways of a porous media or in defined parts of a pore, thus water-based DPR fluid only affects the water network with less or no effect on oil/gas fluid.

5) Wall effect, which is basically due to the presence of the adsorbed polymer layer onto the pore wall, is expected to induce one or a combination of sub-effects that altogether determine the outcome of RPM treatment, and these include: steric effect, lubrication effect, wettability modification effect, and swelling/shrinking effect. The steric effect is defined as a physical pore size restriction that can be caused by the firm and impenetrable layer of the adsorbed polymer on the pore walls. A greater polymer thickness induces a greater water permeability reduction, provided that the polymer layer thickness is not too large thus the minimum effect on non-wetting fluids. Lubrication effect and/or wettability alteration towards water wet counterbalance or compete for steric effect toward less effect on non-wetting phase which eventually aids in DPR. Moreover, the swelling/shrinkage mechanism can help to selectively adjust the polymer layer thickness (i.e. steric effect) depending on flowing fluid (i.e. RPM swells during water flow and shrinks during oil/gas flow) and eventually achieve DPR.

6) A more consistent agreement is found among the studies on the mechanism order that initial rock wettability effect comes first, followed by initial segregation, then adsorption, wall effects (i.e. steric, lubrication, wettability alteration and swelling/shrinkage effects) and then the final segregation.

Chapter 3: Effective Mechanisms to Relate Initial Rock Permeability to Outcome of Relative Permeability Modification

3.1 Introduction

According to the Paris Agreement, the global 2030 agenda for promoting sustainable and clean energy development, 195 countries have pledged to formulate an energy structure that focuses on the utilization of non-fossil resources and natural gas**.** Although natural gas is a fossil fuel, it has been given consideration in the Agreement because its combustion can result in less than half the carbon emissions produced by its coal and oil counterparts. The above is in general indicative of the fact that natural gas is entering a significant development, producing and consuming phase (Wood, 2016b, Wood, 2016a, Xu et al., 2019, Li and Lu, 2019, Cascio et al., 2018, Khan et al., 2019, Qyyum et al., 2019, Yang et al., 2016). However, with many reservoirs reaching their maturity, excessive water production has turned into a major challenge to field operators. It is widely known that water production can lead to a considerable reduction in the productivity of gas wells in particular(Chen et al., 2019b). Furthermore the operating costs associated with handling the water can be as much as $4 per every barrel of the water produced costing the oil and gas industry billions of dollars every year (Kalfayan and Dawson, 2004). It is worth noting that these costs are associated with only treating the water and not associated effects such as corrosion, loss of hydrocarbon production, etc.(Pusch et al., 1995, Evans, 2001, Inikori, 2002, Reynolds, 2002, Mohanty, 2003, Karimi et al., 2014a, Hajilary et al., 2015). Therefore, it is highly desirable to develop viable techniques that can help to reduce the amounts of water produced so the environmental profile of natural gas, as a low carbon transition fuel, can be further improved.

Chemical treatments have been utilized to reduce water production. One class of material that has received widespread attention, due to their outstanding performance, are relative permeability modifiers (RPM) that can selectively reduce the permeability to water while having minimal effect on oil/gas. To date, most studies have focused on the use of RPMs to reduce water production from oil reservoirs, therefore, there is a need for studies focusing on gas reservoirs, as mentioned earlier, since natural gas is deemed as a transition fuel as we move towards renewable sources.

Gas wells have distinct characteristics compared to the oil wells such as special fluid properties (e.g. low viscosity and density of gas) and high production flowrates. Therefore,

the selective behavior of the RPMs to reduce water permeability rather than that of the gas phase may not be as straightforward as that expected for oil wells. That is because factors such as viscosity, capillary pressure and density play important roles in the selective placement of the RPM in the water producing zones and their subsequent behavior. Furthermore, water control in gas wells is not practiced commonly because of the risk of face plugging with high molecular weight polymer solutions(Pusch et al., 1995, Dovan and Hutchins, 1994). Thus, there are only few works in the literatures on the use of polymer treatment in gas reservoirs (Elmkies et al., 2002, Tielong et al., 1996, Ranjbar and Schaffie, 2000, Zaitoun and Pichery, 2001, Zaltoun et al., 1991, Dovan and Hutchins, 1994, Burrafato et al., 1999, Karimi et al., 2014b, Lockhart and Burrafato, 2000, Kalfayan and Dawson, 2004, Nieves et al., 2002, Song et al., 2015, Alshajalee et al., 2019, Chiappa et al., 1997, Chiappa et al., 1999, Mennella et al., 1998, Sharifpour et al., 2016).

The existing literature have reported different physical mechanisms around the mode of action of RPMs. These include wall effect, swelling/shrinking effects, and change in the fluid distribution, with the wall effect considered as the primary mechanism (Zaitoun and Kohler, 1988, Tielong et al., 1996, Zaitoun et al., 1998, Elmkies et al., 2002, Nieves et al., 2002, Dawe and Zhang, 1994, Dovan and Hutchins, 1994, Zaitoun and Pichery, 2001, Alshajalee et al., 2019). In general, the adsorbed polymer layer affects the internal grain surfaces of a rock by causing a wettability change, steric effect and lubrication effect. Solely from steric considerations the adsorption of the polymer onto pore surfaces may reduce the cross-sectional area at the pore throats (or regulate the effective pore throat diameter) for all fluids, thus decrease both water and oil relative permeabilities(Zaitoun and Kohler, 1988, Kalfayan and Dawson, 2004). In addition, the polymer layer may induce a lubricating effect to the non-wetting phase and/or modification of its velocity distribution in the pore channels. Consequently, the non-wetting (gas) phase relative permeability may even experience an increase (Zaitoun and Kohler, 1988, Alshajalee et al., 2019). Moreover, the thickness of the polymer layer may vary with time due to the effects of other parameter such as the fluid phase in the pore space, flowrate (shear rate) and the rheological properties of the polymer (Mennella et al., 1998, Grattoni et al., 2001a, Mishra et al., 2014, Al-Sharji et al., 2001b, Al-Sharji et al., 1999c, Song et al., 2015, Cohen and Christ, 1986, Saphiannikova et al., 1998, Zaitoun and Kohler, 1988).

Furthermore, Grattoni et al.(2001) and Zhang et al.(2017) indicate that during multiphase flow in porous rocks the end-point relative permeabilities are controlled by the fluid

distribution(Grattoni et al., 2001c, Zhang et al., 2017). Zaitoun and Kohler(1988) and Grattoni et al.(2001) also report that fluid distribution in turn depends on pore size distribution of the rock (Zaitoun and Kohler, 1988, Grattoni et al., 2001c, Zhang et al., 2017). Grattoni et al.(2001) propose that after a polymer treatment the induced changes in the pore sizes and the subsequent redistribution of the wetting and non-wetting fluids caused by the polymer are the main cause of the disproportionate permeability reduction (DPR) (Grattoni et al., 2001c). Therefore, analyzing and reporting experimental results with special attention to the role of the adsorbed polymer layer or induced changes in rock pore radii may be insightful and meaningful.

Kalfayan and Dawson(2004) and Qi et al.(2013) claim that the original rock permeability plays an important role in controlling the success of an RPM treatment (Kalfayan and Dawson, 2004, Qi et al., 2013). With the use of different moderate permeability rocks (100-1000mD), various brines (salinity≥1% TDS), different types of polymers and different polymer concentrations (1000-8000ppm), experimental results have shown slight decrease in RPM's performance when the initial rock permeability increases. At the same time, the change in the relative permeability of non-wetting phases (gas and oil) is reported to be much smaller than the reduction to the wetting phase (water) (Mennella et al., 1998, Qi et al., 2013, Elmkies et al., 2002, Zaitoun and Pichery, 2001, Burrafato et al., 1999, Jinxiang et al., 2013, Alshajalee et al., 2019, Chiappa et al., 1997). However, Mennella et al. and Qi et al. report dramatic decrease in RPM's performance when the initial rock permeability increases from medium (100-1000mD) to high (>1000mD) (Mennella et al., 1998, Qi et al., 2013). There are far fewer studies on low permeability rocks. However, Chiappa et al. and Tielong et al. report the same trend as above, similar to the medium and high permeability rocks, in rocks that may be classified as having low permeability (k<100mD) an RPM treatment may affect the permeability to the non-wetting hydrocarbon phase (gas) to a lesser extent (Chiappa et al., 1997, Tielong et al., 1996). It is worth mentioning that Tielong et al. used a brine with about 0.2% TDs in their study (Tielong et al., 1996). Sharifpour et al. and Zaltoun et al. show that brine salinity would play an important role in water shutoff treatment especially in low permeability rocks (Sharifpour et al., 2016, Zaltoun et al., 1991). Zaltoun et al. report that the polymer layer thickness depends on the brine salinty (Zaltoun et al., 1991). Sharifpour et al. conclude that increasing the brine salinity decreases the gas phase accessibility to pores in low permeability media (Sharifpour et al., 2016).

In principle, the critical question in RPM treatment is how to reduce the relative permeability to water but minimize any effect on the non-wetting hydrocarbon phase. This study examines experimentally the performance of a cationic polymer as an RPM agent for a gas/water system in a number of sandstone rocks with different permeabilities. Using the data generated, the underlying mechanisms behind the DPR effect of the RPM agent are discussed. The discussions reveal that the significance of such mechanisms may depend on the permeability of the rock sample being tested. The data generated and the discussions presented are expected to be of broad interest to the technical community and in particular, those concerned with the gas/water system where relevant data are very limited.

3.2 Experimental work

3.2.1 Materials

Eight sandstone core samples (from six different sandstone rock types) with a nominal length and diameter of 7.6 cm and 3.8 cm, respectively were used in this study (Table 3-1). As can be seen from the contact angle values reported, the samples are strongly water-wet in the presence of nitrogen that forms our non-wetting phase. The IFT700 instrument (Vinci Technologies, France) was used to do contact angle measurements using the Sessile Drop approach under the experimental conditions used during our core-flooding experiments as will be defined later. We classified the samples based on their permeabilities into the three categories of low (< 100mD), moderate (100-1000mD) and high (> 1000mD) permeability. The mineralogies of the rocks were typical of a sandstone rock (Table 3-2) as confirmed by X-Ray Diffraction (XRD).

The brine (2wt% KCl) used in these experiments was prepared by adding 20 g/L of analytical grade KCl (Sigma-Aldrich) into distilled water. KCl aqueous ionic solution was selected to examine the effect of rock permeability on the performance of RPM. This is because that KCl would work as a temporary clay stabilizer, which would enable us to solely focus on the effect of rock permeability on the performance of RPM. High purity nitrogen (99.99wt%, BOC Gas) was used as the gas phase to flood the samples. The RPM solution (Table 3-1) was made by dissolving cationic Poly(acrylamide-*co*-diallyldimethylammonium chloride) at 1000ppm concentration in the above mentioned synthetic brine.

It is worth noting that some of our rock samples, in addition to quartz, contained high proportions of other minerals such as albite, illite/muscovite, etc. However, the presence of these minerals may not greatly interfere with the interactions of the RPM solution with the pore surfaces of these rock samples under our experimental conditions. That is because the above minerals would be predominantly negatively charged (Nasralla and Nasr-El-Din, 2014b, Blum and Lasaga, 1991, Shehata and Nasr-El-Din, 2015) and therefore are expected to behave similar to quartz in their interactions with the cationic polymer solution used in this work.

Table 3-1: Basic petrophysical characteristics of core samples as categorised based on their permeability. The error of the permeability measurements are about ±0.05 mD, 0.1 mD and 5mD for the low, moderate and high permeability ranges, respectively.

Sample No.	**Sample name**	**Contact angle (±2°)**	**Porosity, % (±0.1%)**	**Nitrogen permeability, mD**	**Permeability category**
1	Socito	2.9	17.7	2.7	Low
2	Gray Bandera	0.7	20.0	22.7	
3	San Saba	1.3	19.5	66.4	
4	Berea1	2.4	21.9	350.0	Moderate
5	Berea2	2.4	21.0	385.0	
6	Bentheimer1	2.4	23.0	3001	High
7	Bentheimer2	2.4	24.0	3488	
8	Boise	1.0	29.0	5035	

Table 3-2: Mineralogy of rock samples determined using XRD analysis.

	Socito	**Gray Bandera**	**San Saba**	**Berea**	**Bentheimer**	**Boise**
Phase	**Weight%**					
Quartz	88.2	57.7	91.5	81.2	91.1	37.3
Microcline	1.8	1.3	2.3	4.8	6	21.1
Kaolin	5.2	5.4	3.3	5.7	2.9	-
Illite/Muscovite	1.2	10.2	0.9	4.5	-	10.7
Albite	2.7	18.8	1.9	3.0	-	29

Dolomite	0.8	3.9	-	0.5	-	-
Calcite	-	0.2	-	0.3	-	-
Chlorite	0.8	2.5	-	-	-	-
Stilbite	-	-	-	-	-	2

3.2.2 Rheological properties

A HAAKE RheoWin rheometer was used to determine the effect of shear stress on shear rate for our 1000ppm RPM solution. As depicted by Figure 3-1, the viscosity of the solution changes depending on the shear stress applied so it is exhibiting a non-Newtonian shear thickening behavior. This behavior would be desirable for effective delivery of the solution to a porous formation at any scale (i.e. from core/laboratory scale to the wellbore scale).

Table 3-3 The RPM agent used in this study.

Name	Poly(acrylamide-*co*-diallyldimethylammonium chloride)
Molecular Structure	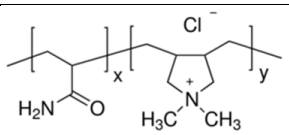
Formula	$(C_8H_{16}ClN)_n.(C_3H_5NO)_m$
Molecular Weight	25000 g/mole
Density	1.02 g/cm^3 at 25 °C
Manufacturer	Sigma-Aldrich

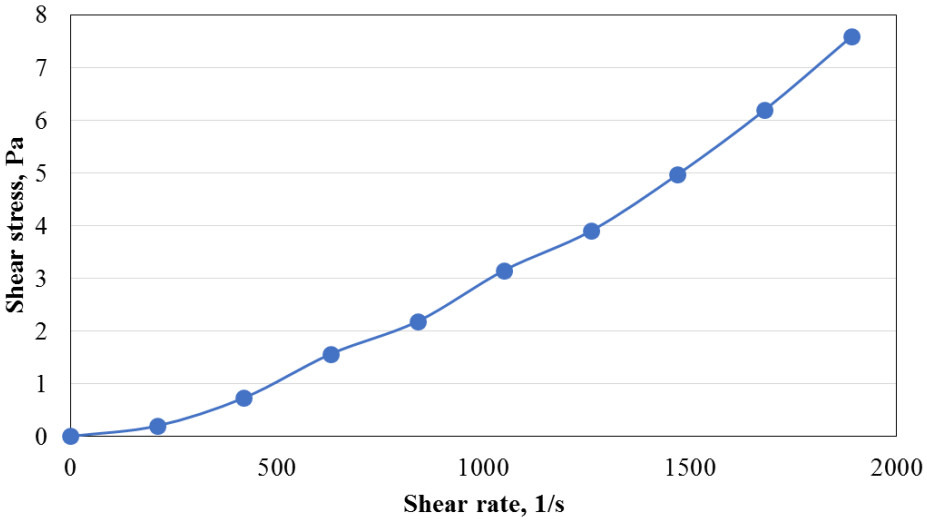

Figure 3-1: The RPM solution exhibits a Newtonian shear thickening behaviour.

3.2.3 Core-flooding procedure and formulations

Figure 3-2 shows a schematic diagram of the instrument used in this work during the core flooding experiments. The rock samples were subjected to a specially designed core-flooding procedure after their initial petrophysical characterization in accordance with the three main stages described below. This flooding procedure, not only enabled us to determine the critically required end-point relative permeabilities to every phase before and after the RPM treatment, but also made it possible to examine the effect of injection flow rate on the performance of the RPM solution used. It is worth noting that a brief version of the flooding procedure is included in this manuscript, as the detailed procedure has been presented elsewhere in our previously published work(Alshajalee et al., 2019).

Before undergoing the flooding procedure, the samples were initially dried in an oven at 65℃ for a period of 24 hours or until reaching weight stability. Subsequently, nitrogen gas was used to measure their porosity and permeability with the relevant data reported in Table 3-1. The AP-680 Automated Permeameter Porosimeter (Coretest Systems Inc., US) has been used for porosity and permeability measurements. This equipment uses a technique based on the Boyle's Law to measure porosity and a pulse decay technique to measure the permeability.

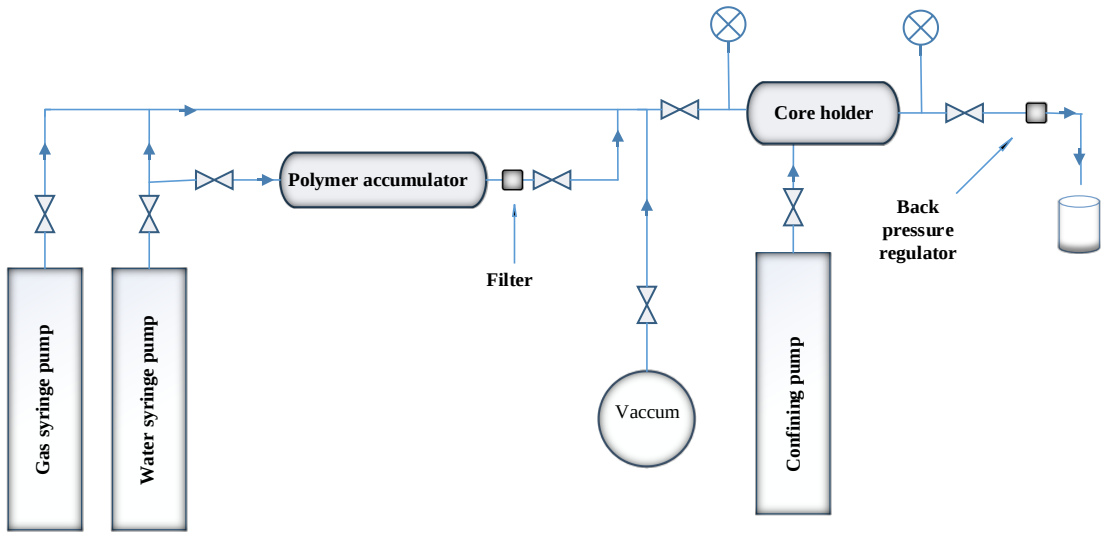

Figure 3-2: Schematic diagram of the core flooding setup.

In this stage, after being vacuumed and brine saturated, the brine permeability of a sample would be measured using a multi-rate brine injection procedure. Subsequently, the samples would be subjected to a sequence of first multi-rate nitrogen and then multi-rate brine (1-160 cc/min) injection, within the Darcy flow regime (Equation 8) (Montillet et al.,

1992). Such constant rate injection steps would be required to determine the necessary irreducible water (S_{wirr}) and residual gas (S_{gr}) saturations as well as the end-point relative permeability of gas at irreducible water saturation ($k_{rg1}(S_{wirr})$) and that of brine at residual gas saturation ($k_{rw1}(S_{gr})$).

1. RPM Treatment:

For effective treatment, three pore volumes of the RPM solution were then pumped through the rock sample and the rock/RPM system was left to age under experimental conditions for 48 hours. The injection flow rate used to deliver the RPM agent was chosen according to the permeability of the sample being tested. It was set at 0.1 cc/min in low permeability samples and 1 cc/min for the moderate and high permeability ones.

2. Post-RPM Treatment Stage:

As part of stage 3 of the flooding procedure, initially a constant flow rate of brine was used to remove any unreacted RPM solution from the pore space of the sample. Subsequently, the sequence of multi-rate gas and brine injections referred to in the description of the first flooding stage were repeated. This was necessary to determine the required post treatment values of S_{wirr} and S_{gr} as well as the relative permeabilities to both brine ($k_{rw2}(S_{gr+polymer})$) and gas ($k_{rg2}(S_{wirr+\ polymer})$) phases which may have been altered due to the presence of the RPM solution.

It is worth noting that the gas relative permeability was measured by injecting gas under constant flow rate until no more brine was produced and achieving constant differential pressure across the sample (i.e. establishing irreducible water saturation (S_{wirr}). A similar procedure was followed to measure the water relative permeability by establishing residual gas saturation (S_{rg}).

In order to proceed with evaluating the outcome of the RPM treatments performed, the above measured data were subsequently used to obtain a number of critical parametric values using the equations outlined below. Some of these equations were included and discussed in our previous publication(Alshajalee et al., 2019), however, we are presenting them in this manuscript again for the ease of referencing and also to make the explanations and discussions presented here complete on their own.

We calculated the water and gas residual resistance factors (Frr_w and Frr_g) using the equations proposed in the literature(White et al., 1973) as a conventional way of determining the outcome of the RPM treatment.

$$Frr_{w=} \frac{K_{before}}{K_{after}} \quad 1$$

$$Frr_{g=} \frac{K_{before}}{K_{after}} \quad 2$$

where; K_{before} and K_{after} are the experimentally measured end-point relative permeability of water/gas before and after the polymer treatment, respectively. The Darcy equation was used to calculate the above permeability values upon reaching steady state conditions. If $Frr_w > 1$ and $Frr_g \approx< 1$ (resulting in $Frr_w/Frr_g > 1$) the RPM treatment may be considered successful. Subsequently, as proposed in the literature, the effective value of the hydrodynamic polymer layer thickness (in μm) adsorbed onto the sample's pore surfaces may be calculated using the equation below (Zaitoun and Kohler, 1988).

$$\mathbf{e = r\left(1 - \frac{1}{Frr^{0.25}}\right)} \quad 3$$

where Frr is the residual resistance factor as defined by equations 1 or 2 and r is the overall average pore radius (μm) of the rock as calculated using Equation 4.

$$\boldsymbol{r = \left(\frac{8\, k_{brine}}{\varphi}\right)^{0.5}} \quad 4$$

where, k_{brine} is the absolute brine permeability (calculated using the Darcy equation) and ϕ is the porosity of a rock sample.

Of note is that depending on the Frr value used (Frr_w or Frr_g), two potentially different values of e (e_w or e_g) may be calculated. Subsequently, r_{eff} or the effective average pore radius (in μm) after the RPM treatment may be calculated using the following equation (Alshajalee et al., 2019).

$$\boldsymbol{r_{eff} = r - e} \quad 5$$

The Young-Laplace equation to calculate capillary pressure for a given pore size is presented below.

$$P_c = \frac{2\,\sigma\,\cos\theta}{r} \qquad 6$$

where P_c is the capillary pressure, σ the interfacial tension, θ the contact angle and r the pore radius. As demonstrated by our contact angle data, in the presence of the strongly non-wetting nitrogen phase, the sandstone rock samples are strongly water-wet or $\theta \approx 0$ which may further simplify the above equation by reducing the term $\cos\theta$ to 1.

The following equation may be used to calculate the average interstitial velocity (Vsi) in cm/sec for fluid flow in porous rocks (Kuo, 2014).

$$Vsi = \frac{Q}{A * \varphi} \qquad 7$$

where, Q is fluid flow rate (cm^3/sec), A the core cross sectional area (cm^2) and ϕ the porosity (fraction) of the rock sample.Lastly, the following equation is used to calculate the interstitial Reynold's number (Rei) , which corresponds to the ratio of inertial forces to the viscous ones (Montillet et al., 1992). This equation is used to determine the fluid flow regimes in porous rocks.

$$Rei = \frac{\rho\,d\,Q}{\mu\,\varphi\,A} \qquad 8$$

where, ρ and μ are the density (g/cm^3) and the dynamic viscosity (Pa-s) of the fluid, respectively, d is the pore equivalent diameter (cm) and parameters Q, A and ϕ have the same meaning and units as that in Equation 7.

3.3 Results and Discussions

Presented in Table 3-4 are the Frr_w and Frr_g values and their ratios for all core plugs examined as calculated using the results of the core-flooding experiments. Every Frr value included in the table is the calculated average value over the 1-4 cm^3/min flow rate range for every fluid phase. It is worth noting that, depending on their initial permeability, some rock samples were tested using flow rates beyond this range. However, the above mentioned range was common across all the rock samples making a comparison between their responses to the RPM treatment meaningful. The individual Frr_w and Frr_g values calculated for every flow rate used can be found in figures 11-12.

Table 3-4: The average $\mathbf{Frr_w}$, $\mathbf{Frr_g}$ and $\mathbf{Frr_w/Frr_g}$ calculated over the 1-4cc/min flow rate range.

Rock name	Porosity, %	Initial Permeability, mD	r, µm (Equation 4)	Permeability category	Frr_g	Frr_w	Frr_w/Frr_g
Socito	17.66	2.7	0.17	Low	6.20	2.35	0.40
Gray Bandera	20.0	22.7	0.58		4.60	2.00	0.45
San Saba	19.5	66.4	1.10		7.60	1.44	0.20
Berea1	21.0	350.0	4.20	Moderate	0.928	2.86	4.20
Berea2	21.0	385.0	4.10		0.90	2.3	2.6
Bentheimer1	23.0	3001	5.80	High	1.00	1.75	1.75
Bentheimer2	24.0	3488	11.40		1.17	1.21	1.04
Boise	29.0	5035	16.00		1.32	1.38	1.05

For visual elaboration, the Frr_w, Frr_g and then their ratio are plotted in Figure 3-3 and Figure 3-4, respectively, against rock permeability.

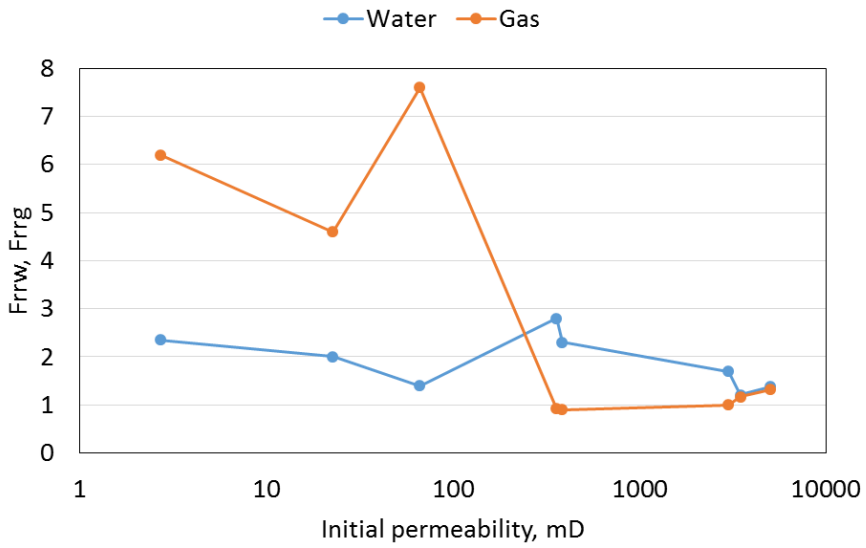

Figure 3-3 Behaviour of water and gas residual resistance factors (Frr_wandFrr_g) versus initial rock permeability (Socito (2.7 mD); Gray Bandera (22.7 mD); SanSaba (66.4 mD); Berea1 (350 mD); Berea2 (385 mD); Bentheimer1(3001); Bentheimer2(3488) and Boise (5035 mD).

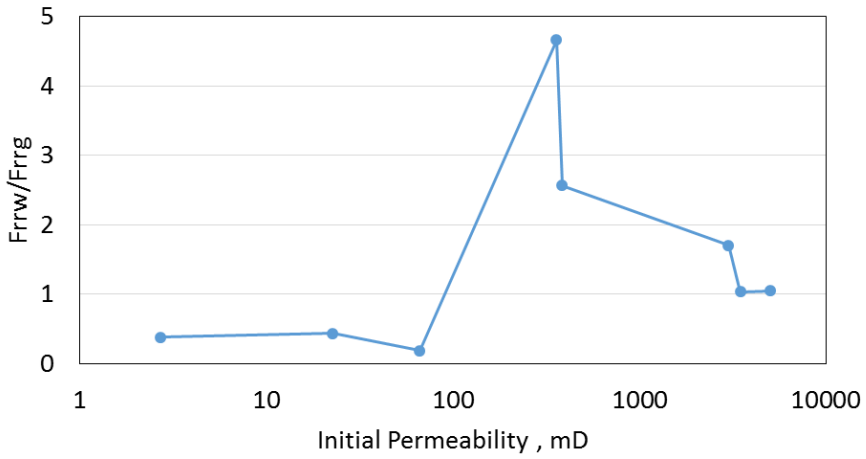

Figure 3-4: Behaviour of residual resistance factor ratio (Frr_w/Frr_g) against initial rock permeability (Socito (2.7 mD); Gray Bandera (22.7 mD); SanSaba (66.4 mD); Berea1 (350 mD); Berea2 (385 mD); Bentheimer1(3001); Bentheimer2(3488) and Boise (5035 mD).

The effect of rock permeability on the RPM treatment examined in this work was explored by evaluating the data presented in Figure 3-3 and Figure 3-4 in the context of the three permeability categories defined for our rock samples in Table 3-4. As can be seen, for moderate permeability rocks, the water relative permeability decreases after the polymer treatment. However, the gas relative permeability either does not change significantly or improves slightly. Therefore, for all rock samples in this permeability range $Frr_w \gg 1$ and $Frr_g \approx< 1$ (Table 3-4 and Figure 3-3), with the same treatment sequence which means the treatment may be considered successful. According to this criteria, various literature have reported a similar trend with the use of different moderate permeability rocks (100-1000mD), various brines (salinity≥1% TDS), different types of polymers and different polymer concentrations (1000-8000ppm) (Mennella et al., 1998, Qi et al., 2013, Elmkies et al., 2002, Zaitoun and Pichery, 2001, Burrafato et al., 1999, Jinxiang et al., 2013, Alshajalee et al., 2019, Chiappa et al., 1997). A summary of such findings is included in Table 3-5.

Table 3-5: Literature review on the outcome of RPM treatment in moderate permeability rocks (100-1000mD).

Literature	Non-wetting phase	Wetting phase	Rock type	Permeability, mD	RPM agent and concentration	Frr_w	Frr_g
(Elmkies et al., 2002, Burrafato et al., 1999)	Gas	Brine	Sandstone	318	Polyacrylamide, Non-ionic, 2500 ppm	21	1.7
(Burrafato et al., 1999)	Gas	Brine	Sandpack	203	Polyacrylamide, Cationic, 2000 ppm	5.1	1.3
				380		7.1	1.1
(Chiappa et al., 1997)	Gas	Brine	Sandstone	120	Polyacrylamide, Cationic, 2000 ppm	5.6	2.1
				330	Polyacrylamide, Non-ionic, 2000 ppm	3.8	1.5
				690	Polyacrylamide, Cationic, 2000 ppm	4.5	1.3

However, in the high permeability rocks the water and gas relative permeability reductions are almost the same resulting in $Frr_w \approx 1$ and $Frr_g \approx 1$. Similarly, experimental results by Mennella et al. and Qi et al. show dramatic decrease in RPM's performance when the initial rock permeability increases from medium (100-1000mD) to high (>1000mD) (Mennella et al., 1998, Qi et al., 2013) especially for the gas-water system (Table 3-6). Therefore, using higher polymer concentration may help to increase permeability reduction (Chiappa et al., 1997, Chiappa et al., 1999, Grattoni et al., 2001a, Mennella et al., 1998, Ogunberu and Asghari, 2004a, Mishra et al., 2014, Zheng et al., 1998, Qi et al., 2013). However, beyond a certain concentration no further adsorption takes place due to saturation of the adsorption capacity of the active adsorption sites (Qi et al., 2013, Chiappa et al., 1997, Zheng et al., 1998, Tekin et al., 2005, Tekin et al., 2010). Therefore as indicated in the literature, using gels to treat high (and even moderate) permeability rocks may be more

effective than using polymers (Burrafato et al., 1999, Lockhart and Burrafato, 2000, Kalfayan and Dawson, 2004, Zaltoun et al., 1991, Karimi et al., 2014b).

Table 3-6: Outcome of literature review on treating moderate (100-1000mD) to high (>1000mD) permeability rocks.

Literature	**Non-wetting phase**	**Wetting phase**	**Rock type**	**Permeability, mD**	**RPM agent and concentration**	**Frr_w**	**Frr_o/Frr_g**
(Mennella et al., 1998)	Gas	Brine	Sandstone	900	Plyacrylarnide, cationic, 2000 ppm	10	1.2
				2000		1.9	1.1
	Oil			600		2.6	1.1
				2000		1.8	1
(Qi et al., 2013)	Oil	Brine	Sandstone	263	Plyacrylarnide, cationic, 2000 ppm	7.7	1.84
				578		6.8	1.49
				1,139		5.3	1.41
				2,300		5	1.35

In the low permeability category (Table 3-4), consistently across all samples $Frr_g \gg 1$, $Frr_w > 1$ resulting in $Frr_w/Frr_g \ll 1$ (Figure 3-3) meaning that the RPM treatment has reduced the relative permeability to both fluid phases. However, since for all samples (Figure 3-4), such reductions would be much more pronounced for the gas phase than the water phase. In other words, the treatment is considered unsuccessful in this category of rocks. However, Chiappa et al. and Tielong et al. reported a different trend using rocks that may be classified as having low permeability (k<100mD) where they indicate that an RPM treatment may affect the permeability to the non-wetting hydrocarbon phase (gas) to a lesser extent (Chiappa et al., 1997, Tielong et al., 1996). It is worth mentioning that Tielong et al. used a brine with about 0.2% TDs in their study (Tielong et al., 1996). Sharifpour et al. and Zaltoun et al. showed that brine salinity would play an important role in water shutoff treatment especially in low permeability rocks (Sharifpour et al., 2016, Zaltoun et al., 1991). Zaltoun et al. reported that the polymer layer thickness depends on brine salinty (Zaltoun et al., 1991). Increasing the brine salinity may increase the polymer layer thickness and eventually this

may decrease the gas phase accessibility to small pores in low permeability media (Sharifpour et al., 2016). Therefore the low permeability candidates may require special RPM technology since the treatment of such formations may be associated with several problems such as plugging, loss of injectivity and limited depth of pentration (Ranjbar and Schaffie, 2000, Noik and Audibert, 1993).

The results presented above may find support in the pre- and post-treatment pore-size and fluid distributions of the different rock samples. As naturally expected and revealed by the calculated values in Table 3-4, as the permeability of a rock increases, its overall pore sizes become larger. This is also visually demonstrated in Figure 3-5, noting that our rock samples to be water-wet in the presence of nitrogen gas. Before the treatment small pores (Figure 3-5-A1) would be fully saturated with the wetting phase (water) and inaccessible to the non-wetting gas phase for reasons of capillarity (Equation 6). On the other hand, in the moderate and large pores (Figure 3-5-B1&C1) the non-wetting phase flows in the center, and the wetting water phase is present in the form of a film covering the pore walls (Zaitoun and Kohler, 1988, Grattoni et al., 2001c). In summary the pore size distribution of a porous medium and hence capillarity in conjunction with wettability control the way fluids are distributed in the pore space of a porous medium.

As pointed out earlier Grattoni et al. have shown that after a polymer treatment, the induced changes in the pore sizes of a porous medium by the RPM and the subsequent redistribution of the wetting and non-wetting fluids are the main cause of DPR(Grattoni et al., 2001c). As a common phenomenon across all rock samples, the adsorbed polymer on the surface of the water-wet grains (Figure 3-5-A2, B2& C2) alters the effective pore size distribution by reducing their actual sizes. However, the relative pore size change (i.e. $\frac{e}{r}$) would be a function of rock's initial pore sizes and therefore would be different in different rock samples.

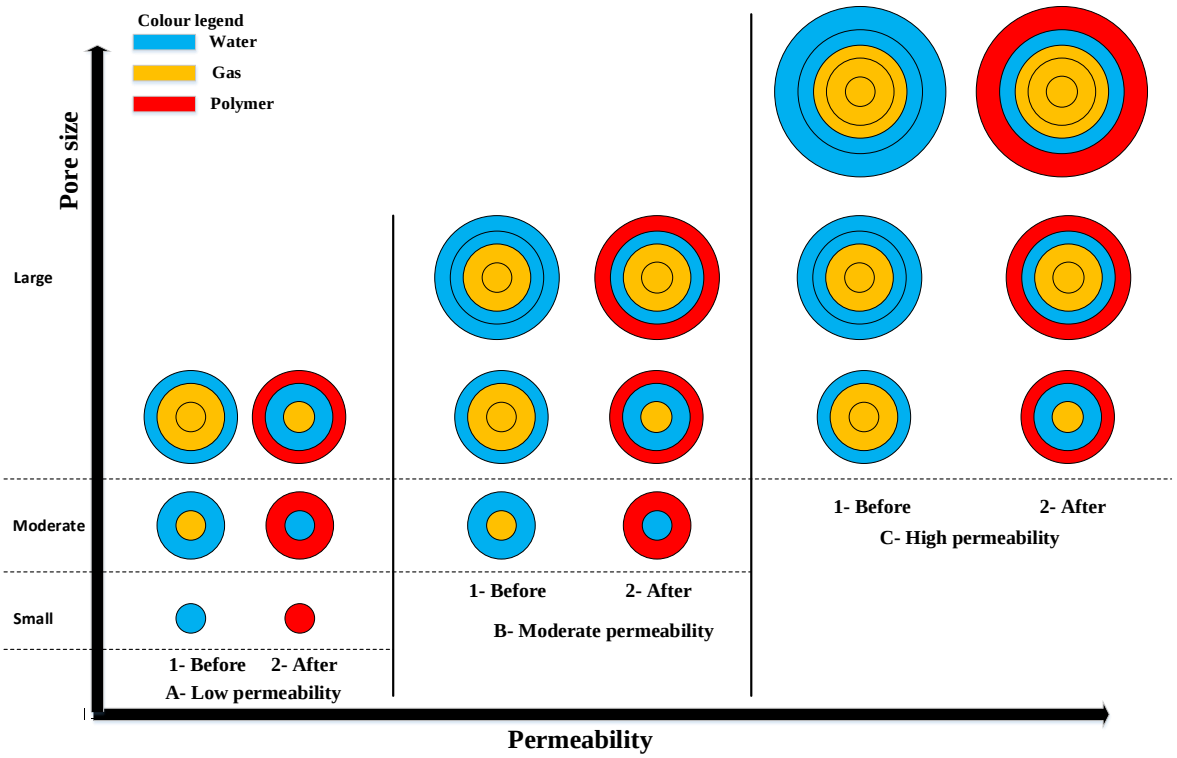

Figure 3-5: The effect of pore sizes distribution on fluid phases distribution before (B) and after (A) the RPM treatment.

As can be seen in Figure 3-5, after treatment, the very small pores that were previously filled with water (Figure 3-5-A1) may become plugged by immobile polymer (Figure 3-5-A2). The moderate pores, that were previously occupied by water and non-wetting phase simultaneously (Figure 3-5-A1 &B1), now have a smaller size (i.e. higher capillary pressure (Equation 6)) and therefore, becomes filled only by water (Figure 3-5-A2 &B2). The largest pores, however, may still remain relatively large so that they would be filled by both of water and gas phases simultaneously (Figure 3-5-A2, B2&C2).

The immediate conclusion from the above is that the amount of pore space available for each fluid to flow through reduces during the post-treatment stage. However, the nature of this reduction is different in samples with different permeabilities. In other words generally after treatment, the relative permeabilities to both of the wetting and non-wetting phases may be reduced. However, in the high permeability rocks, given its relatively larger pores, such a relative reduction is the lowest. This would mean that, as also revealed by our results presented earlier, with such a permeability range the effect of an RPM treatment would be of similar order on the wetting and non-wetting fluids relative permeabilities. Unlike high permeability media, the relative permeability reduction effect would be highly pronounced in low permeability rocks where the relative pore size reduction (i.e. $\frac{e}{r}$) would be the greatest.

In such media, gas (i.e. the non-wetting phase) cannot access a range of pore sizes at all initially due to their very small sizes and this range extends to even more pores after treatment. This means the gas relative permeability reduction may be the highest in a low permeability situation. This conclusion is supported by the experimental results as presented and discussed earlier. Judged based on the discussion presented so far, the best outcome from an RPM treatment may be expected in moderate permeability media. As seen from some of the results for moderate permeability rocks the gas relative permeability may even improve as attributed to influencing factors such as the lubrication effect induced by the adsorbed polymer(Zaitoun and Kohler, 1988, Alshajalee et al., 2019).

In general, the polymer layer thickness (e), as calculated using Equation 3, may increase with increasing rock permeability (i.e. increasing pore sizes). As can be seen from Figure 3-6 and Figure 3-7, the highest polymer layer thickness is observed in the highest permeability sample (i.e. Boise). As discussed earlier, the samples with moderate permeability (i.e. Berea Sandstone) exhibits an exceptionally favorable response to the RPM treatment. As seen from Figure 3-6 and Figure 3-8, this rock reveals negative polymer thickness at low gas flowrate meaning improvements in gas relative permeability during post RPM treatment. In addition, as revealed by Figure 3-3, these rocks show high water relative permeability reduction that would not follow the way the curves for all other rocks are arranged with respect to their permeability.

The low permeability rocks witness the highest effect of polymer layer since, as also indicated in our earlier discussions, the ratio between the polymer thickness and the original pore radius ($\frac{e}{r}$) decreases with increasing the rock permeability. Such a general trend can be seen in the data plotted in Figure 3-8 and Figure 3-9. In Figure 3-8, for low permeability rocks and at the lowest gas flow rate, the average e/r ratio is about 42% while it is in the negative region for the lowest flow rate tested in the moderate permeability samples. Similar results about low permeability rocks have also been reported by other researchers (Park et al., 2015). Park et al. treated low permeability sandstone samples (41-56mD) with 1,500 ppm of a polymer. This treatment resulted in 3.34 μm of polymer layer thickness, where, approximately, 59.8% of the pre-treatment pore radius was blocked. As discussed earlier these researchers also indicate that such an effect would result in a large permeability reduction to the non-wetting phase in particular. One overall conclusion from these results is that the the efficiency of an RPM treatment may strongly depend on the ratio of the adsorbed polymer layer thickness to original effective pore radius of the treated rock which on its own

is one of the major parameters controlling the rock permeability. Eventually this may affect the relative permeability of water and gas differently in each permeability range.

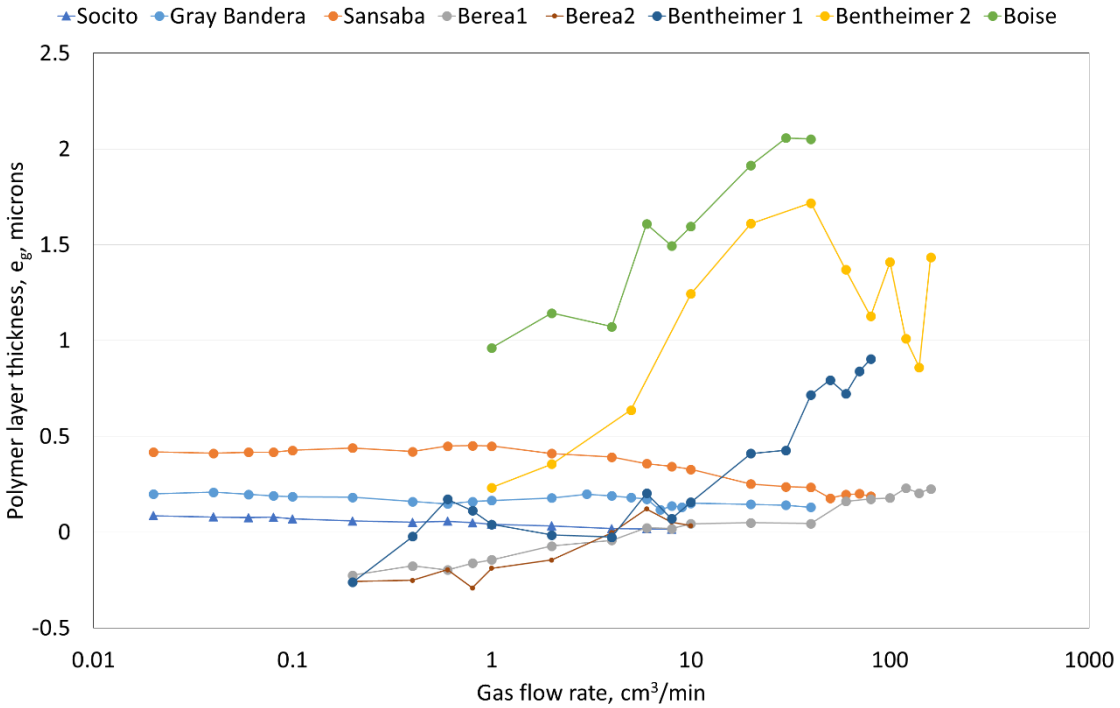

Figure 3-6: Change in polymer layer thickness versus gas flow rate in different rock samples (eg: the adsorbed polymer layer thickness calculated for the gas injection stage).

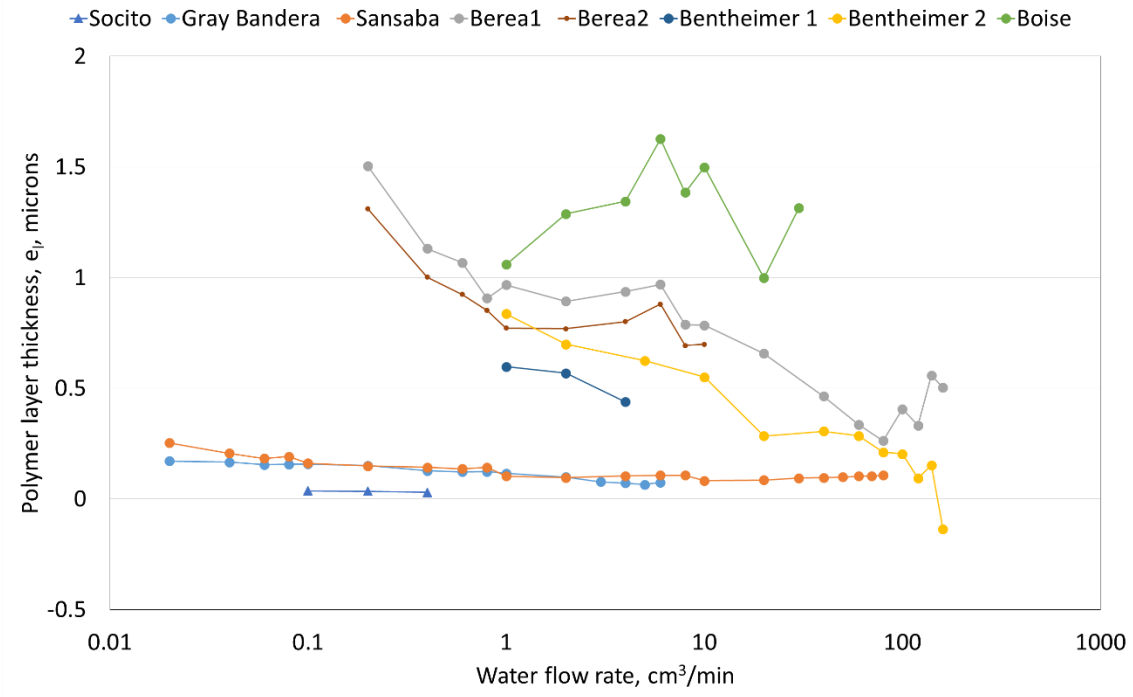

Figure 3-7: Change in polymer layer thickness versus water flow rate in different rock samples (e_l: the adsorbed polymer layer thickness calculated for the water injection stage).

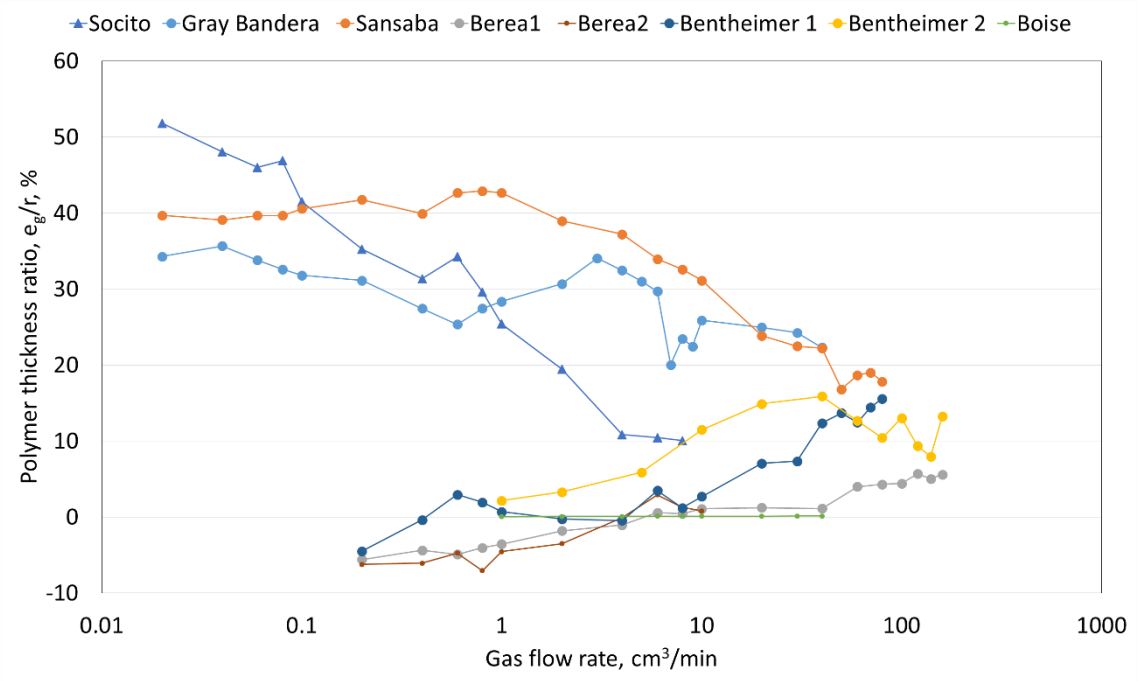

Figure 3-8: Change in the polymer thickness ratio versus gas flow rate.

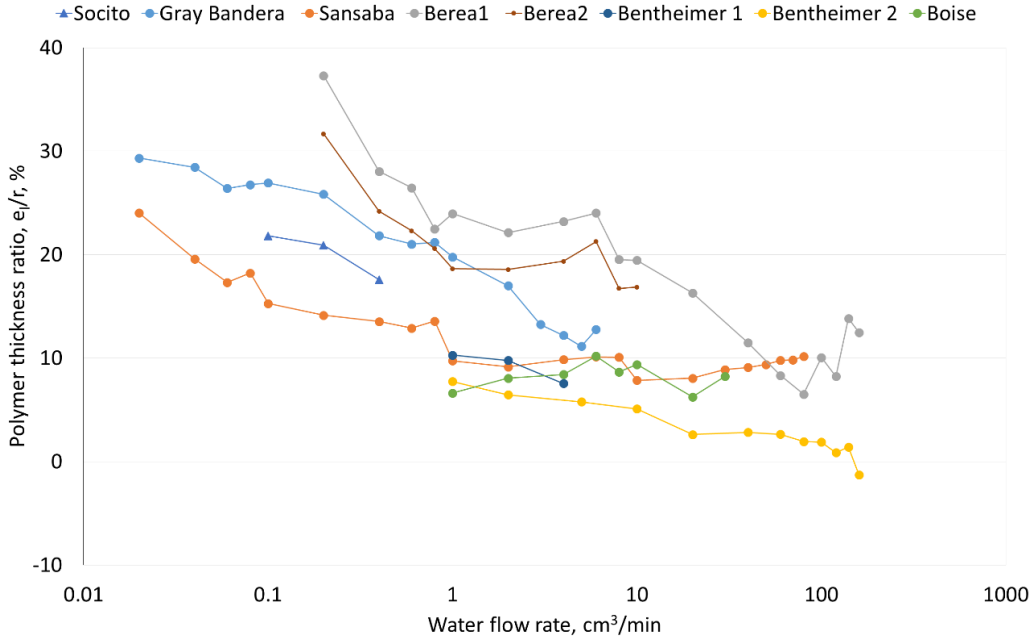

Figure 3-9: Change in the polymer thickness ratio versus water flow rate.

One more observation can be made from the data plotted in Figure 3-8 and Figure 3-9. As the gas flow rate increases the polymer thickness ratio ($\frac{e}{r}$) changes sharply in low permeability rocks. However, in moderate and high permeability rocks this trend in much

less steep. This behavior may be attributed, in general, to the fact that, at a fixed flow rate, the interstitial fluid velocity is higher in lower permeability rock which also has lower porosity. The higher velocity would tend to induce a higher force and cause the polymer layer to compress and therefore decrease in thickness. A similar behavior to that observed from the plots of polymer layer thickness ratio versus flow rate can be transcribed for the more commonly used treatment parameter of Frr_g and Frr_w which are plotted in Figure 3-10 and Figure 3-11, respectively.

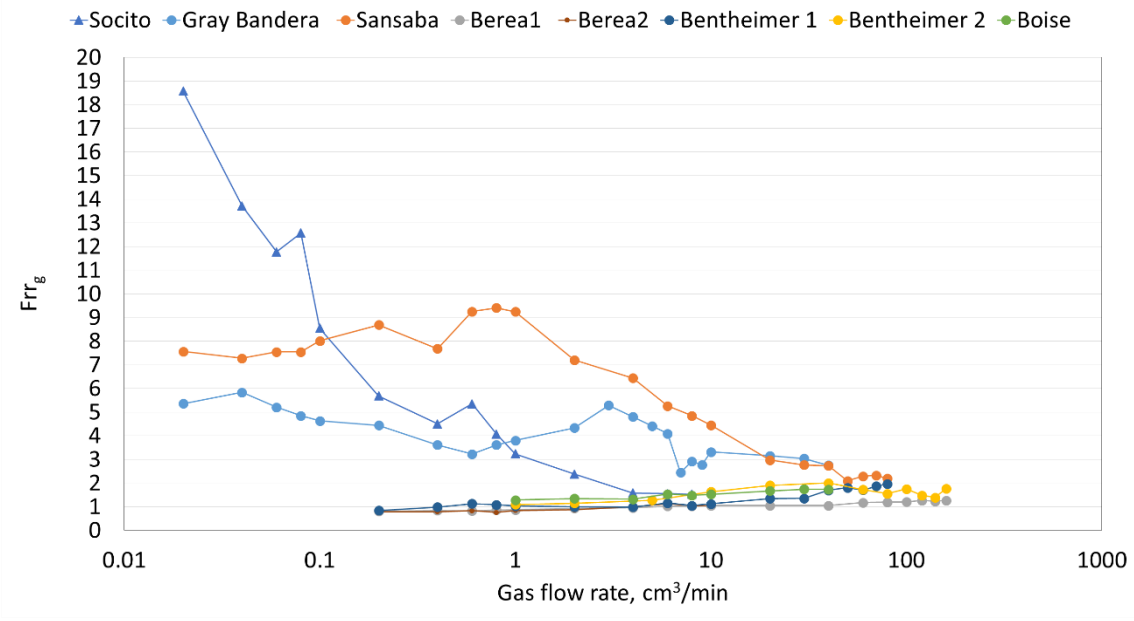

Figure 3-10: Variation in the gas residual resistance factor (Frr_g) versus gas flow rate (Q_g).

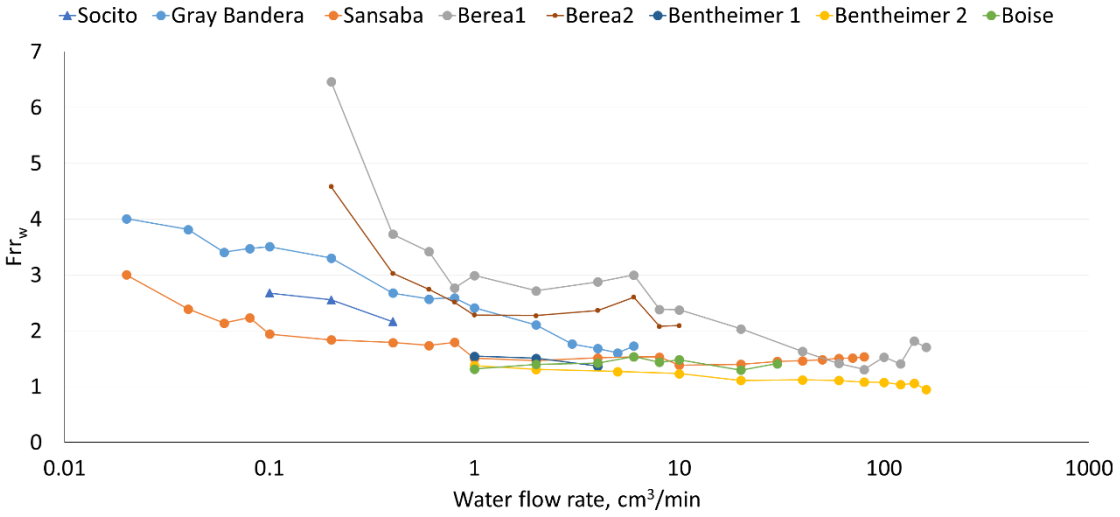

Figure 3-11: Variation in the water residual resistance factor (Frr_w) versus water flow rate (Q_w).

3.4 Summary and conclusions

The major objective of this study is to add to the limited existing data and knowledge around the application of RPMs for the gas/water system in sandstone media. In this work, the effects of initial rock permeability on potential changes to the gas and water relative permeabilities due to an RPM treatment have been studied experimentally. In doing so, the traditional parameters of Frr_w, Frr_g and Frr_w/Frr_g have been used to evaluate the performance of the treatment. What is more, an attempt has been made to explain and interpret the observed trends between the above parameters and rock permeability using possible pore-scale events/mechanisms (e.g. relative pore size changes, redistribution of fluids, steric effect, lubrication effect, etc.) that may come to existence due to the RPM treatment.

According to our results and under the experimental conditions explored in this work, in the high permeability rocks (3001, 3488 and 5035mD), the treatment may have no significant effect on either of the water and gas relative permeabilities. In low permeability rocks (2.7, 22.7 and 66.4mD), the treatment results in high gas relative permeability reductions which are even greater than that induced to the water phase. This may imply that an RPM treatment using our particular polymer solution may be considered strongly unsuccessful in such rocks. In the moderate permeability rocks (350 and 385 mD) however, the polymer treatment reduces water relative permeability significantly but either does not have much of effect on the gas phase or results in an improvement to the gas relative permeability at low gas flow rates.

The above trends may be attributed to the way an RPM treatment may alter the pore size distribution of a rock which then impacts on how the wetting (water) and non-wetting (gas) phases may redistribute and flow in the newly modified pore system. The polymer layer thickness (e), in general, may increase with increase in the rock permeability but the more important ratio of $(\frac{e}{r})$ is expected to decrease as it is a relative parameter whose value depends on the initial rock permeability. The results obtained in this work may be insightful in pointing out that the initial rock permeability may be used as an important screening parameter in planning an RPM treatment for gas producing wells.

Chapter 4: Low-Salinity-Assisted Cationic Polyacrylamide Water Shutoff in Low-Permeability Sandstone Gas Reservoirs

4.1 Introduction

Natural gas remains to be an important geo-energy resource for the rest of the 21st century, which also has a far less pronounced global carbon footprint compared to coal and oil (Chen et al., 2019a, Cascio et al., 2018, Ahmed and Rezaei-Gomari, 2019). However, one of the main technical and economic challenges to produce natural gas from the low permeability reservoirs is to mitigate the water production. This is because increasing water production during gas production leads to a decrease of gas relative permeability thus lowering gas production rate (Elmkies et al., 2002, Tielong et al., 1996, Chiappa et al., 1997, Ranjbar et al., 1995, Ranjbar and Schaffie, 2000).To reduce the water production from gas wells, production engineers and field operators have been paying attention to chemical water control strategies (Seright, 1992, Seright and Martin, 1993, Hajilary et al., 2015b). The chemical water control techniques aim to reduce the water relative permeability nearby the wellbore by injecting a chemical, namely relative permeability modifier (RPM), which would have a minimal effect on relative permeability of the hydrocarbon phase (i.e. gas or oil).

Published work shows that RPM treatments can successfully mitigate water production from moderate and high permeability rocks (Mennella et al., 1998, Qi et al., 2013, Elmkies et al., 2002, Zaitoun and Pichery, 2001, Burrafato et al., 1999, Jinxiang et al., 2013, Al-shajalee et al., 2019b). For example, Burrafato et al. treated sandstone rock samples with permeablity ranging from 203 to 380mD with cationic polyacrylamide (CPAM). These treatments resulted in favorable outcome with relatively high residual resistance factors to water (Frr_w=5.1 and 7.1) but minimal effect on the gas phase (Frr_g=1.3 and 1.1). Chiappa et al treated similar sandstone rock samples (120 and 690 mD) with CPAM, which demonstrated comparable results (Frr_w=5.6 and 4.5, Frr_g=2.1 and 1.3). To interpret the controlling factor(s) of the performance of RPM treatment, a few physical mechanisms have been proposed such

as the wall effect, swelling/shrinking effects, and fluid redistribution. The wall effects (especially steric effects) are considered as the primary mechanism, which originate from the hydrodynamic thickness of the adsorbed polymer layer at the pore surfaces of a rock (Nieves et al., 2002, Tielong et al., 1996, Zaitoun et al., 1998, Zaitoun and Kohler, 1988, Elmkies et al., 2002, Dovan and Hutchins, 1994, Grattoni et al., 2001c, Alshajalee et al., 2019)**.**

However, the application of RPMs to low permeability media remains unsuccessful due to the potential plugging or phase trapping issues after the treatment in such samples. Such issues may arise because in low permebility media the induced polymer layer thikness at the pore surfce by an RPM treatment may take up a much higher proporation of the radius of the pores and throats impeding the effective passage of fluids through them. In other words, in low permeability porous media, the ratio of the adsorbed polymer layer (e) to original pore sizes (r) is expected to be much larger than that in high permeability media (Al-shajalee et al., 2019b, Park et al., 2015). In effect, not only the post-treatment permeability the medium would reduce considerably, the substabtial relative reduction in its pore and throat sizes would result in a noticable increase in the capillary pressure, which would make them effectively inacecssible to the gas phases hence very large Frr_g (Pusch et al., 1995, Ranjbar and Schaffie, 2000, Zaitoun et al., 1990, Dovan and Hutchins, 1994, Tielong et al., 1996, Chiappa et al., 1997, Park et al., 2014, Park et al., 2015, Grattoni et al., 2001d, Kalfayan and Dawson, 2004, Zaitoun and Kohler, 1988, Al-shajalee et al., 2019b).

It has been proven that the polymer hydrodynamic thickness also depends on the electrostatic interactions between the polymer/brine/rock. These interactions in turn depend on the ionic strength of the brine (Chiappa et al., 1999, Pusch et al., 1995, Ranjbar and Schaffie, 2000, Zaitoun and Pichery, 2001, Nieves et al., 2002, Sydansk, 1993, Karimi et al., 2014b, Qi et al., 2013, Zaltoun et al., 1991, Kalfayan and Dawson, 2004, Mishra et al., 2014, Al-Hashmi and Luckham, 2010, Tekin et al., 2005, Tekin et al., 2010). It has been tested that the adsorption of an anionic/non-ionic polymer on negatively charged sandstone increases when increasing the positively charged ionic strength of a brine due to reducing the electrostatic

repulsion in the polymer solution. Moreover, this causes reducing the hydrodynamic radius of polymer molecule. However, the opposite will occur if the polymer is cationic (i.e. the adsorption of cationic polymer increases when decreasing the positively charged ionic strength of a brine) (Mishra et al., 2014, Al-Hashmi and Luckham, 2010, Tekin et al., 2010, Tekin et al., 2005, Chiappa et al., 1999, Zaltoun et al., 1991).

With reference to polymer flooding in low permeability sandstones, Moghadasi et al.(2019) emphasized on the importance of low salinity-polymer synergy, which keeps the polymer adsorption thickness sufficiently low increasing the flood's chance of success (Moghadasi et al., 2019). In addition, it has been shown that decreasing the amount of monovalent positive charged ions in a positively charged polymer solution reduces the electrostatic repulsion in the polymer solution. Consequently, the hydrodynamic thickness of the adsorbed polymer would reduce (compressed) (Mishra et al., 2014, Zaltoun et al., 1991, Tekin et al., 2010, Tekin et al., 2005, Chiappa et al., 1999, Grattoni et al., 2004, Al-Hashmi and Luckham, 2010). Overall, an important factor determining the successful application of a particular RPM in low permeability rocks is achieving a low thickness of the adsorbed polymer, which may be controlled using brine salinity.

Moreover, owing to the alterations in particle surface physicochemical properties after polymer coating, wettability of particles coated with polymers differs from that of uncoated particles (Moen and Richardson, 1984b, Jańczuk et al., 1991, Bae and Inyang, 2001, Terry and Nelson, 1986, Helalia and Letey, 1989, Tekin et al., 2010, Tekin et al., 2005).

Furthermore, we note that the low salinity water flooding technique has generated significant interest in improving hydrocarbon recovery (Myint and Firoozabadi, 2015, Alotaibi et al., 2011, Sheng, 2014, Al Shalabi et al., 2014, Rezaei Gomari and Joseph, 2017). A number of mechanisms are responsible for enhanced oil recovery due to low salinity brine, which include, but are not limited to, double layer effect, wettability alteration towards more water-wet, and increased pH and reduced IFT (Al Shalabi et al., 2014, Sheng, 2014). Note that

while this work focuses on polymer-augmented low-salinity EOR, it may be considered as an extension to the applications of low-salinity EOR.

We thus hypothesize that lowering salinity may expand the application of the cationic polyacrylamide (CPAM) in low permeability gas reservoirs due to the favorable polymer-polymer interaction at pore surfaces. To be more specific, lowering salinity may increase the interaction between the negatively charged sandstone rock and the positively charged polymer, meanwhile, decreasing effective polymer hydrodynamic thickness at pore surface by decreasing the repulsion between polymer/polymer. It is also expected that treating the negatively charged sandstone rocks with the positively charged CPAM and lowering salinity would induce electrochemical alteration to rock pore surfaces (Tekin et al., 2005, Tekin et al., 2010). Such a change may cause render the pore surface less water wet, to some extent, thus decreasing water layer thickness at the rock surface (Zaltoun et al., 1991, Mishra et al., 2014, Xie et al., 2016, Myint and Firoozabadi, 2015, Alotaibi et al., 2011, Arif et al., 2017a, Nasralla et al., 2013).

To test the hypothesis, we performed core flooding experiments using three type of sandstone rocks (e.g., Socito, Gray Bander and San Sab) with permeabilities ranging from 2.7 to 80mD using KCl aqueous ionic solutions with two different salinities (e.g., 0.2 and 2%wt). The rock permeability range selected in this work (i.e. 2 mD to 80 mD) has been categorized as 'low' in accordance with the recent investigations on this subject (e.g. (Al-shajalee et al., 2019b, Zhang et al., 2019, Guetni et al., 2020, Zhao et al., 2019)). Note that a 'low' permeability rock does not mean 'tight or unconventional' as the latter is more rigorously defined by a rock having permeability less than 0.1 mD (Smith et al., 2009, Bennion and Thomas, 2005).

We then examined the relative permeabilities to water and gas before and after CPAM treatment. We also calculated the polymer layer thickness to account for the variation of relative permeabilities for each phase. Moreover, we measured the zeta potentials of the polymer-polymer, rock-polymer and brine-rock (for each rock type) as a function of salinity

before and after the treatment. Furthermore, we measured the contact angles for glass/brine before and after the CPAM treatment as a function of salinity.

4.2 Experimental

4.2.1 Materials

Rocks: Three relatively low permeability sandstone core samples with a nominal diameter and length of 3.8 cm and 7.6 cm, respectively, were used (Table 4- 1). The major objective of the current study is to study the possibility of using CPAM as an RPM agent in relatively low permeability rocks. Therefore, we used the results obtained in our previous study (Al-shajalee et al., 2019b, Al-Shajalee et al., 2019a) to choose a range of sample permeabilities included in this study. The X-Ray Diffraction (XRD) results (Table 4- 2) show a typical sandstone mineralogy for these rocks.

Petrophysical parameters of core samples used in the core-flooding experiments

Table 4- 1 Petrophysical parameters of core samples used in the core-flooding experiments

Sample #	**Sample name**	**Porosity (%)**	**Klinkenberg corrected nitrogen permeability (mD)**	**KCl concertation (%)**
1	**Socito1**	17.7	2.7	2.0
	Socito2	18.2	3.7	0.2
2	**Gray Bandera 1**	20.0	22.7	2.0
	Gray Bandera 2	19.7	23.0	0.2
3	**San Saba 1**	19.5	66.4	2.0
	San Saba 2	21.0	80.0	0.2

Table 4- 2: Rock samples mineralogy

Mineral groups	**Phase**	**Socito**	**Gray Bandera**	**San Saba**
		Weight (%)		
Silicates	Quartz	88.3	57.7	91.6
	Microcline	1.8	1.3	2.3
	Albite	2.7	18.8	1.9

	Sum=	**93**	**78**	**96**
Clay	Kaolin	5.2	5.4	3.3
	Illite/Muscovite	1.2	10.2	0.9
	Chlorite	0.8	2.5	-
	Sum=	**7.2**	**18**	**4.2**
Carbonate	Dolomite	-	3.9	-
	Calcite	-	0.2	-
	Sum=	**0**	**4.1**	**0**

Brine and gas phases: We aimed to test the hypothesis that lowering salinity may compress polymer layer thickness, therefore, to avoid the effect of clay swelling on absolute permeability of rocks, we selected KCl brine (0.2 and 2wt %) as an aqueous ionic solution because KCl can serve as a temporary clay stabilizer to mitigate the clay swelling effect. Moreover, we used KCl here since the adsorption of cationic polymer is not strongly influenced by different concentrations of KCl brine as reported by Chiappa (Chiappa et al., 1999). High purity nitrogen was used as non-wetting fluid phase.

Chemicals: Polymer solutions with concentration of 1000 mg/L were prepared by dissolving the positively charge Polyacrylamide (acrylamide-*co*-diallyldimethylammonium chloride) in either 0.2 or 2wt% KCl brine. We used polyacrylamide since it is the most commonly utilized polymer in oil-gas fields (Uranta et al., 2019). In addition, we used a cationic polymer rather than an anionic/non-ionic one due to its positively charged ions that could adsorb better onto the negatively charged sandstone pore surfaces (Chiappa et al., 1999).

4.2.2 Core-flooding procedure

To examine the relative permeabilities of water and gas before and after the RPM treatment in all three rocks as a function of salinity (0.2 and 2% wt KCl), we conducted six core flooding experiments. The core flooding instrument used in this work is shown schematically in Figure 4-1.

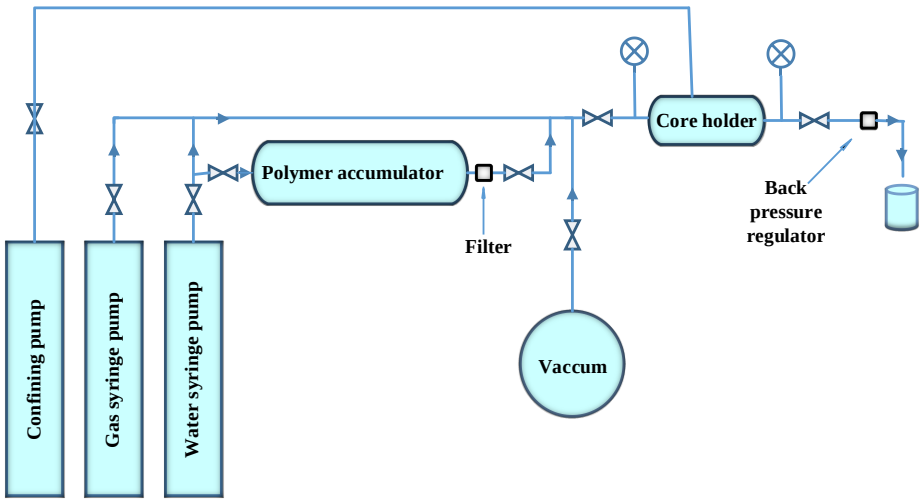

Figure 4-1: Core flooding setup.

First, the samples were dried in an oven at 65 ºC until their weights stabilized (usually 24 hours). The permeability and porosity of core plugs were then measured using the AP-680 Automated Permeameter Porosimeter (Core test Systems Inc., US) under net effective stress using nitrogen gas. Subsequently, similar to our previous research work (Al-Shajalee et al., 2019a), the following procedure was followed to examine the performance of the RPM treatment in modifying the gas and water relative permeabilities.

1. The pre-treatment stage included vacuuming the rock sample and saturating it with the brine. Then, using different gas or brine injection flow rates (0.1-100 cm^3/min), the following pre-treatment parameters were determined: absolute brine permeability, relative gas permeability at residual brine saturation $[k_{rgb}(S_{wirr})]_{Qg}$ (primary drainage) and relative brine permeability at residual gas saturation $[k_{rwb}(S_{gr})]_{Gw}$ (primary imbibition).
2. Subsequently, to treat a rock sample, three pore volumes (PV) of the 1000ppm polymer solution were injected at constant injection rate (0.1 cm^3/min). The polymer concentration and the injection flow rate used to deliver the RPM agent were chosen according to some preliminary injectivity tests performed. This was done to avoid exceeding rock fracturing pressure of the exerting excessively high differential pressures across rock samples. This also can help with devising a suitable injection

procedure for field applications. Then the sample was left to age in contact with the solution for 48 hours. At the time of injecting the polymer solution (which is a product of dissolving our polymer agent in water), much of the rock pore space would be occupied by water and the rest by residual gas. Given the strongly water-wet nature of our rock samples, the residual gas would only occupy the centre of the pores. Therefore, upon injection, the water-based polymer solution would displace the water phase out (and maybe some of the residual gas too) and result in the effective treatment of pore surfaces. To the best of our knowledge, this is the procedure followed in other previously completed research work in this area (Zaitoun and Pichery, 2001, Elmkies et al., 2002, Chiappa et al., 1997, Al-shajalee et al., 2019b, Al-Shajalee et al., 2019a).

3. The post-treatment stage included removing, at a constant brine injection rate of 0.1 cm^3/min, any free polymer from the porous media of the rock sample.
4. Afterward, the gas and brine relative permeabilities were measured at different injection flow rates (0.1-100 cm^3/min). This included the post-treatment relative gas permeability at residual brine saturation $[k_{rwa}(S_{gr+polymer})]_{Qg}$ (primary drainage) and relative brine permeability at residual gas saturation $[k_{rwa}(S_{gr+polymer})]_{Qw}$ (primary imbibition).
5. Finally, to assess the performance of the polymer treatment, we used the measured data from pre-treatment and post-treatment stages to calculate the critical parametric values of water and gas residual resistance factors (Frr_w andFrr_g).

$$Frr_{w=} \frac{K_b\ (Sgr)}{K_a(Sgrp)} \qquad 8$$

$$Frr_{g=} \frac{K_b(Swi)}{K_a(Sgrw)} \qquad 9$$

where K_b and K_a are the end-point effective permeability of water or gas before and after-treatment, respectively. An RPM treatment is considered successful if $Frr_w > 1$ and $\frac{\mathrm{Frr_w}}{\mathrm{Frr_g}} > 1$.

To interpret the Frr_w and Frr_g in terms of the steric effect, we calculated the effective hydrodynamic thickness of the polymer layer onto the sample's pore surfaces using equation 3 as under (Zaitoun and Kohler, 1988):

$$e = r\left(1 - \frac{1}{Frr^{0.25}}\right) \qquad 10$$

where, e is the effective hydrodynamic thickness of the polymer layer (μm), Frr is the residual resistance factor of water or gas as defined by equations 1 or 2, respectively, and r is the average pore radius (μm) of the rock porous media, given as under:

$$r = \left(\frac{8K_w}{\emptyset}\right)^{0.5} \qquad 11$$

Where, K_w is the absolute permeability of brine (using Darcy equation) and ϕ is rock sample porosity. Since e value (Equation 3) depends on either Frr_w or Frr_w, two different values of e (e_w or e_g) may be considered for imbibition and drainage floods separately. Subsequently, the effective polymer layer thickness ratio after the RPM treatment ($\frac{e_w}{r}$ and $\frac{e_g}{r}$) is calculated using Equation 5. As briefly discussed previously, this ratio is a critical factor influencing the outcome of an RPM treatment in low permeability rocks.

$$EHR_w = \frac{e_w}{r} \quad \text{and} \quad EHR_g = \frac{e_g}{r} \qquad 12$$

Where, EHR_w and EHR_g are the effective polymer layer thickness ratios of water and gas, respectively, e_w and e_g are the effective polymer layer thickness for the water (imbibition) and gas (drainage) floods, respectively. The capillary pressure is related to IFT, contact angle and rock pore size using the Young-Laplace equation:

$$P_c = \frac{2\,\sigma\,\cos\theta}{r} \qquad 13$$

Where P_c, σ, θ and r are the capillary pressure, interfacial tension, contact angle and pore radius, respectively. As mentioned previously, change in the pore sizes of a rock due to the

adsorption of the polymer layer would alter the capillary pressure behaviour of the rock impacting on the accessibility of the non-wetting phase (here, the gas phase) to pores.

Note that equation 5 provides estimates of effective polymer thickness ratio and it involves parameters ‘e’ and ‘r (from equations 3 and 4) which in turn are based on bundle-of-capillary-tubes model. However, these equations are still valid to evaluate the effect of pore size (including a layer of adsorbed polymer) on fluid distribution in porous media both qualitatively or quantitatively (Stavland and Nilsson, 2001, Anokwuru, 2015, Zhang et al., 2017, Liu et al., 2019, Letham and Bustin, 2018, Yuan et al., 2019).

4.2.3 Zeta potential tests

To interpret the effect of brine salinity on the RPM treatment at the molecular level ($-NH^+$/-SiO- and K^+Cl/ NH^+), and understanding how salinity and mineralogy of rocks govern the treatment, we measured zeta potential for three systems using a Zetasizer –Nano-Zs Malvern. The evaluated systems included polymer-polymer, rock-polymer and rock-brine before and after the treatment across all rock types, and the procedure is as under:

1. Each rock sample was grinded initially to fine powder form (size: 1-40 microns) (Sari et al., 2019, Mahani et al., 2015, Alotaibi et al., 2011).
2. A 0.2 gm sample of particles was aged in 2 cm^3 of KCl solution (2 and 0.2%wt) in capped vial placed in an oven for 48 hours at 60 ^oC followed by measuring the zeta potential of these samples.
3. Similar to Step 2, another 0.2 gm of particles was aged in 2 cm^3 of polymer solution prepared using the earlier mentioned brines (2 and 0.2%wt) and then their zeta potential was measured.
4. Similar to Step 2, another 0.2 gm of particles was aged in 2 cm^3 of polymer solution prepared using the earlier mentioned brines (2 and 0.2%wt). Then these particles were dried in an oven for 48 hours at 60 ^oC. The treated particles were rinsed with distillated water. Then again, the treated particles in the KCl solution (2 and 0.2%wt, respectively)

were aged in oven for 48 hours at 60 ^{o}C prior to measuring the zeta potential of these samples. It is worth noting that polymer solutions (1000 mg/L) were prepared using the earlier mentioned brines (2 and 0.2%wt) before zeta potential measurements.

4.2.4 Contact angle measurements

In order to determine the wetting characteristics of samples before and after the treatment, contact angle measurements were conducted on sandstone rock samples to determine their natural wettability (results in Table 4- 4). Furthermore, to evaluate the influence of salinity on wettability, the contact angles were measured using a clean pure glass substrate by using the sessile-drop method(Arif et al., 2019). Essentially, a brine droplet (of 2 wt% or 0.2%wt KCl) was added onto the substrate via a needle in the presence of air at ambient conditions (results in Figure 4-16). Note that the glass substrate was used in place of real rock surface to avoid the additional complexities associated with reliable contact angle measurements on rock samples (Arif et al., 2020).

In addition, pure glass (silicate) surface is a representative of sandstone rocks owing to the dominant quartz mineral (Arif et al., 2016, Arif et al., 2019). The glass samples were initially cleaned using a plasma cleaner (Diener electronic-Zepto one). Then, after undergoing brine (2-0.2%wt. KCl) contact angle measurement, they were submerged in the polymer solution prepared using the earlier mentioned brines (2 and 0.2%wt KCl) for 48 hours to assure the polymer adsorption. Then the treated glass samples were removed from the solution and rinsed with distilled water. Afterwards, they were dried in an oven at 60 ^{o}C for an hour. Finally brine contact angle was measured for treated and untreated glass samples as a function of brine salinity (2-0.2%wt. KCl brine).

While the contact angle measurements in the presence of air are not realistic since the fluid distribution during measurements is different than that in porous media, still this is the well-known/only method to measure contact angle of two-phase flow. In addition, since in this study we are looking for qualitative trends rather than quantitative data, these results give a good indication to the effect of salinity on contact angle before and after the treatment.

4.3 Results

4.3.1 The Frr_w and Frr_g in high salinity brine

We used the calculated values of Frr_w and Frr_g to evaluate the performance of the polymer treatments in high salinity brine (2wt% KCl)**.** Figure 4-2-Figure 4-4 present Frr_w and Frr_g as a function of flow rate under this salinity. As can be seen from these Figures, we found that Frr_g clearly decreased with increasing flow rates for the case of 2wt% KCl brine for all types of rocks, while the Frr_w showed distinct behavior i.e. Frr_w decreased with flow rate for Gray sandstone and remained almost constant for the other two sandstones. The decrease in Frr_g with increasing gas flow rate is attributed to the ease of gas flow in reservoir which causes the residual resistance factor to reduce.

In addition, we also found that regardless of flow rate and rock type, in all experiments, $Frr_g > 1$ and $Frr_w > 1$. This shows that the polymer treatment decreases the relative permeability to both water and gas phases. This is largely due to the steric effects, which decreases relative permeabilities for both water (wetting) and gas (non-wetting) relative phases as a result of adsorbed polymer layer at the pore walls (Al-shajalee et al., 2019b, Zaitoun and Kohler, 1988). Furthermore, based on the data presented in Figure 4-2-Figure 4-4, we find that for all rock samples $Frr_w/Frr_g < 1$, meaning that the CPAM treatment in these low permeability rocks can be considered unsuccessful. For example, at 0.1 cm^3/min, Frr_w/Frr_g is equal to 0.24, 0.7 and 0.14 for Socito, Gray Bandera and San Saba rocks, respectively.

Figure 4-2-Figure 4-4 also show that increasing gas flow rate decreases Frr_g (in primary drainage process) across all rock types. However, the minimum value of Frr_g remains to be above 1 for all rock samples. For example, Figure 4-2 (for Soctio rock) shows that with increasing flow rate from 0.02 to 6 cm^3/min the Frr_g decreases from 18.5 to 1.5. This is because the greater gas velocity would induce a greater force and cause the polymer layer thickness to lessen due to compression. However, a similar consistent relationship cannot be

established between Frr_w and water flowrate. As apparent from Figure 4-2-Figure 4-4, Frr_w decreases with flow rate for Gray Bandera rock while for Socito and SanSaba samples only slight variations in Frr_w can be observed over the flow rate range. This discrepancy is likely attributed to the mineralogy of the core plugs, which may play a certain role in controlling the polymer adsorption during the treatment. For example, a treatment in Gray Bandera results in higher water permeability reduction than that of Socito and SanSaba rocks due to the higher percentage of clay minerals in Gray Bandera rock (Table 4- 2). However, the effect of rock mineralogy on the dependency of Frr on flow rate needs more investigation and will be the subject of future publications because that is a standalone study.

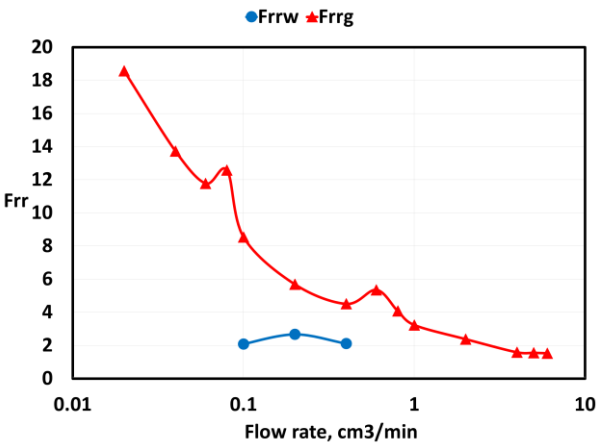

Figure 4-2: The relationship between the water (wetting) and gas (non-wetting) residual resistance factors (Frrw & Frrg) vs. water and gas flow rate, respectively, in presence of 2% KCl for Socito rock.

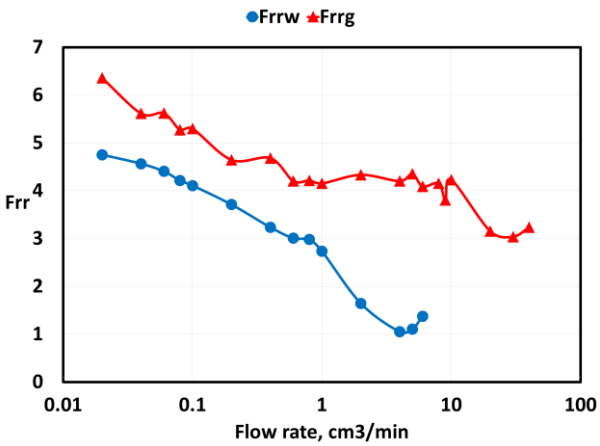

Figure 4-3: The relationship between the water (wetting) and gas (non-wetting) residual resistance factors (Frrw & Frrg) vs. water and gas flow rate, respectively, in presence of 2% KCl for Gray Bandera rock.

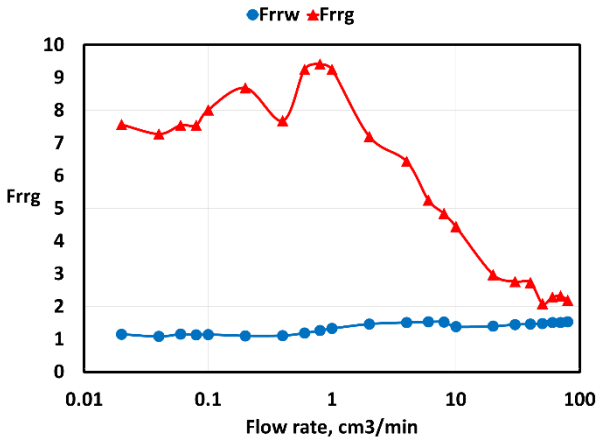

Figure 4-4: The relationship between the water (wetting) and gas (non-wetting) residual resistance factors (Frrw & Frrg) vs. water and gas flow rate, respectively, in presence of 2% KCl for SanSaba rock.

4.3.2 The Frr_w and Frr_g in low salinity brine

To test our hypothesis that lowering brine salinity may improve the performance of CPAM treatment, we repeated the same experimental procedure as in previous section on similar rock samples (Gray Bandera2, 3.7mD; Socito2, 23.0mD and SanSaba2, 80mD), but with the low salinity brine (0.2 wt% KCl). Figure 4-5-Figure 4-7 show Frr_w and Frr_g as a function of flow rate. Results show that lowering salinity to 0.2% wt. KCl, Frr_g remains close to unity and $Frr_w/Frr_g > 1$, suggesting a successful treatment in these low permeability rocks regardless of rock type. For instance, at water and gas flow rate of 0.1 cm^3/min, Frr_w/Frr_g

is equal to 1.2, 6.4 and 1.6 for the Socito, Gray Bandera and San Saba rocks, respectively. In other words, in all rock samples the water relative permeability reduction in presence of low salinity brine (0.2%wt. KCl) was higher than that obtained for the same rocks under high salinity (2%wt. KCL). For example, at water flow rate of 0.1 cm^3/min, the Frr_w was calculated to be 2.7, 3.7 and 1.1 for Socito, Gray Bandera and San Saba rocks, respectively, in presence of 2%wt. KCl brine. Yet, for the same flow rate and in presence of 0.2%wt. KCl brine, the Frr_w increased to 4.7, 27.4 and 1.8 for the Socito, Gray Bandera and SanSaba rocks, respectively.

Thus, our results imply that lowering salinity may lead to a reduction of the adsorbed polymer layer thickness (e) at pore surfaces. This physiochemical process would trigger a reduction in e, which in turn enhances the flow of the non-wetting gas phase through pore channels by reducing the capillary entry pressure and making more pores accessible to gas compared with the high salinity case. Similar observation was made by Sharifpour et al, who report that lowering salinity could significantly decrease the gas flow rate threshold into low permeability porous media (Sharifpour et al., 2016). On the other hand, Figure 4-5 to Figure 4-7 indicate that flow rate would significantly affect the Frr_w by reducing it from very high values at low flow rate to low values comparable to Frr_g at high flow rates. This may be attributed to the fact that increasing flow rate reduces polymer layer thickness as a result of increasing compression force or the ability of polymer layer to hold the water decreases.

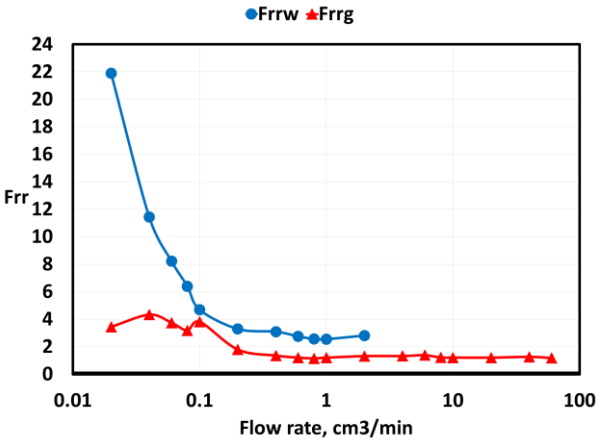

Figure 4-5: The relationship between the water (wetting) and gas (non-wetting) residual resistance factors (Frrw and Frrg) vs. water and gas flow rates respectivelys in presence of 0.2% KCl for Socito rock.

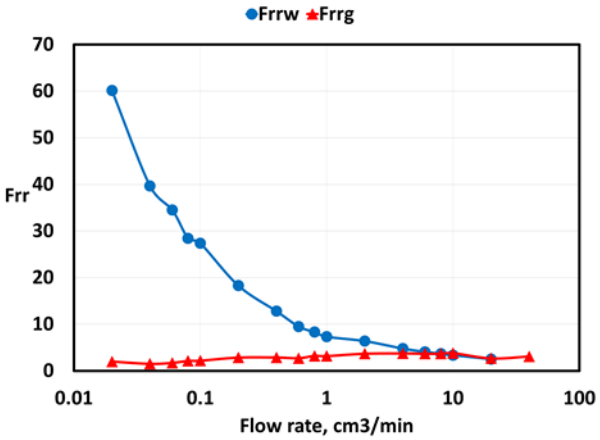

Figure 4-6: The relationship between the water (wetting) and gas (non-wetting) residual resistance factor (Frrw and Frrg) vs. water and gas flow rate, respectively, in presence of 0.2% KCl for Gray Bandera.

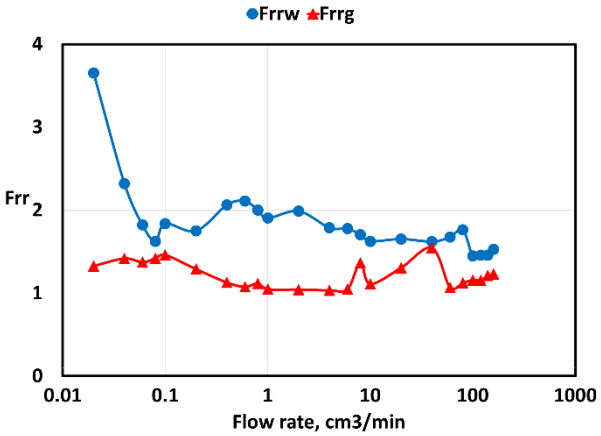

Figure 4-7: The relationship between the water (wetting) and gas (non-wetting) residual resistance factor (Frrw Frrg) vs. water and gas flow rate, respectively, in presence of 0.2wt% KCl for SanSaba rock.

4.4 Discussion

4.4.1 Effect of brine salinity on the effective polymer layer thickness

Figure 4-8 and Figure 4-9 show the calculated effective polymer layer thickness ratio (including the associated water layer) during imbibition flood (EHR_w) as a function of brine salinity (2 and 0.2%wt KCl, respectively) using Eq.5. Results show that lowering salinity increases EHR_w. For instance, at water flow rate of 0.1 cm^3/min, the EHR_w values are approximately 22, 28 and 3.7% in Socito, Gray Bandera and San Saba rocks, respectively, in presence of 2%wt. KCl brine. Yet, at the same flow rate and in presence of 0.2%wt KCl

brine, the EHR_w ratios are approximately 32, 56 and 14% for Socito, Gray Bandera and San Saba rocks, respectively.

Figure 4-10 and Figure 4-11 show the calculated effective polymer layer thickness ratio (including the associated water layer) during gas flooding (EHR_g) as a function of brine salinity (2 and 0.2%wt KCl, respectively). The most important conclusion we can draw from these figures is that overall EHR_g decreases with decreasing brine salinity for all rock samples. For example, at the gas flow rate of 0.1 cm^3/min, the EHR_g values are approximately 42, 41 and 34% for Socito, Gray Bandera and San Saba rocks, respectively, in presence of 2%wt. KCl brine. Yet, at same flow rate and in presence of 0.2%wt. brine, the EHR_g values are approximately 28, 18 and 9% for Socito, Gray Bandera and San Saba rocks, respectively.

The results support the hypothesis that lowering the monovalent cation (K^+) concentration may improve CPAM's performance in low permeability sandstone rocks. The potential mechanisms that are responsible for this improvement include: rock-polymer and polymer-polymer physiochemical interactions, and wettability changes at the interface. The next sections will evaluate these mechanisms.

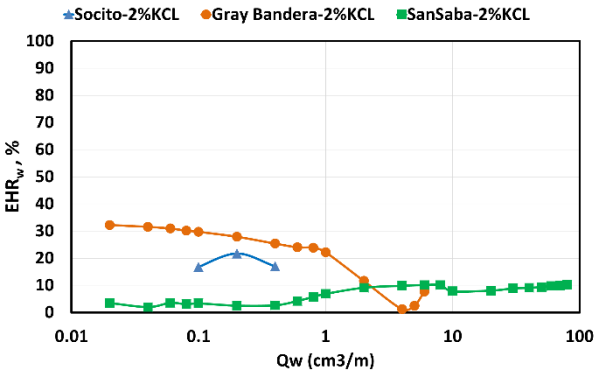

Figure 4-8: the effective polymer layer thickness ratio during water flooding (imbibition), e_w /r, in presence of 2wt% KCl for Socito, Gray Bandera and SanSaba rocks.

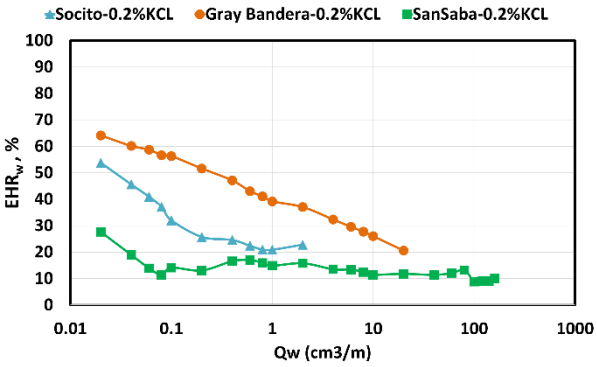

Figure 4-9: the effective polymer layer thickness ratio during water flowing (imbibition), e_w/r, in presence of 0.2wt% KCl for Socito, Gray Bandera and SanSaba rocks.

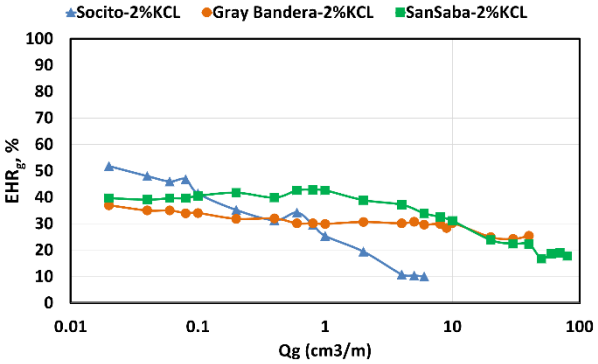

Figure 4-10: the effective polymer layer thickness ratio during gas flooding (draining) e_g /r, in presence of 2wt% KCl, Socito for Gray bandera and SanSaba rocks.

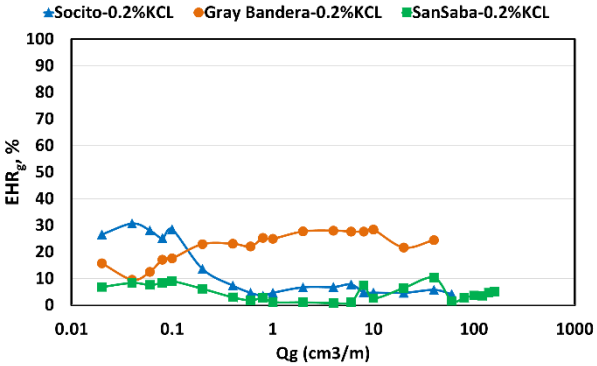

Figure 4-11: the effective polymer layer thickness ratio during gas flooding (draining), e_g/r, in presence of 0.2wt% KCl for Socito, Gray bandera and SanSaba rocks.

Rock-polymer interactions: In this section we will discuss the effect of brine salinity on rock/polymer interactions. Figure 4-12-Figure 4-14 present the measured zeta potential values of the three rock particle types (Gray Bandera, Socito and San Saba) suspended in the polymer solution (rock/polymer) as a function of brine salinity (2 and 0.2wt% KCl). As can be seen, with decrease in brine salinity, the zeta potential becomes less negative (Gray Bandera) or even positive (Socito and San Saba). This means that as the brine salinity deceases, the more positively charged polymer is attached onto the surface of the rock particles. Similar observation has also been reported by Tekin et al. (2005, 2010)(Tekin et al., 2010, Tekin et al., 2005). These researchers indicate that in their experiments the adsorption of positively charged CPAM onto negatively charged expanded perlite (EP) increased with decreasing NaCl concertation due to decreasing salt screening effect (Tekin et al., 2005,

Tekin et al., 2010). To summarize, it seems that reducing the concentration of the monovalent cation (K^+) in the CPAM solution (NH^+) decreases the salt screening effect and increases the rock ($-SiO^-$)-polymer electrostatic attraction, which in turn leads to increase the adsorption of CPAM on the rock surfaces.

Polymer-polymer interactions: To measure the effect of brine salinity on polymer-polymer interactions (repulsion/ attraction), we conducted zeta potential measurements for the polymer solution as a function of brine salinity (2 and 0.2%wt KCl brine) with the results presented in Figure 4-15. This figure indicates that as the salinity deceases, the zeta potential becomes positive which means increasing polymer/polymer attraction (reducing the repulsion). This eventually leads to reduced hydrodynamic polymer/polymer layer thickness at the rock pore surface. Similar observation has been reported by a number of other researchers who state that decreasing the concentration of monovalent positive charged ions in a positively charged polymer reduces the electrostatic repulsion in the polymer solution.

We further note that the zeta potential is measured at the slipping plane and so can include ions that are complexed or move with the polymer. Ionic strength is known to impact the zeta potential as increasing ionic strength can screen this charge. Thus, at the lower ionic strength we see a positive zeta potential, which is in line with the expected charge of the polymer. As ionic strength increases, it would be expected that the zeta potential would get closer and closer to zero. The fact that this does not happen implies the specific interaction of chloride ions with the polymer-polymer structure. For both these zeta potentials however, they are so close to zero that repulsion would not be significant.

Consequently the polymer adsorption capacity increases, however, this also causes the hydrodynamic radius of polymer molecules to reduce (Mishra et al., 2014, Zaltoun et al., 1991, Tekin et al., 2010, Tekin et al., 2005, Chiappa et al., 1999, Grattoni et al., 2004, Al-Hashmi and Luckham, 2010). This may also explain why Frr_g reduces as brine salinity reduces from 2 to 0.2%wt.KCl (Figure 4-2-Figure 4-7) as attributed to reduction in EHR_g (Figure 4-10 and Figure 4-11). Sharifpour et al. also show that decreasing brine salinity

significantly decreases the threshold gas flow rate for the gas to accesses into low permeability porous media, i.e. increasing gas mobility (Sharifpour et al., 2016).

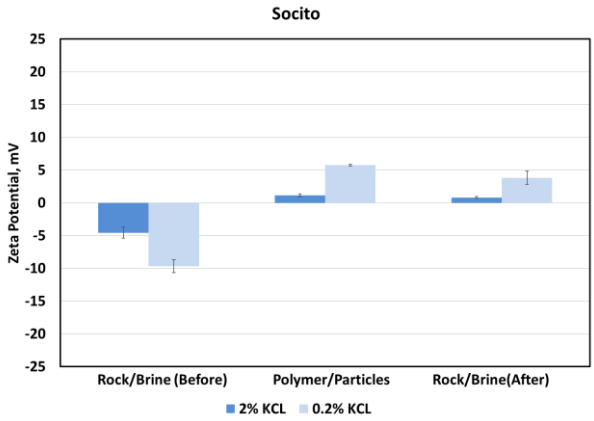

Figure 4-12: Zeta potential of brine/particles, polymer-particles and brine-coated particles in presence of 0.2-2wt% KCl for Socito rock. Error bars are also shown.

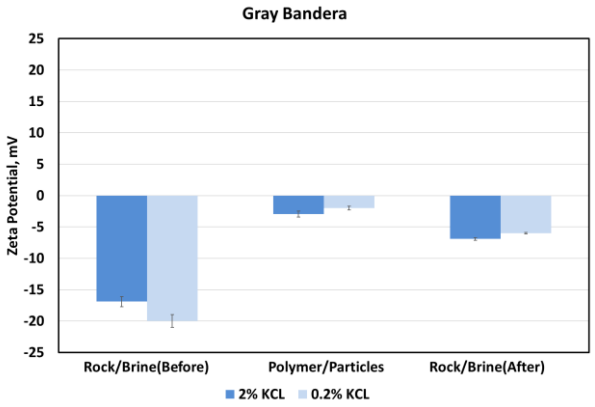

Figure 4-13: Zeta potential of brine/particles, polymer-particles and brine-coated particles in presence of 0.2-2wt% KCl for Gray Bander rock. Error bars are also shown.

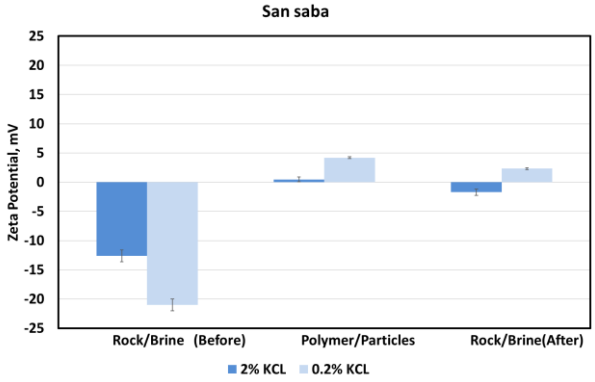

Figure 4-14: Zeta potential of brine/particles, polymer-particles and brine-coated particles in presence of 0.2-2wt% KCl for SanSaba rock. Error bars are also shown.

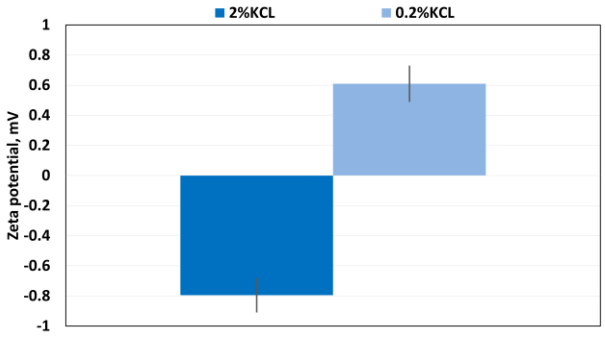

Figure 4-15: Zeta potential of the polymer-polymer as a function of brine salinity (2 and 0.2%wt. KCl%). Error bars are also shown.

4.4.2 Effect of brine salinity on rock surface wettability

We also hypothesized earlier that treating a negatively charged sandstone rock with a positively charged polymer (e.g. CPAM) plus lowering the monovalent cation (K+) in the polymer solution may change the rock surface wettability. To confirm the above, we can look into the results of our zeta potential measurements for the rock-brine system before and after polymer treatment as a function of brine salinity (2 and 0.2wt% KCl) across the all rock types used (Figure 4-12-Figure 4-14). Regardless of the brine salinity, these figures show that

before the treatment the sandstone particles (rock/brine before) exhibit negative zeta potential values across all rock particles. For example, the zeta potential values of Socito, GrayBandera and SanSaba particles in 2wt% KCl brine solution are -4.6, -13 and, -17, respectively. Similarly, the zeta potential values of Socito, GrayBandera and SanSaba particles in 2wt% brine solution are -9.7, -20 and -21 respectively. However, these figures also show that for both salinities, after the treatment (rock/polymer/brine), the zeta potential shifts towards less negative (Gray bandera) and even positive values (Socito and San Saba). For instance, the zeta potential values of Socito, Gray Bandera and SanSaba particles in 2wt% of KCl brine solution are equal to 0.8, -6.9 and -1.7, respectively. Similarly, the zeta potential values of Socito, Gray Bandera and SanSaba particles in 0.2wt% of KCl brine are equal to 3.8, -6.0 and 2.3, respectively. This observation indicates that the particle surfaces become less negative or even positively charged when treated with CPAM. Similar observations have also been made by Tekin when a cationic polymer was adsorbed on negatively charged kaolinite and expanded perlite, respectively. Their results show that such a treatment could change the interface charge of these surfaces from negative to positive as indicated by a shift in zeta potential towards more positive (Tekin et al., 2005, Tekin et al., 2010, Besra et al., 2002, Besra et al., 2003).

The overall conclusion drawn from the above is that (regardless of salinity level) after polymer treatment, the zeta potential shifts to less negative values. Similar reports can be found in the literature where coating rock particles with polymers would alter the physicochemical properties of their surfaces (Tekin et al., 2005, Moen and Richardson, 1984a, Jańczuk et al., 1991, Bae and Inyang, 2001, Terry and Nelson, 1986, Helalia and Letey, 1989, Myint and Firoozabadi, 2015, Xie et al., 2016, Alotaibi et al., 2011, Arif et al., 2017a, Nasralla et al., 2013).

Moreover, to further analyze the wetting behavior with respect to salinity, we measured contact angle of glass (silicate)/brine system, at ambient conditions, before and after polymer treatment as a function of brine salinity (Figure 4-16). We used a glass substrate since it is a

proxy mineral of sandstone (as used by recent investigations e.g. (Arif et al., 2019), and also eliminates the effect of surface roughness to some extent (Arif et al., 2020)). Regardless of the brine salinity, this figure illustrates that after the treatment, contact angle increases. For example, for 2%wt. brine/glass the contact angle shifted from 18 to 20^{o} after the polymer treatment. Similarly, for 0.2%wt. brine/glass the contact angle shifted from 16 to 32^{o} after the treatment. In terms of relating contact angle variation to the corresponding zeta potential variations, a few studies report that with a shift in zeta potential from negative to less negative (or positive), the system shifts towards less water-wet state (e.g. (Arif et al., 2017b, Arif et al., 2017a, Xie et al., 2016)). However, these studies were carried out using simple mineral/brine systems, while in our present case, we have inclusion of complex polymer. Thus, a relation between wettability and zeta potential may not be directly concluded and requires further investigations.

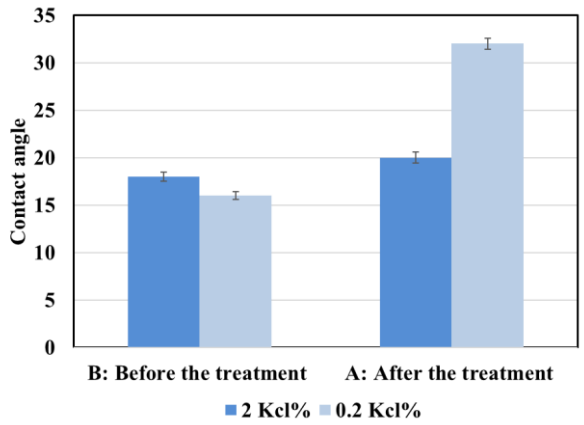

Figure 4-16: Contact angle measurements for brine/glass interface before (B) and after (A) CPAM treatment as a function of brine salinity (2 and 0.2%wt. KCl). Error bars are also shown.

Presented below are discussions around further observations that can be made from our zeta potential and contact angle results as related to the effects of the high and low brine salinity.

Figure 4-12-Figure 4-14 show that before the CPAM treatment as the brine salinity decreases from 2 to 0.2%wt, the zeta potential values of rock/brine system shift to more negative across all rock samples (e.g. from -4.6 to -9.7 for Socito rock particles). Contact angle measurements

indicate a wettability alteration towards more water-wet with the decreasing salinity before the treatment (Figure 4-16, condition: B). Essentially, as brine salinity decreases from 2 to 0.2%wt, contact angle decreases from 18^o to 16^o implying a shift toward more water-wet (though the shift is only minor, i.e. a change of contact angle of only 2^o). However, after the treatment, we note that the rock surface becomes less water-wet when in contact with the lower salinity brine as indicated by contact angles (for case A) in Figure 4-16. This trend in contact angle variation with salinity after the treatment implies that polymer treatment rendered the surface less water-wet. In summary, the salinity effect on contact angle observed here after polymer treatment is that decreasing salinity has resulted in reduced water-wettability of the system. One possible explanation of this trend may be that decreasing salinity from 2 to 0.2%wt after polymer treatment may be causing a reduction in the water film thickness. However, more investigations are required to confirm this observation.

Due to the mechanisms responsible for the RPM effect (as outlined in earlier sections of this manuscript), this type of treatment may be successful in a water-wet systems. Following on from the aforementioned discussion, the salinity induced wettability alteration of the rock samples to a less water-wet state after the polymer treatment may apparently contradict the effective RPM principles. However, an RPM treatment would remain effective as long as a rock remains water-wet regardless of the level of water-wetness.

Overall, taking into account the discussions presented, the polymer and the accompanied water layer thicknesses would be both reduced with the reduction in the KCl concertation from 2 to 0.2wt%. Both of these changes would create a favorable environment to optimize the performance of the CPAM treatment in low permeability reservoirs.

4.4.3 Proposed Mechanism

As discussed earlier, the likely reason behind the observed variation in the performance of the RPM treatment with change in brine salinity (Figure 4-3-Figure 4-8) lies in the rock/polymer/brine physiochemical interactions as controlled by the brine salinity (Gomari et al., 2020). Figure 4-17 shows a schematic illustration of the interactions of

rock/polymer/brine and their influence on the polymer and water thicknesses as a function to brine salinity (0.2-2%wt KCl). These interactions can be divided to three groups of rock-polymer, polymer-brine-polymer and polymer-brine-brine interactions. With reference to the above-mentioned interactions, the polymer layer thickness and the thickness of the associated water layer covering the polymer layer are both functions of brine salinity.

It has been stated in the literature that the adsorbed polymer layer consists of two sub-layers (Grattoni et al., 2004, Ranjbar et al., 1995, Cohen and Christ, 1986, Al-Sharji et al., 2001b). The first one is called the dense layer made of loops-trains close to the rock surface which is responsible for the polymer adsorption (Rock-Polymer: Figure 4-17). Grattoni et al., explain that the arrangement of polymer molecules onto the rock surface and their interactions depend on brine salinity. They state that brine salinity plays an important role in controlling the hydrodynamic size of the polymer molecules and when the size increases, the polymer surface coverage would decrease. The second sub-layer is called the dilute layer containing of stable tails extending into polymer solution that help the adsorbed polymer layer to grow by the entanglement of flowing polymer molecules (Polymer-Brine-Polymer: Figure 4-17) decreasing the pore size (Al-Sharji et al., 2001b).

Overall, reducing the KCl concentration in the polymer solution increases the attraction of first (i.e. dense) polymer layer (rock-polymer) while compressing the second (i.e. dilute) polymer layer (polymer-brine-polymer). In general, the above decreases the water relative permeability as intended, but results in minimal effect on gas productivity. Moreover, it has been shown that the water layer thickness (covering the polymer layer in our case) is salinity dependent (Brine-Brine: Figure 4-17) (Arif et al., 2017a, Myint and Firoozabadi, 2015, Xie et al., 2016).

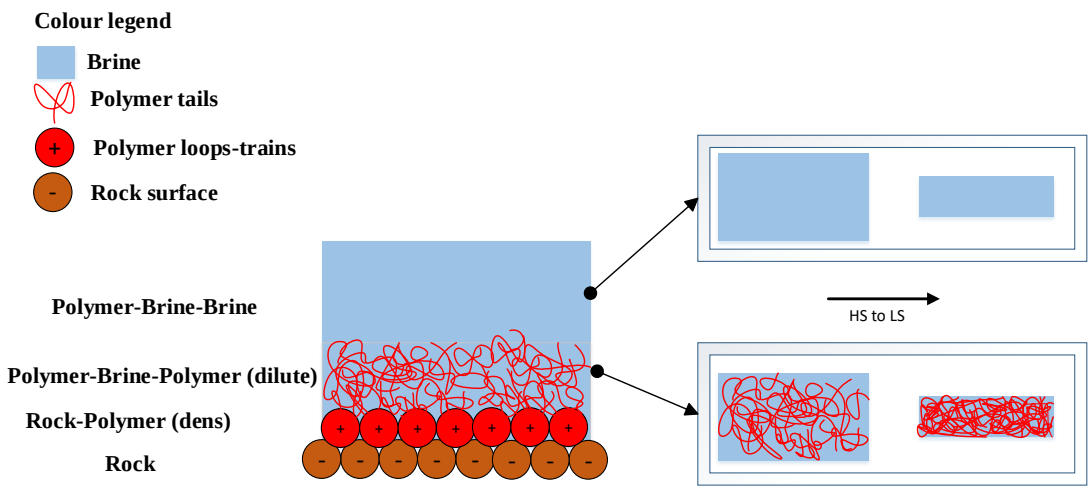

Figure 4-17: The interactions of rock/polymer/brine and their influence on the polymer and water thicknesses as a function to brine salinity (0.2-2%wt KcCl)

Therefore, it may be better to consider the polymer layer thickness and water layer thickness separately which may then be combined in the calculation of the effective polymer layer thickness ratio (HER) as set out in the following equations.

$$\mathrm{EHR}_w = \frac{e_w}{r} = \frac{PH_w + \mathrm{WH}_w}{r} \quad \text{or} \quad \mathrm{EHR}_g = \frac{e_g}{r} = \frac{PH_g + \mathrm{WH}_g}{r} \qquad 14$$

where, $\mathrm{EHR_w}$ is the effective polymer layer thickness ratio during water flooding (imbibition), $\mathrm{EHR_g}$ is the effective polymer layer thickness ratio during gas flooding (drainage), PH is the polymer layer thickness and WH is the associated water layer thickness. Finally, to further elaborate on the results reported in Figure 4-2-Figure 4-7, in the upcoming sections of the manuscript, we will look into the pore size distribution of a rock samples and how it may be altered by the RPM treatment. As will be discussed, such an alteration would result in differing wetting and non-wetting fluid distributions in a rock sample before and after the treatment. We will also explain how this overall phenomenon would be salinity dependent.

4.4.4 The pore size distribution and gas-water distribution in water-wet porous media

As mentioned previously, the adsorption of the polymer layer on the pore surfaces of a rock would alter its pore size distribution. Such an alteration would then impact on the

accessibility and distribution of the non-wetting gas phase in the post-treatment pore space and as a result control the eventual outcome of the RPM treatment. In this section, the impact of the effective polymer layer thickness ratio (EHR) on the performance of CPAM (as characterized by Frr_w and Frr_g) in low permeability sandstones as a function of brine salinity will be discussed.

Interfacial tension (IFT) tests were carried out for the 2%KCl/Nitrogen and 0.2%KCl/Nitrogen systems (Table 4- 3) to find out if brine salinity has an effect on brine-gas flowing (Equation 6). This table shows that the ionic strength of the brine (0.2 and 2wt%) has negligible effect on the interfacial tension (σ) of N_2/brine systems.

Table 4- 3: The IFT measurement results for the KCl brine/Nitrogen systems.

	0.2% KCL	**2% KCL**
IFT, mN/m @1000psi	19.72	19.8

Note that the IFT was measured with a polymer-free solution. This is because the fluid system present in the rock pores after the treatment would generally consist of water and gas and we believe the polymer layer adsorbed onto pore surfaces would not affect the IFT.

In addition, the contact angle values reported in Table 4- 4 show that, in the presence of both brine solutions, the samples are strongly water-wet (i.e. $\theta \approx 0$) in the presence of nitrogen that forms our non-wetting phase in the core flooding experiments. Note that the contact angle in Table 4- 4 represent the natural wettability of the sandstone samples at 1000 psia and 25 ^{o}C.

Table 4- 4: contact angle measurements.

Sample #	**Sample name**	**KCl concertation (%)**	**Contact angle (degree)**

1	**Socito1**	2.0	2.9
	Socito2	0.2	2.8
2	**Gray Bandera1**	2.0	0.7
	Gray Bandera2	0.2	0.7
3	**San Saba1**	2.0	1.3
	San Saba2	0.2	1.1

This would simplify the Young-Laplace capillary pressure equation (Equation 6) by decreasing the term $\cos\theta$ to 1.

$$P_c = \frac{c}{r} \qquad 15$$

Where c is a constant and r the pore radius. Therefore, for our case, the only factor affecting the capillary values in presence of different brine salinity is the pore radii. Zaitoun and Kohler, Grattoni et al. and Al-shajalee et al state that the pore size distribution regulates the way wetting and non-wetting fluids are distributed in the pore spaces of a rock porous media (Zaitoun and Kohler, 1988, Grattoni et al., 2001c, Al-shajalee et al., 2019b) . In general, we can divide the pore sizes into three categories of small, moderate and large (Figure 4-18).

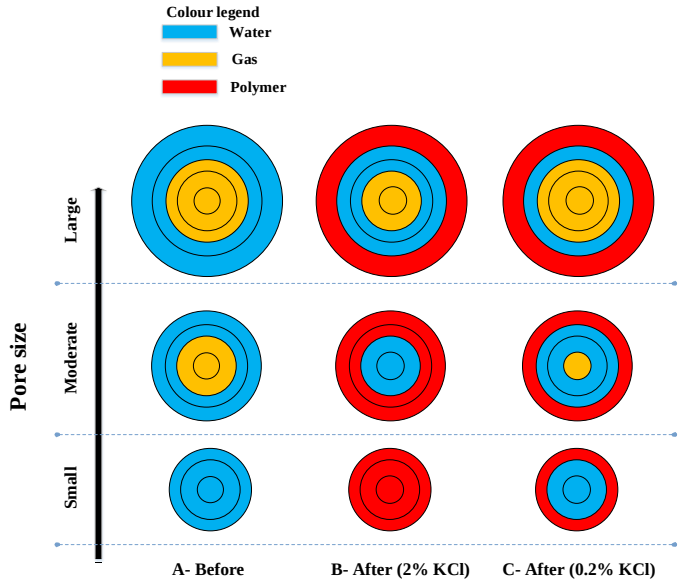

Figure 4-18: The effect of pore sizes distribution on water (wetting) and gas (non-wetting) distribution during draining process. (A) before RPM treatment, (B) after RPM treatment (2%KCl), (C) after RPM treatment (0.2wt%KCl)

Before the treatment (Figure 4-18A), since all of our rock samples were water-wet and due to capillary force (Equation 8), the small pores would be filled with water (as wetting phase) and are unreachable to gas (as non-wetting phase). However, in the moderate and large pores the water film covers the pore walls while the gas phase occupies the centre (Al-shajalee et al., 2019b, Grattoni et al., 2001c, Zaitoun and Kohler, 1988). As mentioned earlier, after a polymer adsorption (treatment), the resultant variation in the pore sizes of a rock porous medium by the adsorbed polymer layer and the consequential redistribution of the wetting phase (water) and non-wetting phase (gas) fluids is the main source of RPM effect (Grattoni et al., 2001c, Al-shajalee et al., 2019b). In other words, for all the rock samples studied, the adsorbed polymer onto the water-wet grain surface changes the effective pore size distribution by decreasing their real sizes (Figure 4-18B and Figure 4-18C). Therefore, as illustrated in Figure 4-18B, after treatment due to relatively high effective polymer layer thickness ratio in the presence of 2wt% KCl, the small pores that were formerly occupied by water may turn out to be plugged by immovable polymer. The moderate pores, that before treatment were filled with both water and gas phases together, now have a reduced size (i.e. greater capillary force (Equation 8) and thus, turn out to be occupied by only water. However, the largest pores may stay comparatively large and therefore remain accessible to both water and gas.

Therefore the treatment under higher salinity would reduce the relative permeability to gas more than that to water (recall Figure 4-2-Figure 4-4). As schematically demonstrated by Figure 4-18C, due to the reduced effective polymer layer thickness ratio (HER) with the use of lower salinity brine, the accessibility of the non-wetting phase to the pore space would improve, which may enhance the performance of the RPM treatment.

4.5 Conclusions

The use of polymer for water shutoff in low permeability sandstone reservoirs is significant for successful applications of polymer treatment, however the factors that control rock-gas-brine interactions and polymer layer thickness are still not well understood. In this paper we

conducted core flooding experiments to study the impacts of brine concentration (0.2% and 2% KCl) on possible variations to the water and gas relative permeabilities due to cationic polyacrylamide treatment (CPAM) on three sandstones of varying permeabilities (from 2 to 80 mD). Zeta potential measurements were also conducted for polymer-polymer system and rock-brine system before and after the treatment as a function of salinity for all rocks investigated. In addition, we measured the contact angles for silicate/brine/gas systems before and after the treatment as a function of salinity.

The overall results showed that decreasing brine salinity (KCl) improved the performance of cationic polyacrylamide in sandstone rocks by decreasing water relative permeability, while the effect on gas relative permeability was relatively low. This is because decreasing the monovalent cation in brine (K^+), increases the $rock^-/polymer^+$ electrostatic attraction. Zeta potential of $rock^-/polymer^+$ confirmed that as brine salinity deceases (from 2 wt% KCl to 0.2wt% KCl), the zeta potential becomes less negative or even becomes positive. In addition, a decrease in monovalent cation concentration leads to a reduction in the effective polymer layer thickness (compressing) as confirmed by zeta potential measurements. Furthermore, zeta potential of $polymer^+/polymer^+$ measurements show as well that as brine salinity deceases the zeta potential becomes positive suggesting an increase in the $polymer^+/polymer^+$ attraction (reducing the repulsion).

Overall, reducing the KCl concentration in the polymer solution increases the attraction of first polymer layer (rock-polymer) while compressing the second polymer layer (polymer-brine-polymer). In general, the above decreases the water relative permeability as intended, but results in minimal effect on gas productivity. Moreover, and importantly, it was seen that before treatment the system showed a small increase in water wettability with decreasing salinity. However, after the treatment of sandstone rocks with positively charged polymer, and lowering the brine salinity, rock surface wettability altered towards less water-wet. This effect was related to a shift in zeta potential towards more positive value at lower salinity

after the treatment. However more investigations are required to relate wettability to zeta potentials.

Altogether, polymer and the accompanied water layer thicknesses will be both reduced (compressed/shrink) with reducing KCl concertation. Under such conditions, the treatment will be suitable as seen by a decline in relative permeability to water and an unaltered gas relative permeability.

Chapter 5: A Multiscale Investigation of Cross-Linked Polymer Gel Injection in Sandstone Gas Reservoirs: Implications for Water Shutoff Treatment

5.1 Introduction

Oil and gas – which are still the major fuel resources – face the problem of excess water production(Al-Shajalee et al., 2020d, Song et al., 2018b, Amir et al., 2019). Such water production can be controlled by mechanical, chemical, or biological methods(Karimi et al., 2014b), chemical methods being most effective and cheapest(Amir et al., 2019, Karimi et al., 2014b). Technically, polymer is injected into the vicinity of producing wells to limit relative water permeability(Broseta et al., 2000). However, it has been shown that the polymer's water shutoff efficiency is reduced dramatically in moderate-to-high permeability rocks(Mennella et al., 1998, Qi et al., 2013, Elmkies et al., 2002, Zaitoun and Pichery, 2001, Chiappa et al., 1999, Jinxiang et al., 2013, Al-shajalee et al., 2019b, Khamees and Flori, 2018).

There is thus a need to develop better polymer shut-off techniques. The application of a cross-linked polymer gel has shown promising efficiency in these more permeable rocks(Karimi et al., 2014b, Hajilary et al., 2015b). Where cross-linked polymer gels are expected to hold themselves inside the porous media by forming 3D-network(Zaltoun et al., 1991, Amir et al., 2019, Zhu et al., 2017, Nguyen et al., 2012). Moreover, El-Karsani et al. (2014) state that all legitimate available studies prove that once the crosslinking take place, which has larger size than pore throats, it will not propagate through the porous media (El-Karsani et al., 2014). However, the efficiency of cross-linked polymers (gels) were found to vary with gas, oil and water flow rate(Al-Sharji et al., 2001b, Al-Sharji et al., 1999a, Song et al., 2015, Mishra et al., 2014). In addition, the relative permeability modifier (RPM) performance decreases as the fluid flow rate increases, posing a risk of overestimating the water-cut reduction potential. Therefore, the influence of fluid flow rate needs to be included in RPM design(Stavland, 2010).

Furthermore, it was previously shown that the efficiency of a water shutoff treatment strongly depends on the gel quality (i.e. the gel's rigidity and stability)(Jia et al., 2010, Wassmuth et al., 2004, Zhao et al., 2011, Sharifpour et al., 2016). Moreover, while there have been recent insights into the mechanism of gel deformation and the associated disproportionate permeability reduction(Hajilary and Shahmohammadi, 2018, Yadav et al., 2020, Salehi et al., 2019, Song et al., 2015, Liang et al., 2017), still further scientific understanding of gel behaviour in relation to injection rates is required to guarantee successful gel placements in gas wells. The previous literature mostly focused on the use of gels to mitigate water production in oil wells. It is well known that gas wells have dissimilar physical characteristics compared to the oil wells, for example distinct fluid properties variations with pressure (e.g. low density and viscosity of gas) and higher flowrates due to gas expansion. Consequently, the disproportionate tendency of the gels to decrease water permeability will not be as simple as that anticipated for oil reservoirs. Thus, there is a need for studies concentrating on gas reservoirs.

Therefore, this work investigates the effect of gel rheology and residual fluid saturation on gas and water permeabilities in moderately permeable rocks as a function of gas/water flow rate. The present study therefore adds to our current understanding of the gel/water/gas interactions in porous media, and aids in the reduction of excess water production.

5.2 Materials and Methods

5.2.1 Materials

Three cylindrical Berea sandstone core samples were used in this study for the core flooding experiments. Porosity and permeability of the rock samples were measured using an automated permeameter and porosimeter [Coretest Systems (USA), model: AP-680], Table 5-1. Prior to the core flooding experiments, the clean rock samples were kept in an oven at 338K for 24 h.

Table 5-1: Petrophysical characteristics of Berea core samples and polymer gels used.

Sample	**Material**	**Length (cm)**	**Diameter (cm)**	**Porosity (%)**	**Permeability (mD)***	**Gel formulation**	
						Polymer (ppm)	**Cr^{3+} (ppm)**
Berea 1	Sandstone	7.61	3.81	18.7	140	20,000	200
Berea 2	Sandstone	7.60	3.80	19.0	166	20,000	300
Berea 3	Sandstone	7.60	3.80	18.6	149	20,000	400
Berea 4	Sandstone	7.61	3.79	20	170	20,000	600
Micromodel	Glass	2	1 (width)	48	2500	20,000	300
Capillary1	Pure glass	15	0.05	-	-	20,000	600

* Klinkenberg-corrected absolute Nitrogen permeability

2 wt. % KCl brine, high purity Nitrogen gas (99.99%, BOC Gas Australia), Chromium (III) acetate hydroxide and Poly (acrylamide-co-acrylic acid) partial sodium salt (P(AAM-co-AA)Na, compare Table 5-2 for details) were procured from Sigma Aldrich (Australia). KCl brine was selected in this work due to a notable clay content in sandstone samples(Al-Shajalee et al., 2020d).

Table 5-2: Relative permeability modifiers (RPM) agents used in this study.

Name	Chromium (III) acetate hydroxide*	Poly (acrylamide-co-acrylic acid) partial sodium salt
Mol. wt.	603.31 g mol^{-1}	520,000 g mol^{-1}
Formula	$(CH_3CO_2)_7Cr_3(OH)_2$	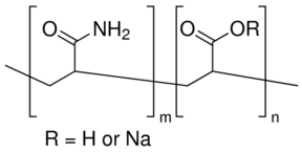

* Abbreviated as Cr^{3+} in the script

** Abbreviated as P(AAM-co-AA)Na in the script

Methylene blue and activated charcoal particles (100 mesh) were procured from Sigma Aldrich and used in the micromodel experiments, see below.

5.2.2 Rheological analysis

The rheological behavior of the P(AAM-co-AA)Na chromium cross-linked solution was examined. It has been reported that high salinity brine and high temperature may affect the behaviour of such gels(Yi et al., 2017, Zhu et al., 2017). However, Karimi et al. (2014) and Zhu et al. (2017) report that chromium cross-linked polyacrylamide gels can be utilized in the reservoirs with high temperatures (≈ 127 ^{o}C) and salinity (Karimi et al., 2014b, Zhu et al., 2017). In addition, to make such polymer gel systems more tolerant to thermal and salinity effects it is suggested to be combined with nanoparticle technology or some additives (Zhu et al., 2017, El-Karsani et al., 2014). It can also improve gels rheological properties and lubricity for different applications, and also making gels more environmentally friendly by reducing its toxicity(Zhu et al., 2017, El-Karsani et al., 2014, Ismail et al., 2016). Moreover, these cost-effective polyacrylamide and chemical additives such as a Chromium (III) acetate has been successfully applied in lab-scale and reservoir-scale sandstone oil/gas-fields operations(Liang et al., 2017, Liang et al., 2018, Karimi et al., 2014b, Ehsan et al., 2017, Jia and Chen, 2018, Zhang et al., 2014, Alvand et al., 2017, Aftab et al., 2016, Heidari et al., 2019, Yi et al., 2017, Zhu et al., 2017, Al-Sharji et al., 1999a, Al-Sharji et al., 2001b, Grattoni et al., 2001b, Dai et al., 2017b, Dovan and Hutchins, 1994, Xindi and Baojun, 2017, Seright, 1995).

P(AAM-co-AA)Na concentration was constant throughout the study (i.e., 20,000 ppm). Experimentally, P(AAM-co-AA)Na powder was added to the brine and stirred (at 300

rpm) by a magnetic stirrer at 333 K till the solution became homogeneous. Later, prescribed amounts of chromium(III) acetate hydroxide powder (i.e., 200, 300, 400, and 600 ppm) were added to the P(AAM-co-AA)Na solution, followed by continuous stirring for 10–12 h. The top of the beaker was sealed throughout the sample preparation procedure to avoid any water evaporation.

A rheometer [Thermofisher (USA), model: Haake Mars] with concentric cone geometry (diameter: 27 mm) was used for the study, and the flow behaviour of the samples was investigated over a wide shear rate range (0.01–100 s^{-1}). In addition, the impact of both the concentration of the cross-linking agent and the temperature were also examined. Thus amplitude, frequency, and temperature sweep tests were performed to study the viscoelastic behaviour of the polymer solutions. Note that the energy accumulated and dissipated in the polymer solutions under oscillatory stress are quantified by the storage modulus (G') and loss modulus (G''), respectively(Larson, 1999). Furthermore, the linear viscoelastic (LVE) region was determined by amplitude sweep tests [at a 0.1 – 100% strain and 1 Hz frequency]. Frequency sweep tests were carried out to gain further insight into the viscoelastic properties of the polymer solutions at a 0.01 – 100 Hz frequency and 5% strain. Finally the influence of temperature on G' and G'' was analyzed over a temperature range of 298 – 338 K at a constant frequency (1 Hz) and constant strain (5 %).

5.2.3 Core flooding experiments

Gas and water permeabilities of the rock samples were measured before and after polymer treatment to assess the gel performance. The samples were thus placed inside a core flooding apparatus and vacuumed for 24 hours under 3.45 MPa confining pressure at room temperature (Figure 5-1). Brine was then injected at 1 cm^3/min, and both pore and confining pressure, were simultaneously and gradually increased (keeping the effective stress constant at 3.45 MPa) to 6.90 and 10.35 MPa, respectively. The samples were then left for 24 h at 60 ^oC temperature to guarantee full saturation.

The absolute brine permeability was then measured (at a different brine injection rates of 0.2-160 cm^3/min). Subsequently gas was injected at a constant flow rate, until no water was produced, and a constant pressure differential across the sample was achieved. This step was repeated for different successively increasing flow rates (0.2–160 cm^3/min) and the differential pressures were recorded for each flow rate. A similar procedure was followed when measuring the water permeability. Finally, three pore volumes (PV) of crossed-linked polymer solution were injected through the rock sample at a constant flow rate of 1 cm^3/min. The polymer solution was then left to form a gel inside the core for 48 h at 60□C and 6.90 MPa pore pressure. In the post-treatment stage, three PV of brine were injected at 1 cm^3/min flow rate, thus removing the free polymer solution from the pore space. Subsequently, as in the pre-treatment stage, gas and then water were successively injected at the same flow rates as before.

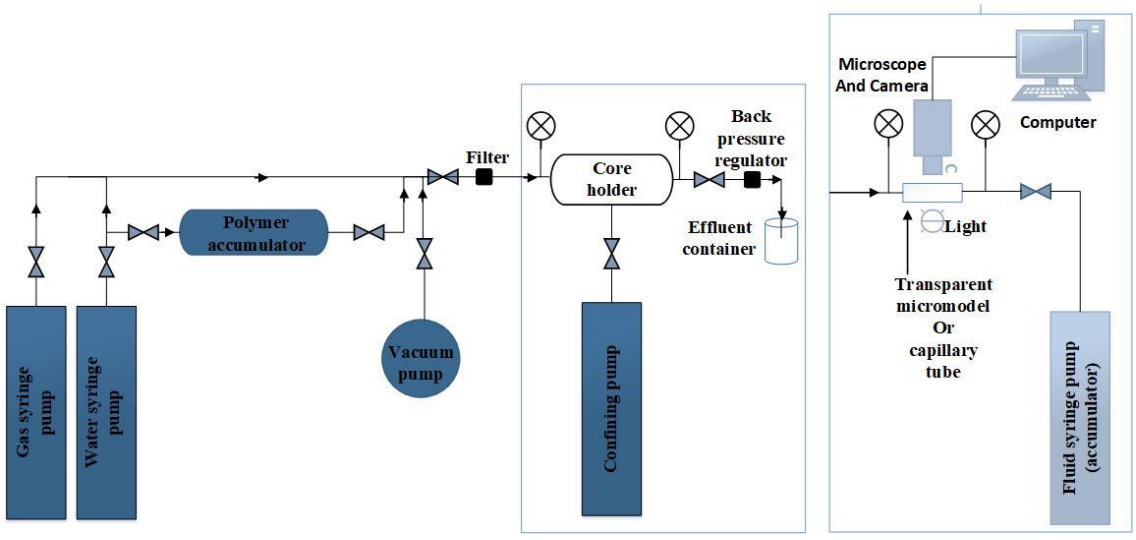

(a) (b)

Figure 5-1**:** Experimental setup of (a) the core flooding apparatus and (b) micromodel and capillary tube.

From the measured data, the water and gas residual resistance factors (Frr_w and Frr_g) before and after polymer treatment were calculated as follows(Al-Shajalee et al., 2019a):

$$Frr_w = \frac{\Delta P_{after}}{\Delta P_{before}} \quad (1)$$

$$Frr_g = \frac{\Delta P_{after}}{\Delta P_{before}} \quad (2)$$

where; ΔP_{before} and ΔP_{after} are the constant pressure differentials across the sample during water or gas injections (at constant flow rate). Note that the ratios in equations 1 and 2 can alliteratively be written as relative permeability before-treatment over relative permeability after-treatment(Al-shajalee et al., 2019b, Al-Shajalee et al., 2020d). RPM treatment is considered successful if $Frr_w > 1$ and $Frr_g \approx 1$ (resulting in $\frac{Frr_w}{Frr_g} >> 1$)(Al-Shajalee et al., 2020d).

Finally the shear rate γ in the porous medium was calculated via equation 3(Wei, 2015):

$$\gamma = \left(\frac{Q}{A(8K\emptyset)^{0.5}}\right) \quad (3),$$

where Q is the flow rate, and A, K and ϕ are the porous medium's cross-sectional area, permeability and porosity, respectively.

5.2.4 Two-dimensional (2D) Micromodel Flow Experiments

To interpret the core flooding results and to visualize the flow behavior of the gel and how it influenced gas flow at pore scale, a set of systematic visualization experiments were conducted on a transparent 2D-micromodel using borosilicate glass and a capillary tube which both mimic the sandstone. The 2D-micromodel flooding experiments were performed using the setup shown in Figure 5-1b, and the glass micromodel is shown in Figure 5-2. A 0.1 wt% methylene blue powder (Sigma Aldrich Australia) was dissolved in the brine to improve the visual observation during micromodel and capillary tube experiments(Dehshibi et al., 2019). To ensure full dissolution of the dye particles, the brine-dye mixture was sonicated (using an UNiSOiCS FXP10M sonicator at 40 kHz for 5 h). A Leica microscope (model: MZ6) and high-speed high-resolution camera (iDS Imaging Development Systems

GmbH (Germany), model: UI-3140CP Rev. 2) connected to a computer recorded the various flow patterns. These were further analysed, see below.

The glass micromodel experiment started with brine injection at 0.02 cm^3/min until the model was fully saturated with the brine; the pore pressure was then gradually increased to 3.45 MPa. The subsequent steps were similar to those used in the core-flooding procedure; first the absolute brine permeability was measured (at constant flow rate, 0.02 cm^3/min), gas was injected at different but constant flow rates (0.1-15 cm^3/min), followed by brine injection at constant flow rate (0.02 cm^3/min). 1 cm^3 of the crossed-linked polymer solution was then injected through the micromodel at constant flow rate (0.02 cm^3/min), and the micromodel was left in a water bath for 48 h at 60 ºC and 6.90 MPa to allow polymer gelation inside the porous medium. Next, 1 cm^3 of brine was injected at 0.02 cm^3/min flow rate, thus removing the free polymer solution from the pore space. Subsequently, as in the pre-treatment stage, gas and then water were injected.

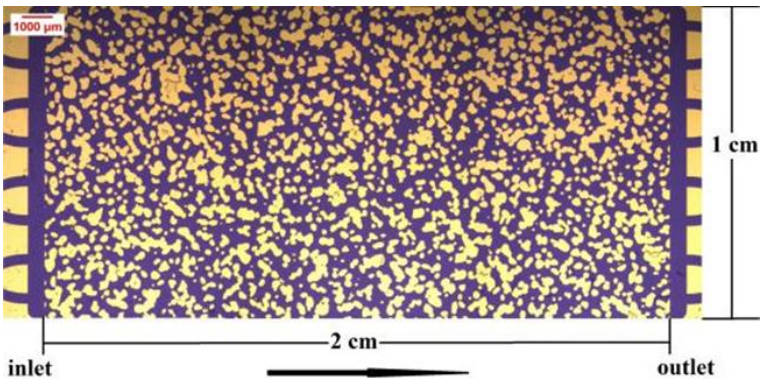

Figure 5-2: Photo of the 2D micromodel used.

5.2.5 Capillary tube tests

To further enhance understanding of the fundamental physics observed in the 2D micromodels, experiments were conducted in a transparent circular capillary tube (Figure 3). Note that as such a tube can be rotated by 360º, a 3D demonstration can be achieved. However, since the diameter of the capillary tube was higher than the average pore diameters in the core samples ($\approx 4\ \mu m$,(Al-shajalee et al., 2019b)) or the micromodel, a higher cross-linker concentration was used to produce a stronger gel and to thus hold the gel inside the

capillary tube (600 ppm Cr^{3+}) during the flow experiment. Activated charcoal particles (0.1 wt. %) were mixed with the gel to assist the visual observation and to confirm the presence of the transparent gel inside the tube during the flow experiments. Note that since the main purpose of this test was to visually observe the flow behavior of water and gas in presence of the gel, a constant flow rate of 0.1 cc/min was used for water and gas injection, before and after treatment. Note that this flow rate value is within the shear rate range used in core sample (middle value), please see Table 5-3.

A polymer solution (600 ppm Cr^{3+} in 20,000 ppm P(AAM-co-AA)Na formulation) solution was injected into the capillary tube (at ambient conditions). The capillary tube was then kept in an oven for 48 h at 60 C^o to assure RPM solution gelation. The gel layer had a non-uniform thickness and covered almost the whole surface area of the inside wall of the capillary tube. Table 3 summarizes the flow and shear rates used in the various flow experiments.

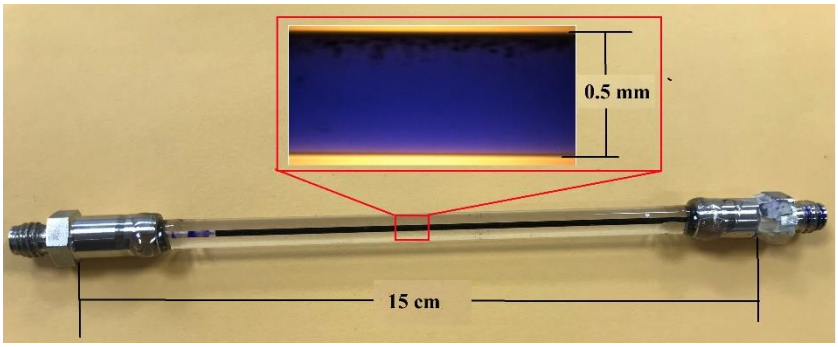

Figure 5-3: Circular capillary glass tube used.

Table 5-3: Flow and shear rates used in the various experiments.

Core sample		Micromodel		Capillary tube	
Q, cm/min	Shear rate, s^{-1}	Q, cm/min	Shear rate, s^{-1}	Q, cm/min	Shear rate, s^{-1}
0.2	6.77924	0.1	2604.52443	0.1	319.4571*
0.4	13.55848	0.15	3906.78664		

0.6	20.33772	0.2	5209.04886		
0.8	27.11696	0.3	7813.57329		
1	33.8962	0.4	10418.0977		
2	67.7924	0.5	13022.6221		
4	135.5848	1	26045.2443		
6	203.3772	2	52090.4886		
8	271.1696	5	130226.221		
10	338.962	10	260452.443		
20	677.924	12	312542.931		
40	1355.848	15	390678.664		
60	2033.772				
80	2711.696				
100	3389.62				
120	4067.544				
140	4745.468				
160	5423.392				

*The micromodel was exposed to the allowable maximum gas shear (within the manufacturing limit of 10.3 MPa maximum operational pressure).

5.3 Results and Discussion

5.3.1 Rheological analysis

To improve RPM performance, it is important to understand the gel's rheological properties(Grattoni et al., 2001d, Karimi et al., 2014b, Idahosa et al., 2014, Zaitoun and Pichery, 2001, Al-Sharji et al., 2001b, Salehi et al., 2019, Yadav et al., 2020, Pereira et al., 2020). Therefore, viscosity measurements were conducted using steady shear flow tests, and the viscoelastic properties of the polymer solutions were examined via oscillation shear flow

tests. Temperature sweeps mimicking true reservoir temperatures were also conducted. The subsequent sections describe the results obtained.

5.3.1.1 Steady shear flow test

At constant shear rate, the viscosity of the aqueous P(AAM-co-AA)Na –Cr^{3+} gel clearly increased with increasing cross-linker concentration (Figure 5-4). For instance, at a shear rate of 10 s^{-1}, the viscosity of the 200 ppm Cr^{3+} gel (a constant 20,000 ppm P(AAM-co-AA)Na concentration was always used) was 23.68 mPa s, which drastically increased to 1775.8 mPa s, when Cr^{3+} concentration increased to 600 ppm, consistent with literature data(Alvand et al., 2017, Audibert et al., 1993, Grattoni et al., 2001b). This drastic viscosity increase is caused by the additional cross-links created in the gel (by the additional Cr3+). Note that carboxyl and amide groups in the P(AAM-co-AA)Na chemically react with the Cr^{3+}. This leads to the cross-linked polymer network and electrostatic interactions between polyacrylamide and Cr^{3+}(Han et al., 1995, Burrafato et al., 1990, Wiśniewska et al., 2015).

We also observed shear thinning behavior, i.e. viscosity decreased with increasing shear rate (Figure 5-4), which is also consistent with literature data(Zhang et al., 2007, Karimi et al., 2014b). The decrease in viscosity with increasing shear rate is caused by the disruption of the polymers' carbon–hydrogen bonds(Xiong et al., 2018), and devaluation in intermolecular interaction between P(AAM-co-AA)Na and Cr^{3+}(Alvand et al., 2017, Machale et al., 2019). Such shear thinning ensures reduction in the local drag force during polymer injection in the field(Harrison et al., 1999). However, small augmentations in viscosity at lower shear rates (i.e. 0.01–0.1 s^{-1}) are attributed to the resistance offered by the polymeric solution to the deformation and is coherent with recent investigations(Dimi-Misic et al., 2019, Umerova and Ragulya, 2017).

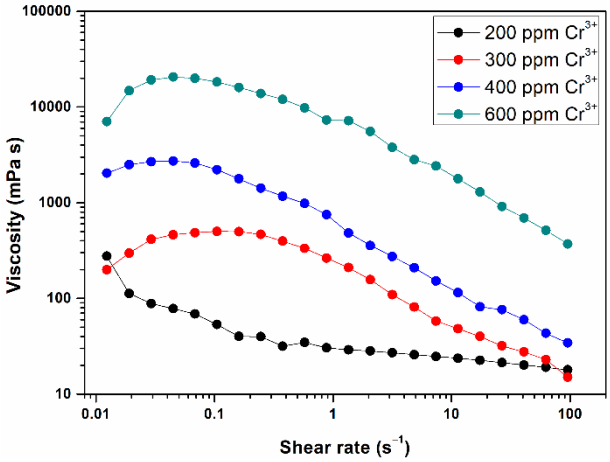

Figure 5-4: Viscosity of aqueous P(AAM-co-AA)Na gels as a function of chromium concentration and shear rate (P(AAM-co-AA)Na concentration = 20,000 ppm, temperature = 298 K; pressure = atmospheric; salinity = 2 wt% KCl).

5.3.1.2 Oscillation shear flow tests

Figure 5-5(a) demonstrates the measured moduli as a function of strain (0.1–1000 %) at constant frequency (1 Hz) for varying Cr^{3+} concentrations (at a fixed P(AAM-co-AA)Na concentration, 20,000 ppm). It is clear that *G′* was higher than *G″* over the full strain range tested. This indicates gel-like characteristics of the P(AAM-co-AA)Na –Cr^{3+} solution. *G′* increased with increasing Cr^{3+} concentration. The only exception however observed for a Cr^{3+} concentration of 200 ppm, when G'' was higher than G'. This implies mainly viscous behavior at 200 ppm Cr^{3+} concentration(Pereira et al., 2020); which is due to fewer network cross-links in the gel. One more note that a sharp decrease in the G' demonstrates the strain-thinning behavior of P(AAM-co-AA) Na–200 ppm Cr3+ solution. This behavior generally demonstrates the destruction of the samples' internal structure while retorting to an externally-applied stimulus.

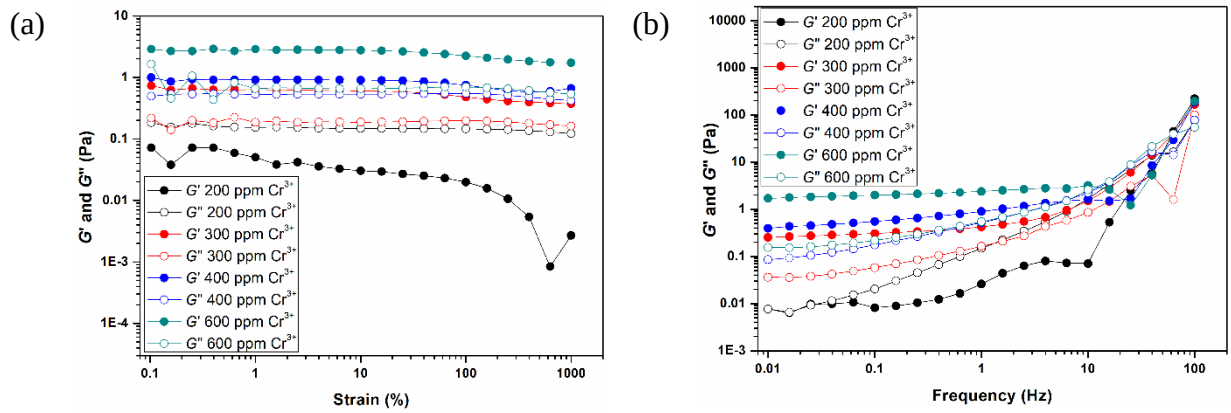

Figure 5-5: G′ and G″ as a function of (a) strain (0.01–1000%) at constant frequency (1 Hz) and (b) frequency (0.01-100 Hz) at constant strain (5 %) for the aqueous P(AAM-co-AA)Na –Cr^{3+} solution. (Temperature = 298 K; pressure = atmospheric; salinity = 2wt% KCl).

After identifying the LVE region, frequency sweep tests were carried out to determine the viscoelasticity of the samples. Figure 5-5(b) demonstrates that the linear viscoelastic behavior of the samples was governed by the elastic component as $G' > G''$. This confirms the gel–like structure of the samples(Song et al., 2006). Notably, the viscous liquid-like behavior of the polymer solution for the 200 ppm Cr^{3+} case (in 20,000 ppm P(AAM-co-AA)Na solution) was again confirmed with these frequency sweep tests.

Importantly, all solutions (except 200 ppm Cr^{3+}) demonstrated a predominantly elastic behavior, while the transition from elastic to viscous regions (i.e., $G'' > G'$)occurs at a relatively higher frequency, as depicted by the crossover point in Figure 5-5b. This elastic behavior also suggests that characteristic three-dimensional gel network was formed(Pereira et al., 2020). Thus, the addition of chromium ions promoted the elastic behavior of the polymer gel possibly due to the attractive intermolecular interactions between polymer and cross-linker.

5.3.1.3 Temperature sweep tests

Temperature sweep studies were also carried out on the Cr^{3+} cross-linked P(AAM-co-AA)Na solutions over a temperature range of 298–338 K at constant frequency (1 Hz) and strain (5

%) (see Figure 5-6). Similar to the other oscillation shear flow tests, a dominance of elastic behavior was observed (i.e. G' was greater than G'') over the whole temperature range tested. Moreover, nominal variations in G' with respect to oscillation shear rate and temperature suggests mechanical and temperature stability of the P(AAM-co-AA)Na –Cr^{3+} solution. The mean velocity of the polymer solution molecules is directly proportional to temperature (Samanta et al., 2010). Consequently, the average intermolecular force between molecules declines. However, the addition of Cr^{3+} cross-linking agent (chromium acetate) in lower-molecular-weight polymer solution results in strong intermolecular interactions and subsequently, the formation of a network structure. In addition, the temperature-dependent rheological properties of polyacrylamide solution could enhance the convective heat transfer (Shin and Cho, 1994, Hartnett and Kostic, 1989). Therefore, a plateau trend has been observed in Figure 5-6.

Figure 5-6(b) demonstrates the complex viscosity of P(AAM-co-AA)Na –Cr^{3+} solutions over a range of temperatures. The complex viscosity of the gel increased with temperature for Cr^{3+} concentrations of 300 ppm and higher, while it decreased for a 200 ppm Cr^{3+} concentration. The interaction between molecules in the solution and the tendency of Cr3+ for the development of aggregates with P(AAM-co-AA)Na are functions of temperature(Wang et al., 2011).

In the P(AAM-co-AA)Na –200 ppm Cr^{3+} solution, the intermolecular interactions between P(AAM-co-AA)Na and Cr^{3+} are limited due to the lower Cr^{3+} concentration. However, the probability of aggregate formation and also intermolecular interaction increases with increasing concentration.

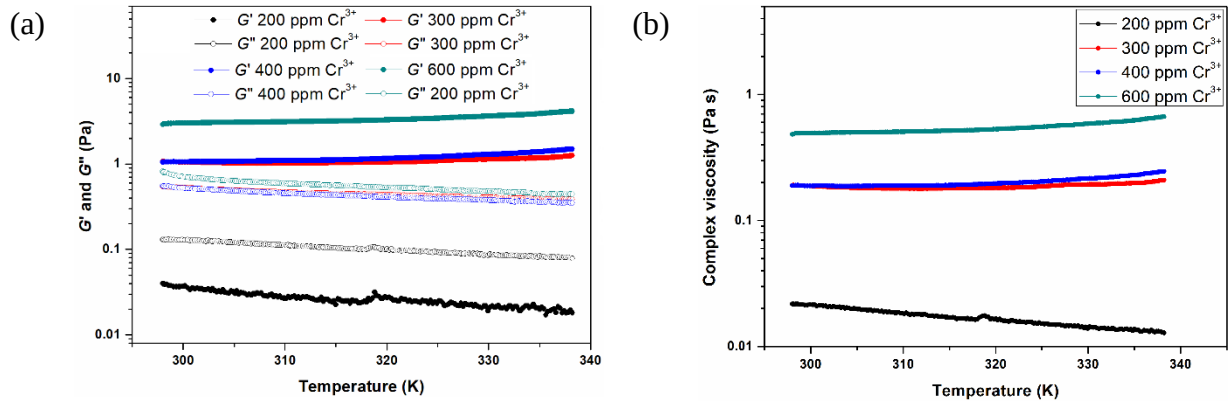

Figure 5-6: (a) Storage G' and loss G'' moduli and (b) complex viscosity of various P(AAM-co-AA)Na –Cr^{3+} gels as a function of temperature. (Brine salinity: 2 wt% KCl, Pressure = Atmospheric).

5.3.2 Core flooding results

We then performed core flooding experiments at reservoir conditions to evaluate the effectiveness of the gel treatment, with a focus on its performance to reduce the relative water permeability. Figure 5-7 shows the relationship between Frr_w, Frr_g , and Frr_w/Frr_g and (water and gas) flow rate as a function of cross-linker concentration. The gel with the higher cross-linker concentration (600 ppm Cr^{3+}) had significantly higher viscosities, especially at low shear rates. Note that the results for the 20,000 ppm P(AAM-co-AA)Na –600 ppm Cr^{3+} solution (in Berea 4 samples) have not been included after the aging time.

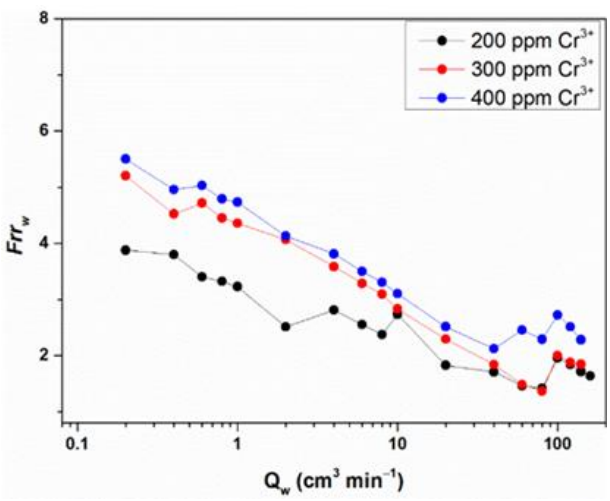

(a)

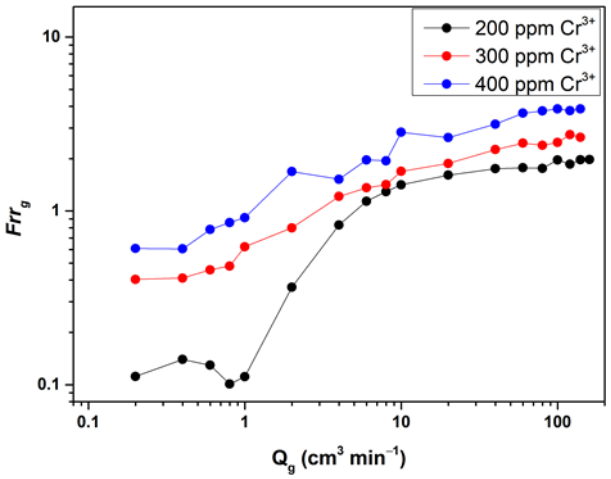

(b)

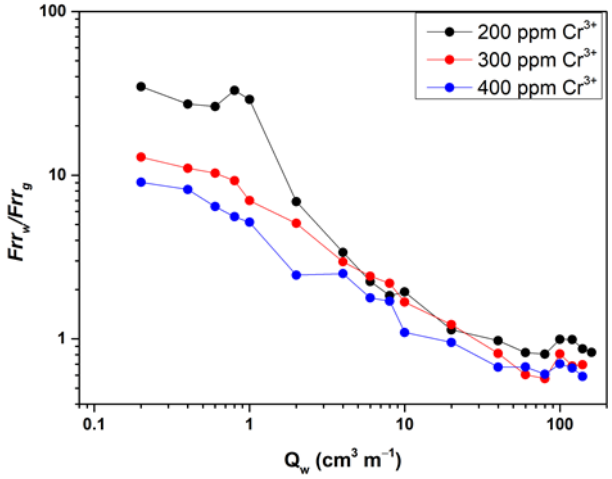

(c)

Figure 5-7**:** Relationships between (a) Frr_w versus water flow rate, (b) Frr_g versus gas flow rate and (c) Frr_w/Frr_g versus water flow rate as a function of cross-linker concentration for Berea sandstone (Pressure = 6.9 MPa, Temperature = 333 K, Salinity = 2%wt. KCl, P(AAM-co-AA)Na concentration = 20,000 ppm).

5.3.2.1 Water residual resistance factor, Frr_w (imbibition)

The water residual resistance factor (Frr_w) was highest for the largest Cr^{3+} concentration (Figure 5-7a). For example, for a water flow rate of 1 cm^3/min, Frr_w was ~ 5 at 400 ppm Cr^{3+}, while it was ~3 at 200 ppm Cr^{3+} concentration. This suggests that stronger gels retain more water in the porous medium. This again can be attributed to the solid-like nature of the gel (see Figure 5-5), which is less deformable during water flow.

Furthermore, and importantly, it was found that as the water flow rate (0.1–160 cm^3/min) increased, Frr_w decreased, irrespective of the cross-linker concentration (Figure 5-7a). Moreover, the minimum Frr_w remained greater than unity for all cross-linker concentrations over the whole water flow rate range tested. For example, the 20,000 ppm P(AAM-co-AA)Na and 200 ppm Cr^{3+} system, as flow rate increased from 0.1 to 160 cm^3/min, Frr_w decreased from 3.8 to 1.7 (i.e. Frr_w depends on the flow and shear rate). This could be mainly caused by two effects, namely a) polymer layer deformation (thinning), and/or b) residual gas saturation (S_{gr}) reduction. Indeed**,** shear thinning behavior of the polymer –Cr^{3+} solutions has been observed in the rheological measurements (see Section 3.1.1 above), it has also been previously reported by numerous researchers(Barrufet and Ali, 1994, Liang and Seright, 1997, Zaitoun and Kohler, 1988, Hajilary and Shahmohammadi, 2018, Nguyen et al., 2006, Song et al., 2015, Yadav et al., 2020, Stavland et al., 2011).

Furthermore it was observed that increasing water flow rate liberated more gas from the core sample (i.e. a lower S_{gr} was achieved). These liberated bubbles were observed in the effluent container which was filled with water (compare Figure 5-1a). Zhang et al. (2016) suggest that as gas saturation decreases, the potential of gel to limit water relative permeability sharply decreases(Zhang et al., 2016). Moreover, recent investigations(Yadav et al., 2020, Liang et al., 2017, Liang et al., 2018, Prado Paez et al., 2009, Connolly et al., 2017) state that significant trapping of residual non-wetting saturation due to RPM treatment results in a greater restriction to water (wetting) flow, and eventually significantly increases Frr_w Considering all above, we conclude that the reduction in Frr_w with increasing water flow rate is due to both, the deformation of the gel layer and decreasing S_{gr}.

5.3.2.2 Gas residual resistance factor (drainage)

We then analysed how the gel influences the drainage (displacement of brine by gas) behaviour in the core. As for imbibition (see Figure 5-7a), the gas residual resistance factor (Frr_g) was highest for the highest Cr^{3+} concentration (Figure 5-7a). For instance, for a gas

flow rate of 1 cm^3/min, Frr_w was ~ 0.9 for a 400 ppm Cr^{3+}, while it was ~0.1 for a 200 ppm Cr^{3+} concentration. However, in contrast to the imbibition process (see Figure 5-7a), the gas flow rate (Q_g) increased, when Frr_g increased for a given Cr^{3+} concentration (see Figure 5-7 b). This implies that the gel is shear thickening when gas is flowing. Similar behaviour was reported by Song et al. (2015) during the second and third water-gas injection cycles, while shear thinning behaviour was observed during the first cycle (Song et al., 2015). However, the majority of published works on the effect of fluid flow rate on gel performance were performed on oil/water systems, and show either shear independency(Nguyen et al., 2006, Hajilary and Shahmohammadi, 2018, Liang et al., 1995, Liang and Seright, 1997, Barrufet and Ali, 1994, Zaitoun and Kohler, 1988) or shear thinning behaviour(Song et al., 2018b) with increasing oil shear rate. Moreover, and interestingly, there is a critical gas flow rate Q_{gc1} (which is different for each Cr^{3+} concentration) below which Frr_g < 1 and above which Frr_g > 1 (see Figure 5-7b). Note that Frrg < 1 indicates an increase in gas permeability due to RPM lubrication effect(Al-shajalee et al., 2019b, Al-Shajalee et al., 2019a). For example, at a Cr^{3+} concentration of 400 ppm, the critical gas flow rate was ~ 1 cm^3/min, while at 200 ppm Cr^{3+} concentration, the critical gas rate was ten times higher (~ 10 cm^3/min; Figure 5-7b). It is thus clear that Frr_g depends on Q_g and Cr^{3+} concentration. Figure 7 b may also suggest that stronger gels have a smaller lubrication effect (i.e. as gel strength increased, Frr_g increased).

Our results aligning with literature show that gels showed shear thickening behaviour during gas flow and shear thinning during water flow. However, the opposite is requested by oil industry. Therefore we recommend that more studies are needed to be done in this regard.

5.3.2.3 Frr_w / Frr_g ratio

Previous studies showed that gel efficiency and water reduction both significantly increase with gel strength(Nguyen et al., 2006). However, a stronger gel decreased the gel lubrication effect (i.e. Frr_g increased, Figure 5-7b). We therefore analyzed the Frr_w / Frr_g ratio, Figure 5-7c. Clearly the 200 ppm Cr^{3+} gels showed optimum behavior. For instance, for a water flow

rate of 1 cm^3/min, Frr_w/Frr_g was ~ 29 for 200 ppm Cr^{3+}, while it was ~5 for a 400 ppm Cr^{3+} concentration. This suggests that weaker gels retain less water in the porous medium, yet they increase the gas permeability. This is an important observation which indicates that there are two counteracting mechanisms (water retention versus lubrication effects) which both determine DPR performance, although in our study the lubrication effect dominated (see also Al-Sharji et al., 2001a(Al-Sharji et al., 2001a), Al-Shajalee et al., 2019a(Al-Shajalee et al., 2019a)).

As mentioned earlier, irrespective of the cross-linker concentration, it was observed that higher water flow rates decreased Frr_w (Figure 5-7a), while higher gas flow rates decreased Frr_g (Figure 5-7b). Therefore, when fluid (water and gas) flow rate increased, Frr_w/Frr_g decreased, also irrespective of the cross-linker concentration (Figure 5-7c). For example, at 200 ppm Cr^{3+} concentration, as the fluid flow rate increased from 0.1 to 160 cm^3/min, Frr_w/Frr_g decreased from 35.0 to 0.8 (i.e. Frr_w / Frr_g depends on the flow and shear rates). Similar trends were observed elsewhere (Song et al., 2018b, Hajilary and Shahmohammadi, 2018). Moreover Figure 5-7c shows that for all gels there is a critical flow rate (~ 30 cm^3/min) above which the treatment becomes unsuccessful (Frr_w/Frr_g <1). It is thus clear that Frr_w / Frr_g depends on fluid flow rate and Cr^{3+} concentration.

5.3.3 Micromodel flooding tests

We then performed 2D micromodel flooding tests (at 3.45-8.9 MPa and 298 K). The key objectives here were to a) analyse the effect of S_{wir} on Frr_g (when $Q_g < Q_{gc1}$), and to b) provide novel insights into the gel shear thickening behaviour (inside a porous medium) at high gas flow rates. The subsequent subsections describe these results.

5.3.3.1 Micromodel flooding results

The core flooding results show that as Q_g increased, Frr_g increased (Figure 5-8b), consistent with the core flooding results (see Figure 5-7b). Moreover, there is a critical gas flow rate Q_{gc1} (~1 cm^3/min) below which $Frr_g < 1$ (improving gas permeability) and above which Frr_g

> 1 (gas permeability reduction). Sharifpour et al. (2016) pointed out that during low gas flow rates, gel performance is mainly controlled by the ability of the polymer to fill-up the rock space, while at higher gas flow rates the gel rigidity controls gel performance (Sharifpour et al., 2016). We thus hypothesized that (for our particular conditions), two factors control the gel behaviour during drainage (as gas flow rate increases), namely: a) the reduction in the irreducible water saturation (S_{wir}), and/or b) polymer layer expansion; these factors were thus examined, and the results are discussed below in sections 3.3.2 and 3.3.3.

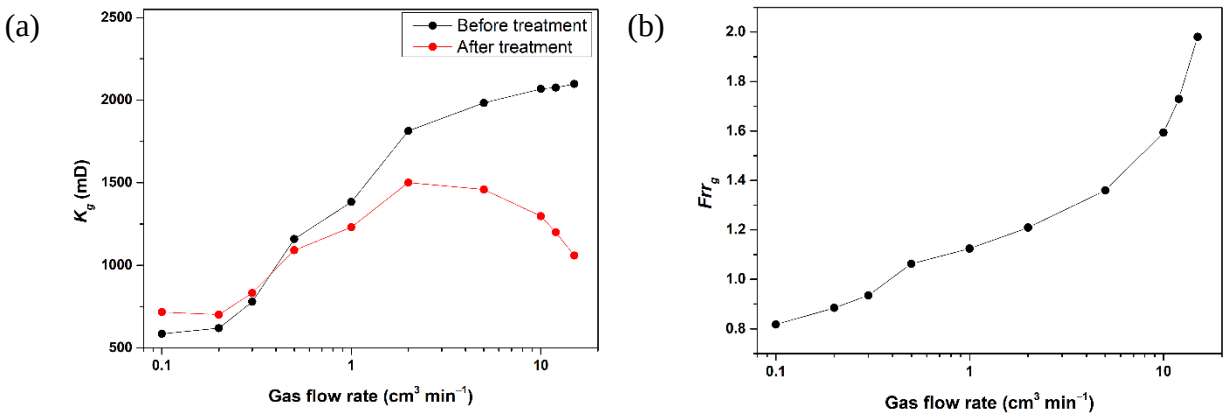

Figure 5-8: a) Relationship between gas flow rate and gas permeability before and after gel treatment, b) relationship between Frr_g and gas flow rate after gel treatment (300 ppm Cr^{3+}concentration, pressure = 3.4 MPa, temperature = 298 K, P(AAM-co-AA)Na concentration = 20,000 ppm, salinity = 2 wt% KCl).

5.3.3.2 The effect of irreducible water saturation (S_{wir})

To understand the pore-scale mechanisms occurring during core flooding observations during increasing gas injection rate, we conducted micromodel experiments for different gas injection rates. Clearly, as gas injection rate increased, S_{wir} decreased across the entire micromodel (Figure 5-9). Furthermore, and consistent with the core flooding results (see Figure 5-7b), as the gas flow rate (Q_g) increased, Frr_g also increased (see Figure 5-8b). Moreover, there was also a critical gas flow rate Q_{gc1} (~ 0.4 cm^3/min) below which Frr_g < 1 (gas permeability increase) and above which Frr_g > 1 (gas permeability reduction). Thus when the gas flow rate increased, S_{wir} decreased and in turn the lubrication effect towards the

gas phase decreased, similar to the results reported previously (Al-shajalee et al., 2019b, Al-Shajalee et al., 2019a). Such lubrication effects are one of the main reasons for DPR when RPM's are used (Alfarge, 2016, Alfarge et al., 2017, Alfarge et al., 2018, Zaitoun et al., 1990, Zaitoun and Kohler, 1988, Dovan and Hutchins, 1994, Scott et al., 2020, Norouzi et al., 2017, Al-Sharji et al., 2001a). Mechanistically, the gel layer on the rock reduces the pore surface roughness, further, it forms a water film on the pore surface, and both effects increase k_{rg} (Zaitoun and Kohler, 1988, Zaitoun et al., 1998).

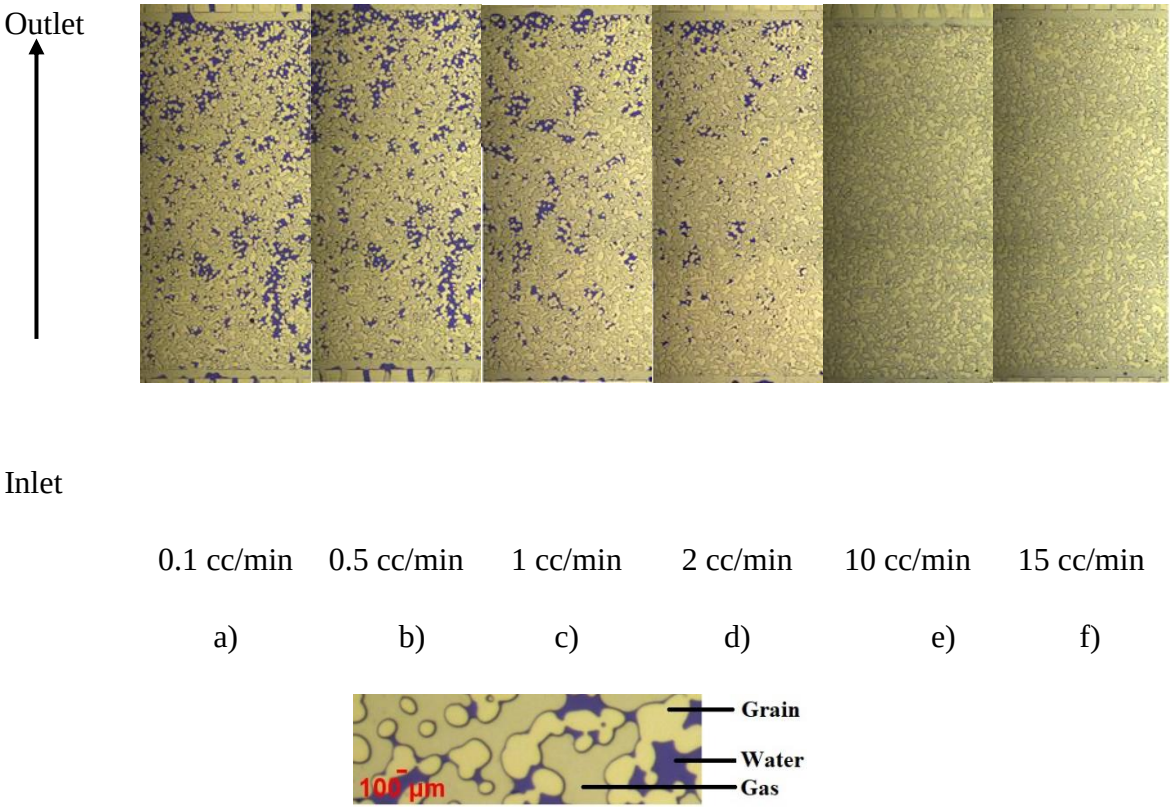

Figure 5-9: Micromodel images of the fluid distribution in the porous medium after gel treatment as a function of gas flow rate. (Pressure = 3.4 MPa, temperature =298 K, salinity = 2 wt% KCl, P(AAM-co-AA)Na concentration = 20,000 ppm, Chromium concentration = 300 ppm).

5.3.3.3 Effect of polymer rheology

Previous studies showed that the reduction in relative oil permeability (oil was non-wetting) after gel treatment is independent of shear rate (Barrufet and Ali, 1994, Zaitoun and Kohler, 1988, Hajilary and Shahmohammadi, 2018, Nguyen et al., 2006). However, the core flooding

and micromodel results presented here clearly show that the reduction in gas (non-wetting phase) permeability after gel treatment is rate dependent. Moreover, gas permeability decreased due to gel treatment when Q_g increased (shear thickening behaviour, see above).

To examine this further we performed additional micromodel experiments at very high gas flow rates (≥ 10 cc/min), Figure 5-9 e and f, and Figure 5-10 a to f). At a critical Q_g value (Q_{gc2} =10 cc/min), gas bubbles were trapped in the gel and some of these bubbles totally dissolved in the gel over time (Figure 5-10 a to f). Moreover, at Q_{gc2} the gel layer on the glass surface expanded (Figure 5-10 d to f). This caused a further gas permeability reduction (i.e. Frr_g increased). We conclude that the gel layer deformation was the underlying mechanism of the shear thickening (dilatant) behaviour. Such dilatant behaviour is caused by the elongation of the adsorbed coiled polymer molecules in the converging flow (Liang et al., 1992). For gas flow rates greater than the critical flow rate, the gel layer underwent a sequential deformation, i.e. first gas bubbles were trapped in the gel, followed by the dissolution of the gas bubbles in the gel, and finally gel layer expansion.

Note that the gas flow rate range used in the micromodel experiments (0.1-15 cc/min) induced higher shear rates (2600-39,000 s^{-1}; equation 3) than those occurring in the core sample (7-5,000 s^{-1}; equation 3). Despite this difference, similar trends between the gas flow rate and Frr_g were observed (shear thickening and gradual increase of Frr_g as gas flow rate increased). This suggests that such shear thickening also occurred in the rock sample, yet to a lesser extent.

In summary, during low gas flow rates gel performance is mainly controlled by the gel lubrication effect, while at higher gas flow rates gel rigidity is the dominant factor.

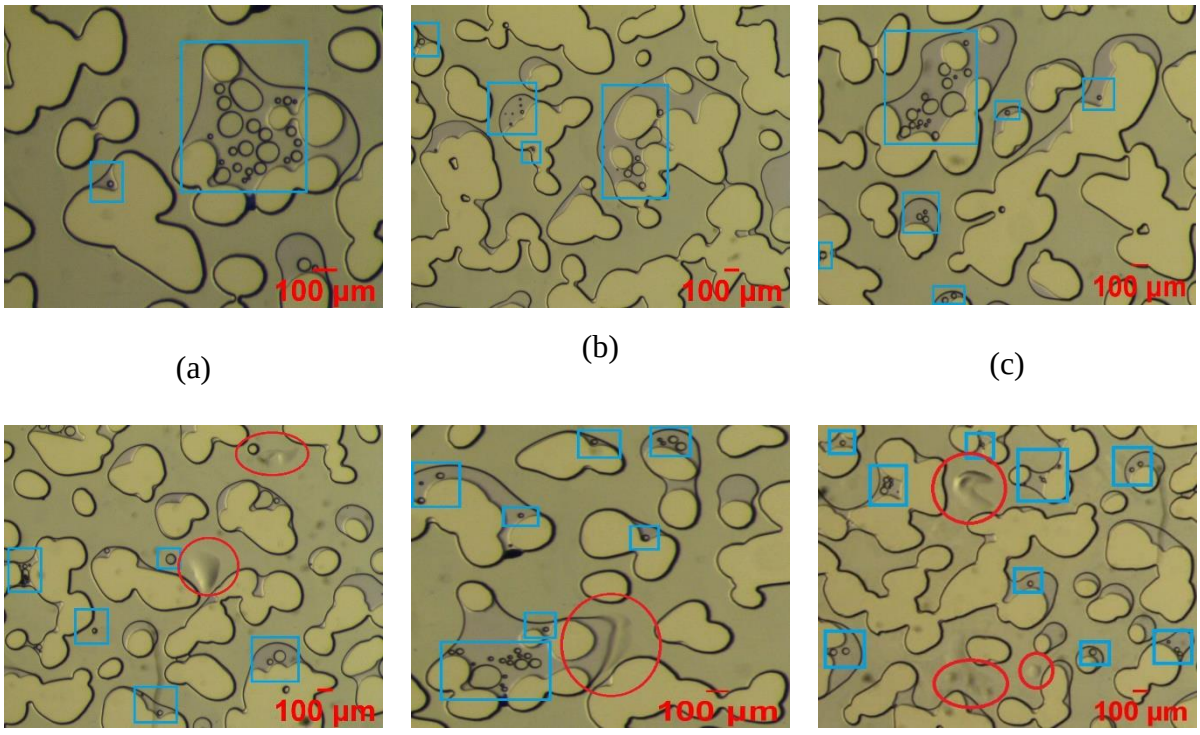

(a) (b) (c)

(d) (e) (f)

Figure 5-10: Visual pore scale micromodel observations (gas flow rate = 10 cm^3/min, pressure = 3.4 MPa, temperature = 298 K, salinity =2 wt% KCl, P(AAM-co-AA)Na concentration = 20,000 ppm , Chromium concentration = 300 ppm). Blue rectangles = trapped gas; red circles = gel expansion.

5.3.4 Capillary tube experiments

Capillary tube experiments were then performed at ambient conditions to further examine the rheological gel behaviour, and to investigate the gel formation at pore walls, and water and gas flow. The subsequent subsections describe the results.

5.3.4.1 Water flooding

Figure 5-11a shows that the 3D-network of gel holds itself(Grattoni et al., 2001b, Amir et al., 2019, Zhu et al., 2017) onto all pore surfaces after 48 h aging period. After one minute of water flooding two separate regions developed (Figure 5-11b-d). In the first region, water flowed through a rapture in the gel (convective flow), while in the second region water flowed through the gel layer (by diffusion).

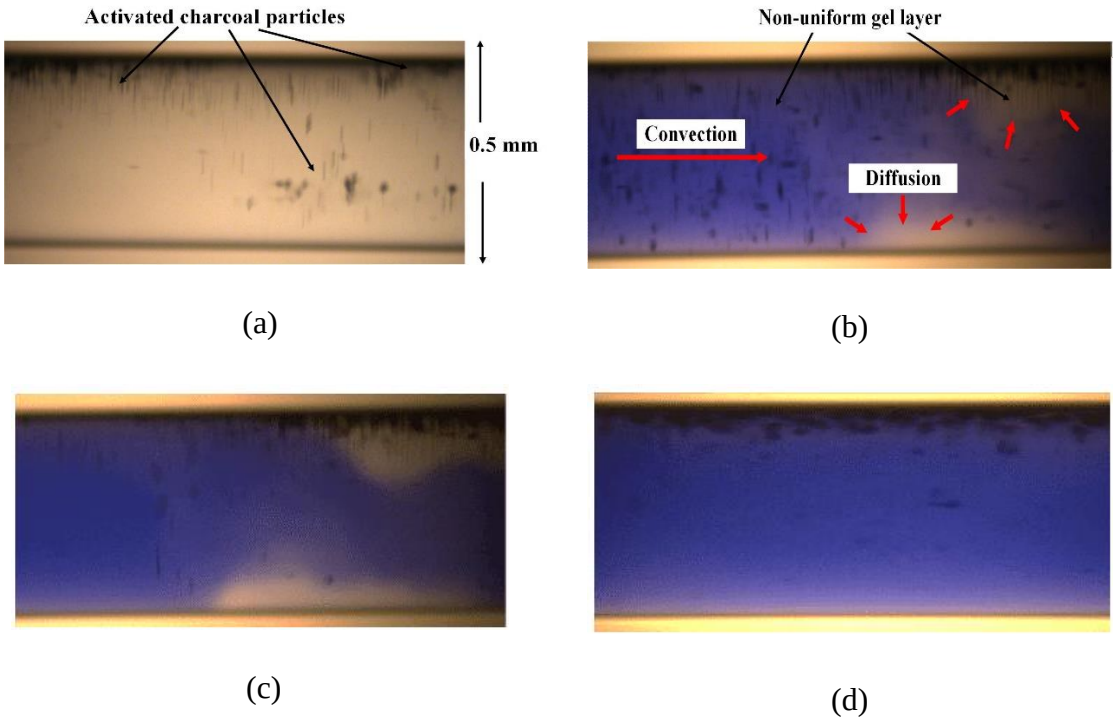

Figure 5-11: Flow visualization images during water injection into gel placed in the capillary tube. Water (blue) flowed convectively through the transparent gel (20,000 ppm P(AAM-co-AA)Na -600ppm Cr^3), and also diffused into the gel (a) transparent gel filling the tube at t = 0 (After ageing the gel inside the capillary tube for 48 h the gel entirely filling the tube), (b) water flowing at time t = 1 min, (c) water flowing and diffusing at time t = 10 min, and (d) water totally diffused in the gel at t = 17 min.

5.3.4.2 Gas flooding

During gas injection, gas slugs migrated through the non-uniform flow channel formed in the raptured gel by the water flood (Figure 5-12). The gas slugs deformed and then split up when they flowed through a narrower constriction in the flow path; beyond the constriction, the split gas slugs sometimes coalesced again. Due to the non-uniform thickness of the gel, this process was repetitive and caused pressure fluctuations. Precisely, as gas flowed through a constriction, the pressure increased until the gas deformed the gel; at this point the gas slugs became elongated and moved further downstream through the gel. The pressure then decreased again, and the gel layer returned to its original state (as before the deformation), thus the elongated gas slug split again into smaller bubbles.

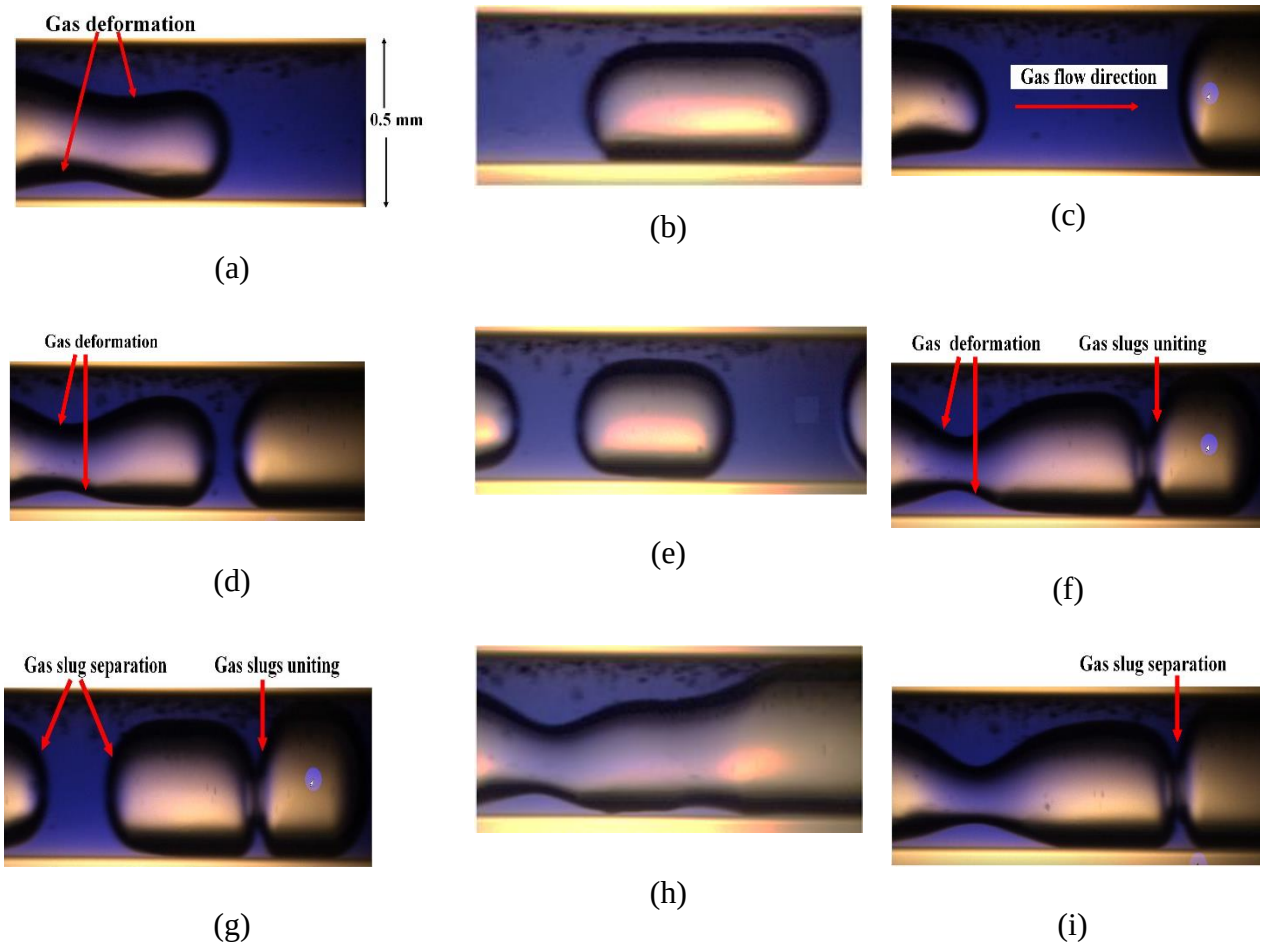

Figure 5-12: Gas slugs flowing through the non-uniform channel in the gel (created by the waterflood) (a) gas slug deformed by the thick gel, (b) gas slug enlarged in the thin gel, (c) another gas slug moving in, (d) the second gas slug deformed, too, (e) gas slugs flowing, (f) gas slugs coalescing, (g) gas slug separation and gas slugs coalesce at the same time, (h) gas slug elongation and (i) elongated gas slug separation.

These observations are considerably different to those reported previously, where the gel formed only in the edges and crevices of grains (Liang et al., 2017, Sharifpour et al., 2016, Al-Sharji et al., 2001b). Most likely in these previous studies gel layer formation was not observed as the layer was too thin and totally transparent (but still existed, see above).

5.4 Conclusions

This work investigated the rheological behaviour of P(AAM-co-AA)Na -chromium gels for a broad range of shear rates (0.01-100 s^{-1}), chromium concentrations (200-600 ppm Cr^{3+} in 20,000 ppm P(AAM-co-AA)Na) and temperatures (298-338 K), followed by core scale and

pore scale flow experiments, to determine the gel performance in terms of reducing water production. A clear increase in viscosity of the P(AAM-co-AA)Na gel with increasing cross-linking agent concentration was measured and shear thinning was observed. Oscillation shear flow tests indicated that all solutions (except for 200 ppm Cr^{3+} concentration) exhibited a predominantly elastic behaviour (with transition from elastic to viscous behaviour occurring at a relatively high frequency). Likewise, a temperature sweep confirmed the dominance of elastic behaviour over viscous behaviour throughout the temperature range tested.

Furthermore, it was found that higher gel strength increased the water retention inside the porous media. Two counteracting mechanisms were responsible for the observed disproportionate permeability reduction (DPR), namely (a) water retention and (b) lubrication (both being functions of gel rheology). While the lubrication effect was the main mechanism behind the DPR especially at low gas flow rates, gel rigidity was prominent at higher flow rates. This was associated with gas diffusion and dissolution in the gel, which in turn expanded the gel layer thickness and reduced gas permeability. Moreover, irrespective of the cross-linker concentration, it was observed that higher water flow rates (during imbibition) decreased Frr_w. This was attributed to: a) gel shear thinning behaviour and b) S_{gr} reduction. However, increasing gas flow rates (during draining) decreased the Frr_g (i.e. shear thinking behaviour). Moreover, there was a critical fluid flow rate above which the treatments became unsuccessful, as both effects (i.e. water retention and lubrication) were significantly reduced.

The micromodel results showed that at high gas flow rate (Q_{gc2}), the gel layer expanded on the glass surface after trapping and dissolving gas bubbles in the gel or water. This in turn increased Frr_g, as the gas flow path became more restricted. In the capillary tube experiment gas slugs pushed themselves through the non-uniform channel without diffusion. The gas slugs repetitively deformed and split up and coalesced again when the gas flowed through the thicker gel layers, also causing pressure fluctuations.

In summary, the results of this study improve our fundamental understanding of the mechanisms associated with gel treatment for water permeability reduction. These results thus aid in the implementation of gel placements for reducing excess water production.

Chapter 6: A New Dimensionless Approach to Assess Relative Permeability Modifiers

6.1 Introduction

Currently many hydrocarbon fields are nearing their maturity and excessive water production from production wells have become a major challenge to the oil and gas industry. Chemical approaches are broadly utilized to reduce water production. This can include polymer gels or inorganic cements but these are only applicable when the water producing zone can be treated. In the case where water producing zones cannot be identified, polymers can be injected in the area around the producing wells. Some classes of polymer can selectively reduce the production of water whilst having a minimal impact on hydrocarbon. These materials are known as relative permeability modifiers (RPMs). To date, a number of experimental investigations and field trials have been carried out to understand the behavior of RPMs with the oil/water system. However, there is very limited data available regarding the gas/water systems.

All the existing literature agrees that by increasing the concentration of the injected polymer the adsorption is enhanced so that the thickness of the adsorbed polymer layer increases on the internal pore walls of a porous medium. This may eventually decrease the permeability to all fluids flowing in the medium (Grattoni et al., 2001a, Mennella et al., 1998, Ogunberu and Asghari, 2004b, Mishra et al., 2014, Zheng et al., 1998, Qi et al., 2013). However, there is no universal consensus about the effect of pre-treatment absolute permeability of the medium on the eventual permeability reduction. Mennella et al. (Mennella et al., 1998) and Qi et al. (Qi et al., 2013) claim that permeability reduction decreases with increasing absolute permeability whereas Jinxing et al. (Jinxiang et al., 2013) have concluded the opposite. Zheng et al. (Zheng et al., 1998) results show both increasing then decreasing of permeability reduction with increasing absolute permeability of their rock samples.

As indicated before, many researchers(Zaitoun and Kohler, 1988, Mennella et al., 1998) indicate that the presence of the adsorbed polymer layer on the pore wall is expected to lessen the flow pore size for all phases in the same way and ultimately modify their permeabilities. However, Mennella et al. (Mennella et al., 1998) claim that assuming the polymer layer thickness not to be constant and depend on every flowing fluid phase would yield a more consistent interpretation of the experimental data. Grattoni et al. (Grattoni et al., 2001a), Mishra et al. (Mishra et al., 2014) and Mennella et al. (Mennella et al., 1998) report that the post-treatment effective pore size would depend on the spatial distribution of expanded and shrunken regions of polymer layer which depends on the flowing fluid phase considered.

Using capillary tubes and sand packs, the measured gas, oil and water permeabilities in the presence of a polymer/gel were found to vary with flow velocity (shear rate) according to a power-law (Al-Sharji et al., 2001b, Al-Sharji et al., 1999c, Song et al., 2015, Mishra et al., 2014). For a non-deformable porous medium, the power-law model can only be attributed to the elastic properties of the non-Newtonian or deformable fluid (polymer/gel), something that may not be expected from a Newtonian fluid (oil, water and gas) (Al-Sharji et al., 1999c, Al-Sharji et al., 2001b, Cohen and Christ, 1986, Saphiannikova et al., 1998) . Zaitoun and Kohler(Zaitoun and Kohler, 1988) and Mishra et al. (Mishra et al., 2014) also report that the adsorbed polymer molecules in a porous medium deform under hydrodynamic forces (shear stress) exerted on it and ultimately this would affect the permeability.

Grattoni et al. (2001a), Ali and Barrufet (2001) and Zaitoun and Pichery (2001) emphasize the importance of shear dependency or the deformation of the adsorbed polymer layer on permeability reduction(Grattoni et al., 2001a, Ali and Barrufet, 2001, Zaitoun and Pichery, 2001). They show in their results that this dependency, which is a function of polymer concentration, would eventually affect flow behaviour of different fluid phases. Zaitoun and Kohler(Zaitoun and Kohler, 1988) imply that the presence of the adsorbed polymer layer, which attracts wetting phase to it, brings about several effects including reduction of the flow of the wetting phase as well as inducing lubrication effect towards the non-wetting phase.

They also state that this lubrication influence increases with increasing the viscosity contrast between the non-wetting and wetting phases and decreases with increasing the viscosity contrast in the case of using a non-wetting phase.

The mechanisms behind the 'Disproportionate Permeability Reduction (DPR)' of RPMs on fluid phases is still a matter of controversy. Wall effect of the adsorbed polymer layer on the inner walls of a porous medium may induce one or all of the four effects of wettability, steric, lubrication and swelling/shrinking. The wall effect is considered a primary mechanism behind the relative permeability modification(Zaitoun and Kohler, 1988, Tielong et al., 1996, Zaitoun et al., 1998, Elmkies et al., 2002, Nieves et al., 2002, Dawe and Zhang, 1994, Dovan and Hutchins, 1994, Zaitoun and Pichery, 2001). Moreover, the polymer layer thickness may change as affected by many parameter such as the phase that is being flowed, flow rate (shear rate) and polymer rheology(Zaitoun and Kohler, 1988, Mennella et al., 1998, Grattoni et al., 2001a, Mishra et al., 2014, Al-Sharji et al., 2001b, Al-Sharji et al., 1999c, Song et al., 2015, Cohen and Christ, 1986, Saphiannikova et al., 1998). Therefore, reporting experimental results in term of polymer thickness or pore radius may be more meaningful.

The first aim of this research was to experimentally study the effect of an RPM agent (i.e. a cationic polymer) and its concentration on water and gas permeability reductions in a number of sandstone rock samples of different permeability. A new dimensionless parameter called the dimensionless effective pore radius (r_{eff}^{-}) that can help to interpret and compare the resulting experimental data in a more insightful, streamlined and objective manner is also outlined. If looked at as a final quantitative figure to evaluate the effectiveness of an RPM treatment, r_{eff}^{-} may seem similar to the commonly used residual resistance factor (Frr). However, this newly developed parameter explicitly reflects the effect of a number important parameters of the rock-fluid-polymer system(e.g. pore sizes, permeability, porosity, thickness of the adsorbed polymer layer,) on the final results of the treatment. Finally, Forchheimer equation has been also used here to observe gas flow regimes changes.

6.2 Experimental work

6.2.1 Materials

Four cylindrical water-wet Berea Sandstone core plugs, with similar porosities were used in this study (Table 6-1). The permeability of each rock varied to some degree across the study. To determine the mineral composition of this Berea Sandstone, X-Ray Diffraction (XRD) was used on an offcut of a sample whose results are shown in Table 6-2 which reveal a mineralogy typical of sandstones. The brine used in core-flooding experiments was a synthetic brine (2wt% KCl) prepared by dissolving an analytical grade KCl (Sigma-Aldrich) in distilled water. The gas phase was a high purity bottled nitrogen gas (99.99wt%, BOC Gas). We also used a cationic Poly(acrylamide-*co*-diallyldimethylammonium chloride) solution(Table 6-3) with four different concentrations as our RPM agent (Table 6-1). The earlier mentioned synthetic brine was used to dilute the polymer and arrive at the concentrations listed in Table 6-1. The reason behind using a cationic polymer was due to its positively charged ions that can be adsorbed well on the negatively charged Berea Sandstone pore surfaces. As discussed in the earlier sections of the manuscript, adequate adsorption of an RPM agent is essential for achieving the possible relative permeability modification effect of the agent.

Table 6-1: Characterization of the rock samples used and the polymer concentration used to treat each during core flooding.

#	L, cm	D, cm	∅, %	K, mD	Polymer concentration, ppm
1	4.881	3.798	21	350	1000
2	4.947	3.792	22	375	2000
3	4.82	3.779	21	410	4000
4	4.77	3.789	21	426	8000

Table 6-2: Berea Sandstone mineral composition as obtained from XRD analysis

Phase	Weight%
Quartz	81.2
Microcline (max)	4.8
Kaolin	5.7
Illite/Muscovite	4.5
Albite, low	3
Dolomite	0.5
Calcite	0.3

Table 6-3: Characteristics of the polymer used in this study as the RPM agent.

Name	Poly(acrylamide-co-diallyldimethylammonium chloride)
Molecular Structure	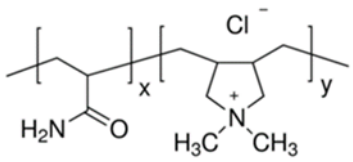
Formula	$(C_8H_{16}ClN)_n.(C_3H_5NO)_m$
Molecular Weight	75000
Viscosity	9,000-25,000 cP(25 °C)
Density	1.02 g/mL at 25 °C
Manufacturer	Sigma-Aldrich https://www.sigmaaldrich.com/catalog/product/aldrich/409081?lang=en&region=AU

6.2.2 Rheological properties

A series of rheological tests were conducted using a HAAKE RheoWin rheometer on different concentrations of the polymer solution to determine its behavior and the effect of shear stress on shear rate (Figure 6-1). According to the results obtained, these solutions show

non-Newtonian shear thickening behavior so the viscosity varies depending on the applied stress or force. The polymers also show enhanced shear thickening behavior with increasing solution concentration so the increasing shear rate and polymer concentration would lead to increase in polymer rigidity.

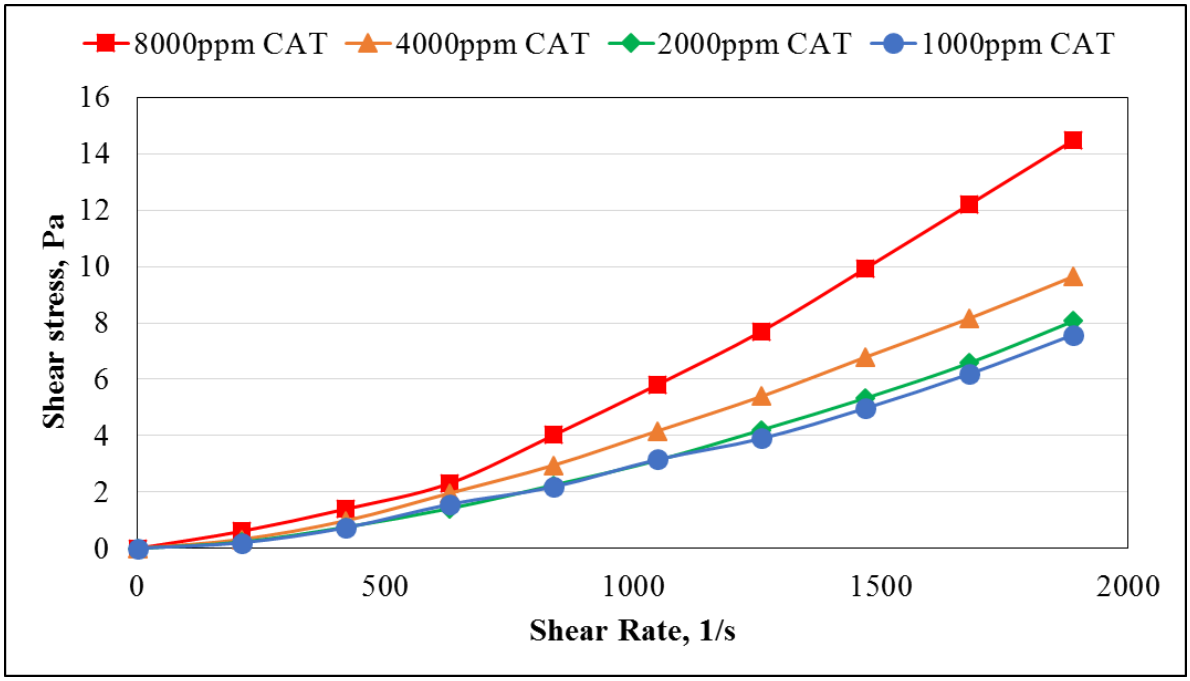

Figure 6-1: Results of the rheology tests: the effect of shear rate on shear stress.

6.2.3 Core-flooding Tests

A schematic of the core-flooding setup used in this work is presented in Figure 6-2. The flooding experiments were conducted at a room temperature with a confining pressures of 10.35 MPa and a pore pressure of 6.90 MPa.

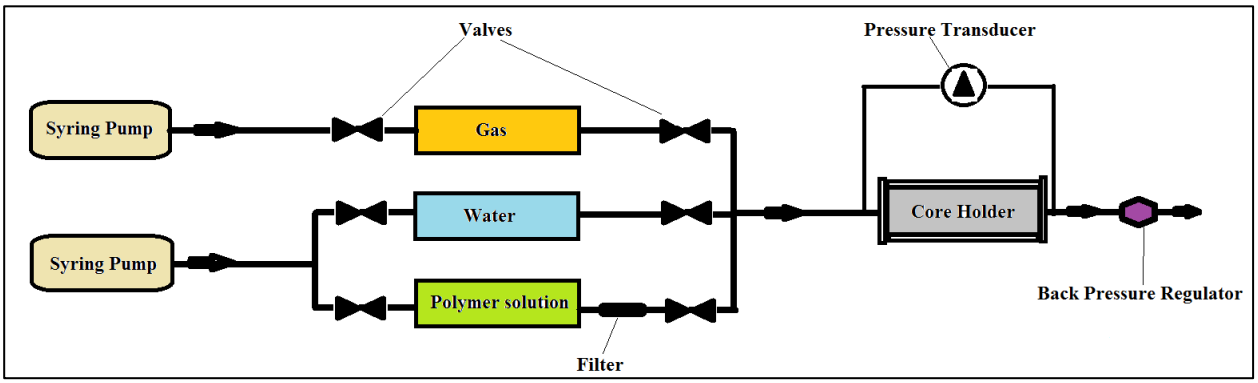

Figure 6-2: Core flooding test equipment.

After petrophysical characterization of the core samples they underwent a core-flooding experiment that consisted of three major steps as outlined below. The basic preliminary characterization included drying the samples in an oven at 65℃ for 24 hours or until their weights stabilized. Subsequently, they underwent nitrogen porosity and permeability measurements whose results are included in Table 6-1.

- Before Polymer Treatment:

1. Installing a core sample inside the core holder. Vacuuming the sample for 24 hours. Then saturating the sample with the 2%KCl brine under constant pressure for another 24 hours.
2. Injecting brine at different flow rates to measure the sample's absolute permeability (k).
3. Injecting gas under constant flow rate until no more brine would be produced and achieving constant differential pressure across the sample (i.e. establishing irreducible water saturation (S_{wirr})). Calculating the relative permeability to gas at irreducible water saturation $k_{rg1}(S_{wirr})$ using the final measured differential pressure. Repeating this step with different gas flow rates (1-70 cc/min).
4. Injecting brine with constant flow rate until no more gas would be produced and achieving constant differential pressure across the sample (i.e. reaching residual gas saturation $S_{gr.}$). Calculating relative permeability to brine at residual gas saturation k_{rw1} (S_{gr}) using the final measured differential pressure. Repeating this step with different brine flow rates (1-4 cc/min).

- Polymer Treatment:

5. Injecting three pore volumes of a polymer solution with a specific concentration (Table 6-1) through the core sample.
6. Aging the sample in contact with the polymer solution for 48 hours.

- After Polymer Treatment:

7. Injecting brine at constant flow rate to displace free/unreacted polymer solution from sample.

8. Injecting gas under constant flow rate until no more brine would be produced and achieving constant differential pressure across the sample (i.e. reaching irreducible water saturation S_{wirr}). Calculating the relative permeability to gas at irreducible water saturation and adsorbed polymer $k_{rg2}(S_{wirr+\ polymer})$ using the final measured differential pressure. Repeating this step with different gas flow rates (1-70 cc/min).
9. Injecting brine under constant flow rates until no more gas would be produced and achieving constant differential pressure across the sample (i.e. reaching residual gas saturation (S_{gr})). Calculating the relative permeability to brine at residual gas saturation and adsorbed polymer $k_{rw2}(S_{gr+polymer})$ using the final measured differential pressure. Repeating this step with different water flow rates (1-4 cc/min).

The data measured or calculated from the above outlined experimental procedure was subsequently used to calculate a number of important parameters using specific equations that will be presented and discussed in the next section of the manuscript.

6.2.4 Dimensionless Parameters

The residual resistance factor (Frr) is a critical parameter introduced in the literature to evaluate the performance of an RPM agent (White et al., 1973). This parameter is calculated separately for each of the fluid phases whose permeability is to be modified. The general equation used to calculate Frr is provided below.

$$Frr = \frac{\Delta P_a}{\Delta P_b} \qquad 16$$

Where; ΔP_a and ΔP_b are the decreases in pressure during injection which is recorded across a core sample for a fluid phase after and before the RPM treatment, respectively.

As indicated earlier, it is expected that DPR effect of an RPM agent would be realized by leaving a very thin layer (~μm) on the internal pore surfaces of the treated porous medium. Since the polymer layer thickness is not always constant and affected by many parameter

such as flowing phase, flow rate (shear rate), polymer rheology and concentration, pore sizes, etc. (Zaitoun and Kohler, 1988, Mennella et al., 1998, Grattoni et al., 2001a, Mishra et al., 2014, Al-Sharji et al., 2001b, Al-Sharji et al., 1999c, Song et al., 2015, Cohen and Christ, 1986, Saphiannikova et al., 1998). Evaluating any experimental results using a parameter expressed in terms of polymer thickness and pore radius may be more meaningful and insightful. The pre-treatment effective or average pore radius for the medium in combination with F_{rr} has been used by Zaitoun and Kohler (Zaitoun and Kohler, 1988) to estimate the effective thickness of the adsorbed layer of the RPM polymer/gel using the following equation.

$$\mathrm{e} = \mathrm{r}\left(1 - \frac{1}{\mathrm{Frr}^{0.25}}\right) \qquad 17$$

Where, e is the estimated average hydrodynamic polymer/gel layer thickness (μm), r is the average pore radius (μm) for brine flow which can be calculated using Equation 18 [8] and F_{rr} is the residual resistance factor as calculated using Equation 1.

$$r = \left(\frac{8.k_{brine}}{\emptyset}\right)^{0.5} \qquad 18$$

Where, k_{brine} is the brine permeability, and ϕ the porosity of the porous medium as modelled using a bundle of capillary tubes.

Subsequently, the post-treatment effective porous radius can be estimated using the following equation by taking into account the fraction of the original radius taken up by the presence of the adsorbed polymer/gel layer.

$$r_{eff} = r - e \qquad 19$$

Where r_{eff} is the post-treatment effective pore radius (μm).

Dimensionless variables have been used in many technical areas, such as fluid dynamics and fluid flow in porous media, as simple and effective comparison tools especially when there

are many cases of similar nature to be evaluated in a study that have different features and are needed to be compared with each other. Thus, for different core samples that, for example, have different permeability (i.e. with different initial pore radii), and have been treated with different polymer concentrations (i.e. resulting in different adsorbed polymer thicknesses), the dimensionless form of Equation 4 would be very helpful for comparing the results obtained for one sample to those obtained for others. Therefore, we propose the dimensionless effective pore radius to be calculated using the following equation.

$$r_{eff}^{-} = \frac{r_{eff}}{r} \qquad 20$$

where r_{eff} and r are defined by equations 3 and 4.

As indicated earlier, r_{eff}^{-} may be regraded very similar to Frr in that it is a ratio between the pre- and pot-treatment of a parameter impacted upon by an RPM treatment (i.e. ΔP for the case of Frr and r_{eff} for the case of r_{eff}^{-}). However, the critical advantageous feature of r_{eff}^{-} is that it explicitly reveals the interlink between the effectiveness of the treatment and important properties of the rock-fluid-polymer system through utilizing outputs of equations 1-4. The Frr may only be explicitly related to permeability of the porous medium under investigation through ΔP as it may be calculated from the Darcy's equations.

6.2.5 Forchheimer Equation

The Forchheimer Equation, as presented in Equation 6, is in the form of an equation for a straight line and has been widely used to interpret the experimental data that show inertial effects (i.e. non-Darcy flow). However Zimmerman et al. (Zimmerman et al., 2004) state that this equation can be also utilized over any range of flow rates as it produces similar results to those obtained from the Darcy's equation at low values of flow rate.

$$Y_g = \frac{1}{k} + \beta X_g \qquad 6$$

Where; β is inertial resistance coefficient (m^{-1}) and also:

$$Y_g = \frac{(P_1^2 - P_2^2)}{2\mu_g L P_1 \left(\frac{Q_{g1}}{A}\right)} \qquad 7$$

and

$$X_g = \frac{P_1 M}{\mu_g RT}\left(\frac{Q_{g1}}{A}\right) \qquad 8$$

Where Y_g and X_g are the Forchheimer-Y (m^{-2}) and Forchheimer-X (m^{-1}) functions, respectively, Q_{g1} is the gas volumetric flow rate at the inlet (m^3/sec), A the cross sectional area (m^2), L the length (m), and P_1 and P_2 the measured pressures at the inlet and outlet of the porous medium, respectively.

6.3 Results and Discussion

This section of the manuscript presents and discuss the experimental results obtained in the current study. Initially, the results are interpreted and discussed in the context of the commonly used Frr. Subsequently, in order to demonstrate its effectiveness, the same experimental data are analyzed, interpreted and discussed using the newly developed r_{eff}^{-}. Another objective of this section is to interpret the results obtained in this work using the Forchheimer equation to determine the possible flow regimes that may be encountered within the porous media as the gas injection flow rate changes with and without the presence of the adsorbed polymer layer.

6.3.1 The effect of rock permeability and polymer concentration

Table 6-4 shows the residual resistance factors of water and gas as obtained from the experiments and the calculated ratio between them along with the rock permeabilities and polymer concentrations used. It is worth noting that each Frr value reported in this table for each fluid phase is the average value calculated across all phase injection flowrates explored (i.e. 1-4cc/min). For visual inspection, the Frr_w and Frr_g values are then plotted in Figure 6-3 and Figure 6-4 against polymer concentration and rock permeability, respectively. As revealed by the figures, Frr_w decreases initially with increase in both rock permeability (from

350 to 410mD) and polymer concentration (from 1000 to 4000ppm), but then increases with further increase in the rock permeability to 426 mD and the polymer concentration to 8000ppm. All the reviewed literature report an ever increasing Frr_w with an increase in the polymer concentration as attributed to the increase in the thickness of the adsorbed polymer layer(Mennella et al., 1998, Qi et al., 2013, Jinxiang et al., 2013, Zheng et al., 1998).

The apparent contradiction between our results and previously published data is believed to have been caused by the increase in rock permeability at the same time as the increase in the polymer concentration. In other words, the final value of Frr_w resulted from every experiment would be dictated by the competing and opposite effects of pore radius (which increases with increase in permeability) and adsorbed polymer layer (which increases with increase in polymer concentration). With regards to the trend observed in Frr_w versus sample permeability, similar behaviour has been reported in the literature(Mennella et al., 1998, Qi et al., 2013, Jinxiang et al., 2013, Zheng et al., 1998). This indicates that a uniform trend of ever decreasing or increasing Frr_w versus rock permeability may not be expected. In our work, this trend can be explained by the discussion presented above when addressing a similar trend observed for variation in Frr_w versus polymer concentration.

With regard to the gas phase, Figure 6-3 and Figure 6-4 reveal an increasing Frr_g with an increase in both rock permeability and polymer concentration. The observed trend in Frr_g versus polymer concentration is in agreement with those presented in all the previously published literature (Grattoni et al., 2001a, Mennella et al., 1998, Ogunberu and Asghari, 2004b, Mishra et al., 2014, Zheng et al., 1998, Qi et al., 2013). The reason for Frr_g behaving differently against the polymer concentration to that observed for Frr_w could be due to the fact that the adsorbed polymer layer may impact on the gas flow in different ways compared with the water flow. Figure 6-3 reveals that 1000, 2000 and 4000ppm polymer concentrations have resulted in even improvement in the gas flowing behaviour as Frr_g for these concentrations is less than unity. This improvement, for the polymer concentrations used and for the range of gas flow rates (1-4cc/min) applied, may have been induced by the lubrication effect of the adsorbed polymer layer facilitating the gas flow as a mechanism which is also

suggested by(Zaitoun and Kohler, 1988). Concerning the observed trend in Frr_g versus rock permeability, as discussed for the water phase before, similar trends have been reported in the literature.

Table 6-4: The average **Frr_w**, **Frr_g** and **Frr_w/Frr_g** (Water and gas flow rate range =1-4cc/min)

Rock No.	Porosity, %	Permeability, mD	Polymer concentration, ppm	Frr_w	Frr_g	Frr_w/Frr_g
1	21	350	1000	2.38	0.6	5.55
2	22	375	2000	2.05	0.8	2.6
3	21	410	4000	1.15	0.8	1.86
4	21	426	8000	2.75	2	1.41

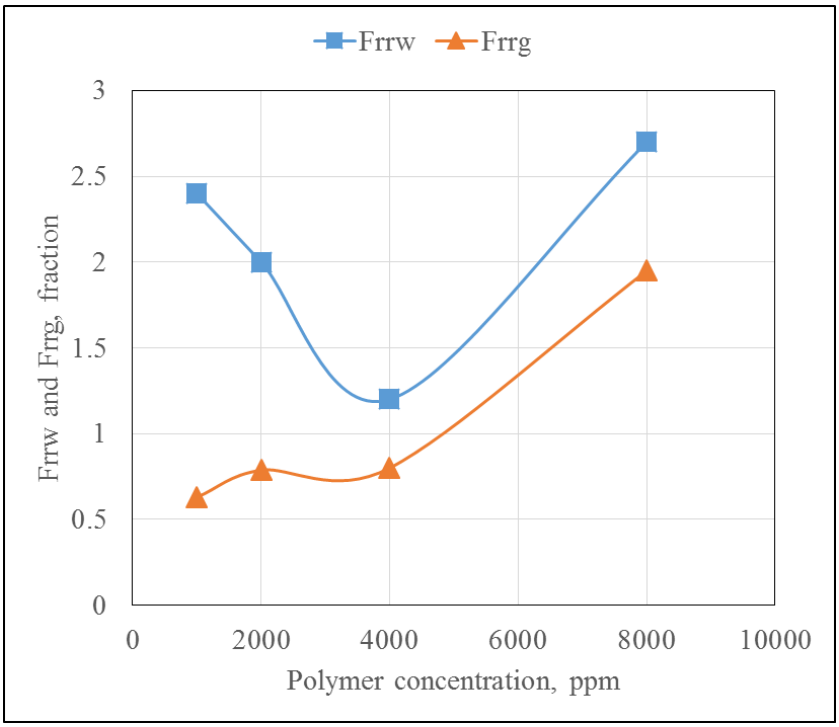

Figure 6-3: The relationship between polymer concentration and **Frr_w** and **Frr_g**.

Technically, for the evaluation of the effectiveness of an RPM treatment, the ratio of Frr_w/Frr_g is often more insightful than individual Frr_w and Frr_g on their own. The best treatment is that with Frr_w/Frr_g values of more than unity and, in general, the higher the value the better the outcome of the treatment. Figure 6-5 and Figure 6-6 show the effect of both rock permeability and polymer concentration on Frr_w/Frr_g for the experiments conducted in this work. According to these figures, the ratio decreases with an increase in concentration and permeability. Most importantly these data reveal that the concentration of 1000ppm is the best treatment concentration for our polymer solution and 8000ppm is the worst.

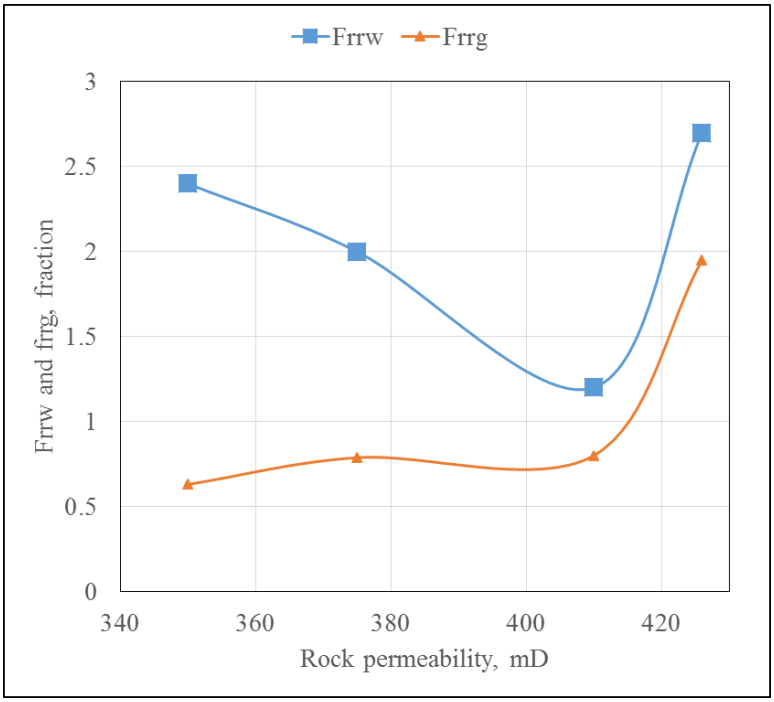

Figure 6-4: The relationship between rock permeability and **Frr_w** and **Frr_g**.

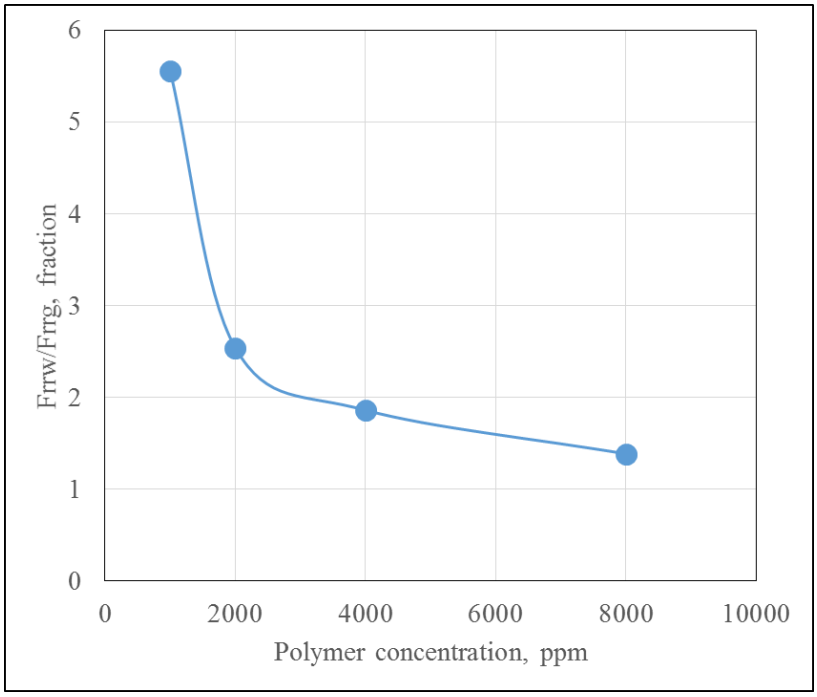

Figure 6-5: The relationship between polymer concentration and $\mathbf{Frr_w/Frr_g}$.

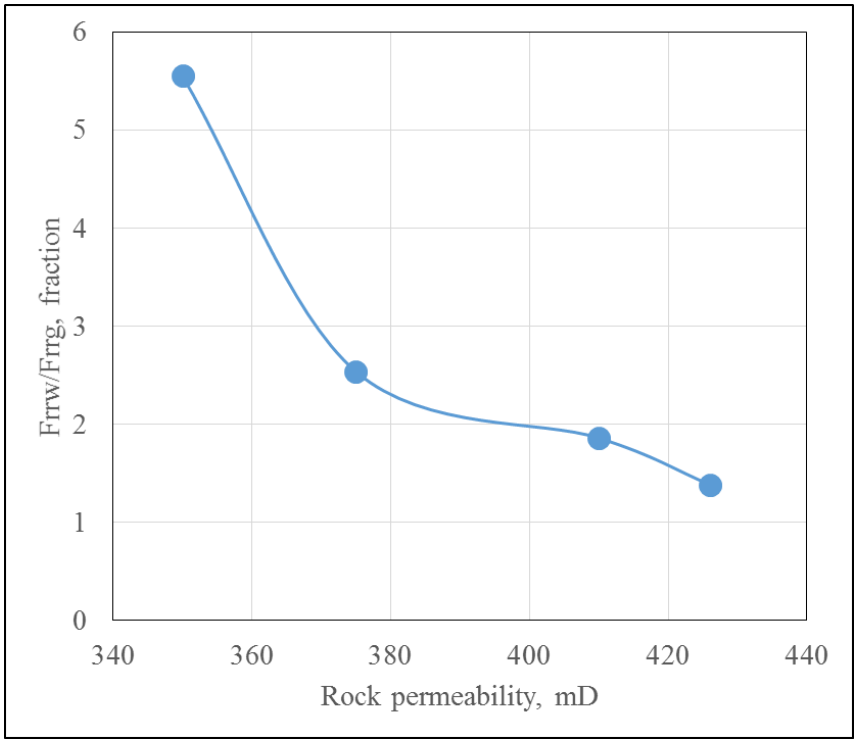

Figure 6-6: The relationship between rock permeability and $\mathbf{Frr_w/Frr_g}$.

6.3.2 Dimensionless Effective Pore Radius

As discussed earlier a primary objective of this section of the manuscript is to put the earlier developed dimensionless effective pore radius (r_{eff}^{-}) into use. The use of this parameter would yield similar final conclusions as those obtained by analyzing Frr. However using r_{eff}^{-} would be more insightful for the same reasons presented and discussed previously.

Figure 6-7 shows the combination effect of rock permeability and polymer concentration and gas flow rate on r_{eff}^{-}. Overall, this figure indicates that r_{eff}^{-} decreases with increasing polymer concentration. Generally, for all polymer concentrations, with increase in gas injection flowrate, the calculated r_{eff}^{-} would eventually approach unity. At relatively low gas flow rate (0.2-1cc/min) and for polymer concentrations of 1000-4000ppm, r_{eff}^{-} is greater than one. This outcome implies improvement in gas permeability after treatment which, as indicated before, may be attributed to the lubrication effect of the adsorbed polymer. Improvement in post-treatment gas permeability have also been obtained by Zaitoun and Kohler(Zaitoun and Kohler, 1988), Zaitoun et al.(Zaitoun et al., 1990) and Dovan and Hutchins (Dovan and Hutchins, 1994).The concentration of 8000ppm results in a reduction in effective permeability to gas which may be caused by the high thickness and increased rigidity of the polymer layer formed under this polymer concentration. With gas flow rates higher than 2cc/min, and across all concentrations, r_{eff}^{-} is almost equal to one which may imply that the polymer layer has lost its effects on flow behavior. This effect may be attributed to increase in polymer layer rigidity because of increase in the shear rate.

Figure 6-8 presents the same data as Figure 6-7 but for the water phase. As can be seen, all the calculated r_{eff}^{-} values are less than one meaning, as also apparent from Figure 6-3, a reduction in effective permeability to water was achieved after all polymer treatments. In general, the less the value of r_{eff}^{-}, the better the outcome overall. Although Figure 6-8 shows that all concentrations used could decrease water effective permeability, different trends are observed in this figure compared with Figure 6-7. This means that the parameters investigated have different effects on water flow compared with the gas flow. Overall, 4000ppm

concentration seems to have the least effect on water effective permeability followed by the concentrations of 2000ppm, 1000ppm and 8000ppm.

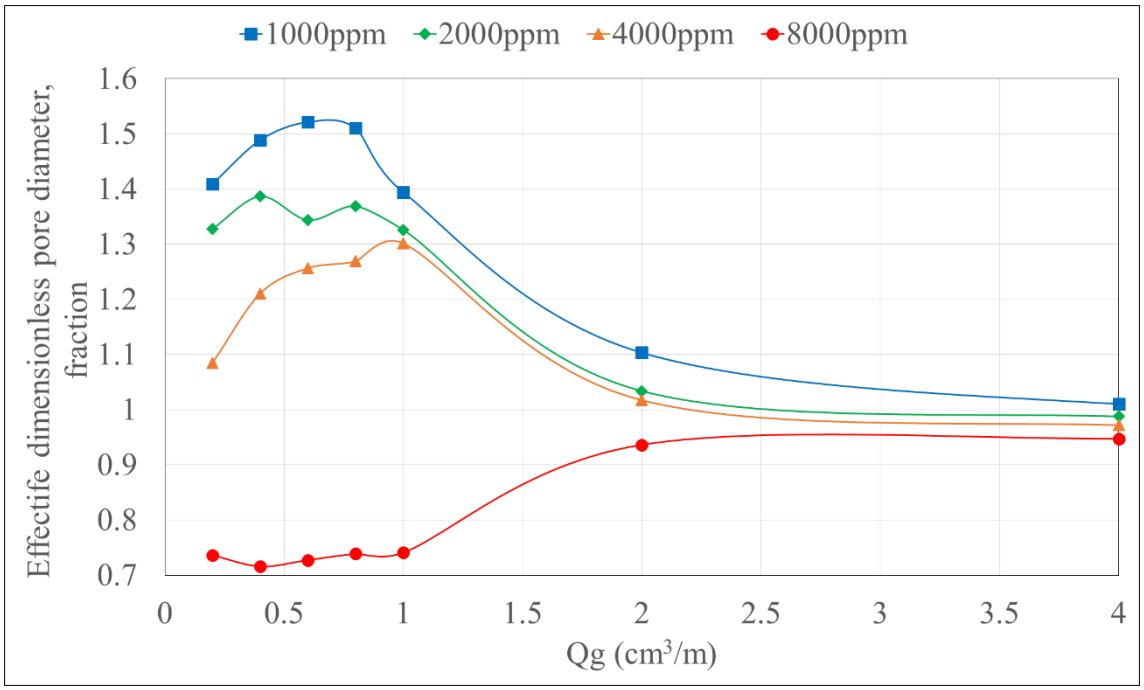

Figure 6-7. The relationship between gas flow rate and $\mathbf{r_{eff}^{-}}$ with changing polymer concentration.

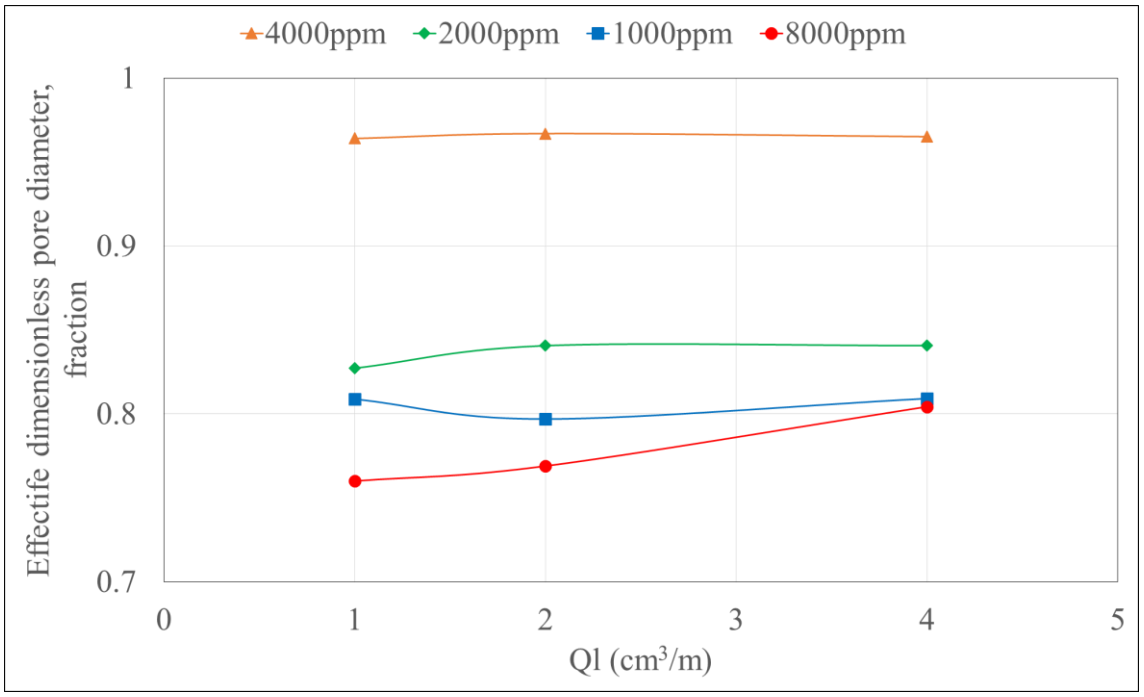

Figure 6-8. The relationship between liquid flow rate and $\mathbf{r_{eff}^{-}}$ with changing polymer concentration.

6.3.3 Flow regime

Since, where possible, the construction of a linear relationship is the easiest way to graphically model and interpret a data set, we have chosen the Forchheimer equation, as characterized by equations 6-8, to discuss the occurrence of different flow regimes that may be induced during our experiments as the fluid injection flow rate varies. Another reason for using this equation is that compared with the Darcy equation, the Forchheimer equation is considered more general in that it can be used over a much wider range of flow rates(Zimmerman et al., 2004)**.**

Figure 6-9-Figure 6-12 present the calculated Forchheimer plots for the gas flow rate range of 0.2-70cc/m with and without the presence of the adsorbed polymer layer whose thickness and behavior may change with change in the polymer concentration. In general, all these figures for the two states of pre- and post-polymer treatment, show three distinct flow regimes. The first and the third regimes show a linear profile while the middle ones may be regarded as a non-linear transition zone from the first linear regime to the second. In the flow rate range explored, treatments with polymer concentrations of 1000, 2000 and 4000ppm result in an improvement in gas flowing behavior over the first flow regime and the transition zone. As indicated before, such an improvement may be due to the lubrication effect induced by the adsorbed polymer layer. When gas flow rate exceeds a critical value (Qg=2cc/m) the polymer layer, very likely, becomes too rigid because of its shear thickening behavior and therefore r_{eff}^{-} would be reduced to a minimum (Figure 6-7) due to the loss of the lubrication effect of the polymer layer. Treatment with 8000ppm show a reduction in gas permeability in all the identified flow regimes. This may be because 8000ppm treatment is expected to induce the highest adsorbed polymer layer thickness or the least r_{eff}^{-} (Figure 6-7) and also the highest thickening effect in the rheology tests (Figure 6-1).

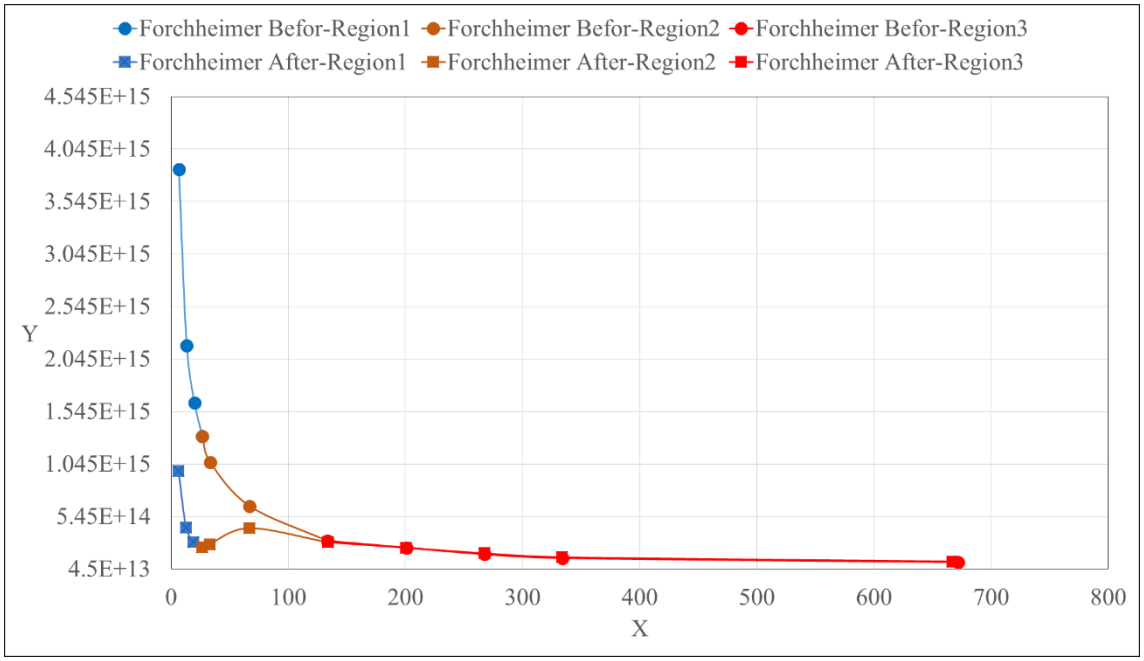

Figure 6-9: Forchheimer relationship, 1000ppm polymer concentration

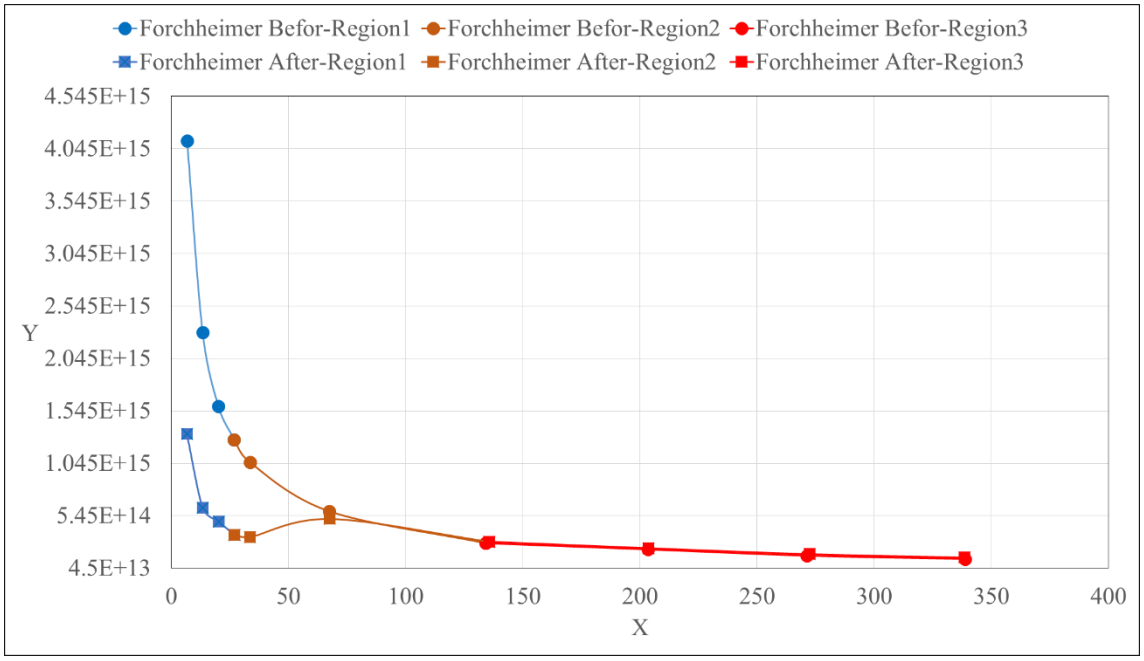

Figure 6-10: Forchheimer relationship, 2000ppm polymer concentration

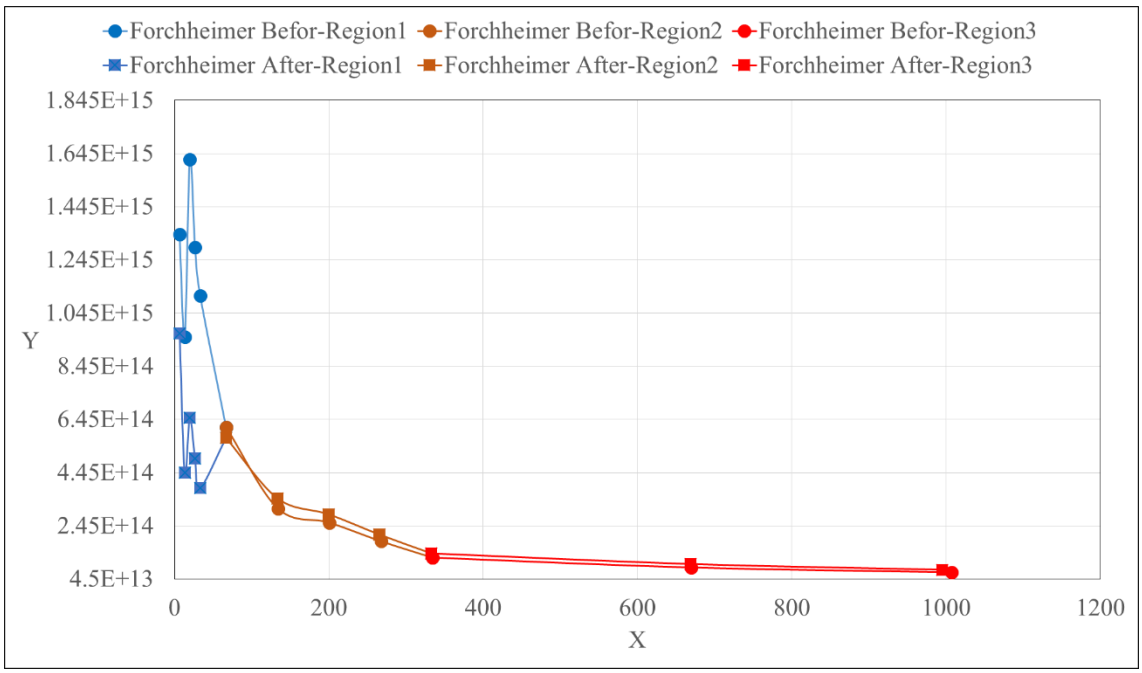

Figure 6-11: Forchheimer relationship, 4000ppm polymer concentration

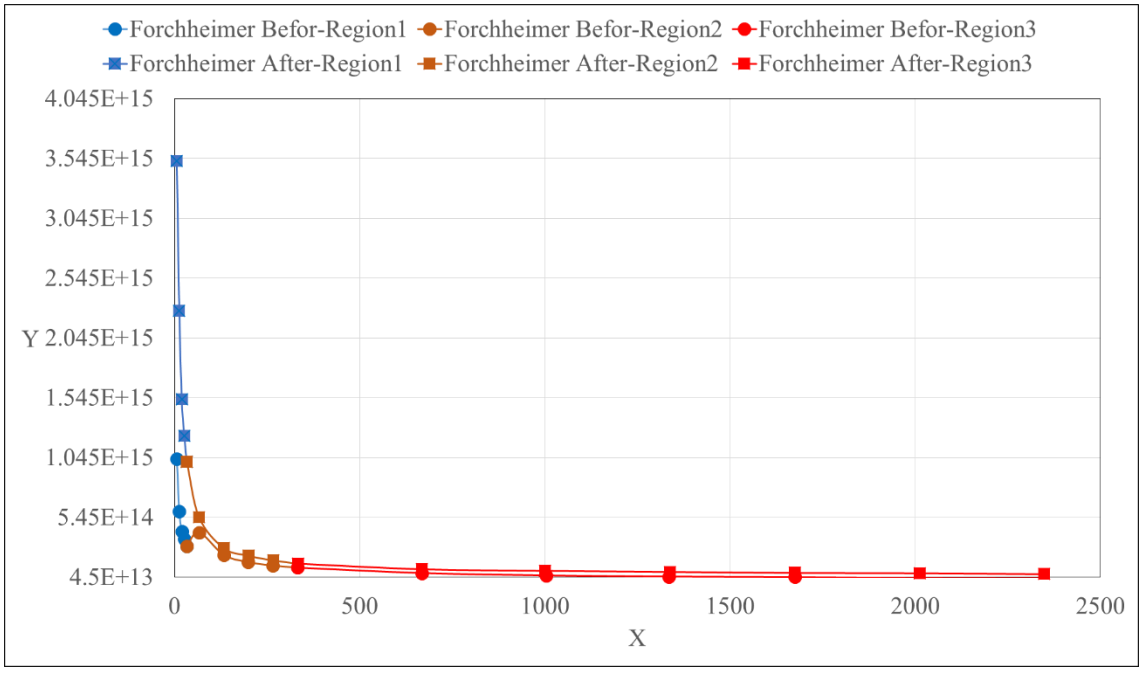

Figure 6-12: Forchheimer relationship, 8000ppm polymer concentration

6.4 Conclusion

In this work we have studied the competing and opposite effects of rock permeability and polymer concentration on water and gas permeability reductions during the experimental evaluation of an RPM treatment. The results of the study have been interpreted and discussed initially using a common technique where Frr is used as a critical parameter in evaluating the effectives of such a treatment. Subsequently, a new dimensionless parameter referred to as the dimensionless effective pore radius ($\bar{r_{eff}}$) was developed and used to interpret the same data. Finally, the Forchheimer equation was used to analyze the possible flow regimes that may be encountered during gas injection as the injection flow rate varies. The following specific conclusions may be drawn from the results obtained and the discussions presented earlier:

- Rheology tests show that the polymer used here is a non-Newtonian shear thickening solution and its rigidity increases with increasing the shear rate and polymer concentration.
- The competing and opposite effects of rock permeability and polymer concentration on Frr_w and Frr_g as reported in the literature were demonstrated by the results obtained in this study.
- Using the ratio of Frr_w/Frr_g was found to easier to determine the effectiveness of an RPM treatment in the context of changing rock permeability and polymer concentration. As expected from an RPM treatment, this ratio was always more than one for all the cases explored in this work.
- By using the more traditional technique based on the use of Frr and the newly developed $\bar{r_{eff}}$ to interpret the results obtained in this work it is demonstrated that while $\bar{r_{eff}}$ can reproduce similar outcomes as those of Frr, $\bar{r_{eff}}$ may be considered a more insightful factor due to the way it is calculated and what it represents .
- Interpreting the data obtained using the Forchheimer equation show three regimes of gas flowing behaviour with increasing injection gas flow rate. The first and third

phase exhibit linear relationships with the gap between the two phases bridged by a non-linear transition flow regime.

Chapter 7: Conclusions, Recommendations and Outlook for Future Work

7.1 Conclusions

As more oil and gas reservoirs are becoming mature, water production from the reservoirs become a problem. Globally the water/oil ratio may reach to 3/1. Water production can cause many problems; reduces the well productivity, increases the costs of oil/gas treatment, equipment damages and environmental problems. Polymer/Gel (relative permeability modifiers, RPM) is injected into the vicinity of production wells to selectively reduce the water permeability with minimal effect on oil/gas fluids. The major objective of this thesis is to add to the limited existing data and knowledge around the application of RPMs for the gas/water system in sandstone media. The major factors were experimentally investigated in this thesis; high range of rock permeability (low, moderate and high), high range of fluid (water and gas) flow rates, RPM strength and rheology and brine salinity. Sandstone core samples with high permeability range were used for the flooding experiment. The main aim of flooding experiments were to measure the relative permeability modification due to the RPM treatment (i.e. RPM efficiency). Additional experiments were also conducted to clarify and interpret the core flooding data; micromodel and capillary flooding, fluid rheology, XRD analysis, Zeta potential, contact angle and IFT.

In general, the results of the study reveal that the rock permeability can be used as an important screening parameter in planning an RPM treatment for gas producing wells. The relative pore size alteration (wall-steric effect) due to the RPM treatment impacts on how water-gas may redistribute and RPM performance. Brine salinity and RPM strength play a significant role on RPM performance. Moreover, RPM performance is significantly fluid (water and gas) flow rate dependent. Therefore, flow rate should be considered during RPM design. The most significant findings of this work are summarized below as sorted according to the way various chapters are presented in this thesis:

7.2 Effective Mechanisms to Relate Initial Rock Permeability to Outcome of Relative Permeability Modification

First, the effects of initial rock permeability (low, moderate, and high) on potential changes to the gas and water relative permeabilities due to cationic polyacrylamide (CPAM) treatment

have been studied experimentally. In doing so, the traditional parameters of Frr_w, Frr_g and Frr_w/Frr_g have been used to evaluate the performance of the treatment. What is more, an attempt has been made to explain and interpret the observed trends between the above parameters and rock permeability using possible pore-scale events/mechanisms (e.g. relative pore size changes, redistribution of fluids, steric effect, lubrication effect, etc.) that may come to existence due to the RPM treatment.

According to our results and under the experimental conditions explored in this work,

- In low permeability rocks (2.7, 22.7 and 66.4mD), the treatment results in high gas relative permeability reductions which are even greater than that induced to the water phase. This may imply that an RPM treatment using our particular polymer solution may be considered strongly unsuccessful in such rocks.
- In the moderate permeability rocks (350 and 385 mD) however, the polymer treatment reduces water relative permeability significantly but either does not have much of effect on the gas phase or results in an improvement to the gas relative permeability at low gas flow rates.
- In the high permeability rocks (3001, 3488 and 5035mD), the treatment may have no significant effect on either of the water and gas relative permeabilities.
- The above trends may be attributed to the way an RPM treatment may alter the pore size distribution of a rock which then impacts on how the wetting (water) and non-wetting (gas) phases may redistribute and flow in the newly modified pore system. The polymer layer thickness (e), in general, may increase with increase in the rock permeability but the more important ratio of ($^{e}/_{r}$) is expected to decrease as it is a relative parameter whose value depends on the initial rock permeability.
- The results obtained in this work are insightful in pointing out that the initial rock permeability can be used as an important **screening** parameter in planning an RPM treatment for gas producing wells.

7.3 Low-Salinity-Assisted Cationic Polyacrylamide Water Shutoff in Low-Permeability Sandstone Gas Reservoirs

The use of polymer for water shutoff in low permeability sandstone reservoirs is significant for successful applications of polymer treatment, however the factors that control rock-gas-brine interactions and polymer layer thickness are still not well understood. In this paper we conducted core flooding experiments to study the impacts of brine concentration (0.2% and 2% KCl) on possible variations to the water and gas relative permeabilities due to cationic polyacrylamide treatment (CPAM) on three sandstones of varying permeabilities (from 2 to 80 mD). Zeta potential measurements were also conducted for polymer-polymer system and rock-brine system before and after the treatment as a function of salinity for all rocks investigated. In addition, we measured the contact angles for silicate/brine/gas systems before and after the treatment as a function of salinity.

The overall results showed that

- Decreasing brine salinity (KCl) improved the performance of cationic polyacrylamide in sandstone rocks by decreasing water relative permeability, while the effect on gas relative permeability was relatively low. This is because decreasing the monovalent cation in brine (K^+), increases the $rock^-/polymer^+$ electrostatic attraction.
- Zeta potential of $rock^-/polymer^+$ confirmed that as brine salinity deceases (from 2 wt% KCl to 0.2wt% KCl), the zeta potential becomes less negative or even becomes positive. In addition, a decrease in monovalent cation concentration leads to a reduction in the effective polymer layer thickness (compressing) as confirmed by zeta potential measurements. Furthermore, zeta potential of $polymer^+/polymer^+$ measurements show as well that as brine salinity deceases the zeta potential becomes positive suggesting an increase in the $polymer^+/polymer^+$ attraction (reducing the repulsion).
- Overall, reducing the KCl concentration in the polymer solution increases the attraction of first polymer layer (rock-polymer) while compressing the second polymer layer (polymer-brine-polymer). In general, the above decreases the water relative permeability as intended, but results in minimal effect on gas productivity.

- Moreover, and importantly, it was seen that before treatment the system showed a small increase in water wettability with decreasing salinity. However, after the treatment of sandstone rocks with positively charged polymer, and lowering the brine salinity, rock surface wettability altered towards less water-wet. This effect was related to a shift in zeta potential towards more positive value at lower salinity after the treatment. However more investigations are required to relate wettability to zeta potentials.
- Altogether, polymer and the accompanied water layer thicknesses will be both reduced (compressed/shrink) with reducing KCl concertation. Under such conditions, the treatment will be suitable as seen by a decline in relative permeability to water and an unaltered gas relative permeability.

7.4 A Multiscale Investigation of Cross-Linked Polymer Gel Injection in Sandstone Gas Reservoirs: Implications for Water Shutoff Treatment

The impact of cross-linked polyacrylamide gel as an RPM for a moderate permeability sandstone/gas/water system was also investigated. This work investigated the rheological behaviour of P(AAM-co-AA)Na -chromium gels for a broad range of shear rates (0.01-100 s^{-1}), chromium concentrations (200-600 ppm Cr^{3+} in 20,000 ppm P(AAM-co-AA)Na) and temperatures (298-338 K), followed by core scale and pore scale flow experiments, to determine the gel performance in terms of reducing water production.

- A clear increase in viscosity of the P(AAM-co-AA)Na gel with increasing cross-linking agent concentration was measured and shear thinning was observed. Oscillation shear flow tests indicated that all solutions (except for 200 ppm Cr^{3+} concentration) exhibited a predominantly elastic behaviour (with transition from elastic to viscous behaviour occurring at a relatively high frequency). Likewise, a temperature sweep confirmed the dominance of elastic behaviour over viscous behaviour throughout the temperature range tested.

- Furthermore, it was found that higher gel strength increased the water retention inside the porous media.
- Two counteracting mechanisms were responsible for the observed disproportionate permeability reduction (DPR), namely (a) water retention and (b) lubrication (both being functions of gel rheology). While the lubrication effect was the main mechanism behind the DPR especially at low gas flow rates, gel rigidity was prominent at higher flow rates. This was associated with gas diffusion and dissolution in the gel, which in turn expanded the gel layer thickness and reduced gas permeability.
- Moreover, irrespective of the cross-linker concentration, it was observed that higher water flow rates (during imbibition) decreased Frr_w. This was attributed to: a) gel shear thinning behaviour and b) S_{gr} reduction. However, increasing gas flow rates (during draining) decreased the Frr_g (i.e. shear thinking behaviour). Moreover, there was a critical fluid flow rate above which the treatments became unsuccessful, as both effects (i.e. water retention and lubrication) were significantly reduced.
- The micromodel results showed that at high gas flow rate (Q_{gc2}), the gel layer expanded on the glass surface after trapping and dissolving gas bubbles in the gel or water. This in turn increased Frr_g, as the gas flow path became more restricted.
- In the capillary tube experiment gas slugs pushed themselves through the non-uniform channel without diffusion. The gas slugs repetitively deformed and split up and coalesced again when the gas flowed through the thicker gel layers, also causing pressure fluctuations.

7.5 A New Dimensionless Approach to Assess Relative Permeability Modifiers

Finally, we have also studied the competing and opposite effects of rock permeability and polymer concentration on water and gas permeability reductions during the experimental evaluation of an RPM treatment. The results of the study have been interpreted and discussed initially using a common technique where Frr is used as a critical parameter in evaluating the effectives of such a treatment. Subsequently, a new dimensionless parameter referred to

as the dimensionless effective pore radius (r_{eff}^{-}) was developed and used to interpret the same data. Finally, the Forchheimer equation was used to analyze the possible flow regimes that may be encountered during gas injection as the injection flow rate varies.

The following specific conclusions may be drawn from the results obtained and the discussions presented earlier.

- Rheology tests show that the polymer used here is a non-Newtonian shear thickening solution and its rigidity increases with increasing the shear rate and polymer concentration.
- The competing and opposite effects of rock permeability and polymer concentration on Frr_w and Frr_g as reported in the literature were demonstrated by the results obtained in this study.
- Using the ratio of Frr_w/Frr_g was found to easier to determine the effectiveness of an RPM treatment in the context of changing rock permeability and polymer concentration. As expected from an RPM treatment, this ratio was always more than one for all the cases explored in this work.
- By using the more traditional technique based on the use of Frr and the newly developed r_{eff}^{-} to interpret the results obtained in this work it is demonstrated that while r_{eff}^{-} can reproduce similar outcomes as those of Frr, r_{eff}^{-} may be considered a more insightful factor due to the way it is calculated and what it represents.
- As the polymer concentration increases, r_{eff}^{-} decreases (i.e. lubrication decreases).
- At low flowrates and low polymer concentration (1000-4000), $r_{eff}^{-} > 1$ (i.e. lubrication).
- At higher flowrates, the $r_{eff}^{-} \sim 1$ across all polymer concentrations. This is possibly due to polymer layer losing its effects or increasing polymer rigidity caused by increasing shear rate).

- Interpreting the data obtained using the Forchheimer equation show three regimes of gas flowing behavior with increasing injection gas flow rate. The first and third phase exhibit linear relationships with the gap between the two phases bridged by a non-linear transition flow regime.
- Treatments with low polymer concentrations showed an improvement in gas flowing behaviour over the first and the transition flow regimes (i.e. lubrication effect) whereas no effect on the second flow regimes.
- Treatment with high ppm showed a reduction in gas permeability in all the identified flow regimes, probably due to higher adsorbed polymer layer thickness and also higher thickening effect with increasing shear rate.

7.6 Recommendations and Outlook for Future Work

The experimental work and literature review conducted indicate that selecting suitable polymers for a reservoir candidate with certain rock characteristics plays a critical role in controlling the adsorption process. The current study also covers sufficient details around the adsorption process and the subsequent mechanisms (i.e. wall effects and fluid segregation pathway) that can govern the ultimate outcome of an RPM treatment. However, there is still a lack of detailed understanding as how some RPM effects can be controlled to further improve the ultimate efficiency of a treatment. In particular, the followings could be the subject of further investigation:

- A suitable simulation software is recommended to be used to upscale the experimental results on reservoir scale. This simulation will help to understand the usefulness of the laboratory data for the larger near wellbore scale and also over a longer period of time. Different scenarios should be considered to simulate the real conditions of gas wells.

- More pore scale studies (experimentally and numerically) are also need for further understanding to RPM mechanisms.

- The adsorbed RPM thickness has a significant effect on the RPM performance. Adjusting RPM thickness as a function of brine salinity/composition is in need of further studies.
- More research is also needed to investigate the polymer adsorption/thickness as a function to polymer injection volume, injection rate, and aging time.
- Moreover, in the same context, swelling agents have not yet received enough interest from researchers.

Appendix A: Contribution of Co-authors

Statement of Contribution of Others for "**Rock/Fluid/Polymer Interaction Mechanisms: Implications for Water Shut-off Treatment**"

AL-SHAJALEE, F., ARIF, M., MYERS, M., TADÉ, M. O., WOOD, C. & SAEEDI, A. 2021. Rock/Fluid/Polymer Interaction Mechanisms: Implications for Water Shut-off Treatment. Energy & Fuels, 35, 12809-12827.

Name	Conceptualization	Methodology	Investigation	Interpretation and Discussion	Original Draft Writing	Review, Editing and Approval
AL-SHAJALEE, F.	X	X	X	X	X	X
I acknowledge that these represent my contributions to the above research output. AL-SHAJALEE, F. Faaiz Al-Shajalee						
ARIF, M.						X
I acknowledge that these represent my contributions to the above research output. ARIF, M. arif						
MYERS, M.						X
I acknowledge that these represent my contributions to the above research output. MYERS, M.						
TADÉ, M. O.						X
I acknowledge that these represent my contributions to the above research output. TADÉ, M. O. 4/16/21						
WOOD, C.	X					X
I acknowledge that these represent my contributions to the above research output. WOOD, C.						
SAEEDI, A.	X					X
I acknowledge that these represent my contributions to the above research output. SAEEDI, A. Ali Saeedi						

Statement of Contribution of Others for "**Effective Mechanisms to Relate Initial Rock Permeability to Outcome of Relative Permeability Modification**"

AL-SHAJALEE, F., WOOD, C., XIE, Q. & SAEEDI, A. 2019. Effective Mechanisms to Relate Initial Rock Permeability to Outcome of Relative Permeability Modification. Energies, 12, 4688.

Name	Conceptualization	Methodology	Investigation	Interpretation and Discussion	Original Draft Writing	Review, Editing and Approval
AL-SHAJALEE, F.	X	X	X	X	X	X
I acknowledge that these represent my contributions to the above research output. AL-SHAJALEE, F. Faaiz Al-Shajalee						
WOOD, C.	X					X
I acknowledge that these represent my contributions to the above research output. WOOD, C.						
XIE, Q.				X		X
I acknowledge that these represent my contributions to the above research output. XIE, Q. Samto						
SAEEDI, A.	X			X		X
I acknowledge that these represent my contributions to the above research output. SAEEDI, A. Ali Saeedi						

Statement of Contribution of Others for "**Low-Salinity-Assisted Cationic Polyacrylamide Water Shutoff in Low-Permeability Sandstone Gas Reservoirs**"

AL-SHAJALEE, F., ARIF, M., SARI, A., WOOD, C., AL-BAYATI, D., XIE, Q. & SAEEDI, A. 2020. Low-Salinity-Assisted Cationic Polyacrylamide Water Shutoff in Low-Permeability Sandstone Gas Reservoirs. Energy & Fuels, 34, 5524-5536.

Name	Conceptualization	Methodology	Investigation	Interpretation, and Discussion	Original Draft Writing	Review, Editing and Approval
AL-SHAJALEE, F.	X	X	X	X	X	X
I acknowledge that these represent my contributions to the above research output. AL-SHAJALEE, F. Faaiz Al-Shajalee						
ARIF, M.				X		X
I acknowledge that these represent my contributions to the above research output. ARIF, M. arif						
SARI, A.		X				
I acknowledge that these represent my contributions to the above research output. SARI, A.						
WOOD, C.	X					X
I acknowledge that these represent my contributions to the above research output. WOOD, C.						
AL-BAYATI, D.		X				
I acknowledge that these represent my contributions to the above research output. AL-BAYATI, D. Duraid						
XIE, Q.				X		X
I acknowledge that these represent my contributions to the above research output. XIE, Q.						
SAEEDI, A.	X			X		X
I acknowledge that these represent my contributions to the above research output. SAEEDI, A.						

Statement of Contribution of Others for "**A Multiscale Investigation of Cross-Linked Polymer Gel Injection in Sandstone Gas Reservoirs: Implications for Water Shutoff Treatment**"

AL-SHAJALEE, F., ARIF, M., MACHALE, J., VERRALL, M., ALMOBARAK, M., IGLAUER, S. & WOOD, C. 2020a. A Multiscale Investigation of Cross-Linked Polymer Gel Injection in Sandstone Gas Reservoirs: Implications for Water Shutoff Treatment. Energy & Fuels, 34, 14046-14057.

Name	Conceptualization	Methodology	Investigation	Interpretation, and Discussion	Original Draft Writing	Review, Editing and Approval
AL-SHAJALEE, F.	X	X	X	X	X	X
I acknowledge that these represent my contributions to the above research output. AL-SHAJALEE, F. Faaiz Al-Shajalee						
ARIF, M.				X		X
I acknowledge that these represent my contributions to the above research output. ARIF, M.						
MACHALE, J.,		X	X	X		
I acknowledge that these represent my contributions to the above research output. MACHALE, J.						
MICHAEL R. VERRALL		X				
I acknowledge that these represent my contributions to the above research output. MICHAEL R. VERRALL						
ALMOBARAK, M.		X				
I acknowledge that these represent my contributions to the above research output. ALMOBARAK, M.						
IGLAUER, S.						X
I acknowledge that these represent my contributions to the above research output. IGLAUER, S.						
WOOD, C.	X			X		X
I acknowledge that these represent my contributions to the above research output. WOOD, C.						

Statement of Contribution of Others for "**A New dimensionless Approach to Assess Relative Permeability Modifiers**"

AL-SHAJALEE, F., SAEEDI, A. & WOOD, C. 2019a. A New Dimensionless Approach to Assess Relative Permeability Modifiers. Energy & Fuels, 33, 3448-3455.

Name	Conceptualization	Methodology	Investigation	Interpretation and Discussion	Original Draft Writing	Review, Editing and Approval
AL-SHAJALEE, F.	X	X	X	X	X	X
I acknowledge that these represent my contributions to the above research output. AL-SHAJALEE, F. Faaiz Al-Shajalee						
SAEEDI, A.	X			X		X
I acknowledge that these represent my contributions to the above research output. SAEEDI, A. Ali Saeedi						
WOOD, C.	X			X		X
I acknowledge that these represent my contributions to the above research output. WOOD, C.						

Appendix B: Official Permissions & Copyrights

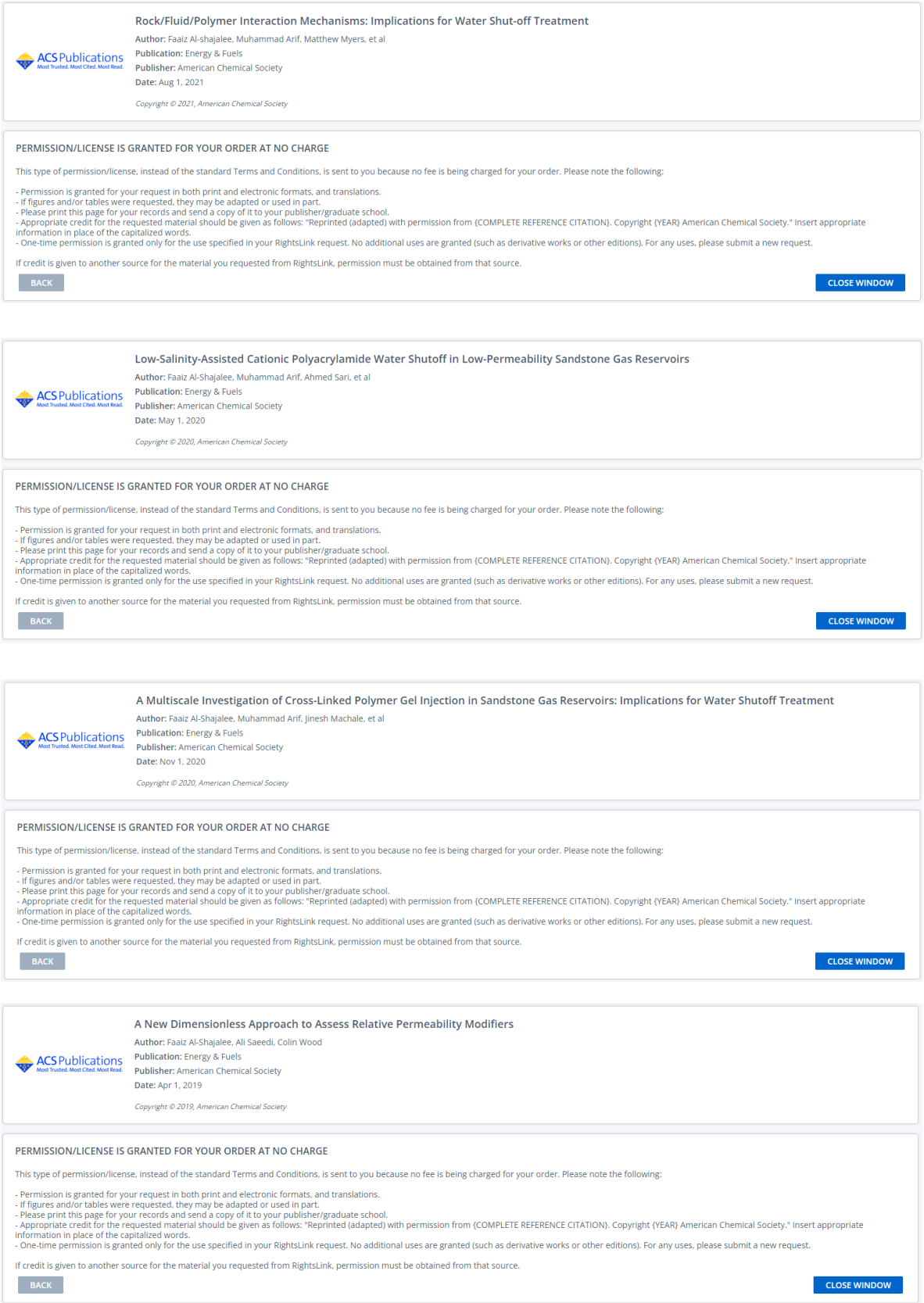

Rock/Fluid/Polymer Interaction Mechanisms: Implications for Water Shut-off Treatment

Author: Faaiz Al-shajalee, Muhammad Arif, Matthew Myers, et al
Publication: Energy & Fuels
Publisher: American Chemical Society
Date: Aug 1, 2021

Copyright © 2021, American Chemical Society

PERMISSION/LICENSE IS GRANTED FOR YOUR ORDER AT NO CHARGE

This type of permission/license, instead of the standard Terms and Conditions, is sent to you because no fee is being charged for your order. Please note the following:

- Permission is granted for your request in both print and electronic formats, and translations.
- If figures and/or tables were requested, they may be adapted or used in part.
- Please print this page for your records and send a copy of it to your publisher/graduate school.
- Appropriate credit for the requested material should be given as follows: "Reprinted (adapted) with permission from {COMPLETE REFERENCE CITATION}. Copyright {YEAR} American Chemical Society." Insert appropriate information in place of the capitalized words.
- One-time permission is granted only for the use specified in your RightsLink request. No additional uses are granted (such as derivative works or other editions). For any uses, please submit a new request.

If credit is given to another source for the material you requested from RightsLink, permission must be obtained from that source.

BACK CLOSE WINDOW

Low-Salinity-Assisted Cationic Polyacrylamide Water Shutoff in Low-Permeability Sandstone Gas Reservoirs

Author: Faaiz Al-Shajalee, Muhammad Arif, Ahmed Sari, et al
Publication: Energy & Fuels
Publisher: American Chemical Society
Date: May 1, 2020

Copyright © 2020, American Chemical Society

PERMISSION/LICENSE IS GRANTED FOR YOUR ORDER AT NO CHARGE

This type of permission/license, instead of the standard Terms and Conditions, is sent to you because no fee is being charged for your order. Please note the following:

- Permission is granted for your request in both print and electronic formats, and translations.
- If figures and/or tables were requested, they may be adapted or used in part.
- Please print this page for your records and send a copy of it to your publisher/graduate school.
- Appropriate credit for the requested material should be given as follows: "Reprinted (adapted) with permission from {COMPLETE REFERENCE CITATION}. Copyright {YEAR} American Chemical Society." Insert appropriate information in place of the capitalized words.
- One-time permission is granted only for the use specified in your RightsLink request. No additional uses are granted (such as derivative works or other editions). For any uses, please submit a new request.

If credit is given to another source for the material you requested from RightsLink, permission must be obtained from that source.

BACK CLOSE WINDOW

A Multiscale Investigation of Cross-Linked Polymer Gel Injection in Sandstone Gas Reservoirs: Implications for Water Shutoff Treatment

Author: Faaiz Al-Shajalee, Muhammad Arif, Jinesh Machale, et al
Publication: Energy & Fuels
Publisher: American Chemical Society
Date: Nov 1, 2020

Copyright © 2020, American Chemical Society

PERMISSION/LICENSE IS GRANTED FOR YOUR ORDER AT NO CHARGE

This type of permission/license, instead of the standard Terms and Conditions, is sent to you because no fee is being charged for your order. Please note the following:

- Permission is granted for your request in both print and electronic formats, and translations.
- If figures and/or tables were requested, they may be adapted or used in part.
- Please print this page for your records and send a copy of it to your publisher/graduate school.
- Appropriate credit for the requested material should be given as follows: "Reprinted (adapted) with permission from {COMPLETE REFERENCE CITATION}. Copyright {YEAR} American Chemical Society." Insert appropriate information in place of the capitalized words.
- One-time permission is granted only for the use specified in your RightsLink request. No additional uses are granted (such as derivative works or other editions). For any uses, please submit a new request.

If credit is given to another source for the material you requested from RightsLink, permission must be obtained from that source.

BACK CLOSE WINDOW

A New Dimensionless Approach to Assess Relative Permeability Modifiers

Author: Faaiz Al-Shajalee, Ali Saeedi, Colin Wood
Publication: Energy & Fuels
Publisher: American Chemical Society
Date: Apr 1, 2019

Copyright © 2019, American Chemical Society

PERMISSION/LICENSE IS GRANTED FOR YOUR ORDER AT NO CHARGE

This type of permission/license, instead of the standard Terms and Conditions, is sent to you because no fee is being charged for your order. Please note the following:

- Permission is granted for your request in both print and electronic formats, and translations.
- If figures and/or tables were requested, they may be adapted or used in part.
- Please print this page for your records and send a copy of it to your publisher/graduate school.
- Appropriate credit for the requested material should be given as follows: "Reprinted (adapted) with permission from {COMPLETE REFERENCE CITATION}. Copyright {YEAR} American Chemical Society." Insert appropriate information in place of the capitalized words.
- One-time permission is granted only for the use specified in your RightsLink request. No additional uses are granted (such as derivative works or other editions). For any uses, please submit a new request.

If credit is given to another source for the material you requested from RightsLink, permission must be obtained from that source.

BACK CLOSE WINDOW

References:

ABDULFARRAJ, M. & IMQAM, A. The Application of Micro-Sized Crosslinked Polymer Gel for Water Control to Improve Zonal Isolation in Cement Sheath: An Experimental Investigation. 53rd US Rock Mechanics/Geomechanics Symposium, 2019. American Rock Mechanics Association.

AFTAB, A., ISMAIL, A., KHOKHAR, S. & IBUPOTO, Z. H. 2016. Novel zinc oxide nanoparticles deposited acrylamide composite used for enhancing the performance of water-based drilling fluids at elevated temperature conditions. *Journal of Petroleum Science and Engineering,* 146**,** 1142-1157.

AGHABOZORGI, S. & ROSTAMI, B. 2016. An investigation of polymer adsorption in porous media using pore network modelling. *Transport in Porous Media,* 115**,** 169-187.

AHMED, A. A., MOHD SAAID, I. & MOHD SHAFIAN, S. 2020. Novel Relative Permeability Modifier using Polymer Grafted Nanoclay. *Energy & Fuels,* 34**,** 2703-2709.

AHMED, M. & REZAEI-GOMARI, S. 2019. Economic Feasibility Analysis of Shale Gas Extraction from UK's Carboniferous Bowland-Hodder Shale Unit. *Resources,* 8**,** 5.

AHSANI, T., TAMSILIAN, Y. & REZAEI, A. 2020. Molecular Dynamic Simulation and Experimental Study of Wettability Alteration by Hydrolyzed Polyacrylamide for Enhanced Oil Recovery: A New Finding for Polymer Flooding Process. *Journal of Petroleum Science and Engineering***,** 108029.

AIT-AKBOUR, R., BOUSTINGORRY, P., LEROUX, F., LEISING, F. & TAVIOT-GUÉHO, C. 2015. Adsorption of PolyCarboxylate Poly (ethylene glycol)(PCP) esters on Montmorillonite (Mmt): Effect of exchangeable cations (Na+, Mg2+ and Ca2+) and PCP molecular structure. *Journal of Colloid and Interface Science,* 437**,** 227-234.

AIT-KADI, A., CARREAU, P. & CHAUVETEAU, G. 1987. Rheological properties of partially hydrolyzed polyacrylamide solutions. *Journal of Rheology,* 31**,** 537-561.

AL-ANAZI, H. A. & SHARMA, M. M. Use of a pH sensitive polymer for conformance control. International Symposium and Exhibition on Formation Damage Control, 2002. Society of Petroleum Engineers.

AL-HAJRI, S., MAHMOOD, S. M., ABDULELAH, H. & AKBARI, S. 2018. An overview on polymer retention in porous media. *Energies,* 11**,** 2751.

AL-HASHMI, A. & LUCKHAM, P. 2010. Characterization of the adsorption of high molecular weight non-ionic and cationic polyacrylamide on glass from aqueous solutions using modified atomic force microscopy. *Colloids and Surfaces A: Physicochemical and Engineering Aspects,* 358**,** 142-148.

AL-HASHMI, A., LUCKHAM, P. & GRATTONI, C. 2013. Flow-induced-microgel adsorption of high-molecular weight polyacrylamides. *Journal of Petroleum Science and Engineering,* 112**,** 1-6.

AL-HULAIL, I., SHAKEEL, M., BINGHANIM, A., ZEGHOUANI, M., RAHAL, R., AL-TAQ, A. & AL-RUSTUM, A. Water Control in High-Water-Cut Oil Wells using

Relative Permeability Modifiers: A Saudi Lab Study. SPE Kingdom of Saudi Arabia Annual Technical Symposium and Exhibition, 2017. Society of Petroleum Engineers.
AL-MUTHANA, A., HURSAN, G. G., MA, S. M., VALORI, A., NICOT, B. & SINGER, P. M. Wettability as a function of pore size by NMR. SCA conference paper, 2012.
AL-SHAJALEE, F., ARIF, M., MACHALE, J., VERRALL, M., ALMOBARAK, M., IGLAUER, S. & WOOD, C. 2020a. A Multiscale Investigation of Cross-Linked Polymer Gel Injection in Sandstone Gas Reservoirs: Implications for Water Shutoff Treatment. *Energy & Fuels*.
AL-SHAJALEE, F., ARIF, M., MACHALE, J., VERRALL, M., ALMOBARAK, M., IGLAUER, S. & WOOD, C. 2020b. A Multiscale Investigation of Cross-Linked Polymer Gel Injection in Sandstone Gas Reservoirs: Implications for Water Shutoff Treatment. *Energy & Fuels,* 34**,** 14046-14057.
AL-SHAJALEE, F., ARIF, M., SARI, A., WOOD, C., AL-BAYATI, D., XIE, Q. & SAEEDI, A. 2020c. Low-Salinity-Assisted Cationic Polyacrylamide Water Shutoff in Low-Permeability Sandstone Gas Reservoirs. *Energy & Fuels,* 34**,** 5524-5536.
AL-SHAJALEE, F., ARIF, M., SARI, A., WOOD, C., AL-BAYATI, D., XIE, Q. & SAEEDI, A. 2020d. Low-Salinity-Assisted Cationic Polyacrylamide Water Shutoff in Low-Permeability Sandstone Gas Reservoirs. *Energy & Fuels*.
AL-SHAJALEE, F., SAEEDI, A. & WOOD, C. 2019a. A New Dimensionless Approach to Assess Relative Permeability Modifiers. *Energy & Fuels,* 33**,** 3448-3455.
AL-SHAJALEE, F., WOOD, C., XIE, Q. & SAEEDI, A. 2019b. Effective Mechanisms to Relate Initial Rock Permeability to Outcome of Relative Permeability Modification. *Energies,* 12**,** 4688.
AL-SHAKRY, B., SKAUGE, T., SHAKER SHIRAN, B. & SKAUGE, A. 2018. Impact of mechanical degradation on polymer injectivity in porous media. *Polymers,* 10**,** 742.
AL-SHARJI, H., GRATTONI, C., DAWE, R. & ZIMMERMAN, R. Disproportionate permeability reduction due to polymer adsorption entanglement. SPE European formation damage conference, 2001a. Society of Petroleum Engineers.
AL-SHARJI, H. H., GRATTONI, C. A., DAWE, R. A. & ZIMMERMAN, R. W. Pore-scale study of the flow of oil and water through polymer gels. SPE Annual Technical Conference and Exhibition, 1999a. Society of Petroleum Engineers.
AL-SHARJI, H. H., GRATTONI, C. A., DAWE, R. A. & ZIMMERMAN, R. W. 1999b. Pore-Scale Study of the Flow of Oil and Water through Polymer Gels. *SPE***,** 50–53.
AL-SHARJI, H. H., GRATTONI, C. A., DAWE, R. A. & ZIMMERMAN, R. W. 1999c. Pore-Scale Study of the Flow of Oil and Water through Polymer Gels. *SPE*.
AL-SHARJI, H. H., GRATTONI, C. A., DAWE, R. A. & ZIMMERMAN, R. W. 2001b. Flow of oil and water through elastic polymer gels. *Oil & Gas Science and Technology-Revue D Ifp Energies Nouvelles,* 56**,** 145-152.
AL-HASHMI, A. A., AL-MAAMARI, R., AL-SHABIBI, I., MANSOOR, A., AL-SHARJI, H. & ZAITOUN, A. 2014. Mechanical stability of high-molecular-weight polyacrylamides and an (acrylamido tert-butyl sulfonic acid)–acrylamide copolymer used in enhanced oil recovery. *Journal of Applied Polymer Science,* 131.

AL ALI, A. 2012. *Application of Polymer Gels as Conformance Control Agents for Carbon Dioxide for Floods in Carbonate Reservoirs.* Texas A&M University.

AL HASHMI, A., AL MAAMARI, R., AL SHABIBI, I., MANSOOR, A., ZAITOUN, A. & AL SHARJI, H. 2013. Rheology and mechanical degradation of high-molecular-weight partially hydrolyzed polyacrylamide during flow through capillaries. *Journal of Petroleum Science and Engineering,* 105**,** 100-106.

AL SHALABI, E. W., SEPEHRNOORI, K. & DELSHAD, M. 2014. Mechanisms behind low salinity water injection in carbonate reservoirs. *Fuel,* 121**,** 11-19.

ALAGIC, E. & SKAUGE, A. 2010. Combined low salinity brine injection and surfactant flooding in mixed− wet sandstone cores. *Energy & fuels,* 24**,** 3551-3559.

ALFARGE, D., BAI, B. & ALMANSOUR, A. 2018. Numerical simulation study to understand the performance of RPM gels in water-shutoff treatments. *Journal of Petroleum Science and Engineering,* 171**,** 818-834.

ALFARGE, D. K., WEI, M. & BAI, B. 2017. Numerical simulation study of factors affecting relative permeability modification for water-shutoff treatments. *Fuel,* 207**,** 226-239.

ALFARGE, D. K. K. 2016. Study on the applicability of relative permeability modifiers for water shutoff using numerical simulation.

ALI, L. & BARRUFET, M. 2001. Using centrifuge data to investigate the effects of polymer treatment on relative permeability. *Journal of Petroleum Science and Engineering,* 29**,** 1-16.

ALI, M. & MAHMUD, H. B. The effects of concentration and salinity on polymer adsorption isotherm at sandstone rock surface. IOP Conference Series: Materials Science and Engineering, 2015. IOP Publishing.

ALLEN, F. J., GRIFFIN, L. R., ALLOWAY, R. M., GUTFREUND, P., LEE, S. Y., TRUSCOTT, C. L., WELBOURN, R. J., WOOD, M. H. & CLARKE, S. M. 2017. An anionic surfactant on an anionic substrate: monovalent cation binding. *Langmuir,* 33**,** 7881-7888.

ALOTAIBI, M. B., AZMY, R. & NASR-EL-DIN, H. A. A comprehensive EOR study using low salinity water in sandstone reservoirs. SPE improved oil recovery symposium, 2010. OnePetro.

ALOTAIBI, M. B., NASRALLA, R. A. & NASR-EL-DIN, H. A. 2011. Wettability studies using low-salinity water in sandstone reservoirs. *SPE Reservoir Evaluation & Engineering,* 14**,** 713-725.

ALSHAJALEE, F., SAEEDI, A. & WOOD, C. D. 2019. A New dimensionless Approach to Assess Relative Permeability Modifiers. *Energy & Fuels*.

ALVAND, E., AALAIE, J., HEMMATI, M. & SAJJADIAN, V. A. 2017. Rheological and thermal stability of novel weak gels based on sulfonated polyacrylamide/scleroglucan/chromium triacetate. *Polymer International,* 66**,** 477-484.

AMIR, Z., SAID, I. M. & JAN, B. M. 2019. In situ organically cross-linked polymer gel for high-temperature reservoir conformance control: A review. *Polymers for Advanced Technologies,* 30**,** 13-39.

ANDERSON, W. G. 1986. Wettability literature survey-part 1: rock/oil/brine interactions and the effects of core handling on wettability. *Journal of petroleum technology,* 38**,** 1,125-1,144.

ANOKWURU, V. C. 2015. *Simulation of water diversion using ECLIPSE Options.* University of Stavanger, Norway.

ARIF, M., ABU-KHAMSIN, S. & IGLAUER, S. 2019. Wettability of rock/CO2/brine and rock/oil/CO2-enriched-brine systems: Critical parametric analysis and future outlook. *Advances in colloid and interface science*.

ARIF, M., ABU-KHAMSIN, S. A., ZHANG, Y. & IGLAUER, S. 2020. Experimental investigation of carbonate wettability as a function of mineralogical and thermo-physical conditions. *Fuel,* 264**,** 116846.

ARIF, M., BARIFCANI, A. & IGLAUER, S. 2016. Solid/CO2 and solid/water interfacial tensions as a function of pressure, temperature, salinity and mineral type: Implications for CO2-wettability and CO2 geo-storage. *International Journal of Greenhouse Gas Control,* 53**,** 263-273.

ARIF, M., JONES, F., BARIFCANI, A. & IGLAUER, S. 2017a. Electrochemical investigation of the effect of temperature, salinity and salt type on brine/mineral interfacial properties. *International Journal of Greenhouse Gas Control,* 59**,** 136-147.

ARIF, M., JONES, F., BARIFCANI, A. & IGLAUER, S. 2017b. Influence of surface chemistry on interfacial properties of low to high rank coal seams. *Fuel,* 194**,** 211-221.

ARIF, M., ZHANG, Y. & IGLAUER, S. 2021. Shale Wettability: Data Sets, Challenges, and Outlook. *Energy & Fuels,* 35**,** 2965-2980.

ARJOMAND, E., EASTON, C. D., MYERS, M., TIAN, W., SAEEDI, A. & WOOD, C. D. 2020. Changing Sandstone Rock Wettability with Supercritical CO2-Based Silylation. *Energy & Fuels,* 34**,** 2015-2027.

ASKARINEZHAD, R. & HATZIGNATIOU, D. G. Improved Disproportionate Permeability Reduction of Silicate-Gelant Treatments: A Laboratory Scale Approach. SPE International Conference on Oilfield Chemistry, 2017. Society of Petroleum Engineers.

ASKARINEZHAD, R., HATZIGNATIOU, D. G. & STAVLAND, A. Disproportionate Permeability Reduction of Water-Soluble Silicate Gelants-Importance of Formation Wettability. SPE Improved Oil Recovery Conference, 2016. Society of Petroleum Engineers.

AUDIBERT, A., NOIK, C. & LECOURTIER, J. 1993. Behaviour of polysaccharides under harsh conditions. *Journal of Canadian Petroleum Technology,* 32.

AWOLAYO, A. N., SARMA, H. K. & NGHIEM, L. X. Numerical Modeling of Fluid-Rock Interactions During Low-Salinity-Brine-CO Flooding in Carbonate Reservoirs. SPE Reservoir Simulation Conference, 2019. Society of Petroleum Engineers.

BABCOCK, H. P., TEIXEIRA, R. E., HUR, J. S., SHAQFEH, E. S. & CHU, S. 2003. Visualization of molecular fluctuations near the critical point of the coil− stretch transition in polymer elongation. *Macromolecules,* 36**,** 4544-4548.

BAE, S. & INYANG, H. 2001. Effects of various polyethylenimine solutions on desiccation of Na-montmorillonite. *Soil and Sediment Contamination,* 10**,** 675-685.

BARRUFET, M. & ALI, L. Modification of relative permeability curves by polymer adsorption. SPE Latin America/Caribbean Petroleum Engineering Conference, 1994. Society of Petroleum Engineers.

BENNION, D. B. & THOMAS, F. B. 2005. Formation damage issues impacting the productivity of low permeability, low initial water saturation gas producing formations.

BERA, A., KUMAR, T., OJHA, K. & MANDAL, A. 2013. Adsorption of surfactants on sand surface in enhanced oil recovery: Isotherms, kinetics and thermodynamic studies. *Applied Surface Science,* 284**,** 87-99.

BESRA, L., SENGUPTA, D., ROY, S. & AY, P. 2002. Flocculation and dewatering of kaolin suspensions in the presence of polyacrylamide and surfactants. *International Journal of Mineral Processing,* 66**,** 203-232.

BESRA, L., SENGUPTA, D., ROY, S. & AY, P. 2003. Influence of surfactants on flocculation and dewatering of kaolin suspensions by cationic polyacrylamide (PAM-C) flocculant. *Separation and Purification Technology,* 30**,** 251-264.

BHATNAGAR, A. & EOFF, L. Stimulation in High Water-Cut Wells: Treatment Optimization Using a Fluid Placement Model. SPE Asia Pacific Oil & Gas Conference and Exhibition, 2016. Society of Petroleum Engineers.

BLUM, A. E. & LASAGA, A. C. 1991. The Role of Surface Speciation in the Dissolution of Albite. *Geochimica Et Cosmochimica Acta,* 55**,** 2193-2201.

BORDEAUX-REGO, F., MEHRABI, M., SANAEI, A. & SEPEHRNOORI, K. 2021. Improvements on modelling wettability alteration by Engineered water injection: Surface complexation at the oil/brine/rock contact. *Fuel,* 284**,** 118991.

BRAGANÇA, F. D. C., VALADARES, L. F., LEITE, C. A. D. P. & GALEMBECK, F. 2007. Counterion effect on the morphological and mechanical properties of polymer− clay nanocomposites prepared in an aqueous medium. *Chemistry of materials,* 19**,** 3334-3342.

BRISCOE, B., LUCKHAM, P. & ZHU, S. 1999. Pressure influences upon shear thickening of poly (acrylamide) solutions. *Rheologica acta,* 38**,** 224-234.

BROSETA, D., MARQUER, O., BLIN, N. & ZAITOUN, A. Rheological screening of low-molecular-weight polyacrylamide/chromium (III) acetate water shutoff gels. SPE/DOE improved oil recovery symposium, 2000. Society of Petroleum Engineers.

BROSETA, D. & MEDJAHED, F. 1995. Effects of substrate hydrophobicity on polyacrylamide adsorption. *Journal of colloid and interface science,* 170**,** 457-465.

BROWNE, C. A., SHIH, A. & DATTA, S. S. 2020. Pore-Scale Flow Characterization of Polymer Solutions in Microfluidic Porous Media. *Small,* 16**,** 1903944.

BURRAFATO, G., ALBONICO, P., BUCCI, S. & LOCKHART, T. P. Ligand-exchange chemistry of Cr13-polyacrylamide gels. Makromolekulare Chemie. Macromolecular Symposia, 1990. Wiley Online Library, 137-141.

BURRAFATO, G., PITONI, E., VIETINA, G., MAURI, L. & CHIAPPA, L. Rigless WSO Treatments in Gas Fields. Bullheading Gels and Polymers in Shaly Sand: Italian Case Histories. SPE European Formation Damage Conference, 31 May–1 June 1999 The Hague, The Netherlands. Society of Petroleum Engineers.

CANSECO, V., DJEHICHE, A., BERTIN, H. & OMARI, A. 2009. Deposition and re-entrainment of model colloids in saturated consolidated porous media: Experimental study. *Colloids and surfaces A: physicochemical and engineering aspects,* 352**,** 5-11.

CASCIO, E. L., DE SCHUTTER, B. & SCHENONE, C. 2018. Flexible energy harvesting from natural gas distribution networks through line-bagging. *Applied energy,* 229**,** 253-263.

CHAUVETEAU, G., DENYS, K. & ZAITOUN, A. New insight on polymer adsorption under high flow rates. SPE/DOE improved oil recovery symposium, 2002. Society of Petroleum Engineers.

CHAUVETEAU, G. & MOAN, M. 1981. The onset of dilatant behaviour in non-inertial flow of dilute polymer solutions through channels with varying cross-sections. *Journal de Physique Lettres,* 42**,** 201-204.

CHAUVETEAU, G., MOAN, M. & MAGUEUR, A. 1984. Thickening behaviour of dilute polymer solutions in non-inertial elongational flows. *Journal of non-newtonian fluid mechanics,* 16**,** 315-327.

CHEN, B., SUN, H., ZHOU, H., YANG, M. & WANG, D. 2019a. Effects of pressure and sea water flow on natural gas hydrate production characteristics in marine sediment. *Applied energy,* 238**,** 274-283.

CHEN, B., YANG, M., SUN, H., WANG, P. & WANG, D. 2019b. Visualization study on the promotion of natural gas hydrate production by water flow erosion. *Fuel,* 235**,** 63-71.

CHEN, X., LI, Y., LIU, Z., LI, X., ZHANG, J. & ZHANG, H. 2020a. Core-and pore-scale investigation on the migration and plugging of polymer microspheres in a heterogeneous porous media. *Journal of Petroleum Science and Engineering***,** 107636.

CHEN, X., LI, Y., LIU, Z., ZHANG, J., CHEN, C. & MA, M. 2020b. Investigation on matching relationship and plugging mechanism of self-adaptive micro-gel (SMG) as a profile control and oil displacement agent. *Powder Technology,* 364**,** 774-784.

CHIAPPA, L., MENNALLA, A. & ORTOLANI, M. Role of Polymer Adsorption and of Petrophysical Properties in Water-Cut Control Treatments by Polymer Injection in Gas Wells. IOR 1997-9th European Symposium on Improved Oil Recovery, 20-22 October 1997 Hague, Netherlands. European Association of Geoscientists & Engineers, cp-106-00047.

CHIAPPA, L., MENNELLA, A. & BURRAFATO, G. Polymer/rock interactions in polymer treatments for water-cut control. SPE/DOE Improved Oil Recovery Symposium, 1998. Society of Petroleum Engineers.

CHIAPPA, L., MENNELLA, A., LOCKHART, T. P. & BURRAFATO, G. 1999. Polymer adsorption at the brine/rock interface: the role of electrostatic interactions and wettability. *Journal of petroleum science and engineering,* 24**,** 113-122.

CISSOKHO, M., BERTIN, H., BOUSSOUR, S., CORDIER, P. & HAMON, G. 2010. Low salinity oil recovery on clayey sandstone: Experimental study. *Petrophysics-The SPWLA Journal of Formation Evaluation and Reservoir Description,* 51.

COHEN, Y. & CHRIST, F. 1986. Polymer retention and adsorption in the flow of polymer solutions through porous media. *SPE Reservoir Engineering,* 1**,** 113-118.

CONNOLLY, P. R., VOGT, S. J., IGLAUER, S., MAY, E. F. & JOHNS, M. L. 2017. Capillary trapping quantification in sandstones using NMR relaxometry. *Water Resources Research,* 53**,** 7917-7932.

COZIC, C., ROUSSEAU, D. & TABARY, R. Broadening the application range of water shutoff/conformance-control microgels: An investigation of their chemical robustness. SPE Annual Technical Conference and Exhibition, 2008. Society of Petroleum Engineers.

COZIC, C., ROUSSEAU, D. & TABARY, R. 2009. Novel insights into microgel systems for water control. *SPE Production & Operations,* 24**,** 590-601.

DAI, C., LIU, Y., ZOU, C., YOU, Q., YANG, S., ZHAO, M., ZHAO, G., WU, Y. & SUN, Y. 2017a. Investigation on matching relationship between dispersed particle gel (DPG) and reservoir pore-throats for in-depth profile control. *Fuel,* 207**,** 109-120.

DAI, C., XU, Z., WU, Y., ZOU, C., WU, X., WANG, T., GUO, X. & ZHAO, M. 2017b. Design and study of a novel thermal-resistant and shear-stable amphoteric polyacrylamide in high-salinity solution. *Polymers,* 9**,** 296.

DANG, T., CHEN, Z., NGUYEN, T. & BAE, W. 2014. Investigation of isotherm polymer adsorption in porous media. *Petroleum science and technology,* 32**,** 1626-1640.

DAWE, R. A. & ZHANG, Y. 1994. Mechanistic study of the selective action of oil and water penetrating into a gel emplaced in a porous medium. *Journal of Petroleum Science and Engineering,* 12**,** 113-125.

DE GENNES, P. 1976. Scaling theory of polymer adsorption. *Journal de physique,* 37**,** 1445-1452.

DEHSHIBI, R. R., MOHEBBI, A., RIAZI, M. & DANAFAR, F. 2019. Visualization study of the effects of oil type and model geometry on oil recovery under ultrasonic irradiation in a glass micro-model. *Fuel,* 239**,** 709-716.

DENG, Y., DIXON, J. B., WHITE, G. N., LOEPPERT, R. H. & JUO, A. S. 2006. Bonding between polyacrylamide and smectite. *Colloids and Surfaces A: Physicochemical and Engineering Aspects,* 281**,** 82-91.

DENYS, K., FICHEN, C. & ZAITOUN, A. Bridging adsorption of cationic polyacrylamides in porous media. SPE international symposium on oilfield chemistry, 2001. OnePetro.

DI LULLO, G., RAE, P. & CURTIS, J. New Insights into Water Control—A Review of the State of the Art—Part II. SPE International Thermal Operations and Heavy Oil

Symposium and International Horizontal Well Technology Conference, 2002. Society of Petroleum Engineers.

DIMI-MISIC, K., PHIRI, J., NIEMINEN, K., MALONEY, T. & GANE, P. 2019. Characterising exfoliated few-layer graphene interactions in co-processed nanofibrillated cellulose suspension via water retention and dispersion rheology. *Materials Science and Engineering: B,* 242**,** 37-51.

DOS SANTOS, A. P., GIROTTO, M. & LEVIN, Y. 2016. Simulations of polyelectrolyte adsorption to a dielectric like-charged surface. *The Journal of Physical Chemistry B,* 120**,** 10387-10393.

DOVAN, H. & HUTCHINS, R. 1994. New polymer technology for water control in gas wells. *SPE Production & Facilities,* 9**,** 280-286.

DUPUIS, D., LEWANDOWSKI, F., STEIERT, P. & WOLFF, C. 1994. Shear thickening and time-dependent phenomena: The case of polyacrylamide solutions. *Journal of non-newtonian fluid mechanics,* 54**,** 11-32.

EHSAN, A., JAMAL, A., MAHMOOD, H. & AHMAD, S. V. 2017. Thermal stability, adsorption and rheological behaviors of sulfonated polyacrylamide/chromium triacetate/laponite nanocomposite weak gels. *Macromolecular Research,* 25**,** 27-37.

EL-HOSHOUDY, A., MOHAMMEDY, M., RAMZI, M., DESOUKY, S. & ATTIA, A. 2019. Experimental, modeling and simulation investigations of a novel surfmer-co-poly acrylates crosslinked hydrogels for water shut-off and improved oil recovery. *Journal of Molecular Liquids,* 277**,** 142-156.

EL-KARSANI, K. S. M., AL-MUNTASHERI, G. A. & HUSSEIN, I. A. 2014. Polymer systems for water shutoff and profile modification: a review over the last decade. *SPE Journal,* 19**,** 135-149.

ELMKIES, P., LASSEUX, D., BERTIN, H., PICHERY, T. & ZAITOUN, A. Polymer effect on gas/water flow in porous media. SPE/DOE Improved Oil Recovery Symposium, 13–17 April 2002 Tulsa, Oklahoma, USA. Society of Petroleum Engineers.

EVANS, R. Produced water management strategy with the aid of decision analysis. In: Paper SPE 66543 Presented at the SPE/EPA/DOE Exploration and Production Environmental Conference, 26-28 February., 2001 San Antonio, Texas. SPE.

FARASAT, A., SEFTI, M. V., SADEGHNEJAD, S. & SAGHAFI, H. R. 2017. Effects of reservoir temperature and water salinity on the swelling ratio performance of enhanced preformed particle gels. *Korean Journal of Chemical Engineering,* 34**,** 1509-1516.

FERREIRA, V. H. & MORENO, R. B. 2019. Polyacrylamide adsorption and readsorption in sandstone porous media. *SPE Journal*.

GAO, H.-B., LI, H., ZHANG, X.-Q., WANG, X.-H., LI, C.-Y. & LUO, M.-B. 2021. Computer Simulation Study on Adsorption and Conformation of Polymer Chains Driven by External Force. *Chinese Journal of Polymer Science,* 39**,** 258-266.

GEORGELOS, P. N. & TORKELSON, J. M. 1988. The role of solution structure in apparent thickening behavior of dilute peo/water systems. *Journal of non-newtonian fluid mechanics,* 27**,** 191-204.

GOMARI, K. E., GOMARI, S. R., ISLAM, M. & HUGHES, D. 2020. Studying the effect of acidic and basic species on the physiochemical properties of polymer and biopolymer at different operational conditions. *Journal of Molecular Liquids,* 112424.

GRATTONI, C., LUCKHAM, P., JING, X., NORMAN, L. & ZIMMERMAN, R. W. 2004. Polymers as relative permeability modifiers: adsorption and the dynamic formation of thick polyacrylamide layers. *Journal of petroleum science and engineering,* 45**,** 233-245.

GRATTONI, C. A., AL-SHARJI, H. H., DAWE, R. A. & ZIMMERMAN, R. W. 2002. Segregated pathways mechanism for oil and water flow through an oil-based gelant. *Journal of Petroleum Science and Engineering,* 35**,** 183-190.

GRATTONI, C. A., AL-SHARJI, H. H., YAN, C., MUGGERIDGE, A. H. & ZIMMERMAN, R. W. 2001a. Rheology and Permeability of Crosslinked Polyacrylamide Gel. *Journal of Colloid and Interface Science* 240, 601–607

GRATTONI, C. A., AL-SHARJI, H. H., YANG, C., MUGGERIDGE, A. H. & ZIMMERMAN, R. W. 2001b. Rheology and permeability of crosslinked polyacrylamide gel. *Journal of colloid and interface science,* 240**,** 601-607.

GRATTONI, C. A., JING, X. D. & ZIMMERMAN, R. W. 2001c. Disproportionate Permeability Reduction When a Silicate Gel is Formed In-Situ to Control Water Production. *SPE*.

GRATTONI, C. A., JING, X. D. & ZIMMERMAN, R. W. 2001d. Disproportionate Permeability Reduction When a Silicate Gel is Formed In-Situ to Control Water Production. *SPE Latin American and Caribbean Petroleum Engineering Conference.* Buenos Aires, Argentina: Society of Petroleum Engineers.

GRIFFIN, L., BROWNING, K., LEE, S., SKODA, M., ROGERS, S. & CLARKE, S. 2016. Multilayering of calcium aerosol-OT at the mica/water interface studied with neutron reflection: Formation of a condensed lamellar phase at the CMC. *Langmuir,* 32**,** 13054-13064.

GUETNI, I., MARLIÈRE, C., ROUSSEAU, D., PELLETIER, M., BIHANNIC, I. & VILLIÉRAS, F. 2020. Transport of EOR polymer solutions in low permeability porous media: impact of clay type and injection water composition. *Journal of Petroleum Science and Engineering,* 186**,** 106690.

HAJILARY , N., SEFTI, M. V. & KOOHI , A. D. 2015. Experimental study of water shutoff gel system field parameters in multi-zone unfractured gas-condensate reservoirs.

HAJILARY, N., SEFTI, M. V. & KOOHI, A. D. 2015a. Experimental study of water shutoff gel system field parameters in multi-zone unfractured gas-condensate reservoirs. *Journal of Natural Gas Science and Engineering,* 27**,** 926-933.

HAJILARY, N., SEFTI, M. V., SHAHMOHAMMADI, A., KOOHI, A. D. & MOHAJERI, A. 2015b. Development of a novel water shut-off test method: Experimental study of polymer gel in porous media with radial flow. *The Canadian Journal of Chemical Engineering,* 93**,** 1957-1964.

HAJILARY, N. & SHAHMOHAMMADI, A. 2018. New permeability model for gel coated porous media with radial flow. *Journal of Applied Fluid Mechanics,* 11**,** 397-404.

HAMOUNA, M., DELBOS, A., DALMAZONNE, C. & COLIN, A. 2021. Can unmixed complex forming polymer surfactant formulations be injected into oil reservoirs or aquifers without clogging them? *Soft Matter*.

HAN, M., ALSHEHRI, A. J., KRINIS, D. & LYNGRA, S. State-of-the-art of in-depth fluid diversion technology: enhancing reservoir oil recovery by gel treatments. SPE Saudi Arabia section technical symposium and exhibition, 2014. Society of Petroleum Engineers.

HAN, M., SHI, L., YE, M. & MA, J. 1995. Crosslinking reaction of polyacrylamide with chromium (III). *Polymer Bulletin*, 35**,** 109-113.

HARRISON, G., FRANKS, G., TIRTAATMADJA, V. & BOGER, D. 1999. Suspensions and polymers-Common links in rheology. *Korea-Australia Rheology Journal*, 11**,** 197-218.

HARTNETT, J. P. & KOSTIC, M. 1989. Heat transfer to Newtonian and non-Newtonian fluids in rectangular ducts. *Advances in heat transfer*. Elsevier.

HASSAN, A. M., AYOUB, M., EISSA, M., BRUINING, H. & ZITHA, P. 2020. Study of surface complexation modeling on a novel hybrid enhanced oil recovery (EOR) method; smart-water assisted foam-flooding. *Journal of Petroleum Science and Engineering*, 195**,** 107563.

HEIDARI, A., VASHEGHANI-FARAHANI, E. & VAFAIE-SEFTI, M. 2019. Preformed particle gels of sulfonated polyacrylamide: preparation, characterization, and application as permeability modifier. *Iranian Polymer Journal*, 28**,** 1001-1013.

HELALIA, A. M. & LETEY, J. 1989. Effects of different polymers on seedling emergency, aggregate stability, and crust hardness. *Soil Science*, 148**,** 199-203.

HIRASAKI, G. & POPE, G. 1974. Analysis of factors influencing mobility and adsorption in the flow of polymer solution through porous media. *Society of Petroleum Engineers Journal*, 14**,** 337-346.

HOAGLAND, D. A. & PRUD'HOMME, R. K. 1989. Hydrodynamic chromatography as a probe of polymer dynamics during flow through porous media. *Macromolecules*, 22**,** 775-781.

IDAHOSA, P. E., OLUYEMI, G. F., PRABHU, R. & OYENEYIN, B. 2014. Rheological behaviour of single-phase non-Newtonian polymer solution in complex pore geometry: a simulation approach.

IMQAM, A. H. 2015. *Particle gel propagation and blocking behavior through high permeability streaks and fractures*, Missouri University of Science and Technology.

IMQAM, A. H., BAI, B., XIONG, C., WEI, M., DELSHAD, M. & SEPEHRNOORI, K. Characterisations of Disproportionate Permeability Reduction of Particle Gels Through Fractures. SPE Asia Pacific Oil & Gas Conference and Exhibition, 2014. Society of Petroleum Engineers.

INIKORI, S. O. 2002. *Numerical Study of Water Coning Control with Downhole Water Sink (DWS) Well Completions in Vertical and Horizontal Well (Master thesis).* , Baton Rouge Benin City-Nigeria., Louisiana State University.

ISMAIL, A., AFTAB, A., IBUPOTO, Z. & ZOLKIFILE, N. 2016. The novel approach for the enhancement of rheological properties of water-based drilling fluids by using multi-walled carbon nanotube, nanosilica and glass beads. *Journal of Petroleum Science and Engineering,* 139**,** 264-275.

JAAFAR, M., NASIR, A. M. & HAMID, M. 2014. Measurement of isoelectric point of sandstone and carbonate rock for monitoring water encroachment. *Journal of Applied Sciences,* 14**,** 3349-3353.

JAAFAR, M., VINOGRADOV, J. & JACKSON, M. 2009. Measurement of streaming potential coupling coefficient in sandstones saturated with high salinity NaCl brine. *Geophysical Research Letters,* 36.

JACKSON, M., VINOGRADOV, J., HAMON, G. & CHAMEROIS, M. 2016. Evidence, mechanisms and improved understanding of controlled salinity waterflooding part 1: Sandstones. *Fuel,* 185**,** 772-793.

JAŃCZUK, B., BIAŁOPIOTROWICZ, T., KLISZCZ, A., BILIŃSKI, B. & STAWIŃSKI, J. 1991. Influence of polyacrylamide on the surface free energy and wettability of a chernozem soil. *Geoderma,* 50**,** 173-184.

JARIPATKE, O. A., DALRYMPLE, E. D., PROKHOROV, A. V., GAPONOV, M. A. & FAKHREEVA, A. Field-Application Results of HMWSP in Western Siberia: Design Optimization, Conclusions, and Recommendations. International Petroleum Technology Conference, 2009. International Petroleum Technology Conference.

JENNINGS, R., ROGERS, J. & WEST, T. 1971. Factors influencing mobility control by polymer solutions. *Journal of Petroleum Technology,* 23**,** 391-401.

JHA, N. K., ALI, M., IGLAUER, S., LEBEDEV, M., ROSHAN, H., BARIFCANI, A., SANGWAI, J. S. & SARMADIVALEH, M. 2019a. Wettability alteration of quartz surface by low-salinity surfactant nanofluids at high-pressure and high-temperature conditions. *Energy & Fuels,* 33**,** 7062-7068.

JHA, N. K., IGLAUER, S., BARIFCANI, A., SARMADIVALEH, M. & SANGWAI, J. S. 2019b. Low-salinity surfactant nanofluid formulations for wettability alteration of sandstone: role of the SiO2 nanoparticle concentration and divalent cation/SO42– ratio. *Energy & fuels,* 33**,** 739-746.

JHA, N. K., IVANOVA, A., LEBEDEV, M., BARIFCANI, A., CHEREMISIN, A., IGLAUER, S., SANGWAI, J. S. & SARMADIVALEH, M. 2021. Interaction of low salinity surfactant nanofluids with carbonate surfaces and molecular level dynamics at fluid-fluid interface at ScCO2 loading. *Journal of Colloid and Interface Science,* 586**,** 315-325.

JHA, N. K., LEBEDEV, M., IGLAUER, S., ALI, M., ROSHAN, H., BARIFCANI, A., SANGWAI, J. S. & SARMADIVALEH, M. 2020. Pore scale investigation of low salinity surfactant nanofluid injection into oil saturated sandstone via X-ray micro-tomography. *Journal of colloid and interface science,* 562**,** 370-380.

JIA, H. & CHEN, H. 2018. Using DSC technique to investigate the non-isothermal gelation kinetics of the multi-crosslinked Chromium acetate (Cr3+)-Polyethyleneimine (PEI)-Polymer gel sealant. *Journal of Petroleum Science and Engineering,* 165**,** 105-113.

JIA, H., PU, W.-F., ZHAO, J.-Z. & JIN, F.-Y. 2010. Research on the gelation performance of low toxic PEI cross-linking PHPAM gel systems as water shutoff agents in low temperature reservoirs. *Industrial & engineering chemistry research,* 49**,** 9618-9624.

JINXIANG, L., XIANGGUO, L., JINGFA, L., SHUQIONG, H. & BAOQING, X. 2013. Mechanism and gelling effects of linked polymer solution in the core. *Petroleum Exploration and Development,* 40**,** 507-513.

JOSEPH, A. & AJIENKA, J. A review of water shutoff treatment strategies in oil fields. Nigeria Annual International Conference and Exhibition, 2010. Society of Petroleum Engineers.

KALFAYAN, L. J. & DAWSON, J. C. Successful implementation of resurgent Relative Permeability Modifier (RPM) technology in well treatments requires realistic expectations. SPE Annual Technical Conference and Exhibition, 26-29 September 2004 Houston, Texas, U.S.A. Society of Petroleum Engineers.

KALGAONKAR, R., SARDA, A. & SABHAPONDIT, A. Novel Fluid System for Efficient Downhole Placement of Water Swellable Polymers. Offshore Mediterranean Conference and Exhibition, 2013. Offshore Mediterranean Conference.

KAMAL, M. S., SULTAN, A. S., AL-MUBAIYEDH, U. A. & HUSSEIN, I. A. 2015. Review on polymer flooding: rheology, adsorption, stability, and field applications of various polymer systems. *Polymer Reviews,* 55**,** 491-530.

KARIMI, S., ESMAEILZADEH, F. & MOWLA, D. 2014a. Identification and selection of a stable gel polymer to control or reduce water production in gas condensate fields. *Journal of Natural Gas Science and Engineering***,** 940-950.

KARIMI, S., ESMAEILZADEH, F. & MOWLA, D. 2014b. Identification and selection of a stable gel polymer to control or reduce water production in gas condensate fields. *Journal of Natural Gas Science and Engineering,* 21**,** 940-950.

KARIMI, S., KAZEMI, S. & KAZEMI, N. 2016. Syneresis measurement of the HPAM-Cr (III) gel polymer at different conditions: An experimental investigation. *Journal of Natural Gas Science and Engineering,* 34**,** 1027-1033.

KARMAKAR, G., GRATTONI, C. & ZIMMERMAN, R. Relative permeability modification using an oil-soluble gelant to control water production. SPE Annual Technical Conference and Exhibition, 2002. OnePetro.

KARMAKAR, G., GRATTONI, C. & ZIMMERMAN, R. 2018. An oil-based gel system for reservoir rock permeability modification. *Advances in Materials and Processing Technologies,* 4**,** 669-679.

KATIKA, K., SAIDIAN, M. & FABRICIUS, I. L. Wettability of chalk and argillaceous sandstones assessed from T1/T2 ratio. 78th EAGE Conference and Exhibition 2016, 2016. European Association of Geoscientists & Engineers, 1-5.

KAWELAH, M., HE, Y., ALAMRI, H., GIZZATOV, A., SWAGER, T. M. & ZHU, S. S. 2020. Dynamic adsorption of functionalized zwitterionic copolymers on carbonate surfaces under extreme reservoir conditions. *Energy & Fuels,* 34**,** 12018-12025.

KHAMEES, T. K. & FLORI, R. E. 2018. A comprehensive evaluation of the parameters that affect the performance of in-situ gelation system. *Fuel,* 225**,** 140-160.

KHAN, M. I., SHAHRESTANI, M., HAYAT, T., SHAKOOR, A. & VAHDATI, M. 2019. Life cycle (well-to-wheel) energy and environmental assessment of natural gas as transportation fuel in Pakistan. *Applied Energy,* 242**,** 1738-1752.

KOBAYASHI, K., LIANG, Y., MURATA, S., MATSUOKA, T., TAKAHASHI, S., AMANO, K.-I., NISHI, N. & SAKKA, T. 2017. Stability evaluation of cation bridging on muscovite surface for improved description of ion-specific wettability alteration. *The Journal of Physical Chemistry C,* 121**,** 9273-9281.

KOHLER, N., RAHBARI, R., HAN, M. & ZAITOUN, A. Weak gel formulations for selective control of water production in high-permeability and high-temperature production wells. SPE International Symposium on Oilfield Chemistry, 1993. Society of Petroleum Engineers.

KUO, J. 2014. *Practical design calculations for groundwater and soil remediation*, CRC Press.

LADUTKO, A., GOSS, M. L., DALRYMPLE, E. D. D. & CHANG, K.-T. Field Application Results of Water Permeability Modifier in Fracture Stimulation Treatments in Western Siberia. SPE Annual Technical Conference and Exhibition, 2012. Society of Petroleum Engineers.

LAGER, A., WEBB, K. J., BLACK, C., SINGLETON, M. & SORBIE, K. S. 2008a. Low salinity oil recovery-an experimental investigation1. *Petrophysics-The SPWLA Journal of Formation Evaluation and Reservoir Description*, 49.

LAGER, A., WEBB, K. J., COLLINS, I. R. & RICHMOND, D. M. LoSal enhanced oil recovery: Evidence of enhanced oil recovery at the reservoir scale. SPE symposium on improved oil recovery, 2008b. OnePetro.

LARSON, R. G. 1999. *The structure and rheology of complex fluids*, Oxford university press New York.

LE MAOUT, V., SCIUME, G. & BERTIN, H. 2021. Modeling Monophasic Flow of Polymer Solutions in Porous Media: Assessing Relative Impact of Intrinsic Fluid Properties and Pore Microstructure. *Transport in Porous Media,* 137**,** 233-254.

LETHAM, E. A. & BUSTIN, R. M. 2018. Quantitative validation of pore structure characterization using gas slippage measurements by comparison with predictions from bundle of capillaries models. *Marine and Petroleum Geology,* 91**,** 363-372.

LEVER, A. & DAWE, R. A. 1984. Water-sensitivity and migration of fines in the hopeman sandstone. *Journal of Petroleum Geology,* 7**,** 97-107.

LEWIS, R. 2014. *Water Shutoff in the Dunbar Field, Identification of Candidates and Production Gains.* Centre for Petroleum Studies, Department of Earth Science and Engineering.

LI, K., SUN, W., LI, F., QU, Y. & YANG, Y. 2014. Novel method for characterizing single-phase polymer flooding. *SPE Journal,* 19**,** 695-702.

LI, Q., PU, W., WEI, B., JIN, F. & LI, K. 2017. Static adsorption and dynamic retention of an anti-salinity polymer in low permeability sandstone core. *Journal of Applied Polymer Science,* 134.

LI, W. & LU, C. 2019. The multiple effectiveness of state natural gas consumption constraint policies for achieving sustainable development targets in China. *Applied energy,* 235**,** 685-698.

LIANG, B., JIANG, H., LI, J., CHEN, F., MIAO, W., YANG, H., QIAO, Y. & CHEN, W. 2018. Mechanism study of disproportionate permeability reduction using nuclear magnetic resonance T2. *Energy & Fuels,* 32**,** 4959-4968.

LIANG, B., JIANG, H., LI, J., SERIGHT, R. & LAKE, L. W. Further insights into the mechanism of disproportionate permeability reduction. SPE annual technical conference and exhibition, 2017. Society of Petroleum Engineers.

LIANG, J.-T. & SERIGHT, R. 1997. Further investigations of why gels reduce water permeability more than oil permeability. *SPE Production & Facilities,* 12**,** 225-230.

LIANG, J.-T., SUN, H. & SERIGHT, R. 1995. Why do gels reduce water permeability more than oil permeability? *SPE Reservoir Engineering,* 10**,** 282-286.

LIANG, J., SUN, H. & SERIGHT, R. Reduction of oil and water permeabilities using gels. SPE/DOE Enhanced Oil Recovery Symposium, 1992. Society of Petroleum Engineers.

LIAO, J. 2014. Gel treatment field application survey for water shut off in production wells.

LIU, J.-X., ZHANG, Y.-H. & REN, S.-R. 2009. Hydrodynamic adsorption of cationic polymer in porous media. *Journal of Petrochemical Universities,* 1.

LIU, L. 2015. Effect of polymer on disproportionate permeability reduction to gas and water for fractured shales.

LIU, L., DAI, S., NING, F., CAI, J., LIU, C. & WU, N. 2019. Fractal characteristics of unsaturated sands− implications to relative permeability in hydrate-bearing sediments. *Journal of Natural Gas Science and Engineering,* 66**,** 11-17.

LOCKHART, T. & BURRAFATO, G. Water production control with relative permeability modifiers. 16th World Petroleum Congress, 2000. World Petroleum Congress.

LOPEZ, G. M. C., MYERS, M. B., XIE, Q., WOOD, C. D. & SAEEDI, A. 2021. Wettability alteration using benzoxazine resin: A remedy for water blockage in sandstone gas reservoirs. *Fuel,* 291**,** 120189.

MACHALE, J., MAJUMDER, S. K., GHOSH, P. & SEN, T. K. 2019. Development of a novel biosurfactant for enhanced oil recovery and its influence on the rheological properties of polymer. *Fuel,* 257**,** 116067.

MAHANI, H., KEYA, A. L., BERG, S., BARTELS, W.-B., NASRALLA, R. & ROSSEN, W. Driving mechanism of low salinity flooding in carbonate rocks. EUROPEC 2015, 2015. Society of Petroleum Engineers.

MAIA, A., VILLETTI, M. A., VIDAL, R. R., BORSALI, R. & BALABAN, R. C. 2011. Solution properties of a hydrophobically associating polyacrylamide and its polyelectrolyte derivatives determined by light scattering, small angle x-ray scattering and viscometry. *Journal of the Brazilian Chemical Society,* 22**,** 489-500.

MAIA, A. M., COSTA, M., BORSALI, R. & GARCIA, R. B. Rheological Behavior and Scattering Studies of Acrylamide-Based Copolymer Solutions. Macromolecular symposia, 2005. Wiley Online Library, 217-227.

MENNELLA, A., CHIAPPA, L., BRYANT, S. L. & BURRAFATO, G. Pore-scale mechanism for selective permeability reduction by polymer injection. SPE/DOE Improved Oil Recovery Symposium, 19-22 April 1998 Tulsa, Oklahoma. Society of Petroleum Engineers.

MENNELLA, A., CHIAPPA, L., LOCKHART, T. P. & BURRAFATO, G. 2001. Candidate and chemical selection guidelines for relative permeability modification (RPM) treatments. *SPE Production & Facilities,* 16**,** 181-188.

MISHRA, S., BERA, A. & MANDAL, A. 2014. Effect of polymer adsorption on permeability reduction in enhanced oil recovery. *Journal of Petroleum Engineering,* 2014.

MOAN, M. & OMARI, A. 1992. Molecular analysis of the mechanical degradation of polymer solution through a porous medium. *Polymer degradation and stability,* 35**,** 277-281.

MOEN, D. & RICHARDSON, J. 1984a. Ultrasonic Dispersion of Soil Aggregates Stabilized by Polyvinyl Alcohol and T403-Glyoxal Polymers 1. *Soil Science Society of America Journal,* 48**,** 628-631.

MOEN, D. E. & RICHARDSON, J. L. 1984b. Ultrasonic Dispersion of Soil Aggregates Stabilized by Polyvinyl Alcohol and T403-Glyoxal Polymers1. *Soil Science Society of America Journal,* 48**,** 628-631.

MOGHADASI, L., PISICCHIO, P., BARTOSEK, M., BRACCALENTI, E., ALBONICO, P., MORONI, I., VESCHI, R., MASSERANO, F., SCAGLIOTTI, S. & DEL GAUDIO, L. Laboratory Investigation on Synergy Effect of Low Salinity-Polymer Water Injection on Sandstone Porous Media. Offshore Mediterranean Conference and Exhibition, 2019. Offshore Mediterranean Conference.

MOHANTY, K. K. 2003. The near-term energy challenge. *AIChE J.***,** 49, 2454-2460.

MONTILLET, A., COMITI, J. & LEGRAND, J. 1992. Determination of structural parameters of metallic foams from permeametry measurements. *Journal of Materials Science,* 27**,** 4460-4464.

MORROW, N. & BUCKLEY, J. 2011. Improved oil recovery by low-salinity waterflooding. *Journal of petroleum Technology,* 63**,** 106-112.

MYINT, P. C. & FIROOZABADI, A. 2015. Thin liquid films in improved oil recovery from low-salinity brine. *Current Opinion in Colloid & Interface Science,* 20**,** 105-114.

NASRALLA, R. A., BATAWEEL, M. A. & NASR-EL-DIN, H. A. 2013. Investigation of wettability alteration and oil-recovery improvement by low-salinity water in sandstone rock. *Journal of Canadian Petroleum Technology,* 52**,** 144-154.

NASRALLA, R. A. & NASR-EL-DIN, H. A. 2014a. Double-layer expansion: is it a primary mechanism of improved oil recovery by low-salinity waterflooding? *SPE Reservoir Evaluation & Engineering,* 17**,** 49-59.

NASRALLA, R. A. & NASR-EL-DIN, H. A. 2014b. Impact of cation type and concentration in injected brine on oil recovery in sandstone reservoirs. *Journal of Petroleum Science and Engineering,* 122**,** 384-395.

NGUYEN, N., TU, T., BAE, W., DANG, C., CHUNG, T. & NGUYEN, H. 2012. Gelation time optimization for an HPAM/chromium acetate system: The successful key of conformance control technology. *Energy Sources, Part A: Recovery, Utilization, and Environmental Effects*, 34**,** 1305-1317.

NGUYEN, T. Q., GREEN, D. W., WILLHITE, G. P. & MCCOOL, C. S. 2006. Effects of gelant composition and pressure gradients of water and oil on disproportionate permeability reduction of sandpacks treated with polyacrylamide-chromium acetate gels. *SPE Journal*, 11**,** 145-157.

NIEVES, G., FERNANDEZ, J., DALRYMPLE, E. D., SIERRA, L., EOFF, L. & REDDY, B. Field application of relative permeability modifier in Venezuela. SPE/DOE Improved Oil Recovery Symposium, 13-17 April 2002 Tulsa, Oklahoma, USA. Society of Petroleum Engineers.

NILSSON, S., STAVLAND, A. & JONSBRATEN, H. Mechanistic study of disproportionate permeability reduction. SPE/DOE Improved Oil Recovery Symposium, 1998. Society of Petroleum Engineers.

NOIK, C. & AUDIBERT, A. New polymers for high salinity and high temperature. 7th IOR Eur. Symp., Proceedings, 27-29 October 1993 Moscow. 366-375.

NOROUZI, M., PANJALIZADEH, H., RASHIDI, F. & MAHDIANI, M. R. 2017. DPR polymer gel treatment in oil reservoirs: A workflow for treatment optimization using static proxy models. *Journal of Petroleum Science and Engineering*, 153**,** 97-110.

OGUNBERU, A. L. & ASGHARI, K. 2004a. Water permeability reduction under flow-induced polymer adsorption. *Journal of Canadian Petroleum Technology*, 44.

OGUNBERU, A. L. & ASGHARI, K. Water permeability reduction under flow-induced polymer adsorption. Canadian International Petroleum Conference, 2004b. Petroleum Society of Canada.

OGUNBERU, A. L. & ASGHARI, K. 2005. Water permeability reduction under flow-induced polymer adsorption. *Journal of Canadian Petroleum Technology*, 44.

OMARI, A., TABARY, R., ROUSSEAU, D., CALDERON, F. L., MONTEIL, J. & CHAUVETEAU, G. 2006. Soft water-soluble microgel dispersions: Structure and rheology. *Journal of colloid and interface science*, 302**,** 537-546.

PARK, H., HAN, J., LEE, M., JANG, Y. & SUNG, W. 2014. Experimental investigation of polymer adsorption-induced permeability reduction in low permeability reservoirs. *J Pet Environ Biotechnol*, 5**,** 2.

PARK, H., HAN, J. & SUNG, W. 2015. Effect of polymer concentration on the polymer adsorption-induced permeability reduction in low permeability reservoirs. *Energy*, 84**,** 666-671.

PEREIRA, K. A., AGUIAR, K. L., OLIVEIRA, P. F., VICENTE, B. M., PEDRONI, L. G. & MANSUR, C. R. 2020. Synthesis of Hydrogel Nanocomposites Based on Partially Hydrolyzed Polyacrylamide, Polyethyleneimine, and Modified Clay. *ACS omega*, 5**,** 4759-4769.

PINGO-ALMADA, M., PIETERSE, S., MARCELIS, A., VAN HAASTERECHT, M., BRUSSEE, N. & VAN DER LINDE, H. Experimental investigation on the effects of

very low salinity on Middle Eastern sandstone corefloods. SPE European Formation Damage Conference & Exhibition, 2013. OnePetro.

PRADO PAEZ, M., RAUSEO, O., REYNA, M. & FERREIRA, I. Evaluation of the Effect of Oil Viscosity on the Disproportionate Permeability Reduction of a Polymeric Gel Used for Controlling Excess Water Production. Latin American and Caribbean Petroleum Engineering Conference, 2009. Society of Petroleum Engineers.

PUSCH, G., KOHLER, N. & KRETZSCHMAR, H. Practical Experience with Water Control in Gas Wells by Polymer Treatments. IOR 1995-8th European Symposium on Improved Oil Recovery, 16 - 17 May 1995 Vienna, Austria. European IOR

QI, Z., WANG, Y., LIU, C., YU, W., WANG, S. & LI, K. 2013. A Laboratory Evaluation of a Relative Permeability Modifier for Water Production Control. *Petroleum science and technology,* 31**,** 2357-2363.

QIN, L., ARJOMAND, E., MYERS, M. B., OTTO, C., PEJCIC, B., HEATH, C., SAEEDI, A. & WOOD, C. 2020. Mechanistic Aspects of Polymeric Relative Permeability Modifier Adsorption onto Carbonate Rocks. *Energy & Fuels,* 34**,** 12065-12077.

QIN, L., MYERS, M. B., OTTO, C., VERRALL, M., ZHONG, Z., ARJOMAND, E., SAEEDI, A. & WOOD, C. D. 2021. Further Insights into the Performance of Silylated Polyacrylamide-Based Relative Permeability Modifiers in Carbonate Reservoirs and Influencing Factors. *ACS omega*.

QYYUM, M. A., QADEER, K., HAIDER, J. & LEE, M. 2019. Nitrogen self-recuperation expansion-based process for offshore coproduction of liquefied natural gas, liquefied petroleum gas, and pentane plus. *Applied Energy,* 235**,** 247-257.

RANJBAR, M., CLAUSTHAL, T., CZOLBE, P. & KOHLER, N. Comparative laboratory selection and field testing of polymers for selective control of water production in gas wells. SPE International Symposium on Oilfield Chemistry, 1995. Society of Petroleum Engineers.

RANJBAR, M., CZOLBE, P. & KOHLER, N. 1996. Polymers for selective control of water production in gas wells. Comparative laboratory selection and field testing. *OIL GAS-EUROPEAN MAGAZINE,* 22**,** 38-41.

RANJBAR, M., RUPP, J. & PRUSCH, G. Influence of pore radi distribution on polymer retention in natural sandstones. IOR 1991-6th European Symposium on Improved Oil Recovery, 1991.

RANJBAR, M. & SCHAFFIE, M. 2000. Improved treatment of acrylamide co-and terpolymers for water control in gas-producing and storage wells. *Journal of Petroleum Science and Engineering,* 26**,** 133-141.

RELLEGADLA, S., PRAJAPAT, G. & AGRAWAL, A. 2017. Polymers for enhanced oil recovery: fundamentals and selection criteria. *Applied microbiology and biotechnology,* 101**,** 4387-4402.

REYNOLDS, D. B. 2002. *Scarcity and Growth Considering Oil and Energy: an Alternative Neo-classical View. ,* New York, Edwin Mellen Press.

REZAEI GOMARI, S. & JOSEPH, N. 2017. Study of the effect of clay particles on low salinity water injection in sandstone reservoirs. *Energies,* 10**,** 322.

REZAEIDOUST, A., PUNTERVOLD, T. & AUSTAD, T. A discussion of the low salinity EOR potential for a North Sea sandstone field. SPE Annual Technical Conference and Exhibition, 2010. OnePetro.

RUBINSTEIN, M. & COLBY, R. H. 2003. *Polymer physics*, Oxford university press New York.

SALEHI, M. B., SOLEIMANIAN, M. & MOGHADAM, A. M. 2019. Examination of disproportionate permeability reduction mechanism on rupture of hydrogels performance. *Colloids and Surfaces A: Physicochemical and Engineering Aspects,* 560**,** 1-8.

SALIS, A., PARSONS, D. F., BOSTROM, M., MEDDA, L., BARSE, B., NINHAM, B. W. & MONDUZZI, M. 2010. Ion specific surface charge density of SBA-15 mesoporous silica. *Langmuir,* 26**,** 2484-2490.

SAMANTA, A., BERA, A., OJHA, K. & MANDAL, A. 2010. Effects of alkali, salts, and surfactant on rheological behavior of partially hydrolyzed polyacrylamide solutions. *Journal of Chemical & Engineering Data,* 55**,** 4315-4322.

SANDIFORD, B. 1964. Laboratory and field studies of water floods using polymer solutions to increase oil recoveries. *Journal of Petroleum Technology,* 16**,** 917-922.

SAPHIANNIKOVA, M. G., PRYAMITSYN, V. A. & COSGROVE, T. 1998. Self-consistent Brownian dynamics simulation of polymer brushes under shear. *Macromolecules,* 31**,** 6662-6668.

SARI, A., CHEN, Y., XIE, Q. & SAEEDI, A. 2019. Low salinity water flooding in high acidic oil reservoirs: Impact of pH on wettability of carbonate reservoirs. *Journal of Molecular Liquids,* 281**,** 444-450.

SATKEN, B., BERTIN, H. & OMARI, A. Adsorption/Retention of HPAM Polymer in Polymer Flooding Process: Effect of Molecular Weight, Concentration and Wettability. IOR 2021, 2021. European Association of Geoscientists & Engineers, 1-14.

SCHMIDT, J., MIRZAIE YEGANE, M., DUGONJIC-BILIC, F., GERLACH, B. & ZITHA, P. Novel method for mitigating injectivity issues during polymer flooding at high salinity conditions. SPE Europec featured at 81st EAGE Conference and Exhibition, 2019. Society of Petroleum Engineers.

SCHNEIDER, F. & OWENS, W. 1982. Steady-state measurements of relative permeability for polymer/oil systems. *Society of Petroleum Engineers Journal,* 22**,** 79-86.

SCHROEDER, C. M., BABCOCK, H. P., SHAQFEH, E. S. & CHU, S. 2003. Observation of polymer conformation hysteresis in extensional flow. *Science,* 301**,** 1515-1519.

SCOTT, A. J., ROMERO-ZERÓN, L. & PENLIDIS, A. 2020. Evaluation of Polymeric Materials for Chemical Enhanced Oil Recovery. *Processes,* 8**,** 361.

SERIGHT, R. Impact of permeability and lithology on gel performance. SPE/DOE Enhanced Oil Recovery Symposium, 1992. Society of Petroleum Engineers.

SERIGHT, R. 1995. Reduction of gas and water permeabilities using gels. *SPE Production & Facilities,* 10**,** 103-108.

SERIGHT, R. & BRATTEKAS, B. 2021. Water shutoff and conformance improvement: an introduction. *Petroleum Science*, 1-29.

SERIGHT, R. & MARTIN, F. 1993. Impact of gelation pH, rock permeability, and lithology on the performance of a monomer-based gel. *SPE Reservoir Engineering,* 8**,** 43-50.

SERIGHT, R., PRODANOVIC, M. & LINDQUIST, W. B. X-ray computed microtomography studies of disproportionate permeability reduction. SPE/DOE Symposium on Improved Oil Recovery, 2004. Society of Petroleum Engineers.

SERIGHT, R. S., PRODANOVIC, M. & LINDQUIST, W. B. 2006. X-ray computed microtomography studies of fluid partitioning in drainage and imbibition before and after gel placement: Disproportionate permeability reduction. *Spe Journal,* 11**,** 159-170.

SHARIFPOUR, E., ESCROCHI, M., RIAZI, M. & AYATOLLAHI, S. 2016. On the importance of gel rigidity and coverage in a smart water shutoff treatment in gas wells. *Journal of Natural Gas Science and Engineering,* 31**,** 808-818.

SHEHATA, A. M. & NASR-EL-DIN, H. A. Zeta potential measurements: Impact of salinity on sandstone minerals. SPE International Symposium on Oilfield Chemistry, 13-15 April 2015 The Woodlands, Texas, USA Society of Petroleum Engineers.

SHENG, J. 2014. Critical review of low-salinity waterflooding. *Journal of Petroleum Science and Engineering,* 120**,** 216-224.

SHI, L., ZHU, S., YE, Z., XUE, X., LIU, C. & LAN, X. 2020. Effect of microscopic aggregation behavior on polymer shear resistance. *Journal of Applied Polymer Science,* 137**,** 48670.

SHIN, S. & CHO, Y. I. 1994. Laminar heat transfer in a rectangular duct with a non-Newtonian fluid with temperature-dependent viscosity. *International journal of heat and mass transfer,* 37**,** 19-30.

SHOAIB, M., QUADRI, S. M. R., WANI, O. B., BOBICKI, E., GARRIDO, G. I., ELKAMEL, A. & ABDALA, A. 2020. Adsorption of enhanced oil recovery polymer, schizophyllan, over carbonate minerals. *Carbohydrate Polymers,* 240**,** 116263.

SIDIQ, H. 2007. *Advance water abatement in oil and gas reservoir.* Curtin University.

SKAUGE, A., ZAMANI, N., GAUSDAL JACOBSEN, J., SHAKER SHIRAN, B., AL-SHAKRY, B. & SKAUGE, T. 2018. Polymer flow in porous media: Relevance to enhanced oil recovery. *Colloids and Interfaces,* 2**,** 27.

SKRETTINGLAND, K., HOLT, T., TWEHEYO, M. T. & SKJEVRAK, I. 2011. Snorre low-salinity-water injection—coreflooding experiments and single-well field pilot. *SPE Reservoir Evaluation & Engineering,* 14**,** 182-192.

SMITH, T. M., SAYERS, C. M. & SONDERGELD, C. H. 2009. Rock properties in low-porosity/low-permeability sandstones. *The Leading Edge,* 28**,** 48-59.

SONG, K.-W., KUK, H.-Y. & CHANG, G.-S. 2006. Rheology of concentrated xanthan gum solutions: Oscillatory shear flow behavior. *Korea-Australia Rheology Journal,* 18**,** 67-81.

SONG, Z., BAI, B. & CHALLA, R. 2018a. Using screen models to evaluate the injection characteristics of particle gels for water control. *Energy & Fuels,* 32**,** 352-359.

SONG, Z., HOU, J., ZHANG, L., CHEN, Z. & LI, M. 2018b. Experimental study on disproportionate permeability reduction caused by non-recovered fracturing fluids in tight oil reservoirs. *Fuel,* 226**,** 627-634.

SONG, Z., LIU, L., WEI, M., BAI, B., HOU, J., LI, Z. & HU, Y. 2015. Effect of polymer on disproportionate permeability reduction to gas and water for fractured shales. *Fuel,* 143**,** 28-37.

STAVLAND, A. 2010. How To Apply the Flow Velocity as a Design Criterion in RPM Treatments. *SPE Production & Operations,* 25**,** 223-231.

STAVLAND, A., JONSBRATEN, H. C., VIKANE, O., SKRETTINGLAND, K. & FISCHER, H. In-depth water diversion using sodium silicate on snorre-factors controlling in-depth placement. SPE European Formation Damage Conference, 2011. Society of Petroleum Engineers.

STAVLAND, A. & NILSSON, S. Segregated flow is the governing mechanism of disproportionate permeability reduction in water and gas shutoff. SPE annual technical conference and exhibition, 2001. Society of Petroleum Engineers.

SUGAR, A., TORREALBA, V., BUTTNER, U. & HOTEIT, H. 2020. Assessment of Polymer-Induced Clogging Using Microfluidics. *SPE Journal*.

SUN, W., ZENG, H. & TANG, T. 2021. Enhanced Adsorption of Anionic Polymer on Montmorillonite by Divalent Cations and the Effect of Salinity. *The Journal of Physical Chemistry A,* 125**,** 1025-1035.

SYDANSK, R. A new conformance-improvement-treatment chromium (III) gel technology. SPE enhanced oil recovery symposium, 1988. Society of Petroleum Engineers.

SYDANSK, R. D. 1993. Acrylamide-polymer/chromium (III)-carboxylate gels for near wellbore matrix treatments. *SPE Advanced Technology Series,* 1**,** 146-152.

TAKEYA, M., UBAIDAH, A., SHIMOKAWARA, M., OKANO, H., NAWA, T. & ELAKNESWARAN, Y. 2020. Crude oil/brine/rock interface in low salinity waterflooding: Experiments, triple-layer surface complexation model, and DLVO theory. *Journal of Petroleum Science and Engineering,* 188**,** 106913.

TAMSILIAN, Y., SHIRAZI, M., SHENG, J. J., AGIRRE, A., FERNANDEZ, M. & TOMOVSKA, R. 2020. Advanced oil recovery by high molar mass thermoassociating graft copolymers. *Journal of Petroleum Science and Engineering***,** 107290.

TANG, G.-Q. & MORROW, N. R. 1999. Influence of brine composition and fines migration on crude oil/brine/rock interactions and oil recovery. *Journal of petroleum science and engineering,* 24**,** 99-111.

TEKIN, N., DEMIRBAŞ, Ö. & ALKAN, M. 2005. Adsorption of cationic polyacrylamide onto kaolinite. *Microporous and Mesoporous Materials,* 85**,** 340-350.

TEKIN, N., DINÇER, A., DEMIRBAŞ, Ö. & ALKAN, M. 2010. Adsorption of cationic polyacrylamide (C-PAM) on expanded perlite. *Applied Clay Science,* 50**,** 125-129.

TERRY, R. E. & NELSON, S. D. 1986. Effects of polyacrylamide and irrigation method on soil physical properties. *Soil Science,* 141**,** 317-320.

THOMPSON, K. E. & FOGLER, H. S. 1997. Pore-level mechanisms for altering multiphase permeability with gels. *SPE Journal,* 2**,** 350-362.

TIELONG, C., YONG, Z., KEZONG, P. & WANFENG, P. 1996. A relative permeability modifier for water control of gas wells in a low-permeability reservoir. *SPE Reservoir Engineering,* 11**,** 168-173.

UMEROVA, S. & RAGULYA, A. 2017. Coexistence of Rheopexy and Dilatancy in Polymer Suspensions Filled with Ceramic Nanoparticles. *Rheol: open access,* 1**,** e102.

URANTA, K. G., GOMARI, S. R., RUSSELL, P. & HAMAD, F. 2019. Application of polymer integration technique for enhancing polyacrylamide (PAM) performance in high temperature and high salinity reservoirs. *Heliyon,* 5**,** e02113.

VASQUEZ, J. & EOFF, L. Field implementation of a relative permeability modifier during stimulation treatments: case histories and lessons learned after more than 3,000 treatments. EAGE Annual Conference & Exhibition incorporating SPE Europec, 2013a. Society of Petroleum Engineers.

VASQUEZ, J. & EOFF, L. A relative permeability modifier for water control: Candidate selection, case histories, and lessons learned after more than 3,000 well interventions. SPE European Formation Damage Conference & Exhibition, 2013b. Society of Petroleum Engineers.

VERMÖHLEN, K., LEWANDOWSKI, H., NARRES, H.-D. & SCHWUGER, M. 2000. Adsorption of polyelectrolytes onto oxides—the influence of ionic strength, molar mass, and Ca2+ ions. *Colloids and Surfaces A: Physicochemical and Engineering Aspects,* 163**,** 45-53.

WANG, J., ZHU, X., GUO, H., GONG, X. & HU, J. 2011. Synthesis and behavior evaluation of a relative permeability modifier. *Journal of petroleum science and engineering,* 80**,** 69-74.

WANG, L., LIANG, H. & WU, J. 2010. Electrostatic origins of polyelectrolyte adsorption: Theory and Monte Carlo simulations. *The Journal of chemical physics,* 133**,** 044906.

WASSMUTH, F., GREEN, K. & HODGINS, L. Water shutoff in gas wells: Proper gel placement is the key to success. SPE/DOE symposium on improved oil recovery, 2004. Society of Petroleum Engineers.

WEI, B. 2015. β-Cyclodextrin associated polymeric systems: Rheology, flow behavior in porous media and enhanced heavy oil recovery performance. *Carbohydrate polymers,* 134**,** 398-405.

WHITE, J., GODDARD, J. & PHILLIPS, H. 1973. Use of polymers to control water production in oil wells. *Journal of Petroleum Technology,* 25**,** 143-150.

WILLHITE, G. P., ZHU, H., NATARAJAN, D., MCCOOL, C. & GREEN, D. Mechanisms causing disproportionate permeability in porous media treated with chromium acetate/HPAAM gels. SPE/DOE Improved Oil Recovery Symposium, 2000. Society of Petroleum Engineers.

WIŚNIEWSKA, M., CHIBOWSKI, S. & URBAN, T. 2015. Impact of polyacrylamide with different contents of carboxyl groups on the chromium (III) oxide adsorption properties in aqueous solution. *Journal of hazardous materials,* 283**,** 815-823.

WOOD, D. A. 2016a. Natural gas needs to compete more innovatively and cooperatively with coal and renewable energies to sustain growth. *Journal of Natural Gas Science and Engineering,* 35**,** A1-A5.

WOOD, D. A. 2016b. The natural gas sector is changing rapidly: Research and technology development remain the keys to overcoming challenges and unlocking opportunities. *Journal of Natural Gas Science and Engineering,* 100**,** A1-A3.

WU, D., ZHOU, K., HOU, J., AN, Z., ZHAI, M. & LIU, W. 2020. Review of experimental and simulation studies of enhanced oil recovery using viscoelastic particles. *Journal of Dispersion Science and Technology***,** 1-14.

XIE, Q., SAEEDI, A., POORYOUSEFY, E. & LIU, Y. 2016. Extended DLVO-based estimates of surface force in low salinity water flooding. *Journal of Molecular Liquids,* 221**,** 658-665.

XINDI, S. & BAOJUN, B. 2017. Comprehensive review of water shutoff methods for horizontal wells. *Petroleum Exploration and Development,* 44**,** 1022-1029.

XIONG, C., WEI, F., LI, W., LIU, P., WU, Y., DAI, M. & CHEN, J. 2018. Mechanism of polyacrylamide hydrogel instability on high-temperature conditions. *ACS omega,* 3**,** 10716-10724.

XU, B., YUAN, B., WANG, Y., ZENG, S. & YANG, Y. 2019. Nanosilica-latex reduction carbonation-induced degradation in cement of CO2 geological storage wells. *Journal of Natural Gas Science and Engineering,* 65**,** 237-247.

YADAV, U. S., KUMAR, H. & MAHTO, V. 2020. Experimental investigation of partially hydrolyzed polyacrylamide–hexamine–pyrocatechol polymer gel for permeability modification. *Journal of Sol-Gel Science and Technology***,** 1-12.

YANG, K.-L., YIACOUMI, S. & TSOURIS, C. 2004. Electrical double-layer formation. CRC Press: Boca Raton, FL.

YANG, L.-P., SONG, E.-Z., DING, S.-L., BROWN, R. J., MARWAN, N. & MA, X.-Z. 2016. Analysis of the dynamic characteristics of combustion instabilities in a pre-mixed lean-burn natural gas engine. *Applied energy,* 183**,** 746-759.

YEFEI, Z. F. D. C. W. & KAI, F. D. C. 2006. Comprehension of water shutoff in oil wells and its technical keys [J]. *Acta Petrolei Sinica,* 5.

YI, Q., LI, C., MANLAI, Z., YULI, L. & RUIQUAN, L. 2017. Dynamic thickening investigation of the gelation process of PAM/PEI system at high temperature and high pressure. *Journal of Dispersion Science and Technology,* 38**,** 1640-1646.

YOU, Q., DAI, C., TANG, Y., GUAN, P., ZHAO, G. & ZHAO, F. 2013. Study on performance evaluation of dispersed particle gel for improved oil recovery. *Journal of Energy Resources Technology,* 135.

YUAN, X., YAO, Y., LIU, D. & PAN, Z. 2019. Spontaneous imbibition in coal: Experimental and model analysis. *Journal of Natural Gas Science and Engineering,* 67**,** 108-121.

ZAITOUN, A., BERTIN, H. & LASSEUX, D. Two-phase flow property modifications by polymer adsorption. SPE/DOE improved oil recovery symposium, 1998. Society of Petroleum Engineers.

ZAITOUN, A. & KOHLER, N. Two-phase flow through porous media: effect of an adsorbed polymer layer. SPE Annual Technical Conference and Exhibition, 2-5 October 1988 Houston, Texas SPE-18085-MS: Society of Petroleum Engineers.

ZAITOUN, A., KOHLER, N., MARRAST, J. & GUERRINI, Y. 1990. On the use of polymers to reduce water production from gas wells. *In Situ;(USA)*, 14.

ZAITOUN, A. & PICHERY, T. A successful polymer treatment for water coning abatement in gas storage reservoir. SPE annual technical conference and exhibition, 30 September–3 October 2001 New Orleans, Louisiana, USA. Society of Petroleum Engineers.

ZALTOUN, A., KOHLER, N. & GUERRINL, Y. 1991. Improved polyacrylamide treatments for water control in producing wells. *Journal of Petroleum Technology*, 43**,** 862-867.

ZHANG, J., HE, H., WANG, Y., XU, X., ZHU, Y. & LI, R. 2014. Gelation performance and microstructure study of chromium gel and phenolic resin gel in bulk and porous media. *Journal of Energy Resources Technology*, 136.

ZHANG, J., TAN, X., ZHAO, X., HE, Q. & WANG, Y. 2019. Experimental and numerical study of small-sized polymeric microgel (SPM) in low-or median-permeability reservoirs. *Journal of Petroleum Science and Engineering***,** 106829.

ZHANG, T., LI, X., SUN, Z., FENG, D., MIAO, Y., LI, P. & ZHANG, Z. 2017. An analytical model for relative permeability in water-wet nanoporous media. *Chemical Engineering Science,* 174**,** 1-12.

ZHANG, X., YANG, S.-L., ZHANG, L., CHEN, H., LIANG, Q.-M. & MA, Q.-Z. 2016. Characteristics and factors of gas-water relative permeability in volcanic gas reservoir. *Energy Sources, Part A: Recovery, Utilization, and Environmental Effects,* 38**,** 370-375.

ZHANG, Y., GAO, P., CHEN, M. & HUANG, G. 2007. Rheological behavior of partially hydrolyzed polyacrylamide hydrogel produced by chemical gelation. *Journal of Macromolecular Science, Part B,* 47**,** 26-38.

ZHAO, G., DAI, C. & ZHAO, M. 2014. Investigation of the profile control mechanisms of dispersed particle gel. *PLoS One,* 9**,** e100471.

ZHAO, J.-Z., JIA, H., PU, W.-F. & LIAO, R. 2011. Influences of fracture aperture on the water-shutoff performance of polyethyleneimine cross-linking partially hydrolyzed polyacrylamide gels in hydraulic fractured reservoirs. *Energy & fuels*, 25**,** 2616-2624.

ZHAO, X., ZHANG, J., HE, Q. & TAN, X. 2019. Experimental study and application of anti-salt polymer aqueous solutions prepared by produced water for low-permeability reservoirs. *Journal of Petroleum Science and Engineering,* 175**,** 480-488.

ZHENG, C., GALL, B., GAO, H., MILLER, A. & BRYANT, R. Effects of polymer adsorption and flow behavior on two-phase flow in porous. SPE/DOE Improved Oil Recovery Symposium, 19-22 April 1998 Tulsa, Oklahoma. Society of Petroleum Engineers.

ZHU, D., BAI, B. & HOU, J. 2017. Polymer gel systems for water management in high-temperature petroleum reservoirs: a chemical review. *Energy & fuels,* 31**,** 13063-13087.

ZIMMERMAN, R. W., AL-YAARUBI, A., PAIN, C. C. & GRATTONI, C. A. 2004. Non-linear regimes of fluid flow in rock fractures. *International Journal of Rock Mechanics and Mining Sciences,* 41**,** 163-169.